

**Factors affecting the durability of 5.25 inch Floppy Diskette Media
and its Mechanisms of Wear.**

Pamal Jit Sharma, B.Sc., M.Sc.

Doctor of Philosophy

The University of Aston in Birmingham

April 1989

This copy of the thesis has been supplied on condition that anyone who consults it is understood to recognise that its copyright rests with its author and that no quotation from the thesis and no information derived from it may be published without the author's prior, written consent.

The University of Aston in Birmingham

**Factors affecting the durability of 5.25 inch Floppy Diskette Media
and its Mechanisms of Wear.**

Pamal Jit Sharma, B.Sc., M.Sc.

Doctor of Philosophy

April 1989

Summary.

This project was concerned with establishing the factors affecting the durability and mechanisms of wear of 5.25 inch magnetic floppy diskettes. The samples used in the present work were produced specifically for this project but the data suggests that the conclusions are more generally applicable.

A variety of rigs have been employed to investigate the durability and wear mechanisms. These are production diskette drive units, simulation rigs, in-situ friction measuring apparatus and computer controlled bit analysis. The simulation rigs have been developed to avoid unrealistic situations. The in-situ friction measuring device has been developed to reduce the effects of external vibration and temperature effects. The bit analysis software has been extended to provide on-line data analysis; the hardware computer interface has also been simplified. All of these rigs produce data showing very similar trends in the durability of the media and its mechanisms of deterioration.

The samples examined were produced by the 3M Company on their pilot plant at St. Paul, USA and represent different lubrication conditions. One set of samples are unlubricated; the second set are internally lubricated only; the third set are surface lubricated only and the final set contains both lubricants. All of the categories have been produced with four different surface roughnesses by varying the degree of burnishing. Burnishing has been found to have a profound effect on the media's durability. Although initial burnishing appears to be beneficial, further such treatment causes premature failure in the media. The process of burnishing itself is considered to initiate the wear of the media.

An hypothesis has been proposed to explain the mechanisms of wear and degeneration of this form of magnetic media. It is suggested that the initial degradation of the media is caused by a fatigue process. The process of sub-surface fatigue produces delaminative wear of the surface. The debris thus generated leads to catastrophic failure through a three body interaction. This has been found to be quite independent of the conditions of lubrication.

**Key words: Floppy / Flexible Diskette, Magnetic Media,
Magnetic Recording, Tribology, Wear.**

To my Mum and Dad

Acknowledgements.

My first, and most sincere, expression of gratitude must go to my supervisor, Dr. John L. Sullivan. The academic advice he offered throughout the duration of this project was invaluable and gratefully accepted. His general guidance is separately and equally gratefully acknowledged.

Thanks are also due to Mr. Andrew M. Abbot whose technical assistance was indispensable. He has often helped in his own time. This was appreciated then and is acknowledged now with thanks.

Mssrs. Howard H. Arrowsmith and Dick A. Blunt have now retired from the Mechanical Workshop but their expertise in producing the devices illustrated in Figs. 4.4 and 5.1 must be noted.

The 3M Company, Minnesota, USA is gratefully thanked for completely funding this project. They have also produced all of the samples tested and provided much of the equipment utilised.

My final thanks are due to my parents whose constant encouragement and special understanding has made everything possible.

Contents.

	<u>Page</u>
Summary	3
Acknowledgements	5
List of Table and Figures	10
Chapter 1. Introduction	24
Introduction	25
1.1 Pre-amble	26
1.2 Objectives	32
1.3 Presentation	32
Chapter 2 What is a Floppy Diskette?	33
Introduction	34
2.1 The Diskette Jacket	35
2.2 The Magnetic Media	37
2.3 Some general considerations	47
2.4 Process and Methods of Magnetic Recording	48
2.4.1 Processes of Recording and Playback	49
2.4.2 Data Encoding Techniques	51
2.4.3 The Diskette Drive	57
Chapter 3 Previous work: A Literature Survey	59
Introduction	60
3.1 Basic Principles of Friction and Wear	62
3.1.1 Friction in Polymers	63
3.1.2 Wear of Polymers	70

Contents

3.2	Lubrication	76
3.2.1	The Stribeck Curve	76
3.3	Floppy Diskettes and Hard Discs	87
3.4	Tape	103
3.5	General Durability and Wear Considerations	118
Chapter 4	Experimental Rigs and Rig Development	130
	Introduction	131
4.1	Tandon TM100-2A Diskette Drives	132
4.2	Supported Sample Simulation Rig	134
4.3	Unsupported Sample Simulation Rig	141
4.4	In-Situ Friction Testing Device	144
4.5	Bit Analysis Software	148
Chapter 5	Instrumentation and Techniques: A Review	157
	Introduction	158
5.1	Optical Microscopic Analysis	158
5.2	Scanning Electron Microscopy	159
5.3	X-ray Photoelectron Spectroscopy	160
5.4	Transmission Electron Microscopy	169
5.5	Computer Analysed Optical Interferometry	172
Chapter 6	Presentation of Results	177
	Introduction	178
6.1	The Samples Coded 58759-4	178
6.2	Experimental Procedures and Criteria for Wear	185
6.3	Mechanical measurements: Friction and Wear	189
6.3.1	Drives	190

Contents

6.3.2	In-Situ Friction Tester	196
	(a) Effects of Burnishing	207
	(b) Effects of Lubrication	210
6.3.3	The Simulation Rigs	215
	(a) Effects of Burnishing	228
	(b) Effects of Lubrication	229
6.4	Electrical Measurements in the Drives	239
6.5	Physical Analysis of Samples	246
6.5.1	Interferometry	246
6.5.2	Transmission Electron Microscopy	247
6.5.3	Optical Microscopic Examination	249
6.5.4	Scanning Electron Microscopy	270
6.5.5	X-ray Photoelectron Spectroscopy	285
Chapter 7	Discussion of Results	296
	Introduction	297
7.1	Durability	297
7.1.1	Durability: The Effect of Burnishing	298
	7.1.1.1 Drives	300
	7.1.1.2 In-situ Friction Tester	304
	7.1.1.3 Supported Sample Simulation Rig	306
	7.1.1.4 Unsupported Sample Simulation Rig	307
7.1.2	Durability: The Effect of Lubrication	308
	7.1.2.1 Unlubricated Media: SR2 Samples.	309
	7.1.2.2 Surface Only Lubricated: SR1 Samples	309
	7.1.2.3 Bulk Only Lubricated: SR4 Samples	311
	7.1.2.4 Fully Lubricated Media: SR3 Samples	313
7.2	Mechanisms of Wear	314

Contents

7.2.1	Effect of Lubrication on Wear	324
7.2.1.1	The Surface Lubricant	324
7.2.1.2	The Bulk Lubricant	327
7.3	Justification of the Simulation Rigs	328
7.4	Effect of Head Wear on Media	329
Chapter 8	Conclusions and Recommendations	331
	Introduction	332
8.1	Conclusions	332
8.1.1	Media	332
8.1.2	Rigs	334
8.2	Recommendations	335
8.3	Further Work Suggestions	335
References		338
Appendix A	Calibrations	351
Appendix B	Computer Programs - Bit Analysis	354

Table

Table 6.1	The values of surface roughness (RA) of sample 58759-4 SR1 to SR4.	182
-----------	--	-----

List of Figures

Figure 2.1	Construction of the jacket and how it encloses the media.	36
Figure 2.2	The construction of the magnetic media.	37
Figure 2.3	Transmission Electron Micrograph showing some of the acicular magnetic particles protruding from the surface 60 K \times .	39
Figure 2.4	Polyester - polyurethane binder co-polymer: (a) its skeletal structure, (b) schematic representation of one element, and (c) in the binder.	41
Figure 2.5	Hydrogen bonding in the Polyurethane causing crystalline grain formation as seen in Fig. 2.4 (c) above.	41
Figure 2.6	The Alumina particles of the HCA fit into the magnetic layer.	44
Figure 2.7.	Different possible modes of magnetic recording.	48
Figure 2.8.	The essence of the recording and replay head and process.	49
Figure 2.9	The two heads in the diskette drive (a) under static conditions viewed in the media's tangential direction and (b) with the media rotating and creating the "Side 0 bubble" as seen in the media's radial direction.	52
Figure 2.10	The obsolete RZ and the two most commonly use techniques for encoding digital data on floppy diskette	

Table and Figures

	media, the FM and MFM methods.	54
Figure 2.11	The more realistic flux reversal transition profile and read-back voltage pulse detected.	56
Figure 2.12	The Tandon TM100-2A 5.25 inch diskette drive employed in this work [45].	58
Figure 3.1	The deformation component of friction in polymers.	68
Figure 3.2	The Stribeck Curve showing the different regimes of lubrication.	77
Figure 3.3	The process of Hydrodynamic lubrication (a) for a polymer-polymer interaction and (b) as expected for the diskette-media interface.	79
Figure 3.4	The nature of the Elasto-hydrodynamically lubricated interface (a) for a polymer-polymer interface and (b) for the head-media interface expected.	82
Figure 3.5	Mixed lubrication means significant penetration of the lubricating film.	83
Figure 3.6	Boundary lubrication of interacting surfaces.	84
Figure 3.7	How a worn track implies loss of signal through spacing loss and a reduction in the amount of material remaining to record the data.	88
Figure 3.8	Depth profile of the lubricant performed on a diskette sample by Chambers [75].	99
Figure 3.9	Schematic representation of magnetic particle distribution (a) The ideal magnetic particle distribution, (b) A polymer-rich magnetic layer and (c) A particle-rich magnetic layer.	112
Figure 3.10	Transmission Electron Micrographs showing voids in the	

	media in two separate samples, one (upper, SR2(4.5)) shown at 120 K \times and the other (lower, SR3(0)) at 60 K \times magnification.	114
Figure 3.11	Hydrolytic degradation of an ester link to carboxylic acid and alcohol (R and R' may be similar or different organic radicals).	115
Figure 3.12	The hydrolytic degradation of the binder co-polymer with the aid of Lewis acids which are the Iron oxide and Aluminium oxide particles in the magnetic layer. (R and R' maybe similar or different organic entities).	117
Figure 3.13	Wear of a highly elastic polymer by a hard and smooth abrader moving over it in a manner which causes cyclical stressing of the surface.	120
Figure 4.1	The circuit enabling gating of the drives' motors to their drive select lines. The circuit is shown in the "gated" mode. All lines are active at a logic LOW.	133
Figure 4.2	The supported sample simulation rig.	135
Figure 4.3	(a) The circuit diagram for the counter constructed to count the total number of passes made by the media and (b) the sensors used on either simulation rig.	137
Figure 4.4	(a) The low inertia head loading device for the simulation rigs and (b) the carriage arm onto which it is mounted.	139
Figure 4.5	The run-out in the supported sample rig.	141
Figure 4.6	The rotating platform used in the flexing sample rig.	142
Figure 4.7	The role of the supportive sponge in the flexing wear studies.	143
Figure 4.8	Heads and transducer arrangement in the In-situ Friction	

Table and Figures

	tester.	146
Figure 4.9	The variation of the output of the load cells before compensation due to changes in the ambient temperature; this output has been taken under zero load conditions.	147
Figure 4.10	Circuit used to achieve temperature stabilisation of Load Cells.	149
Figure 4.11	The circuit diagram of the interface used to communicate between the computer and diskette drives for the Bit Analysis Tests.	155
Figure 5.1	Specially constructed rotating platform for examining diskettes with the optical microscope.	158
Figure 5.2	Mechanism for producing the photoelectrons detected in XPS.	161
Figure 5.3	An example XPS spectrum of PET.	163
Figure 5.4	TEM sample preparation (a) Cured resin block with diskette sample embedded in it (b) The roughly trimmed block (c) The diamond knife and trough (d) How the sample is sectioned (e) The section of diskette on the Copper grid.	171
Figure 5.5	Schematic beam path of the Mirau interference system.	172
Figure 6.1	The skeletal structures of the bulk and surface lubricant molecules.	179
Figure 6.2	Interferometric scans showing the surface of samples JLS01 and JLS02 corresponding to the samples CN20714 and CN20718 respectively.	181
Figure 6.3	Interferometric scans of samples (a) SR2(0) and (b) SR2(1.5).	183

Table and Figures

Figure 6.3	Interferometric scans of samples (c) SR2(3) and (d) SR2(4.5).	184
Figure 6.4 (a)	A typical example of Grade 2 failure seen on a sample examined by optical microscopy (200 ×).	187
Figure 6.4 (b)	A typical example of Grade 3 failure seen on a sample examined by optical microscopy (200 ×).	187
Figure 6.5 (a)	Durability of differently burnished SR1 samples in the drives.	191
Figure 6.5 (b)	Durability of differently burnished SR2 samples in the drives.	192
Figure 6.5 (c)	Durability of differently burnished SR3 samples in the drives.	193
Figure 6.5 (d)	Durability of differently burnished SR4 samples in the drives.	194
Figure 6.6 (a)	A typical example of plastic flow on the surface of a diskette sample seen under SEM examination.	197
Figure 6.6 (b)	A wear site on the media showing the edges of the damaged area lifting up around a void.	197
Figure 6.7 (a)	Friction trace from the in-situ Friction tester: SR2(0).	199
Figure 6.7 (b)	Friction trace from the in-situ Friction tester: SR2(1.5).	200
Figure 6.7 (c)	Friction trace from the in-situ Friction tester: SR2(3).	201
Figure 6.7 (d)	Friction trace from the in-situ Friction tester: SR2(4.5).	202
Figure 6.7 (e)	Friction trace from the in-situ Friction tester: SR4(0).	203
Figure 6.7 (f)	Friction trace from the in-situ Friction tester: SR4(1.5).	204
Figure 6.7 (g)	Friction trace from the in-situ Friction tester: SR4(3).	205
Figure 6.7 (h)	Friction trace from the in-situ Friction tester: SR4(4.5).	206
Figure 6.8	Friction trace for a sample with surface lubrication applied: note the time scale shown.	212

Table and Figures

Figure 6.9 (a)	How initial friction varies with burnish time for Samples SR1 in the in-situ friction tester.	213
Figure 6.9 (b)	How initial friction varies with burnish time for Samples SR2 in the in-situ friction tester.	213
Figure 6.9 (c)	How initial friction varies with burnish time for Samples SR3 in the in-situ friction tester.	214
Figure 6.9 (d)	How initial friction varies with burnish time for Samples SR4 in the in-situ friction tester.	214
Figure 6.10 (a)	Durability of differently burnished SR1 samples on the supported sample simulation rig.	216
Figure 6.10 (b)	Durability of differently burnished SR2 samples on the supported sample simulation rig.	217
Figure 6.10 (c)	Durability of differently burnished SR3 samples on the supported sample simulation rig.	218
Figure 6.10 (d)	Durability of differently burnished SR4 samples on the supported sample simulation rig.	219
Figure 6.11 (a)	Durability of differently burnished SR1 samples on the unsupported sample simulation rig.	220
Figure 6.11 (b)	Durability of differently burnished SR2 samples on the unsupported sample simulation rig.	221
Figure 6.11 (c)	Durability of differently burnished SR3 samples on the unsupported sample simulation rig.	222
Figure 6.11 (d)	Durability of differently burnished SR4 samples on the unsupported sample simulation rig.	223
Figure 6.12 (a)	Catastrophic failure shown by a sample on the supported sample simulation rig with plastic flow and ploughing clearly visible (1 K \times).	225
Figure 6.12 (b)	Similar to the above but clear ploughing wear on the	

unsupported sample simulation rig (550×).	225
Figure 6.13 (a) How initial friction varies with burnish time for samples SR1 on the simulation rigs (U=unsupported, S=supported sample rig).	226
Figure 6.13 (b) How initial friction varies with burnish time for samples SR2 on the simulation rigs (U=unsupported, S=supported sample rig).	226
Figure 6.13 (c) How initial friction varies with burnish time for samples SR3 the simulation rigs (U=unsupported, S=supported sample rig).	227
Figure 6.13 (d) How initial friction varies with burnish time for samples SR4 on the simulation rigs (U=unsupported, S=supported sample rig).	227
Figure 6.14 (a) Friction for the sample SR2 on the unsupported sample rig showing (i) SR2(0), (ii) SR2(1.5), (iii) SR2(3), and (iv) SR2(4.5).	230
Figure 6.14 (b) Friction for the sample SR2 on the supported sample rig showing (i) SR2(0), (ii) SR2(1.5), (iii) SR2(3), and (iv) SR2(4.5).	231
Figure 6.15 (a) Friction for the sample SR4 on the unsupported sample rig showing (i) SR4(0), (ii) SR4(1.5), (iii) SR4(3), and (iv) SR4(4.5).	232
Figure 6.15 (b) Friction for the sample SR4 on the supported sample rig showing (i) SR4(0), (ii) SR4(1.5), (iii) SR4(3), and (iv) SR4(4.5).	233
Figure 6.16 (a) Friction for the sample SR1 on the unsupported sample rig showing (i) SR1(0), (ii) SR1(1.5), (iii) SR1(3), and (iv) SR1(4.5).	234

Table and Figures

Figure 6.16 (b)	Friction for the sample SR1 on the supported sample rig showing (i) SR1(0), (ii) SR1(1.5), (iii) SR1(3), and (iv) SR1(4.5).	235
Figure 6.17 (a)	Friction for the sample SR3 on the unsupported sample rig showing (i) SR3(0), (ii) SR3(1.5), (iii) SR3(3), and (iv) SR3(4.5).	236
Figure 6.17 (b)	Friction for the sample SR3 on the supported sample rig showing (i) SR3(0), (ii) SR3(1.5), (iii) SR3(3), and (iv) SR3(4.5).	237
Figure 6.18	Bit analysis software durability data for the SR2 and SR4 samples.	242
Figure 6.19	The read/write gap in the ferrite loop of a typical M-R head. Wear of the glass bonding can be seen where the ferrite bonds to the ceramic; pull-outs from the glass have left voids (100 ×).	243
Figure 6.20 (a)	The surface of SR2(0) media seen using optical microscopy before testing using the bit analysis software (50 ×).	244
Figure 6.20 (b)	Typical optical micrograph of a sample after testing using the bit analysis software showing patches where the total removal of the magnetic layer has occurred (50 ×, SR2(0)).	244
Figure 6.20 (c)	Sample SR2(4.5), 50 ×.	245
Figure 6.20 (d)	Sample SR4(0), 50 ×.	245
Figure 6.21	Examples of damage caused to the media surface during burnishing: illustrated here are sample (a) SR1(3) and (b) SR3(4.5).	248
Figure 6.22 (a)	The polymer rich areas which may be seen in the samples using TEM: SR2(0) 60 K×.	250

Figure 6.22 (b) Sample SR2(4.5) 60 K \times .	250
Figure 6.22 (c) Sample SR2(4.5) 80 K \times .	251
Figure 6.22 (d) Sample SR2(4.5) showing a crack in the magnetic layer which was probably produced during microtoming, 38 K \times .	251
Figure 6.22 (e) Sample SR3(0) showing slightly more uniform particle distribution 35 K \times .	252
Figure 6.22 (f) Sample SR3(4.5) with particles protruding from the surface, 30 K \times .	252
Figure 6.23 (a) Unlubricated sample tested in the drives: SR2(0), 200 \times .	254
Figure 6.23 (b) Lubricated sample tested in the drives: SR3(0), 100 \times .	254
Figure 6.23 (c) Unlubricated sample tested in the drives: SR2(1.5), 400 \times .	255
Figure 6.23 (d) Lubricated sample tested in the drives: SR3(1.5), 400 \times .	255
Figure 6.23 (e) Unlubricated sample tested in the drives: SR2(3), 400 \times .	256
Figure 6.23 (f) Lubricated sample tested in the drives: SR3(3), 400 \times .	256
Figure 6.23 (g) Unlubricated sample tested in the drives: SR2(4.5), 200 \times .	257
Figure 6.23 (h) Lubricated sample tested in the drives: SR3(4.5), 200 \times .	257
Figure 6.24 (a) Unlubricated sample tested on the unsupported sample simulation rig: SR2(0), 200 \times .	259
Figure 6.24 (b) Lubricated sample tested on the unsupported sample simulation rig: SR3(0), 400 \times .	259
Figure 6.24 (c) Unlubricated sample tested on the unsupported sample simulation rig: SR2(1.5), 400 \times .	260
Figure 6.24 (d) Lubricated sample tested on the unsupported sample simulation rig: SR3(1.5), 400 \times .	260
Figure 6.24 (e) Unlubricated sample tested on the unsupported sample	

simulation rig: SR2(3), 400 ×.	261
Figure 6.24 (f) Lubricated sample tested on the unsupported sample simulation rig: SR3(3), 400 ×.	261
Figure 6.24 (g) Unlubricated sample tested on the unsupported sample simulation rig: SR2(4.5), 400 ×.	262
Figure 6.24 (h) Lubricated sample tested on the unsupported sample simulation rig: SR3(4.5), 400 ×.	262
Figure 6.25 (a) Unlubricated sample tested on the supported sample simulation rig: SR2(0), 400 ×.	263
Figure 6.25 (b) Lubricated sample tested on the supported sample simulation rig: SR3(0), 400 ×.	263
Figure 6.25 (c) Unlubricated sample tested on the supported sample simulation rig: SR2(1.5), 200 ×.	264
Figure 6.25 (d) Lubricated sample tested on the supported sample simulation rig: SR3(1.5), 400 ×.	264
Figure 6.25 (e) Unlubricated sample tested on the supported sample simulation rig: SR2(3), 200 ×.	265
Figure 6.25 (f) Lubricated sample tested on the supported sample simulation rig: SR3(3), 200 ×.	265
Figure 6.25 (g) Unlubricated sample tested on the supported sample simulation rig: SR2(4.5), 400 ×.	266
Figure 6.25 (h) Lubricated sample tested on the supported sample simulation rig: SR3(4.5), 400 ×.	266
Figure 6.26 (a) Typical fine debris found on wear tracks, 400 ×.	268
Figure 6.26 (b) Wear debris laying on a track with a wear patch visible in the background, 200 ×.	268
Figure 6.26 (c) More debris on a sample which shows only a little plastic flow of the surface, 50 ×.	269

Table and Figures

Figure 6.26 (d) Debris particle which shows clear curling, 400 ×.	269
Figure 6.27 (a) Polymeric wear debris which has been rolled up, 50 ×.	271
Figure 6.27 (b) A close up of the largest features with extensive plastic flow visible on the wear track in the background, 100 ×.	271
Figure 6.27 (c) Wear damage is visible in the middle of the plastic flow of the wear track in the background, 200 ×.	272
Figure 6.27 (d) The black specs visible in the rolled polymer debris are the acicular magnetic particles, 400 ×.	272
Figure 6.28 (a) Unlubricated sample tested on the in-situ friction tester showing wear sites as for the other rigs: SR2(0).	273
Figure 6.28 (b) Typical wear sites on the media tested on the friction tester SR2(1.5).	273
Figure 6.28 (c) SR2(3).	274
Figure 6.28 (d) SR2(4.5).	274
Figure 6.29 (a) Typical plastic deformation of the type caused by a ploughing mechanism.	276
Figure 6.29 (b) As with the above micrograph, the plastic flow is clearly visible but this may be compared more easily to the surrounding surface.	276
Figure 6.30 (a) Typical wear site showing a void where material appears to have been removed leaving raised edges.	278
Figure 6.30 (b) An enlarged view of the feature showing clearly raised edges.	278
Figure 6.30 (c) Wear site showing smoothing in the area where material has been removed possibly suggesting that the high local friction led to wear.	279
Figure 6.31 (a) Clear ploughing type plastic deformation on a sample tested on the simulation rigs.	280

Table and Figures

Figure 6.31 (b) Another typical wear site with the remaining material showing raised edges; the edge of the feature appears to be raised suggesting it is only weakly in contact with the sub-surface material.	280
Figure 6.32 (a) A large particle which appears to be of the same constitution as the diskette surface.	282
Figure 6.32 (b) Another wear particle showing more typical curling and having a laminar appearance.	282
Figure 6.32 (c) Another wear particle which appears to be a curled lamina.	283
Figure 6.32 (d) A typical wear site with clear plastic flow around it in a direction from the bottom right hand corner to the top left hand corner.	283
Figure 6.33 (a) Typical head R/W gap showing wear of head, 200 \times .	284
Figure 6.33 (b) A close up of one of the worn regions of the head showing material has been removed through "pull-outs"; this head has not been worn in the present tests, 2 K \times .	284
Figure 6.34 (a) Typical wear of the type of heads fitted in the drives used for this investigation showing the R/W gap and one erase gap.	286
Figure 6.34 (b) Similar damage at the other erase gap.	286
Figure 6.35 (a) The trailing edge of a side 1 head showing apparently preferential wear of the ceramic, 120 \times .	287
Figure 6.35 (b) A close up of the worn area shows pits left by material which has been pulled out, 600 \times .	287
Figure 6.36 (a) A side 0 head shows greater wear of the ferrite, 600 \times .	288
Figure 6.36 (b) A close up shows the mechanism of wear appears to be the same as for the side 1 head, 1.2 K \times .	288
Figure 6.37 XPS scans for Carbon on (a) Unused side 0 head	

Table and Figures

	(b) Used side 0 head.	291
Figure 6.38	XPS Scans for Carbon on (a) Unused side 1 head (b) Used side 1 head.	292
Figure 6.39	XPS Scans for Oxygen on (a) Unused side 0 head (b) Used side 0 head.	293
Figure 6.40	XPS Scans for Oxygen on (a) Unused side 1 head (b) Used side 1 head.	294
Figure 7.1	The curve "A" shows that the desired material would show elastic deformation even for relatively large stresses as well as having a high elongation strain before it fractures.	303
Figure 7.2	The effect of Side 0 head tilt (a) negative gradient, (b) ideal orientation and (c) positive gradient.	304
Figure 7.3	The surface lubricant reduces wear by separating the transducer and the media as well as distributing the loading of the head.	310
Figure 7.4	The three body interaction which is of primary importance.	316
Figure 7.5	Method of sub-surface crack propagation: (a) compression of the leading tip of the crack, and (b) tensioning of the same region.	319
Figure 7.6	Micro-scratch caused on the surface of a fully lubricated media probably by a three body action.	326
Figure 7.7	The protection afforded by the surface lubricant from a third-body ploughing wear action.	325

Table and Figures

Figure A.1	Operating calibration for the supported sample rig.	352
Figure A.2	Operating calibration for the unsupported sample rig. The discontinuity at the dial setting of 100 is due to switching from one range to another on the control face.	352
Figure A.3	Calibration for the friction measuring transducer used on the supported sample and unsupported sample simulation rigs.	353

Chapter 1
Introduction

Chapter 1.

Introduction.

Introduction.

This short chapter is intended to introduce the reader to recording media, and especially that utilising magnetic techniques for recording, with particular emphasis on the floppy diskettes which are the subject of this work. It presents some background on this medium and competitive media as well as an indication as to where the subject of this study stands in the commercial world in relation to the latest innovations in data storage. The aims of the project are then presented before an outline of the presentation is given.

One point which needs to be stressed at the outset is that the field covered by this work is one not often reported in literature and for this reason the work carried out is of a fundamental nature. Indeed, the work previously reported does not appear to be of a basic nature looking at the initial process of degradation.

Furthermore, the work on diskettes reported elsewhere has usually not been of a systematic nature targeted towards finding the mechanisms of wear or isolating particular parameters for study. Aspects that have been studied are methods of producing worn samples and their subsequent analysis using various techniques. It was intended to depart from this approach and to adopt a more systematically progressive method of study for both durability and wear mechanisms for this work and it is felt that methods of testing have been used in non-traditional ways in order to achieve this aim.

1.1 Pre-amble.

The magnetic recording concept was demonstrated in 1900 at the World Fair in Paris where a machine for recording magnetic signals and replaying them back was displayed by a Dane, Valdemar Poulsen [1][2]. Oberlin Smith had suggested recording with the use of magnetic materials in 1888 [3]. He had, however, envisaged particulate media (as, in fact, employed in the majority of magnetic recording media today) whereby discrete particles of magnetically sensitive material were held on a cotton or silk thread. He had apparently dismissed the idea of using a continuous medium, such as steel wire, because he thought that discrete pairs of magnetic north and south poles could not exist in such a medium. However, steel wire was later used by Poulsen in his machine, the "Telegraphone". Poulsen produced magnetic impressions on the wire electromagnetically by the translation of an electro-magnet relative to the wire as electrical signals were produced in the coil of this electro-magnet from a microphone.

The replaying of the sound was achieved by the reversal of this process, that is by the varying magnetic field causing an electrical excitation in the coil. Poulsen applied this technique to a helical winding of steel wire on a drum which rotated below a sensing coil. As the drum rotated, the coil mounting moved parallel to the axis of the cylinder at a speed related to the pitch of the helical winding and thereby followed the recording wire medium. This sensing coil then represented the read/write heads used today which are discussed later. It was thus that Poulsen managed to reproduce the original recorded signal.

The more familiar plastic tape was introduced in 1935 by Allgemeine Elektrizistâts Gesellschaft and I. G. Farben [3] having taken over the work of Pfleumer who had produced particulate media using paper and plastic substrates coated with large magnetic particles in 1927 [3]. This was a much improved

medium with the cost of recording for unit time reduced by a factor of over six. A further improvement was made by Hickman [3] in the form of a reduction in the transducer-medium relative speed with a speed of slightly over 0.4 m.sec^{-1} being used when he utilised a new magnetic material. This compared with the speed of over 2 m.sec^{-1} employed by Poulsen in his original machine, an improvement by a factor of five. The reason for this being a significant development was in its implication that more data could be recorded on a given length of medium thereby increasing the data density by a corresponding factor of five.

These developments have led to the existence of today's well established magnetic recording industry with the virtually obsolete domestic reel-to-reel audio tape recorder and its now common successor, the audio compact Philips type cassette which was introduced in 1963. These are both methods of analogue recording but recording on tape for computer data storage purposes employs digital techniques. In fact these techniques have also been considered for audio recording as described by many researchers, for example Bellis [4] who considers the advantages of this method such as the improvement in signal-to-noise ratio; digital video recording has been discussed by, amongst others, Baldwin [5] for broadcast standard video recording. More recently, there have been developments which have led to announcements concerning the availability of digital audio tape (DAT) in the near future for home use [6]; similar claims for video recording have also appeared [7]. These digital methods are employed for rotating media in the form of hard discs and floppy diskettes as well as for recording on tape. The floppy diskette has arrived relatively recently on the popular market and it supersedes the magnetic computer tape in terms of speed of data access. Floppy diskettes offer data access times of the order of milliseconds for data anywhere on the diskette, compared to possibly minutes for tape. They were originally introduced in their 8 inch diameter format (see

Chapter 2 for structural details) by the International Business Machines Corporation in the early 1970s, but were superseded by the much more popular 5.25 inch diameter format media used in this investigation. The latter media was introduced by Schugart Associates of USA in 1975 and at that time was designed to work on drives with a single read/write head transducer with the media having 40 concentric tracks on each of the two surfaces at a radial density similar to the 8 inch diskettes of 48 tracks per inch. They had a linear recording density of 103 binary digits (or BITS) per millimetre [8] compared to the media used in this investigation which has a density of 218 Bits.mm^{-1} ; the track density on samples used in this investigation is the same as that of the original media.

Although the data bit density available on commercially available computer tape has increased from slightly over 30 Bits.mm^{-1} to some 246 Bits.mm^{-1} , in a similar period, the data access times available on the rotating media has made it far more popular as all of the tape preceding the required portion must be read before the desired data may be read. This contrasts with diskettes having concentric tracks each of which may be accessed directly thereby saving time.

This transfer from tape to diskette use has been further aided by the introduction of micro-computers into the home and relatively cheap and ready availability of diskette drives. The "floppy", or "flexible", diskette has become a very major and extremely popular form of magnetic media for storing digital data both for home computer applications and for applications in the commercial environment: in the USA alone the rate of sale stood at some 15 million units per month in 1982 [9] with projections for an annual growth rate of over 30%. Since this time the home computer market has expanded dramatically as hardware, software and media have all become more affordable. It is more for reasons concerned with this expansion than other aspects that the floppy diskette is likely to dominate the popular, that is less specialised, digital data storage market for quite a long time in the future.

Of course technology is moving at a very fast pace in the field of digital data storage and other media such as optical discs [10] are now fairly freely available. At the present moment, however, these are of the ROM (Read Only Memory) or, at best, WORM (Write Once Read Many) type: an example of the former is the commonly available compact disc for musical entertainment, and an example of the latter is the media which may be found advertised in the popular technical press (for example, Personal Computer Magazine, Vol. 1, Issue 6, July 1988, page 64) and is manufactured by many producers, including 3M. Further advances have enabled the production of magneto-optical rigid and flexible media which is many times erasable such as the flexible type produced for experimental purposes by ICI in the UK and rigid discs produced by 3M in the USA [11] as well as "purely optical" erasable technology which may soon be available [12]. It must be noted, however, that neither is yet ready for commercial launch and is expected to be too uncompetitively priced for it to be accepted readily in the popular market. So despite the greater data density promise with these devices (of the order of GigaBytes on a single disc, as compared to "purely" optical media today where 800 MBytes are available on a 5.25 inch disc [13]), they are unlikely to directly replace the magnetic floppy diskette for some considerable time as new associated hardware also needs to be installed in order to benefit from them. Furthermore, it is suspected that the optical media may suffer from data loss through aging a problem which has been described recently for compact discs [14]. It would appear that the aluminium coating used in the manufacture of these compact discs may be found to deteriorate through atmospheric oxidation after as little as three years. In fact, some of the media, which may have been manufactured under less stringently controlled conditions, has been found to exhibit lifetimes of only 18 month, according to Fox [15]; errors are found when methods are employed for detecting the number of digital errors caused by faults in the aluminium coating. New coatings to overcome this problem, using the

chemically very much less reactive precious metals instead of aluminium, are only at the experimental stage. Furthermore, Burke et al, [16], have reported that despite emerging technologies such as opto-magnetic media, magnetic media will still be necessary for the foreseeable future.

Magnetic technology has also not stood still offering ever increasing data density [17]: 1.6 MByte and 2 MByte capacity is currently available on 5.25" media. The advent of perpendicular, as opposed to the present longitudinal, recording techniques (see Chapter 2 for details) promises a very much greater increase in density as problems of demagnetisation are reduced at higher densities by this method of recording, according to Osaka et al [18]. Advances in this technology are being hampered by tribological problems which are also the major problems associated with the present media. In the present case the wear is predominantly that of the media whereas in perpendicular recording it is predominantly that of the head slider. This is because in perpendicular recording Co-Cr acicular particles are used almost exclusively at present and these sharp magnetic particles must be aligned to have their major axes predominantly in the direction perpendicular to the plane of the media surface. The reasons for this become clear when the size of the particles is considered both for the present longitudinally magnetised γ - Fe_2O_3 and the perpendicularly magnetised Co-Cr: they are approximately 0.5 μm long and 0.1 μm in cross-sectional diameter. Such a size makes their dimensions smaller than a single magnetic domain and means that there are no "Bloch walls" [19] domain boundaries formed within these particles as in the case of "continuous" materials where these "walls" form such boundaries creating individual magnetic domains. Thus the individual particles behave as whole magnetic domains in their own right. This causes each particle to be permanently magnetised in one of the two directions along its major morphological axis; it is the anisotropic nature of the particles' shape which causes this preferential magnetic alignment as alignment in a direction

perpendicular to the major axis implies a greater magneto-static energy being stored leading to it not being the lowest possible energy state for such a particle. Obviously, in order to switch between the two directions, it is necessary to apply a saturating external magnetic field which is in excess of the coercive force for the material being used.

It is because of this anisotropic behaviour that the acicular Co-Cr particles in perpendicularly recorded media must be physically aligned as described above. The sharp ends of these particles then cause tribological difficulties through rapid ploughing type wear (see later in Chapter 3 for details of this process) of the head slider. In the present, longitudinally recorded media, a very small fraction of the magnetic particles are perpendicularly orientated and how they contribute to the durability of the media is proposed and discussed later as is their action on the heads.

This illustrates the fact that, neither the present media nor those expected to be its high density successors, are close to perfection, far from it, in fact. In spite of the fact that diskettes are regarded by most users as being (almost) infinitely reliable when used in accordance with manufacturers' general directions, their use in an "intensive use" environment can lead to failures in the media, both "soft" (recoverable) and "hard" (non-recoverable). It is with this durability problem that this work is concerned and with considerations for modification of the media in order to improve the durability. Problems concerning increased linear and track densities, associated head air-gap and accurate tracking difficulties, have been addressed by media and drive manufacturers. Some of the major problems confronting the industry are, as mentioned earlier, of a tribological nature: wear of the media and the mechanisms responsible for this wear process. This situation has been recognised by Skelcher [20]. Obviously this is a very important area for study and appears to be one of the greatest problems limiting the production of better diskette media.

The problem has not, it appears, been studied in a rational, systematic and logically sequential fashion (see later literature survey of Chapter 3) and clearly needs to be tackled in order that progress be made on the production of better, more reliable media in respect of its wear characteristics and durability. This is even more important as ever increasing data density leads to the use of ever thinner magnetic layers in the interest of limiting the interactions between the magnetic fields of adjacent bits.

1.2 Objectives.

The objectives of this project have been listed below and necessarily cover a very broad field of study. These were to:

- (a) Investigate the effects on media durability of different lubrication conditions,
- (b) Investigate effects of the media's surface roughness on the same,
- (c) Establish the mechanisms of wear for the media,
- (d) Investigate the use of various simulation rigs for accelerated testing.

1.3 Presentation.

This work is presented in a fashion which is considered to lead the reader to understand naturally the reasons for carrying out the various tests. As far as possible, information gained up to any point has been used to relate to and explain further tests.

The intention has been to progress through each of the above aims such that the progress made regarding each one has been clearly identified. Obviously, it is impossible, and perhaps undesirable, to completely divorce one objective from another and as a result some overlap is unavoidable and will be noticeable.

Chapter 2

What is a Floppy Diskette?

Chapter 2.

What is a Floppy Diskette?

Introduction.

This chapter concerns the description of diskettes and their construction. This is essential knowledge for the study of wear, its mechanisms and the enhancement of durability which may be brought about by consideration of these.

As indicated earlier, the floppy diskette is a reliable form of extra-computer **Random Access Memory (RAM)** which is less than perfect. It is often referred to as a RAM device but this is not, strictly, quite true as each byte (group of eight bits) of data cannot be accessed directly irrespective of its physical position on disc in the same way as true RAM which has a structure enabling data to be retrieved from any location through these locations being individually and directly addressable. In the case of diskettes (and hard discs), if a particular byte of data on a track is to be accessed, all of the bits which comes before that byte on that track must first be read. This is, however, a rapid process as individual tracks may be accessed directly. The direct location of the tracks is made possible through these being sequentially numbered concentric circles rather than a continuous spiral groove as in the case of vinyl records.

The diskette consists physically of the wafer thin magnetic media, described later, inside a jacket. In the case of the media used here, the 5.25 inch type (and in the case of the older 8 inch type), this jacket is itself not particularly rigid and is made of PVC; the newer 3 inch and, the more popular, 3.5 inch media are enclosed in a hard plastic cassette type case. As this work has been done on 5.25 inch media, the jacket for this type of diskette is illustrated in Fig. 2.1 and described below but the principles of writing to and reading from the

other three versions, as well as the structure of the actual media, is essentially the same. As a result the problems, and their solutions, are expected to be extremely similar but more acute in the case of physically smaller media due to the thinner magnetically sensitive layer and greater number of tracks per unit radial length (track density) on them: 135 and 100 tracks per inch (TPI) are placed on the 3.5 inch and 3 inch media [21] respectively compared to the maximum track density used on the 5.25 inch media being 96 TPI and that on the 8 inch media being half of this at 48 TPI. The reason for limiting this radial track density in the older media was due to the tracking problems encountered when the media experiences thermal expansion or contraction. In the case of the smaller media, although the fractional expansion is the same, since similar materials are employed, the physical error in the track position is smaller. The description of the drive in a later sub-section will show that the heads used for the reading and writing processes are moved a carefully controlled, constant, distance between tracks and will mis-track if the tracks are displaced by amounts greater than their tolerance through these thermal effects.

2.1 The Diskette Jacket.

The jacket performs the function of enclosing the 79 μm thick media for easy use and storage. It has various slots and holes cut in it as shown in Fig. 2.1; the functions of these are detailed below:

- (1) Spindle hole: a hole in the jacket corresponding to a 1.125 inch hole in the centre of the circular magnetic disc is designed to enable the accurate location of the media in a diskette drive.
- (2) Head access slot: to permit the magneto-resistive (M-R) head to contact the media in order to perform data read/write (R/W) operations

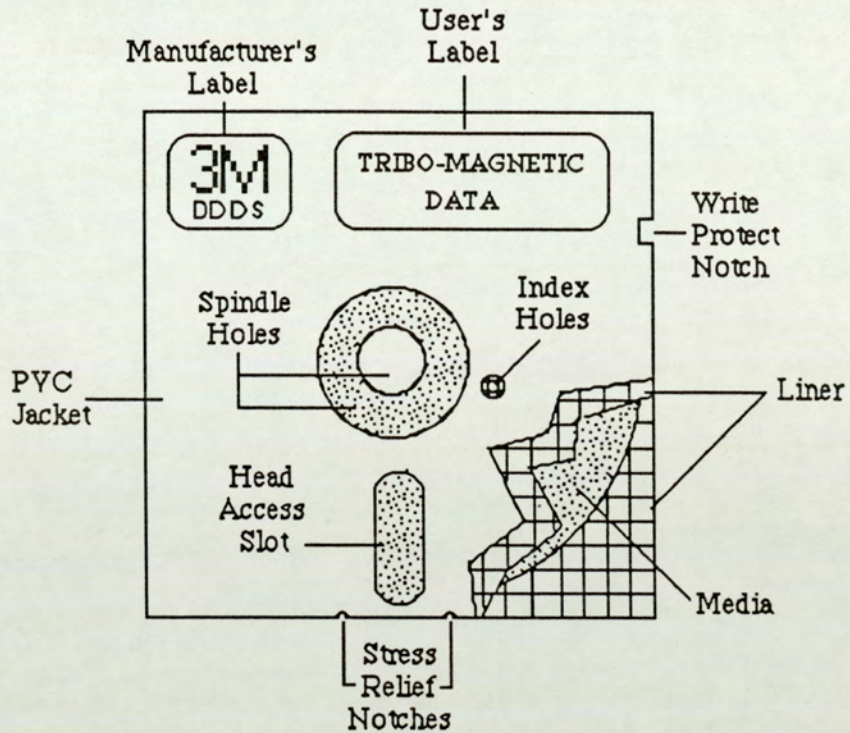


Figure 2.1 Construction of the jacket and how it encloses the media.

- (3) Index hole: a hole which, when aligned with one in the rotating media, allows transmission of an infra-red beam from a transmitter, above, to a receiver below the diskette inside the drive. This enables the drive electronics to locate the start of each of the concentric tracks on the diskette.
- (4) Stress relief notches: to enable the bending of the jacket on head loading etc. for smoother running of the media.
- (5) Write-protect: when open, to allow writing of data to the diskette. A push-switch detector is operated which enables or disables the drive's write electronics depending on its position: when the slot is covered, it depresses this switch and prevents accidental over-writing of existing data. In the newest drives this switch has been replaced by a similar

opto-electronic arrangement to the index hole sensor. In this case the covered slot interrupts the infra-red beam which disables the write electronics.

- (6) Liner: This is a non-woven material designed to collect any dust or debris particles continuously as the diskette rotates in the jacket. It is also thought to contribute to the smooth running of the plastic media. The usual material utilised is Rayon but this is of some contention with some researchers promoting the use of polyester materials as performing the task better [22].
- (7) Labels: the manufacturer's label specifies the type of diskette, the track density, the linear density, control number etc. and the user's identification label is obviously to enable the user to identify the data on a particular unit.

2.2 The magnetic media.

The basic construction of the magnetic media is shown in Fig. 2.2 and consists of

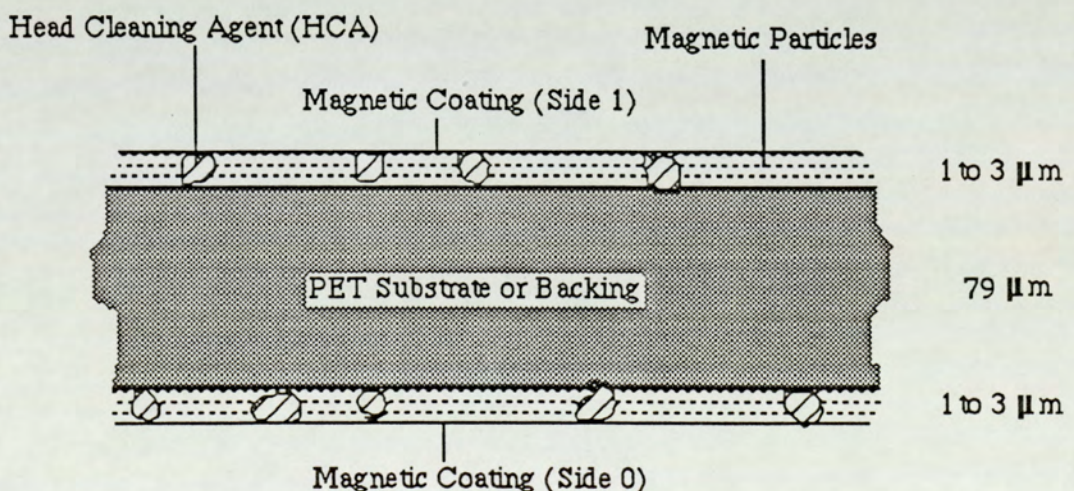


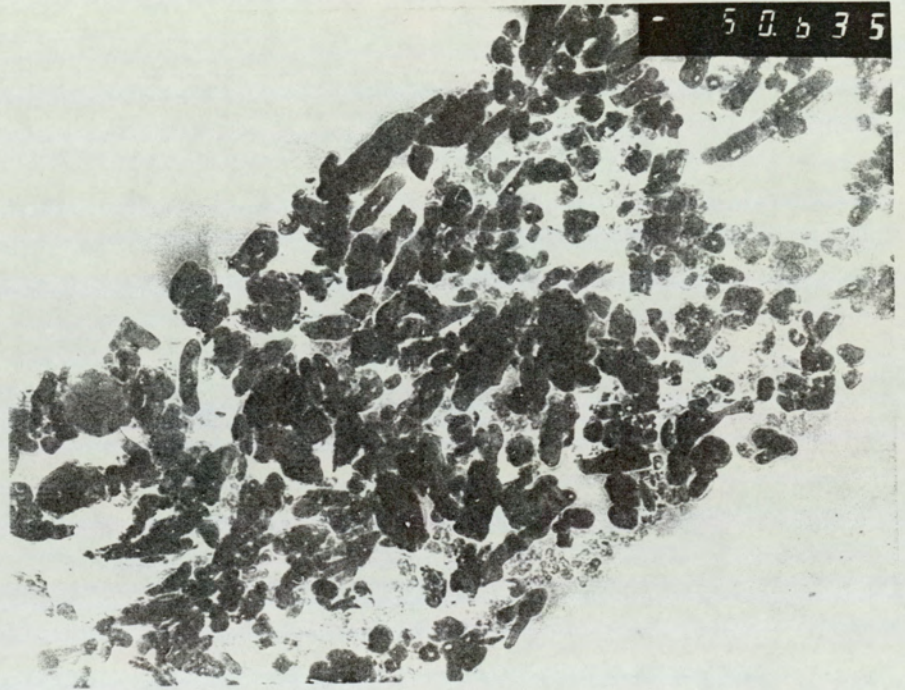
Figure 2.2 The construction of the magnetic media.

two magnetically sensitive layers on either side of the thick substrate of polyethylene terephthalate (PET) comprising the diskette.

The physical and chemical properties of the two different types of layer are, obviously, critical to the proper functioning and durability of the whole system. The substrate or backing has to be flexible and not suffer fatigue fracture and it also has to bond well chemically to the magnetic layers on either side. The latter must also be flexible but, as it is in intimate contact with the magnetic read/write head (or more commonly now, as in this study, with two such heads) made of hard ceramic and ferrite materials, the magnetic layer must also have other qualities. The constituents of the magnetic layer determine these qualities and knowledge of such constituents is essential before any progress can be made on improving the design of the media with these properties in mind. The constituents of this magnetic layer are described below along with the function that each one fulfills:

- (1) γ - Fe_2O_3 : The most important constituent of the magnetic layer of the diskette are the γ - Fe_2O_3 particles. These are the magnetic particles which carry the recorded signal. They are needle-like in shape having a length of approximately $0.5 \mu\text{m}$ and a cross-sectional diameter of the order of $0.1 \mu\text{m}$. They normally reside within the polymer of the binder described below but may be brought to the surface by abrasive removal of the top layers of polymer. In fact, the transmission electron micrograph of Fig. 2.3 shows some of the particles at the surface and protruding from it. The process of burnishing used to smooth the media can also facilitate the exposure of these particles. Being a metal oxide, they are very hard and, as considered below, can contribute to some abrasive degradation of the head in the same fashion as the alumina particles of the HCA. This has also been described

Figure 2.3 Transmission electron micrograph showing some of the acicular magnetic particles protruding from the surface 60 K \times .



below. The nature of the diskette's, and other polymeric magnetic media's, magnetic layer is as that of a highly filled polymer and the properties that this implies: the magnetic layer contains some 70% by weight and 50% by volume of magnetic particles in magnetic tapes according to Bradshaw et al [23] and is expected to be very similar for floppy diskettes.

- (2) Binder: The inherent demand for flexibility on floppy diskettes due to the nature of the head media interface as described by Greenberg [24], Adams [25] and Stromsta et al [26] means that the materials used to produce the binders are usually polymeric thermoplastics. These materials are such that they may be melted and cooled without appreciably affecting their properties. Although undesirable, this melting can occur under high frictional heating. Dickens' work, [27], involved polymers and he indicated that these may, when cooled from the softened or molten state, take either an amorphous or crystalline solid form [27]. The materials normally used for the binder, at least in the case of the 3M floppy diskette media used in this work, are polyester - polyurethane co-polymers which exhibit these properties. The structure of these polyester-polyurethane organic macro-molecules is shown in Fig. 2.4 where their intrinsic "hard" and "soft" phases, or segments, are indicated. The "soft", amorphous polyester section of the binder's organic molecular chains are usually constructed through the reaction of di-functional carboxylic acids with di-functional alcohols for both tapes as described by Bradshaw et al [23] and for various 3M diskettes according to Skelcher [28]. This gives the binder its flexibility as well as, through their elasticity, giving it some desirable durability properties (see later).

The "hard" polyurethane segments form grains and are rigid

through hydrogen bonding between the $-(NH)C(O)O-$ chemical groups incorporated into them: this is illustrated in Fig. 2.5. Cross-linkers in the form of isocyanates are also used here to aid the formation of crystalline grains. This gives a crystalline type rigidity which is further enhanced by the fact that these groups, with highly electronegative Oxygen and Nitrogen in them, participate in dipole-dipole type interactions. The cohesive energies between the polyurethane groups have been measured and are reported by Bradshaw et al [23] as having values of more than 35.3 kJ mol^{-1} . These compare to the corresponding values of 12.1 kJ mol^{-1} between the ester groups of the "soft" polyester section of the co-polymer as reported by the same authors.

The polyurethane sections of the co-polymer, with their grains, increase the hardness of the binder and are less prone to flow plastically at increased temperatures and they reduce the elasticity of the whole structure; they may possibly make the binder more brittle[23].

It should also be mentioned that the other obvious properties of the binder are that it bonds well to the other constituents of the magnetic layer and thus enhances the mechanical properties of the whole layer as well as bonding strongly to the PET substrate.

In the case of media expected to be used under harsh environmental conditions, fungicidal agents may also be added to the binder mix but this does not apply to the media in this present case.

- (3) Carbon black: when two different materials rub against each other, the difference in their surface work functions leads to the transfer of charge at their mutual interface from one surface to the other as can be understood from solid state and atomic physics and as cited for magnetic tapes by Bhushan et al [29]. This will be limited by various relative

parameters but if left unchecked can lead to increasing charge separation causing an electrostatic adhesion, particularly in non-conducting surfaces such as polymers. This extra adhesive force leads to an increase in the coefficient of friction which, in this instance, as discussed later, can be extremely detrimental. Also, discharges could be very harmful to the diskette's surface causing drop-outs through demagnetisation problems; surface smoothing through softening and melting with consequential further plastic flow caused by increased friction. A further consequence of polymer melting is the possibility of producing a polymer-rich upper layer leading to greater than normal separation of the read/write head transducer and the magnetic particles described above. Obviously, the reduction in signal that this is likely to cause, one version of the so called "spacing losses", is undesirable.

It is in order to prevent such charge from building up and creating these problems that the magnetic layer contains an amorphous form of conducting Carbon, carbon black. The amorphous form, rather than the similarly conducting graphite, is used presumably due to the better mixing with the polyester sections of the binder and the anisotropic nature of the charge conduction in graphite.

- (4) Aluminium oxide (alumina): The particles of alumina (Al_2O_3) added to the binder are the biggest particles contained in the magnetic layer and are present to serve two separate, but equally important, purposes. How the particles fit into the layer is shown in Fig. 2.6 and in order to ensure such a fit the (gaussian) spread in the size of the particles is required to have quite a small half-width resulting in the size being quite closely monitored.

One of the functions of the alumina is as a head cleaning agent (HCA) and these particles achieve this by removing any of

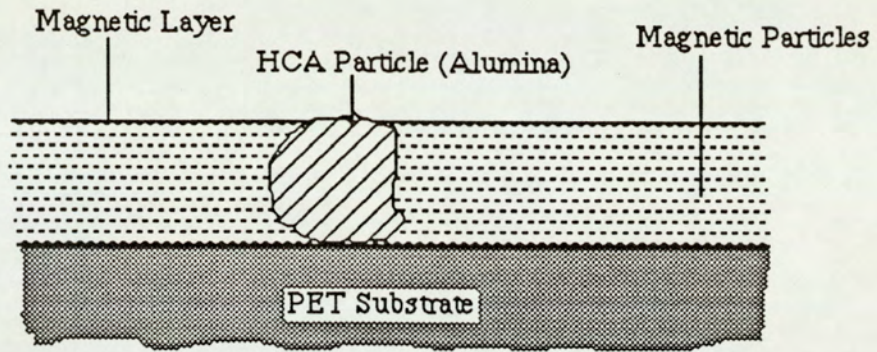


Figure 2.6 The Alumina particles of the HCA fit into the magnetic layer.

the transferred layers of polymer etc. from the surfaces of the heads in a micro-abrasive action. In fact, on a very much longer time scale, this can lead to greater damage than merely cleaning of the slider. This has been borne out in the tests carried out by Talke and Su [30] using steel balls on magnetic media which confirm this abrasive action. Talke and Tseng, [31], also studied wear and transfer of slider materials using radio - activity methods. Irradiated materials were used as sliders with radiation detected from the media then confirming wear of the sliders as well as confirming transfer of slider material to the media surface. How this can be detrimental to the head has been described by many researchers [31], [32], [33]. The discussion of Weiss [32] concerns wear of the head and media. It is made clear that read-back signal loss cannot be totally attributed to media wear. In fact, using the sliders employed in tests with reference media reveals that the visibly worn slider samples produce a lower signal than new heads on the the same reference media. This is obviously not desirable. Blevins et al, [33], have also studied the abrasivity of diskette media. They reported details concerning the preferential wear of certain parts of the head. This has led to their discovering the nature of the head-media interface,

this is clearly very important and is discussed in more detail later. The effect of worn heads has been briefly considered in the final parts of this work as well as being discussed as one factor complicating the study of media durability. There has been some evidence presented by Blevins et al [33] that in addition to the undoubtable wear of the heads caused by the normal proportion of HCA contained in the diskettes, the wear characteristics of the media are improved without degradation of the read signal if the alumina content is increased from the usual 1.5% to (up to a maximum before significant head wear, of) 3.5%. It is not clear, however, whether the signal degradation has been studied over a long period to establish whether it takes fewer of these diskettes to cause significant wear of the heads compared to the number required with 1.5% alumina to cause the same damage.

The other function of the alumina particles is to act as a load bearing agent which distributes stresses in the media's surface magnetic coating. Clearly the relatively soft polymer is not, by itself, sufficiently strong to cope with all the stresses imposed on it by the head. The alumina particles transfer these stresses directly to the backing layer of PET so that the thicker layer takes the weight of the head, which is often loaded at 0.2 N, thus distributing the loading stresses and minimising local damage. One other function that could be performed in addition is to reduce the direct physical interaction between the head and the acicular magnetic particles and hence reducing the amount of wear of the head that these may cause. The increase in the alumina proportion may thus produce no increase in the wear of the head when its own proportion is increased but could still increase the lifetime of the media by improved stress distribution. Of course, any signal degradation (although none was detected at 3M by Blevins et al

[33]) due to "spacing losses" needs then to be investigated; "spacing losses" being caused simply by a reduced magnetic coupling of the head and magnetic particles as they are separated by a larger distance.

- (5) Lubricants: the diskette is lubricated primarily to reduce the friction at the head/media interface as this is believed to reduce wear. Much research has been done to make lubricants compatible with magnetic media such as the work regarding the Fomblin fluorocarbons discussed by Bagatta [34]. Although two different types of lubricants are used in floppy diskette media, "bulk" and "surface" lubricants, their importance is somewhat debatable. Some researchers have suggested changes in the lubrication of polymers such as increasing the viscosity of the surface lubricant to take more stress and thereby preventing high stress caused wear of the diskette surface [34]. Others have suggested improvements in the interaction of the lubricant with the binder such as chemical inertness in order to prevent changing the bonding between the binder and substrate backing material of polyethylene terephthalate [34]. It is not their role which is contested but rather their relative importance; it has been suggested that getting the binder consistency right is more important [35] but arguments can probably be presented to show the contrary and it would be expected that lubricants and binder consistency are equally important. This must be interpreted as meaning that the lubricant system requires less improvement. This conclusion can be drawn with the benefit of the information gained from the present work details of which may be found in later sections but from which it may be concluded that the lubricant is essential in order to regulate wear. It has also been suggested later, as a conclusion of this project, that the binder does indeed require improvement and specific areas for this improvement have been suggested.

Surface roughness has been suggested by Cummings [36] as an equally important factor affecting the coefficient of friction and through it the durability. This is also considered in the present study.

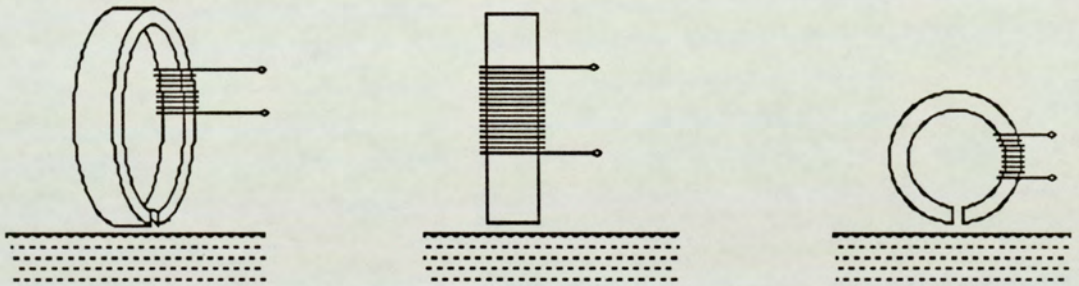
2.3 Some general considerations.

The floppy diskettes are manufactured to closely monitored standards of size etc. as defined by the American National Standards Institute (ANSI). These determine the sizes and positions of the holes in the media and the holes and notches in the protective jacket. They do not, however, specify such details as the constituents of the magnetic layer which are closely guarded commercial secrets. It may, however, be noted as an example that the Japanese manufacturer Fuji has begun to market a product using Barium, rather than Iron, based magnetic particles. The Barium ferrite medium's active particles are just as easy to produce as the Iron oxide particles according to Speliotis [37]. Furthermore, the same author has suggested that the same head-media interface may be used as is employed at present. The potential for further increasing the data recording density through the large extent of perpendicular magnetisation experienced by the Barium ferrite particles has also been observed there and by others such as Fujiwara [38]. In addition to this the particles also offer the advantage, for analogue recording, of a much flatter frequency response which leads to better high frequency playback characteristics and, for digital recording purposes, the possibility of higher density recording [39]. Naturally, disadvantages also exist for this new material such as overwrite problems. This can be overcome, however, as suggested by Speliotis [37], by the use of a thinner magnetic coating. The consequences of wear will, however, then be much more significant and this project's results more important. Of course, the fact that the Barium ferrite particles are not acicularly shaped, may imply slight differences in the wear characteristics but the disc shape which is employed would still be

expected, predominantly at least, to exhibit a very similar mechanism to that discovered from the present work.

2.4 Process and Methods of Magnetic Recording.

In general, the process of magnetic recording entails the moving media being in close proximity to or, in the case of flexible diskette media, in actual contact with the slider of the read/write head transducer. The general process of recording has many forms as is illustrated in Fig. 2.7 below.



(a) Transverse

(b) Vertical or Perpendicular

(c) Longitudinal

Figure 2.7. Different possible modes of magnetic recording.

Transverse recording, Fig. 2.7(a), magnetises the media in a direction perpendicular to the direction of relative motion at the head-media interface but parallel to the surface of the media. Vertical or perpendicular recording may use a single pole, as illustrated in Fig. 2.7(b), or a double pole where the other pole is then below the media but in either case entails magnetising the media perpendicular to its direction of travel and simultaneously perpendicular to its surface.

The process of longitudinal recording, shown in Fig. 2.7(c), is by far

the most commonly used mode and involves magnetisation of the media in its plane and parallel or anti-parallel to the direction of travel: this method is used in both analogue audio etc. and digital data recording onto magnetic computer tape, hard discs and flexible rotating media. It is with the latter process that the media used in this project is concerned.

2.4.1 Process of Recording and Playback.

It may be useful to clarify terminology here: in analogue recording, the process of storing information is usually referred to as "recording" and its retrieval as "playback"; the analogous terms in digital storage are "writing" and "reading" respectively. Since this terminology is not in any way confusing both terms have been used throughout this work as has been considered contextually appropriate.

Fig. 2.8 shows in more detail the process of recording on magnetic floppy diskette along with a more realistic form of the heads' magnetic part.

This consists essentially of a magnetically soft ferrite material (Nickel-Zinc ferrite in this case) which is magnetised by an electric current flowing in a coil as shown. The loop of ferrite "conducts" this magnetic flux through a

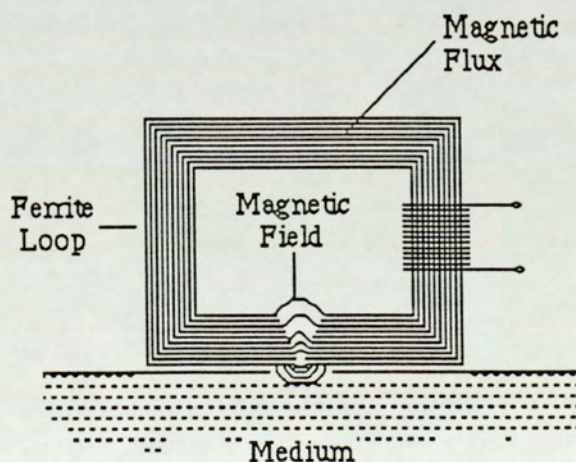


Figure 2.8. The essence of the recording and replay head and process.

uniform reluctance except at the air gap where there is a discontinuity in the permeability. The gap, which is of higher reluctance than the ferrite, is magnetically "short-circuited" by the magnetic material in the recording medium.

In an actual head, this fragile assembly is surrounded and supported by a hard ceramic material, often Barium or Calcium titanate; a photographic illustration of this is given later when head wear is considered. Also, in a real head three ferrite loops exist with one either side of that used for reading and writing data. The other two create "sub-tracks" parallel to and either side of the one on which data is stored. These sub-tracks contain no information. In fact they contain unmagnetised material to prevent interference in the form of "pick-up" from adjacent tracks, when reading, and accidental partial over-writing of adjacent tracks when writing thereby improving the signal-to-noise ratio.

The contacting surface of the whole assembly is finished to a very high degree of smoothness (typically better than $0.1 \mu\text{m}$) in order to prevent damage to the relatively soft media.

The recorded signal for analogue recording is directly dependent in the case of audio recording, for example, on the amplitude of the input. This is achieved by varying the current in the coil on recording resulting in a similar variation of the extent to which the medium is magnetised. On reproduction the relative motion at the head-media interface results in the time varying magnetic field at the head gap electromagnetically inducing a voltage in the coil which may be detected and processed further as desired by electronic means.

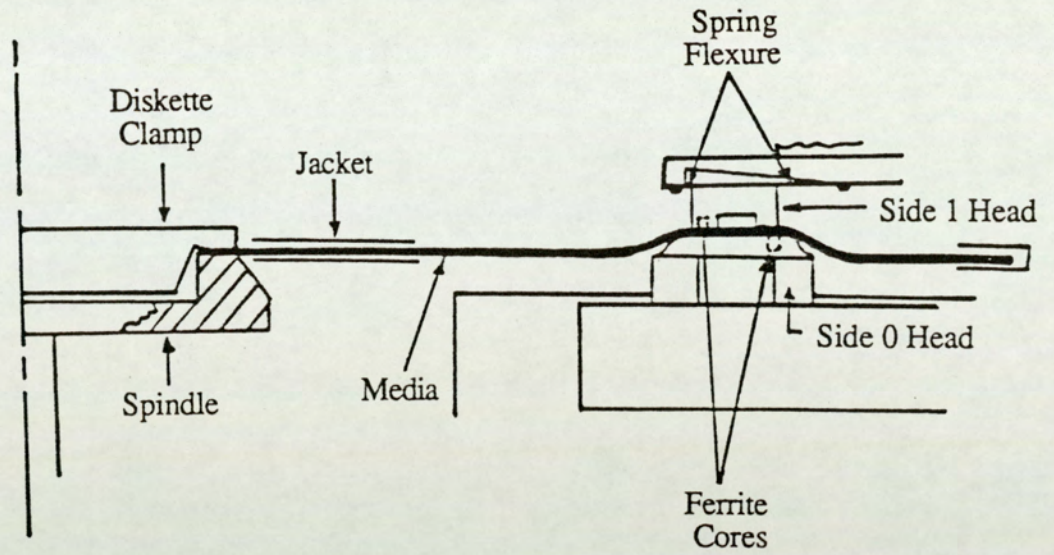
Digital recording involves a mechanism which is the same in principle but a concept known as "saturation recording" is employed: magnetisation in either of the two longitudinal directions is then such that the maximum alignment of particles is attained.

It can be seen from Fig. 2.8 that for the best recording of a signal, either

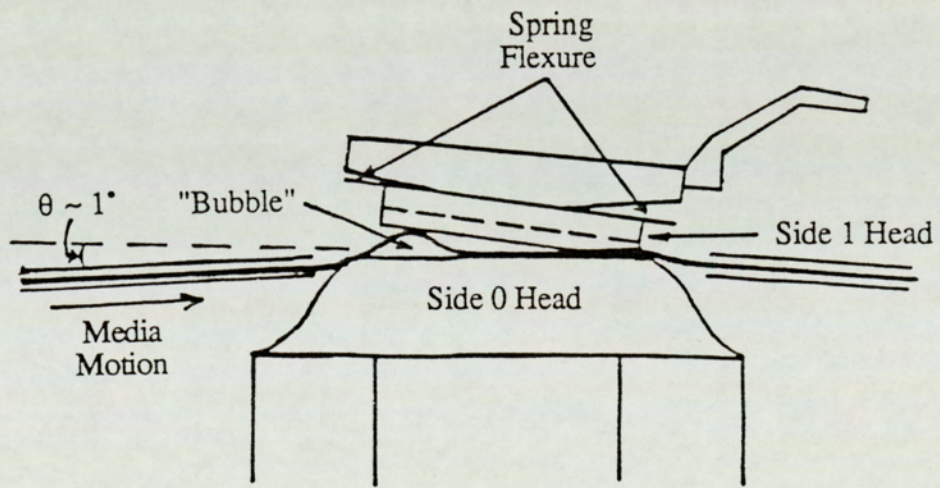
of an analogue or digital nature, the media needs to be as close to the head gap as possible. In fact, for analogue signals, such as the recording of music, the faithful recording of each part is not crucial as a musical piece will appear continuous even if one note, say, is lost. In digital recording, however, one wrongly recorded or replayed bit can result in the wrong ASCII (American Standard Code for Information Interchange) character, for instance, being read back. This can cause errors in processing data using a computer. The heads in a floppy diskette drive are normally in full contact with the media. The exact head-media interface is actually very much more complex and has its own implications. The true interface is shown in Fig. 2.9 but discussed more fully later. The reason for mentioning it here is that spacing losses, as briefly discussed for one instance earlier, can occur during the writing and reading processes whereby the amplitude of the signal written or read is reduced or lost altogether through the physical separation of the media and the read/write transducer. As will be discussed later, this can result from air-borne dust particles coming in between one of the heads and the floppy diskette media or by wear debris from the diskette doing the same. In technical terms, the loss of signal is described as a "drop-out" if the signal falls to below 80% of the signal found for the full head-media contact. The reason for this being that at this point the processing electronics tends to produce errors.

2.4.2 Data encoding techniques.

The methods for encoding data for digital recording are numerous and may be found in general literature such as the general magnetic recording text edited by Pear [40] which deals with many topics including analogue recording, digital recording and media manufacture (primarily tape). Hickman [3] deals exclusively with analogue recording but the principles of magnetic recording are covered. Similar discussion may also be found in the texts by Begun [41] and



(a)



(b)

Figure 2.9 The two heads in the diskette drive (a) under static conditions viewed in the media's tangential direction and (b) with the media rotating and creating the "side 0 bubble" as seen in the media's radial direction.

Stewart [42] in addition to the fundamentals of magnetism and some historical aspects of magnetic recording.

Digital recording methods, which became of greater interest from the early 1960s with the advent and wider use of the digital computers, are discussed in the text by Hoagland [43]. Hoagland has offered details of the different encoding techniques for recording as has Hudson [44]. Hudson has studied each technique for his research with a view to the improvement of the presently available recording densities.

In view of the above literature, it is considered necessary to discuss only the two most commonly used encoding techniques: the so called "Frequency Modulation" (FM), or "single density", and the "Modified Frequency Modulation" (MFM), or "double density" methods and to compare these with the first methods used.

The FM and MFM encoding techniques are both methods which involve the media particles being magnetised either in one direction or the other of the longitudinal recording mode and are termed "Non-Return-to-Zero" (NRZ) techniques as opposed to the very early "Return-to-Zero" techniques which involved parts of the media being of zero magnetisation (that is, with parts of the media being, on the macroscopic scale, unmagnetised). All of these encoding methods are illustrated for a typical data "bit stream" in Fig. 2.10. If the positive part of a square wave is used to represent magnetisation in one direction, and the negative part magnetisation in the other, then the diagrams of Fig. 2.10 may be used to explain the differences between the codes. Essentially, it may be observed that the RZ techniques involve two flux reversals for each recorded bit whereas the FM and MFM methods require only one with the MFM method requiring only half as many reversals to store the same data as the FM code. Since these may be stored in half of the physical space as a consequence, this provides for twice as much data to be stored in unit length, hence the single and

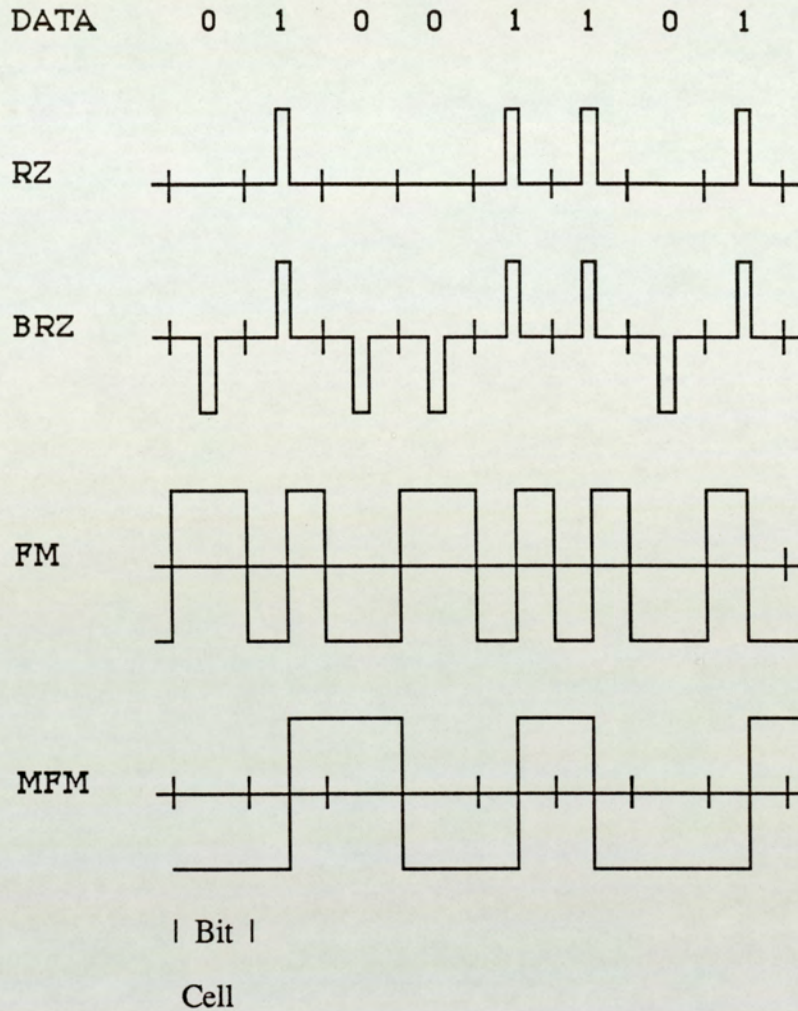


Figure 2.10 The obsolete RZ and the two most commonly used techniques for encoding digital data on floppy diskette media, the FM and MFM methods.

double density terminology.

The RZ techniques involve a pulse of relatively short duration compared to the size of the "bit cell" as illustrated above. In the top RZ technique such a pulse exists only if a logic "1" is to be recorded and a logic "0" is represented by unmagnetised media. This has important implications in over-writing data with the necessity to erase the media before any re-recording can take place and has implications on the time taken to re-write data on pre-recorded media. In the

lower RZ technique, the **Bipolar-RZ (BRZ)**, the erasing step is eliminated by the logic "0" being represented by saturation of the media in the opposite direction to that used for a logic "1". This latter method also has one further feature in that it is termed as being "self - clocking" as each bit of the data is guaranteed to provide a pulse; the RZ method has to be externally clocked, or timed for each bit cell, to detect logic "0" bits.

Earlier NRZ techniques were simply a modified version of the BRZ method such that the two different data bits were represented by two different directions of magnetisation. However, the requirement for increased data densities has necessitated the abandoning of this coding method. The FM code always produces a reversal in magnetisation, or flux reversal, at the start of every bit cell, giving it an inherent self-clocking property; a second flux reversal at the centre of the bit cell then represents a logic "1" and the absence of such a second reversal is used to represent a logic "0" by default. In the case of the MFM coding, flux reversals occur only at the centre of a bit cell and then only for a logic "1" and are absent for a "0" except in the case of two such bits in adjacent bit cells. In this latter case, a flux reversal occurs at the start of the second bit cell of the "0's" and one in the centre for the following "1" as usual. This code is not self-clocking [44]. The chronometric length of each bit cell for MFM recording is half as long as that for FM since a maximum of one flux reversal is required per recorded bit as opposed to two for the latter. These times for the 5.25" media, as used in this project, are 2 μ Sec and 4 μ Sec respectively [21].

The read-back process detects reversals in flux by detection of a voltage pulse as the dictated by the familiar expression:

$$|E(t)| \propto d\phi / dt \quad (2.4.2.1)$$

where $|E(t)|$ is the magnitude of the time dependent voltage detected

ϕ is the flux which changes as a result of head-media relative motion

The ideal, square, flux reversal transitions indicated in the Fig. 2.10 do not, in fact, occur and, although they are sharp, each transition occurs over a finite period of time as shown in Fig. 2.11 below where the corresponding voltage pulse generated and detected is also shown.

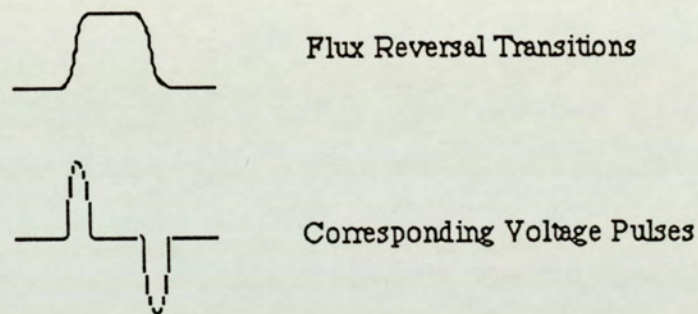


Figure 2.11 The more realistic flux reversal transition profile and read-back voltage pulse detected.

Details of pulse detection and subsequent conversion using the relevant electronics, such as voltage comparators, is not necessary here and is documented elsewhere by other authors including Hudson [44]. However, one method for increasing the data density may be considered here. This involves the forcing closer together of consecutive flux reversals as can be appreciated from Fig. 2.11. This can, however, lead to the positive and negative cycles of the induced voltage to merge and become electronically "confused" posing problems of timing errors etc. These problems are also discussed in more depth by Hudson [44] but imply that the data density may be improved if the media can be caused to run more smoothly. This is the case for studying improved lubrication and friction characteristics.

2.4.3 The Diskette Drive.

The diskette drives used in the work carried out for this project are typical of those commercially available for 5.25 inch media. The more important features of the drive are indicated in Fig. 2.12 [45]. The illustrated drive is the one actually employed (Tandon Model TM100-2A).

The diskette, in its PVC jacket, is inserted into the drive through the opening at the front and is guided in by rails at either side on the inside of the drive to its correct location. Upon closing the front latch, the cone assembly accurately locates and clamps the media itself to the hub, which is driven through a belt by the D.C. drive motor shown. At the same time the heads are automatically loaded onto the two surfaces of the media via a spring mechanism with a loading force of 0.2 N. The rate of rotation of the drive motor is closely monitored, to within 1.5% of $300 \text{ rev. min}^{-1}$, and adjusted accordingly by a servo mechanism on the servo circuit board.

The head assembly is accurately stepped radially across the diskette at the head access gap in the jacket using the four phase stepper motor to enable each of the 40 tracks per surface to be accessed. The voltage signal from the heads is fed directly to the logic circuit board to a point which is not shown in the cut-away view of the drive but is situated at the nearest corner of the board as displayed. The processing of the signal is performed fully on this board to produce digital output at the standard industry interface provided at its rear. Other necessary information required by a drive controller is also available at this point on the board such as the index pulse generated by the index sensor shining through the index hole in the media, as described earlier, once every revolution.

The drive is externally powered by a dual voltage power supply providing +12 V (900 mA) and +5 V (600 mA).

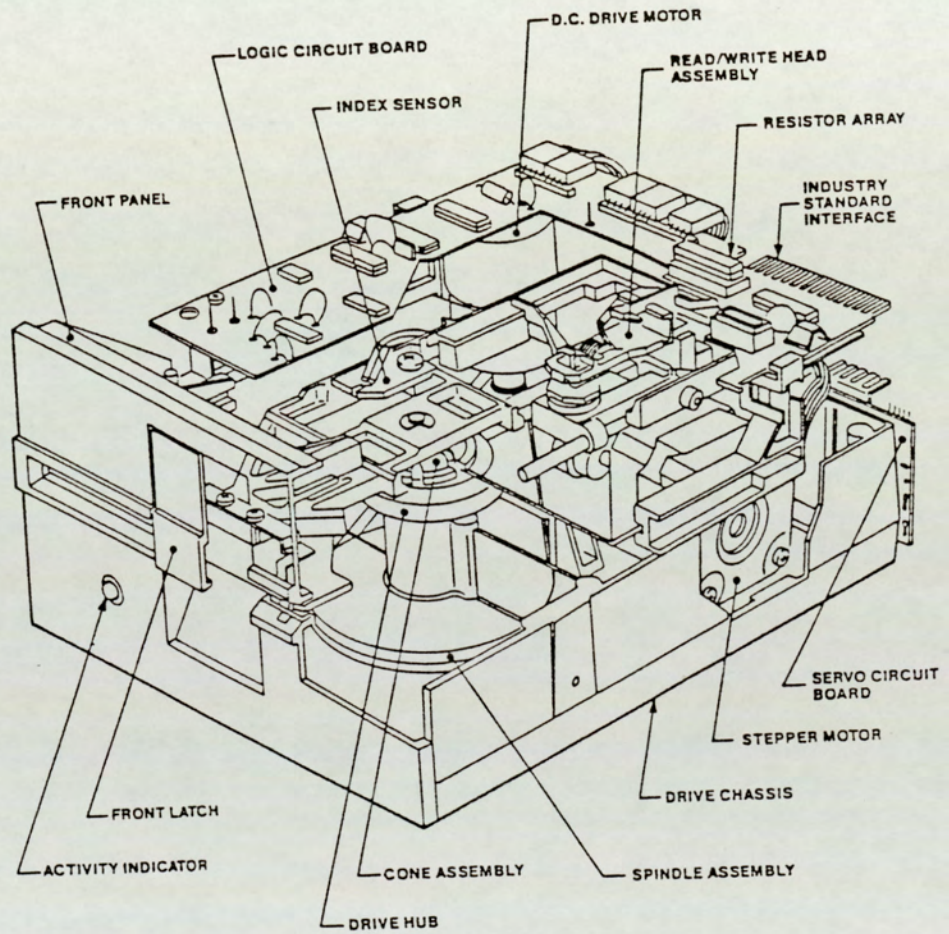


Figure 2.12 The Tandon TM100-2A 5.25 inch diskette drive employed in this work [45].

Chapter 3

Previous Work: A Literature Survey

Chapter 3.

Previous work: A Literature Survey.

Introduction.

It was intended that this chapter present a review of the work that has been carried out in the field of floppy diskette media but since, as mentioned earlier, this project explores a very much unresearched topic, not much literature is available which is directly relevant. Work has been published, however, relating to the magnetic tape medium (particularly for computer data tape and some audio tape as well as, more recently, some on video tape). Some work has also been done on "hard" (or "rigid"), Winchester type, discs which consist of an aluminium disc coated with magnetic particulate coatings or continuous layer coatings. Both of these media work on very similar magnetic principles to those employed for floppy diskettes, but there the similarity often ends because of the differences in their head-media interface and environment. As an example, each of the media may be considered in turn:

- (a) The tape is very much more flexible than floppy diskettes and is designed to withstand the stresses of being wound and stored under longitudinal tension as well as the surface stresses imposed by the layers of tape being wound on top of each other on a reel. Furthermore, computer tape is started and stopped quite suddenly in between reading at fast translational speeds. This can often mean acceleration from stationary to over 5 m.sec^{-1} in a space of approximately 8 mm and of course, similar decelerations. So the tape is under considerable tension during data read and suffers abrasion at the point where it is

stopped as it makes full contact with the read head from a position of almost full hydrodynamic separation (explained fully later) during the read operation. In contrast, floppy diskette media spins at a constant rate and is stored under "relaxed" conditions. The video tape does imitate the frequent contact of a single point with the head as it is helically scanned and thereby each point is stressed more than once by the rotating head-drum assembly. However, the media is not stressed as frequently as diskettes. Again there is also evidence for some hydrodynamic separation of the media from the head [46].

- (b) Hard discs invariably use a hydrodynamically separated media/slider interface with read or write operations taking place without contact. Although this separation is constantly being reduced to enable greater data densities to be achieved, it does not resemble the head/media interface in the floppy diskette drive where both heads are in constant and intimate contact with the media. In fact, the only times at which the hard disc and its associated head are in contact are at the power up and power down stages. When this head-media contact does occur, it is at tracks specifically constructed for this purpose and the media is not rotating at full speed (discussed later in this chapter). This is with the exception of accidental, and undesirable, "head crashes" when the slider lands on the media at some random point while the latter is rotating at its full operating speed of $3600 \text{ rev.min}^{-1}$.

The work reviewed in this chapter, in light of the above comments, has been categorised into three sections: floppy diskettes / hard discs, tapes, and a more general section which includes work on relevant and associated research. In addition to this it is necessary, initially, to review the general subject of tribology and to indicate the relevant theories here as well as the wear of

polymers.

3.1 Basic Principles of Friction and Wear.

This section deals with the fundamentals of the basic concepts of tribology: those of friction and wear. The different contributions to friction at the microscopic level and the different types of wear are considered. In these considerations, particular attention needs to be paid to the "elastic" and "plastic" forms of contact which are especially important in polymers and, therefore, also in floppy diskette friction and wear.

In considering each of the above, the different contributions to the friction and the type of wear are related to the specific case of floppy diskettes. It is then possible to indicate whether that particular concept is important in this context.

Before looking at the details, however, two experimentally determined fundamental laws of friction may be noted:

- (a) The force of friction between two bodies, F , is directly proportional to the normal load, L , applied in forcing them together. That is to say:

$$F / L = \text{constant} = \mu \quad (3.1.1)$$

where μ = coefficient of friction, by definition.

The coefficient of friction is a constant only under fixed material and environmental conditions; it is different between different materials and may be affected by ambient conditions.

- (b) The force F is independent of the apparent area of the mutual interface

between the two bodies. This law arises from the fact that when one body makes contact with another under a normal loading force, this contact occurs at the tips of their surface asperities. The loading causes these asperities to be deformed (flattened) until a sufficient area is in contact to support the loading. The sum of the microscopic areas making contact is the "real area of contact". This real area of contact is given by:

$$A_r = L / P_p \quad (3.1.2)$$

where P_p = critical pressure for plastic flow of the softer material.

Bowden and Tabor [47] developed this idea. In their case metals were considered and P_p was then the yield pressure of the softer metal as the deformation of asperities is plastic in nature.

In polymers, however, some of the deformation may be recoverable, that is elastic in nature. In the present project, deformation of the media's polymeric surface is caused by the very much harder ceramic materials and the magneto-resistive materials used in the construction of the head. The head is not expected to deform appreciably.

3.1.1 Friction in Polymers.

Friction in polymers can arise, essentially, from only two sources. One of these is the adhesion of the polymer, at an asperity level, and gives rise to the related concept of "real" and "apparent" area of contact. The latter is easily understood as the area which appears, macroscopically, to be in contact between two interacting surfaces; the former is the sum of the microscopic areas which make

actual contact at the interface and is usually very much smaller than the apparent area of contact. The other source of friction is that due to the deformation of the polymer under stress and is due to the relatively low bulk modulus of polymers. The deformation term in the friction may be further sub-divided into the contribution due to elastic and plastic deformation and that due to "ploughing" of the softer surface.

These contributions to the friction in polymers are normally termed the "adhesive" and the "deformation" components respectively.

- (a) The adhesive component: Considering the adhesive term first, the force of adhesion, F_a , between the polymer and the other interacting body is given by the familiar equation:

$$F_a = A_r \cdot s \quad (3.1.1.1)$$

where A_r = the real area of contact

s = the shear strength of the junction formed at A_r .

The real area of contact is as described above by equation (3.1.2) and the shear strength is an average value taken over the contacting asperities. One point to consider in the process of averaging over the microscopic asperity contacts is that when sliding occurs, some of the contacts are transient. As a result, the real area of contact is not as high as for the static case. This accounts for the lower value of kinetic friction compared to static friction.

The adhesion at the asperity contacts can have various components as discussed by Dickens [27] but possibly the most important of these are the Van der Waals' forces which exist between all

atoms. Van der Waals' forces are electrostatic in nature and are produced by transient dipoles in the atomic electron clouds. Electrostatic forces may also arise due to polarisation of certain interatomic bonds in the polymer such as those between Carbon and Oxygen due to the difference in their electronegativity (that is, affinity for electrons).

When sliding is caused to occur by a translational force parallel to the interface of the interacting bodies, the microscopic junctions comprising the real area of contact must be forced apart. That is to say that a force F_a of equation (3.1.1.1) is required to break the junctions.

Using the usual definition of the coefficient of friction as given in equation (3.1.1), the adhesive component of the coefficient of friction can thus be realised to be μ_a where,

$$\mu_a = F_a / L \quad (3.1.1.2)$$

Using equations (3.1.2) and (3.1.1.1), the equation quoted by Bowden and Tabor [47] is arrived at:

$$\mu_a = (A_r \cdot s) / (P_p \cdot A_r)$$

$$\therefore \mu_a = s / P_p \quad (3.1.1.3)$$

An important cause of adhesion in polymers is charging of the polymer due to the transfer of charge. This aspect has been discussed in Chapter 2 as described by Bhushan et al [29] for magnetic media. Bowden and Tabor [48] have observed this electrostatic effect with solid films deposited on a surface. If this film is then peeled off, very

large electric potentials can be produced. The charge separation causing these potentials can contribute to adhesive friction, particularly where non-conducting materials are used. In the case of magnetic recording, both the media and the read/write transducer are non-conducting. The addition of carbon black to the media's magnetic layer probably serves to reduce this electrostatic adhesion through charge dispersion over the whole surface. However, some electrostatic adhesion must remain as the charge is only delocalised not removed. The adhesive contribution due to the real area of contact formed by asperity deformation also remains.

Equation (3.1.1.3), however, cannot be quite correct for polymers as this area of contact has been assumed to be proportional to the normal loading force. This is substantially true in metals, provided that the loading is not exceptionally light. In polymers, however, there is considerable elastic deformation and the Hertzian relationship is more accurate [48]:

$$A_r \propto L^{2/3} \quad (3.1.14)$$

This elastic deformation leads to a hysteresis component in the frictional force.

- (b) The ploughing component: The ploughing component of friction may not be present until actual wear begins to occur. In this case, the wear is of an abrasive nature, as considered by Athwal [49] for metals. In polymers, ploughing may cause plastic deformation only rather than abrasive wear. This results in the displacement of material by the slider. This displaced material is then deposited to both sides of the slider's path producing a groove under the slider.

The occurrence of ploughing may be due to two different conditions. In the first case, the asperities of the harder material penetrate the softer material and cut material out of the former. In the second case, a body entrapped between the interacting surfaces may be found to do this due to increased stresses. The details of this mechanism of wear are discussed later in the specific context of polymeric media with reference to the results obtained. It may be appreciated here, however, that increased resistance to motion will be offered. Since the resistance to motion is a friction force, an increase in this force can be observed. The reasons for this increase are that a greater force is required to shear the chemical bonds as is necessary for abrasive wear. Furthermore, substantial material builds up in front of the abrader (whether asperity or third body) which has to be pushed aside in order for progress to be made. This built up material is often plastically deformed to a high degree in the process and requires more force to remove it.

This term in the friction force is very important and evidence for its importance has been found in this study. It has been found that an increase in friction has accompanied the formation of a ploughed track in the media. This is discussed in more detail later in Chapters 6 and 7 where all of the results are presented and discussed.

- (c) The hysteresis component: As mentioned above, the asperity deformation in metals is of a plastic nature but in polymers there is also a substantial elastic component because of the low elastic modulus of polymers [50]. Even on a macroscopic scale, evanescent tracks can be formed on polymeric materials' surface which disappear on elastic or visco-elastic recovery by the material. This means that the deformation component can be very important. In fact, adhesion between the ceramic of the head and the polymer of the magnetic media may

sometimes be less important than the deformation of the softer media except when the adhesion is due to such effects as electrostatic adhesion.

In considering the polymer deformation component of the friction, however, it must be stated that the details of the interaction are important in order to reveal the actual value of this component and may be different for each situation. In general, however, the diagram of Fig. 3.1 reveals the origin of this term.

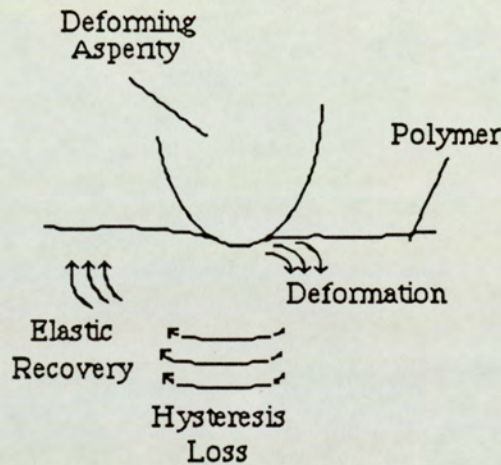


Figure 3.1 The deformation component of friction in polymers.

Unlike the μ_a term, the hysteresis factor has its origin in elastic deformation of the polymer. Here the interacting body deforms the polymer elastically ahead of its contact as can be seen from the above figure. This stores energy within this region of the body of the polymer material. However, that region of the polymer which is behind the deforming body experiences relaxation through elastic recovery, since it is no longer being stressed. This tends to propel the deforming body forwards. The key point here, however, is that the

amount of energy released through elastic relaxation is less than that input during deformation. The loss of energy to the polymer means that the deforming body tends to continually lose energy and a translational force is required to keep it in motion.

Briscoe [51] has considered the elastic work done in deforming polymer materials. If W is the work done by a slider in unit distance of sliding in deforming the polymer, then the energy lost in the hysteresis process is some fraction proportional to W such that:

$$F_d = \alpha W / r \quad (3.1.1.5)$$

where F_d = Deformation component of the frictional force
 r = distance slid by slider = 1, for unit distance of sliding

It is reasonable to consider that this lost energy is gained by the polymer and can cause a rise in its temperature. The implications of this rise are very important and will be discussed in the context of the floppy diskette later. The energy is provided by the external work done in sustaining the motion, that is in overcoming the friction. The amount of work (αW) is done by the friction force in unit distance, as indicated by equation (3.1.1.5).

It may be shown that for a spherical hard body deforming the polymer with a normal loading L , the work done per unit distance is a complex function of various parameters related to the polymer and the hard body. Briscoe [51] has shown the relationship to be:

$$W = 0.17 L^{4/3} R^{-2/3} (1 - \nu^2)^{1/3} E^{-1/3} \quad (3.1.1.6)$$

where R = radius of deforming body
 ν = Poisson's ratio for the polymer
 E = Real part of Young's modulus for polymer

Thus, assuming spherical asperities, it is possible to quantify F_d if α is assumed. α can be as high as 0.35 for high loss polymers such as some rubbers [51].

More practically, the friction force may be measured. It can be reasonably expected that adhesion between such dissimilar materials as the polymers in the magnetic media and the ceramic of the head would be less than for a metal-metal interface. For this reason, a significant contribution to the friction can be expected to be due to the deformation term. Thus the total friction force, F_t , is:

$$F_t = F_d + F_a = (\mu_d + \mu_a).L \quad (3.1.1.7)$$

where μ_d = deformation component of the friction coefficient.

Using this the work done on the polymer may be quantified.

Equation (3.1.1.7) may be violated, if the polymer is penetrated either by the asperities of the hard deforming body or by a third body coming in between them. Either situation can lead to the removal of material through a cutting action causing ploughing wear: this an important phenomenon and is discussed below.

3.1.2 Wear of Polymers.

There are various mechanisms which are responsible for wear and each has its own characteristics. These different mechanisms of wear are discussed below

and each is discussed briefly in relation to floppy diskette media.

- (a) Abrasive wear: Probably the most familiar form of wear, it usually occurs when a harder body cuts through a softer one. For this type of wear to take place, plastic deformation of the abraded surface must occur.

According to Halliday [52], plastic deformation of the softer body occurs at some base angle, θ , of the abrading body where:

$$\theta = C (H / E) (1 - \nu^2) \quad (3.1.1.8)$$

where $C = \text{constant} = 1$, for initiation of plasticity

$H = \text{Indentation hardness of the polymer (directly related to plastic flow pressure)}$

$E = \text{Young's modulus for polymer}$

$\nu = \text{Poisson's ratio for polymer}$

Furthermore, Greenwood and Williamson [53] have suggested that plastic deformation only occurs when the value of the plasticity index, Ψ , that they have define is unity or greater. They define Ψ such that:

$$\Psi = (E/H) (\sigma_p / \beta_p) \quad (3.1.1.9)$$

where $\sigma_p = \text{standard deviation of the asperity peak heights}$

$\beta_p = \text{mean radius of these peaks}$

Once the conditions of equations (3.1.1.8) and (3.1.1.9) are

satisfied for abrasive wear to occur the rate of wear, volume removed per unit distance travelled by the slider, is defined by the equation used by Rabinowicz [54]:

$$dV / dr = k (L / H) \tan \theta \quad (3.1.1.10)$$

where r = the distance travelled by the slider

k = constant reflecting the fact that only a fraction of the polymer being deformed actually becomes wear debris

Skelcher [50] and Dickens [27] have concluded that θ must be of the order of 5° to 10° for abrasive wear to occur in polymers. This compares with 1° for metals. Angles as large as this are encountered only on very rough surfaces such as abrasive papers which have roughnesses of $12 \mu\text{m Ra}$ or greater [50]. The reason for this order of magnitude difference in the base angle of the abrading asperity, as compared to metals, is that the Young's modulus for polymers is very much lower than metals and results in their capability to take very much greater loading stress through elastic deformation.

The wear of polymers by abrasive papers has been considered by Ratner et al [55] and they arrived at an expression for the polymer wear rate in terms of the properties of the polymer:

$$dV / dr = (\mu L) / (H S e) \quad (3.1.1.11)$$

where μ = Coefficient of friction

S = Ultimate breaking strength of the polymer

e = Elongation at fracture; it is the fractional increase in length

The important parameter in this equation is the product (Se) as this relates closely to the work done in reaching the fracture point from the initial disturbance of the material. Lancaster [56] has also observed a correlation between polymer wear rate and $(1 / Se)$.

In concluding this part, the above needs to be considered in relation to the magnetic media used:

- (1) In the special case of magnetic media, the above described two body abrasive interaction is not important as the head is very smooth compared to the roughness of the abrasive paper described. In this case, fatigue wear would be expected to play a larger role in wear. However, any third body introduced at the interface, either from environmental sources or wear debris, may cause abrasive wear.
- (2) It is important to note that the filled polymer nature of magnetic media makes them hard compared to the polymers considered in the studies by Ratner et al [55]. This means that media surfaces require a non-trivial treatment. This results from sub-surface activity needing to be considered at a much more fundamental level.
- (3) The active layer of the magnetic media consists of a co-polymer, as described in Chapter 2, one phase of which is crystalline and the other amorphous. This affects the value of the modulus, E , of the whole structure as discussed for partially crystalline polymers by Bush [57]. He has assigned the symbols E_c and E_a to the crystalline and amorphous parts of E respectively. E_a is said to operate above the glass transition temperature, T_g , and E is close to

E_C below this transition. The effective value of the modulus may be calculated if the fractions of crystalline, f_C , and amorphous material, f_a , are known. Bush [57] quotes:

$$1/E = (f_C / E_C) + (f_a / E_a) \quad (3.1.1.12)$$

It can be appreciated that

$$E_C \gg E_a \quad \text{and} \quad f_a = (1 - f_C)$$

so,

$$E \approx E_a / (1 - f_C) \quad (3.1.1.13)$$

This is clearly non-linear with respect to the crystalline fraction and so the wear properties of the media can be expected to depend similarly on the polyurethane-polyester mixing ratio in the binder.

- (4) Although wear of the polymer is important in magnetic media, the wear rates are usually negligibly small. The surface deformation caused by plastic flow is used as the criterion for discarding samples and little real wear, in fact, occurs. Any wear of the thin magnetic coating which does occur tends to lead rapidly to catastrophic failure and no rates of volume of material removed can be, or need be, measured.

The metal oxide fillers found in the magnetic coating are very hard and tend to cause abrasive wear of the heads. This matter of hard fillers causing wear has been addressed by Anderson [58]. He reported the abrasivity of different fillers on brass balls and concluded from his study that the fillers can roughen the

counterface by their abrasive action. Clearly in the case of magnetic media, a roughened head can then cause ploughing wear of the media and so this is an important observation.

- (b) Erosive wear: This occurs when the surface is bombarded with projectiles which cause wear through a cutting action. On an atomic scale this may be found in the field of surface analysis where beams of ions or atoms are employed as projectiles to remove the top layers of the sample under investigation. This is not important in diskette wear under normal use. Fluid erosion can also occur, for instance when slurries are pumped through plastic conduits
- (c) Corrosive wear: If the wear interface is a material which is reactive, then corrosive wear is possible. Under these conditions, the exposed surfaces may form, for example, oxides on a metal surface in oxidational wear. Another form of corrosive wear results from reactive additives causing chemical corrosion when they react with the lubricated surfaces. This mechanism is not thought possible in magnetic media where, although liquid lubricants are employed, care is taken to utilise relatively inert substances.
- (d) Adhesive wear: Adhesion at the polymer/conterface mutual interface may be imagined to lead to wear if the shear strength of the junction is greater than the shear strength of the bulk material. This is, however, difficult to imagine under any regime and it would be more likely that the bulk property may become reduced in time such that it is then less than that of the adhesive junction. This reduction in the bulk shear strength may occur through a fatigue process.
- (e) Fatigue wear: Wear through a fatigue process may be caused by repeated loading of a single point resulting in sub-surface damage and occurs during cyclic stressing. One such mechanism of wear is that of

delamination whereby thin flakes, or laminae, of material are removed due to a similar process to that described here; details of this process are discussed later in the present chapter.

3.2 Lubrication.

Lubricants are usually employed to achieve either one or both of two aims: to reduce the frictional force and to reduce the rate of wear. In the case of diskette media, it will become clear later, the reduction of friction is important. In fact, as mentioned earlier, two lubricants are used in flexible magnetic media.

Described here are the different regimes of lubrication associated with the four different regions of the familiar Stribeck curve [59] which is illustrated in Fig. 3.2. The diskette media is considered in relation to the various regimes illustrated there and discussed below.

3.2.1 The Stribeck Curve.

The Stribeck curve plots the dimensionless parameter known as the "Bearing Number" against the coefficient of friction. The bearing number (**BN**) is defined by the equation:

$$BN = (\eta v) / P \quad (3.2.1.1)$$

where η = viscosity of the lubricating fluid,
 v = relative sliding speed (in rev.sec⁻¹),
 P = pressure due to the loading of one body against the other.

The curve was originally produced for journal bearings and studied in

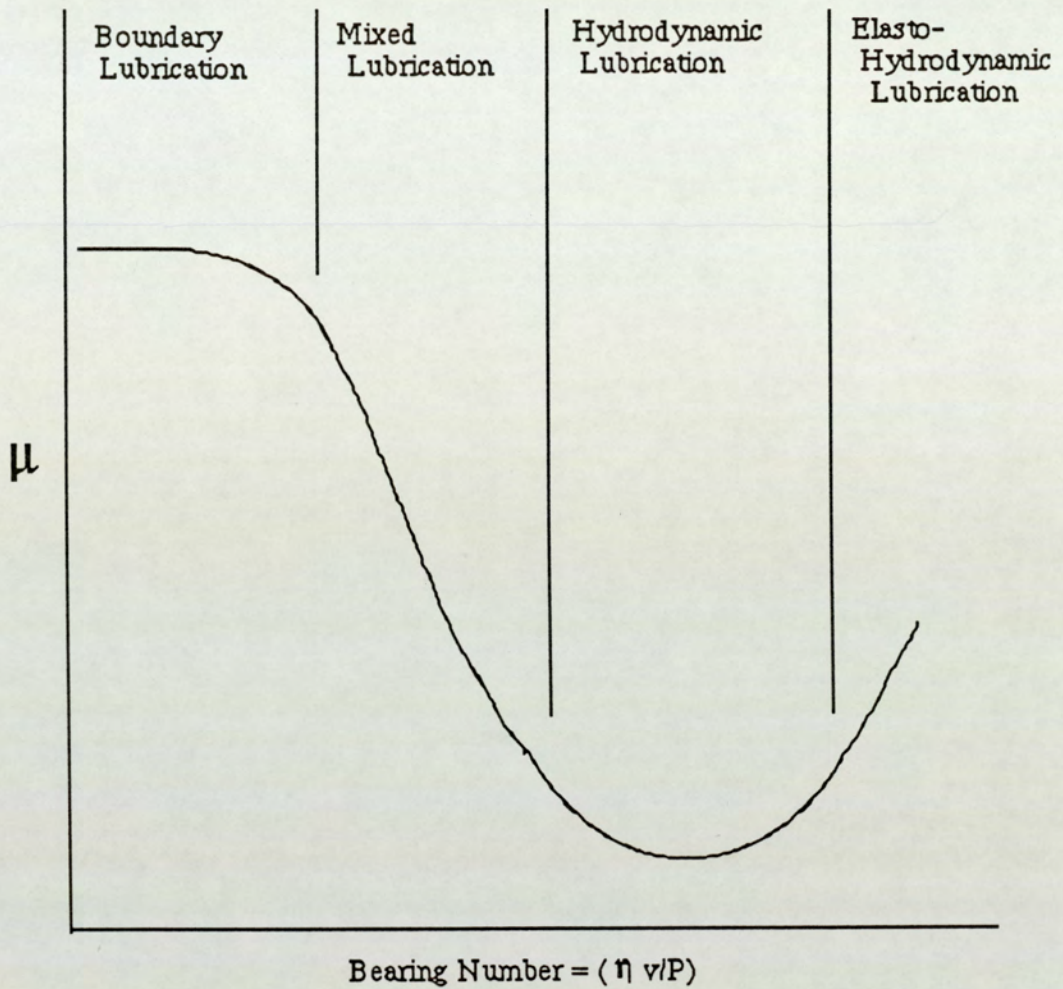


Figure 3.2 The Stribeck curve showing the different regimes of lubrication.

the context of this metal-metal interface. Since then, however, the general shape of the curve has been found to be much more generally applicable. An example of this for magnetic media is Skelcher's work [60] where he has measured friction forces for different head-media interface conditions. This has enabled the determination of the lubrication regimes under which floppy diskettes operate.

Looking at the Stribeck curve in more detail reveals that this plot shows the existence of four distinct regions. Each one of these corresponds to a different regime of lubrication. These regimes have been individually identified

on the curve of Fig. 3.2 and are described below in terms of the lubrication regime that each describes:

- (a) Hydrodynamic (or fluid-film) lubrication: At the highest bearing number values this regime of lubrication is found to operate and is often a result of low loading or high speeds. This is illustrated in Fig. 3.3 overleaf and, as can be seen from there, entails complete separation of the two surfaces by a "wedge" composed of the lubricating fluid.

The wedge is formed such that the fluid at the entry point is at a lower pressure than the exiting fluid. This maintains the separation of the two surfaces to an extent which depends on the relative speed of motion and the viscosity of the fluid.

The friction force in this case is provided by the force required to shear the fluid film of lubricant and rises, as can be seen from the Stribeck curve, for increasing bearing number. The reasons for this are obvious as, for example, if the fluid viscosity is increased, then a greater force would be required to shear the lubricant film. Also, if the relative speed of motion of the two surfaces is increased, then a higher frictional force results as a consequence of the resistance of the fluid to more rapid shearing. Equally, if the vertical loading is reduced, a larger body of fluid must be sheared. In fact the friction force depends on the viscosity of the body of fluid sheared and the rapidity of shearing as described by Petroff's law. Applied to journal bearing, the law states that:

$$F = 2\pi R l \eta v / c \quad (3.2.1.2)$$

where F = frictional force

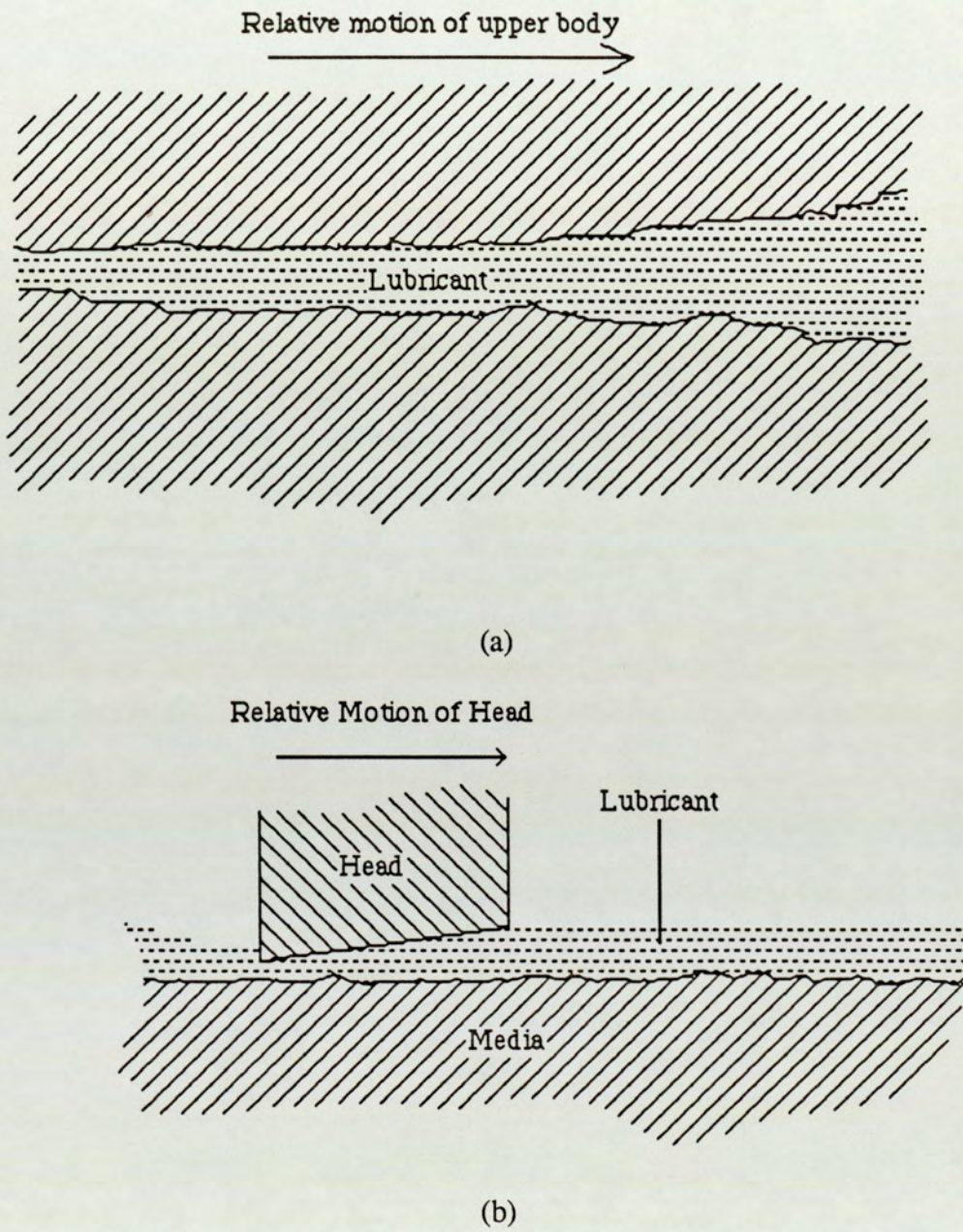


Figure 3.3 The process of hydrodynamic lubrication (a) for a polymer-polymer interaction and (b) as expected for the head-media interface.

R = radius of journal

l = length of journal

η = viscosity of lubricating fluid

v = relative speed of journal

c = thickness of fluid film.

This may be applied in general as some of the terms in equation (3.2.1.2) may be replaced by more relevant terms. This produces the equation:

$$F = A \eta .v / c \quad (3.2.1.3)$$

where A = overlap area of the interacting bodies.

No appreciable hydrodynamic lift is believed to occur in floppy diskette media in normal use despite the common misconception in popular scientific literature such as the report by Hall [61]. In fact, as described in the introduction to this chapter, computer tape often operates under this lubrication regime as do hard, or rigid, discs as used in the common "Winchester" drives; in both cases, computer tape and Winchester disc, the lubricating fluid is air under this regime, the mobile part (the tape and Winchester drive's head) is said to be experiencing hydrodynamic "flying". If the loading becomes slightly too high then, especially in the case of polymers which are relatively easily deformable, the regime of lubrication becomes "elasto-hydrodynamic".

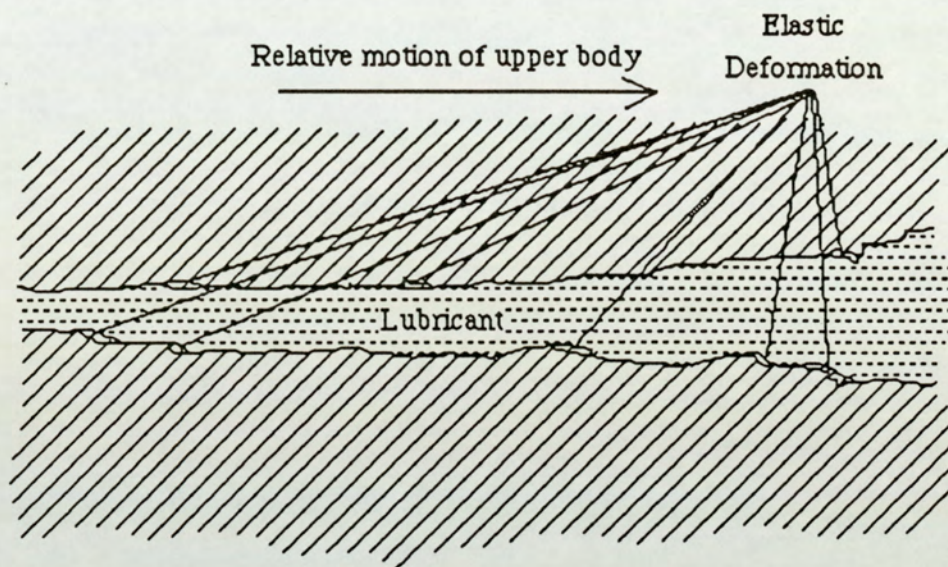
- (b) Elasto-hydrodynamic lubrication: This regime of lubrication still maintains complete separation of the two surfaces involved but elastic

deformation of one or both of the surfaces occurs due to the stresses imposed. The reduction in the value of the bearing number, compared to the hydrodynamic regime, is normally caused by increased loading. The loading stresses are transmitted through the fluid and are responsible for the surface deformation. As mentioned above, this deformation is relatively readily achieved in polymeric materials and so this regime of lubrication is often to be found. The physical nature of the interface is illustrated on the following page in Fig. 3.4

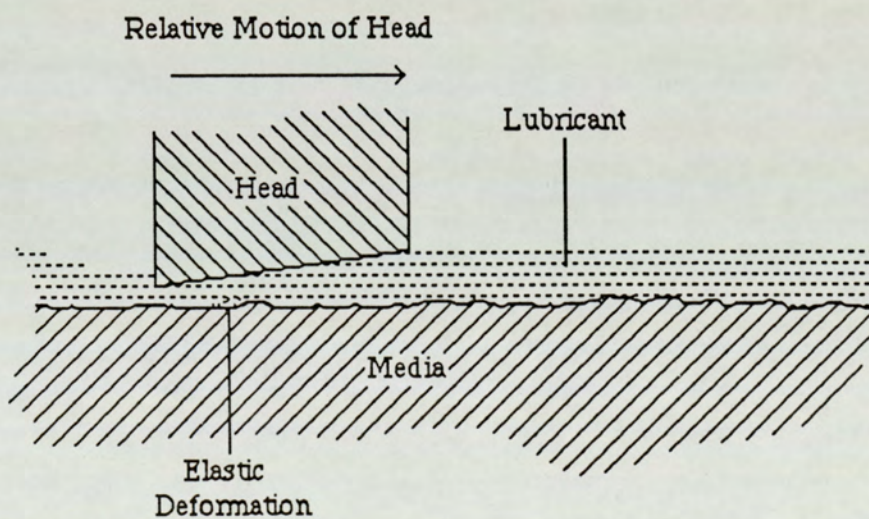
Since deformation of the polymer occurs, this tends to have the effect of distributing the stress imposed on the lubricating fluid film which then does not need to be sheared as much as happens in fully hydrodynamic lubrication. The increase in loading also increases the fluid viscosity resulting in an increase in the frictional force. Naturally, this form of lubrication, as with the closely related hydrodynamic regime, requires large amounts of fluid to be available. Such large quantities are not found on the surface of floppy diskette media and so this regime is not found to be operating.

- (c) Mixed lubrication: If the loading is increased further, or the relative speed is reduced, then the regime of lubrication changes to that of a "mixed lubrication". Under this regime the lubricating film found in the two regimes described above is penetrated. This results in parts of the interface being separated by only a molecular layer. Furthermore, complete penetration of the lubricant can occasionally occur resulting in direct contact between the two bodies. This contact can in turn produce wear of either of the two surfaces.

This regime is illustrated in Fig. 3.5 and is found to be operating under certain conditions at the head-media interface for floppy diskettes.



(a)



(b)

Figure 3.4 The nature of the elasto-hydrodynamically lubricated interface (a) for a polymer-polymer interface and (b) for the head-media interface expected.

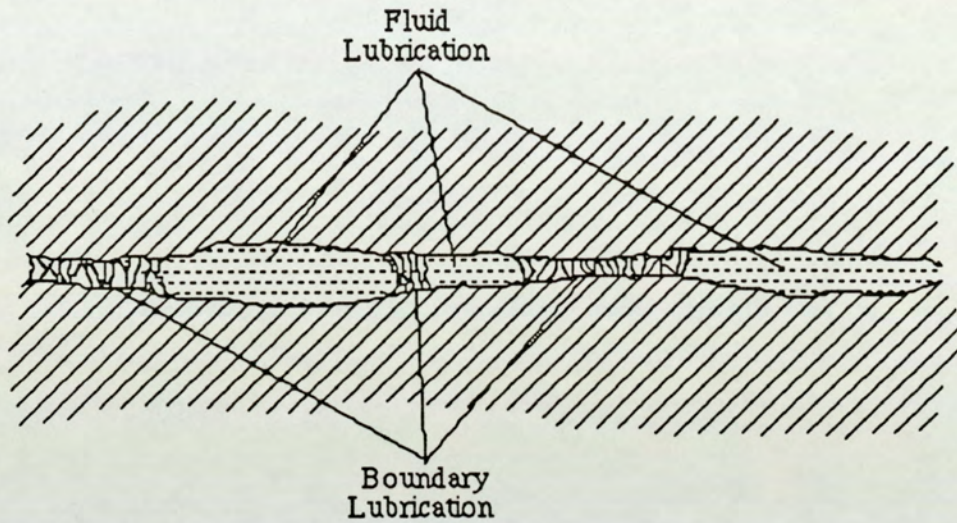


Figure 3.5 Mixed lubrication means significant penetration of the lubricating film.

- (d) Boundary lubrication: This type of lubrication occurs at low values of the bearing number, which may be achieved by any of the following: a low value of sliding speed, low lubricant viscosity, or a high loading pressure. In fact, it is commonly a combination of all of these individual factors.

Under this regime the lubricant is adsorbed either through a chemical action, "chemisorption", or through a physical mechanism, "physisorption", or (more usually) a combination of the two, onto the surfaces of the two interacting bodies. This physisorbed and chemisorbed lubricant forms a molecular layer which, under ideal circumstances, physically separates the two surfaces. In addition to forming a molecular layer, the lubricant can migrate into the sub-surface layers of the interacting bodies. In the case of polymers, this

lubricant migration often does occur. The lubricant which is then resident in the sub-surface region of the polymer can be important in diskette lubrication. The bulk lubricant mentioned in the last chapter is situated below the surface and operates from there.

The larger asperities on the surface can break through the boundary layer and asperity contact can take place between the two surfaces although the intention of boundary lubrication is to keep these surface separated.

As can be seen from the Stribeck curve, the coefficient of friction in boundary lubrication remains virtually constant. The reason for this is that μ is dependent on the shear strength of the molecular layer of lubricant film and those few asperity contacts which are formed. Thus, so long as the penetration of the mono-layer remains similar for changes in the bearing number, the value of μ should remain similar.

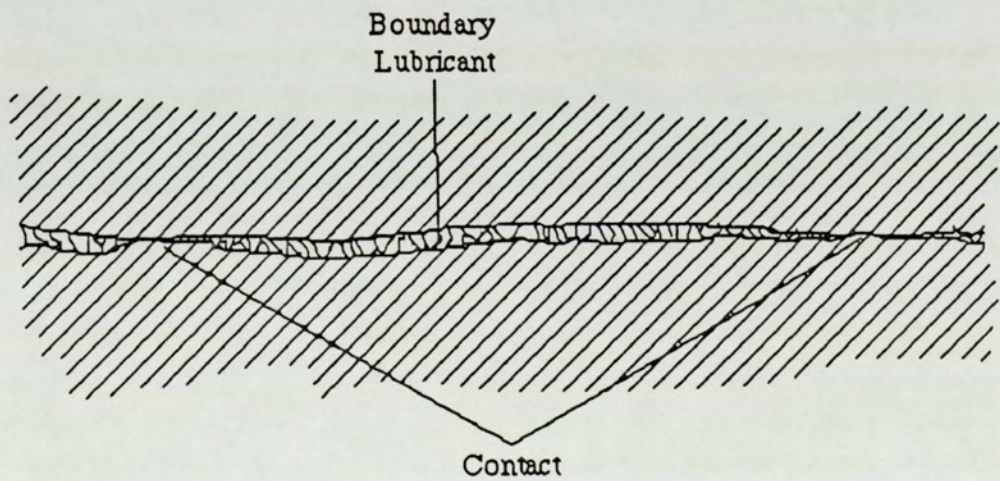


Figure 3.6 Boundary lubrication of interacting surfaces.

The boundary lubricated situation is illustrated in the schematic diagram of Fig. 3.6.

The lubricants used in boundary lubrication are often of the polar organic chain type and in metal-metal tribological interfaces this results in the electrostatic adhesion of such molecules to the surface with the molecular chains pointing away from that surface. In polymers similar results may be observed but the picture is complicated by the fact that electrostatic adhesion is less pronounced. In polymers, there is a tendency for the lubricant to be absorbed into the sub-surface as has been described earlier.

Work carried out on 3M floppy diskettes by Skelcher [60] has shown that the regime of lubrication operating on the two heads in a diskette drive is different with the side 1, or upper, head operating predominantly under Mixed Lubrication whereas the side 0 head, which experiences much greater stress, operates under boundary lubrication conditions. In fact, he has found that the side 0 head may be found to operate at the extreme end of the boundary region of the Stribeck curve towards higher bearing numbers.

Regardless of the regimes of lubrication which operate, the nature of the lubricants can be important. The exact nature of the lubricants used in magnetic media are discussed in later sections where different media are also considered.

The reasons for the difference in the lubrication regimes of the two heads may be two-fold. The first is that the side 1 head is free to move both perpendicular to and, to a limited degree, parallel to the diskette surface. As a result, it does move away from the the media surface if forced to do so. In contrast, the side 0 head is fixed and not able to move in any direction. As a

result, it experiences greater stresses especially in light of its greater consequential penetration into the plane of the media: the nature of the head-media interface makes this clearer as shown in Fig. 2.9. The second reason may be that the construction of the two heads is completely different with the side 0 head having a flat circular surface and the side 1 head having a catamaran type dual rail structure. This results in different areas of contact being exposed to the media.

In fact, Skelcher's work [60] used different values of the parameters of relative speed and head penetration into the plane of the media and he has shown that it is possible to operate the side 0 head under mixed lubrication conditions. This, however, tends to reduce the magnetic signal obtained as it entails reducing the side 0 head penetration. This results in the head being physically moved away from the media. Moving this head away can also result in increased wear rates as more contact is obtained through greater compliance of the media to the head topography. This greater compliance is a consequence of the removal of the "side 0 bubble" illustrated in Fig. 2.9. As will be seen from there, the removal of the "bubble" causes the media to make contact with more of the side 0 head's surface. Furthermore, the side 1 head which is normally forced up as a result of the formation of the bubble also becomes lowered and more contact with the media then results at both head-media interfaces.

Clearly, the side 0 bubble is an interesting and necessary feature. For this reason, it deserves some discussion. As Fig. 2.9 shows, the side 0 head is positioned such that it penetrates into the plane of the media, this penetration is usually about 0.5 mm. As a result, the rotating media has to rise upwards on approaching the heads. The curves, or "blends", at the leading edges of the side 0 head aids the media to rise. However, the media is not sufficiently flexible to follow the curve and continues to rise. No air can enter the bubble region at the leading edge of the side 0 head due to this edge being in full contact with the media. However, air is removed due to the motion of the media towards the

trailing edge of this head. A low pressure region is thus developed. The media is caused to "snap" down onto the head further down due to this pressure differential and the side 1 head. The media then exists at the trailing edge aided by the exit blends. These blends are provided to prevent excessive ploughing wear.

3.3 Floppy diskettes and hard discs.

Much of the earlier work on the tribological aspects relating to magnetic media was done on hard discs and is not directly relevant but some ideas on lubrication and contact-start/stop, applied to hard discs and tapes are of relevance. For this reason they will be discussed here. Similarly the work done without using Winchester type sliders, that is, where no hydrodynamic separation occurs, is also of relevance despite not exactly representing the same head-media interface as that encountered in the system studied for this project. The interesting features are those such as the response of the magnetic layer's polymer binder, γ -Fe₂O₃, alumina head cleaning agent etc. to changes in parameters such as the loading and relative speeds of sliding.

One such investigation was carried out by Talke and Su [30] where a study has been made of the wear caused on steel balls which were placed in contact with moving magnetic media. This study used steel balls specifically to prevent hydrodynamic separation of the probes from the hard disc used. In looking at the wear of the media, they found that at low loads (less than 0.1 N, diskettes are loaded by a head loading force of 0.2 N) and relative speeds (below 1.25 m.sec⁻¹) no appreciable wear occurred in 10³ passes of the abrader over the same point. The wear of the slider, however, was seen to increase monotonically with both parameters. This obviously has important implications for the heads used for magnetic recording.

The rate of media wear was found to increase, however, as speed was

increased and "complete breakdown" of the media was observed to occur when the tests were prolonged. The wear of the media is an important factor affecting the read-back signal. As part of the same study, Talke and Su [30] investigated the wear dependence of the read-back signal for media wear caused by an alumina probe. A wear track of width slightly greater than the read/write core of the head was created. This track, and an unworn one, were then written with square waves. The read-back signal from the worn track showed a reduction of approximately 28% in peak-to-peak amplitude due to an effective increase in the flying height of the M-R head slider causing a spacing loss. The signal is also reduced due to the reduction of the thickness of the magnetic layer at the worn track and consequent reduction in material to give a remanent magnetic field: Fig. 3.7 below illustrates why this occurs.

For the present project, diskette drives designed for diskettes with a track density of 48 tracks per inch (48 TPI) were used. Of the 40 concentric tracks on each side of the media, track 16 is the reference track and is located at a

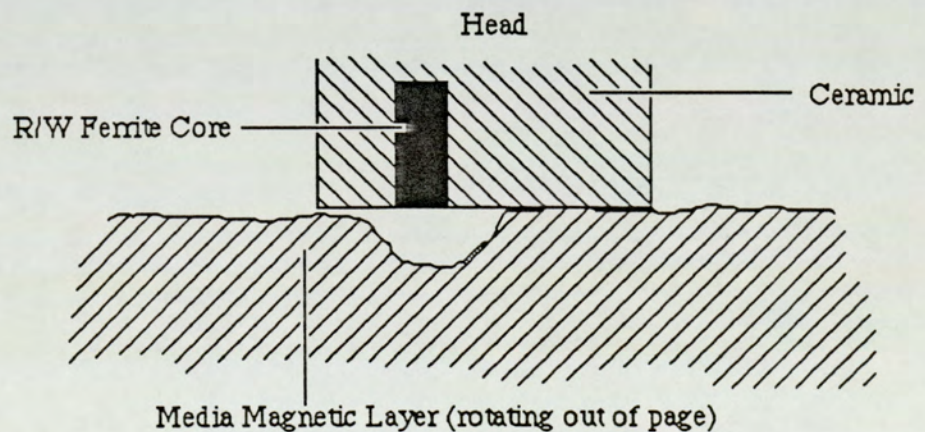


Figure 3.7 How a worn track implies loss of signal through spacing loss and a reduction in the amount of material remaining to record the data.

radius of 1.9167" = 48.684 mm [45]. From this it may be noted that the outermost track, track 0, is located at a radius r_0 such that:

$$\begin{aligned} \text{Radius of track 0} = r_0 &= (1.9167 + 16/48) \times 25.4 \\ \text{so, } r_0 &= \underline{57.151 \text{ mm.}} \end{aligned} \quad (3.3.1)$$

and for track 39, the innermost track at a radius r_{39} :

$$\begin{aligned} r_{39} &= (1.9167 - 23/48) \times 25.4 \\ r_{39} &= \underline{36.513 \text{ mm.}} \end{aligned} \quad (3.3.2)$$

Thus, for an angular frequency of $f = 300 \text{ rev.min}^{-1} = 5 \text{ rev.sec}^{-1}$, the relative speeds at the two tracks may be calculated as this speed at some track t is:

$$v_t = \omega \cdot r_t \quad (3.3.3)$$

where ω is the angular velocity and $\omega = 2\pi f$.

r_t = radius of track t

v_t = relative speed at track t

Therefore,

$$v_0 = 1.795 \text{ m.sec}^{-1} \quad (3.3.4)$$

$$v_{39} = 1.147 \text{ m.sec}^{-1} \quad (3.3.5)$$

Thus, since the loading in the diskette drives is greater than that required for wear initiation, and the relative speed between head and media even at track 39, the innermost track, is close to 1.25 m.sec^{-1} , one would expect wear to occur.

In fact, all of the tests have been carried out on track 20 of the media as it is the directory track and, therefore, most frequently accessed. Also, it displays median head-media relative speed:

$$v_{20} = 1.463 \text{ m.sec}^{-1} \quad (3.3.6)$$

so that wear should definitely be expected considering the results of the study by Talke and Su [30] reported above.

Another investigation in respect of loading and speed was made by Stromsta and Egbert [26]. This study was made in order to determine the performance of diskette drives rather than media durability. The head to diskette compliance was investigated with the drive performance as the important factor. Of course, the nature of the media will also affect compliance - its flexibility will be an important factor in this and it can be seen that the nature of the head media interface thus formed will also determine the durability of the media. The study of compliance, showing how the heads in a double-sided drive interact with the media, points out the existence of, and variation with speed and load of, a "bubble", the side 0 "bubble", as shown in Fig. 2.9. This study also showed, as described earlier, that the bubble has negative pressure (and is formed by a lack of flexibility in the media) and that the media snaps down onto the head further downstream. As a result of the bubble phenomenon, the contact that the media forms with the side 0 head is greater than that with the side 1 head. This may explain the fact that the side 0 of the media is almost invariably the first to wear. Also, the motion of the diskette away from the side 1 head leads to less interaction with its edges.

The one thing to note is that the work done by Stromsta and Egbert [26] was consistently at higher speeds than in a drive in normal use and, so, it is possible that the study does not relate as accurately as it might to the in-situ wear.

Another investigation on the design of diskette drives and the influence on wear of media was undertaken by Green [63]. He discussed the causes of media wear: *viz.* load/unload tapping wear and abrasive wear. The former is caused by repeatedly loading the magnetic heads onto a particular track and then unloading it again before reloading. The latter, abrasive wear, is caused by the "permanent" loading of the head onto a particular track of the media which rotates as under normal read/write operation. Suspicion of a third contribution to the causes of wear was reported: the collision of the two heads in use. There is a complete absence, as in other studies, of any study of the mechanisms of wear initiation and propagation.

Another dimension to the study of the influence of the load and/or speed on wear was added by von Behren [64] who employed accelerated techniques to wear diskettes on specially designed rigs. An attempt was made to study phenomena such as the formation of wear tracks by sliders, which might reveal a mechanism of wear. No conclusions were reached on the latter, however. One of the problems with this study was that unreal sliders, the bottoms of glass test-tubes, were used and films of polymer were seen to accumulate on the slider after as little as a few seconds! Another problem was that the inertial loads applied were high even if the nominal loading was similar to that found in diskette drives.

The use of glass sliders is wrong because there is a possible chemical interaction between the slider material (especially the Sodium in the Pyrex glass) which may lead to a different mechanism of wear to that occurring in the real environment where ceramic heads are used. The essence of the problem is that the surface of glass tends to present free radical type entities which, under normal atmospheric conditions bond with, for example, Oxygen in the atmosphere. However, in the case of the test-tubes acting as abraders on the media, the place of the bonded atmospheric contaminant atoms may be taken by the active groups of the polar molecules in the diskette's lubricants to form soapy materials after

reaction with the Sodium. The wear polymers thus formed can be expected to complicate the picture considerably. They may change the distribution of stresses which are placed on the media surface by the head.

The other problem, that of high inertial loading, was not addressed by von Behren [64] in his study. If the body loaded onto the media is not permitted to follow the undulations of the media, or any run out of the supporting platform, then very large forces are developed at the interface. These forces then rapidly produce wear scars under conditions which are unrealistic compared to those prevailing in the diskette drives. Before being used for the work presented in this thesis, the rigs were modified to overcome this difficulty.

Nevertheless, load/speed results obtained by von Behren [64] showed that there was little effect on wear rates for a constant distance travelled for speeds between 1 and 10 rev.sec⁻¹ (drives: 5 rev.sec⁻¹) leading to the conclusion that the speed of the slider is not a significant factor. It can reasonably be said that until the slider begins to exhibit some degree of flying through hydrodynamic separation from the media, the effects of relative speed may be neglected. Once hydrodynamic separation occurs, a decrease in wear rates can be expected. Similarly, no measurable difference was noticed in wear rates for loads of up to 0.1 N (drives loaded at 0.2 N). Once again the prevention of hydrodynamic separation can be used to explain the fact that no decrease in wear was detected. However, in explaining the fact that wear did not increase either, the nature of the interface must be considered. The usual concept whereby increased loading causes increased wear through an increased real area of contact may not apply here. The reason for this may be that the increased loading may still cause only elastic deformation resulting in hysteresis friction rather than in an adhesive mechanism. As a consequence the amount of material transferred may remain unchanged resulting in no appreciable increase in the wear being observed. Another factor is that the inertial loading is so high in von Behren's work [64] that the relatively small nominal loading forces make no difference to the wear

rate. So, a change from 0.1 N to 0.2 N is negligible compared to the inertial load.

One other interesting factor mentioned by von Behren [64] was that concerning the penetration of the slider which occurs in drives for the side 0 head [26]: this may be seen illustrated in Fig. 2.9. In his work, the test-tube was not pushed too far into the plane of the diskette as the two dimensional head contact model for tapes applies here. Details of the model may be found in literature [64] but basically, it says that if the radius of curvature of the abrader is different to the wrap angle of the media, then different parts of the abrader are worn depending on the exact relationship of the two profiles. Equally, since different parts of the abrader make contact with the media, different wear rates for the media may also be expected with different penetrations. For example, if the penetration is large, the sharp edges of the head slider may be expected to cause ploughing wear of the media. However, the fundamental problems of the glass sliders still apply to all of this study.

As has been pointed out by Chiou [65] the issue of whether any media separation from the magnetic transducer occurs at the speeds encountered in the drives is contentious. A study was made of penetration and relative speeds to discover how these parameters affect the wear of the media. It should be noted, however, that, as was done by von Behren [64], the head is replaced in the drives by glass abraders: this time plano-convex lenses of a similar contour to that of the head were used. Although the more realistic profile of the head in this case leads to a better test than using test-tubes, the chemical interaction between the glass and the polymers of the binder and lubricants would still be expected to be the same. For this reason, the compliance of the media is the only true observable here and information regarding the durability and wear mechanism aspects can not be reliable as wear polymers are again likely to be formed with the glass heads. The other point to note is that the single sided drives used are expected to show

different patterns of wear as the side 1 head is replaced by a soft felt pad and the side 0 head is smaller than in a double-sided drive. These investigations were carried out at relative speeds varying between 80 and 600 rev.min⁻¹. It was reported that the penetration of the head and the loading of the pad act in different ways. The head penetration (since the head contour is spherical) tends to give non-uniform force distribution on the spinning diskette; the pad gives a more uniform loading distribution. At lower speeds the diskette complies well to the head and there is little flying (possibly resulting in more wear through increased contact) but as the relative speed is increased, the system exhibits hydrodynamic lubrication to the degree of forming the side 0 bubble of Fig. 2.9 as discussed earlier. This can lead to reduced compliance and, by implication, less wear. The flexibility of the diskette was said to be important for durability when the bubble forms. This can be appreciated as significant amounts of flexing in the media are involved. This continual flexing and unflexing may cause fatigue fractures in the media. This is likely to happen more rapidly with reduced media flexibility.

Most of the reports discussed so far have concentrated on loading and relative speed at the abrader-media interface. The last report has, however, also looked at the media to slider compliance. This is obviously a very important area for investigation, as a lack of compliance can lead to data loss simulating a false "worn/faulty media condition". The reports which look at compliance tend to use glass sliders or discs in order to enable observations to be made by optical means such as interference fringes to determine the degree of separation and positions of contact on the head. In the case of glass sliders, chemical problems can occur as discussed above and glass discs are too smooth to represent a realistic picture. The glass discs are also rigid, not flexible, and are usually employed in the simulation of Winchester discs for the study of flying characteristics of

Winchester type sliders. This may be a more accurate reflection of reality.

One investigation which reported using this technique combined with white light interferometry was by Lin and Sullivan [66] where both glass disc and glass slider were used for a hard disc application.

A very interesting set of reports were those concerned with the friction and/or lubrication at the head-media interface. This concerns the surface of the media and surface analysis techniques are often employed to study the surface before and after wear. These techniques are described more fully later in the chapter on instrumentation, Chapter 4.

The problem of friction and wear was illustrated for a hard disc in the work done by Weiss [32] who noted that heating due to local friction may be reduced by the use of boundary lubricants. It was also reported that although both the lubricated and the unlubricated disc initially showed a fall in the coefficient of friction with temperature, at about 125 °C the unlubricated disc showed an almost vertical rise in this coefficient whereas that of the lubricated sample continued to fall. The unlubricated one was thought to have been worn away to such an extent that the magnetic coating had been penetrated by the probe. This may be due to plastic flow of the polymer. This increase in μ may be taken as an indicator of wear initiation and was recognised as such by Bengal and Boyles [67] who have suggested the use of a transducer to measure the dynamic friction and normal forces to detect when the media begins to wear. This idea has been used with great effect in a specially constructed rig which has been employed in part of the work carried out for this project. A chemical method of showing the worn area was suggested by Anderson and Yen [68] whereby a solution of Potassium ferricyanide doped with Copper is poured onto the media surface. Any iron in the form of its oxide, Fe_2O_3 , turns the solution a distinctive blue colour.

The authors have suggested that this reaction could only occur where

Fe_2O_3 particles had been revealed at the surface due to the removal of the binder polymer through wear of this polymer.

Anderson and Yen [68] further suggested that the technique described above may also be employed to detect areas where the surface lubricant was absent. This might be done because some of the magnetic particles are always detectable at the surface even for unworn media. The surface lubricant is supposed to cover the whole surface and any such uncovered particles may be detected using the method suggested by Anderson and Yen [68].

Perhaps a better solution for looking at the surface lubricant is offered by Linder and Mee [69] and Hedlund [70] where Electron Spectroscopy for Chemical Analysis or X-ray Photoelectron Spectroscopy (ESCA or XPS) was used to detect the amount of lubricant on the surface of a sample (see Chapter 4 for a full description of this technique). Linder and Mee [69] have studied the lubricants on Winchester type media, but similar fluoro-carbons may also be used on floppy media and the same considerations apply. Many advantages of XPS are given in this study: only approximately the top 100 Å are sampled by this technique so that no background signal due to other materials is seen. This contrasts to techniques such as the Fourier Transform Infra-Red Spectroscopy (FTIR) described by many researchers [70], [71], [72], [73]. In fact, Walder [73] explicitly states that the FTIR technique is used to look at all of the lubricant in one go. Usually, however, it is not necessary to know how much lubricant is potentially available in the bulk but, how much is immediately available on the surface. Comparisons of XPS with extraction techniques show that around 80% of the lubricant resides in a sub-surface environment. Since only the lubricant on the surface is directly effective in lubrication, it is felt that only this should be detected by any technique. This would then enable comparisons to be made as to which of the materials available provides the best surface lubrication. It is thought that the sub-surface lubricant acts as a reservoir to replenish any loss of lubricant at the surface. This loss of lubricant at the surface can occur through,

for example, evaporation. Another function of the sub-surface lubricant is to prevent the situation where there is no lubrication. If the surface layers of the media become worn away, then the surface lubricant becomes removed with them. The lubricant in the immediate sub-surface then becomes the new surface lubricant as a new surface is revealed. The sub-surface lubricant can thus be revealed at the newly formed surface.

Such mechanisms of lubrication by absorbed lubricant have been considered in the field of polymer bearings by Skelcher [50]. He considered the life of polymer bearings which had been lubricated, but had had the excess lubricant removed. Skelcher [50] found that the life of the bearings was extended beyond expectation and he explained it by this absorption of the lubrication fluid. As the results of this present work, presented in Chapter 6, reveal Skelcher's speculations that the mobility of the lubricant is important for this mechanism to work has been confirmed. In fact, Dickens [27] showed that there was no absorption of lubricant in the polymers used by Skelcher because these polymers were not porous. Magnetic media, however, has a porous surface and Skelcher's [50] proposed mechanism is expected to be operative.

For the purpose of determining the distribution over the entire diskette, however, the FTIR technique is superior and faster as it can cover the whole diskette in a single scan. Other methods of lubricant distribution detection are considered by Hinkel et al [74] but are not as simple to use as FTIR. In the case of the surface lubricant layer, alternative, equally surface sensitive, techniques compete with XPS. These include Auger Electron Spectroscopy (AES) and Scanning Auger Microprobes (SAM). However, these are less suitable as the incoming electron beam has a tendency to graphitise the lubricant [69]. Thus, the best, and possibly the most convenient, method for the determination of the amounts and categorising the chemical nature of the lubricants at the surface is XPS. Other techniques using particulate probes, for example Secondary Ion

Mass Spectrometry (SIMS), may be expected to cause damage similar to AES. Techniques employing neutral probes, such as Fast Atom Beams SIMS (FABSIMS), may be less destructive of the surface but neither of these was readily available.

XPS has been used with great success by Chambers [75]. The observations made there are very relevant to the present work. He used a fluoropolymer identified only by the trade name "Krytox" by its manufacturer (Du Pont Company, USA). It was found that Krytox is the only lubricant which does not migrate completely into the bulk of the media, this observation is not possible using FTIR. Spectra presented by Chambers [75] show that the Krytox lubricated diskette blocked out some of the signal from the Fe^{2+} ion whereas the other lubricants used did not block any of this signal. A depth profile of the lubricant showing distribution with depth has also been performed for the same study by Chambers [75] and is reproduced here in Fig. 3.8. From this it can be seen that lubricant level is highest at the surface and decreases quite rapidly to a steady level with depth.

The amount of lubricant on the surface is an important factor in performance and its lack can obviously cause wear as noted earlier in other literature and also discussed in this study as shown by the results presented in Chapter 6. The presence of an excessive amount, however, can also be problematic in that it can cause "pooling" resulting in a very large and sudden increase in the viscous drag, "stiction", to occur [69].

This can also lead to wear being initiated by transmitted stresses in the region of the pool of lubricant. Stiction has been widely studied for Winchester discs, but not so intensely for floppy media with only a few methods suggested for its reduction, for example by Hinkel [76]. The detection of the onset of stiction has been suggested by Heinrich et al [77]. In the latter report, a simple method was suggested whereby a pre-recorded signal written to the media was

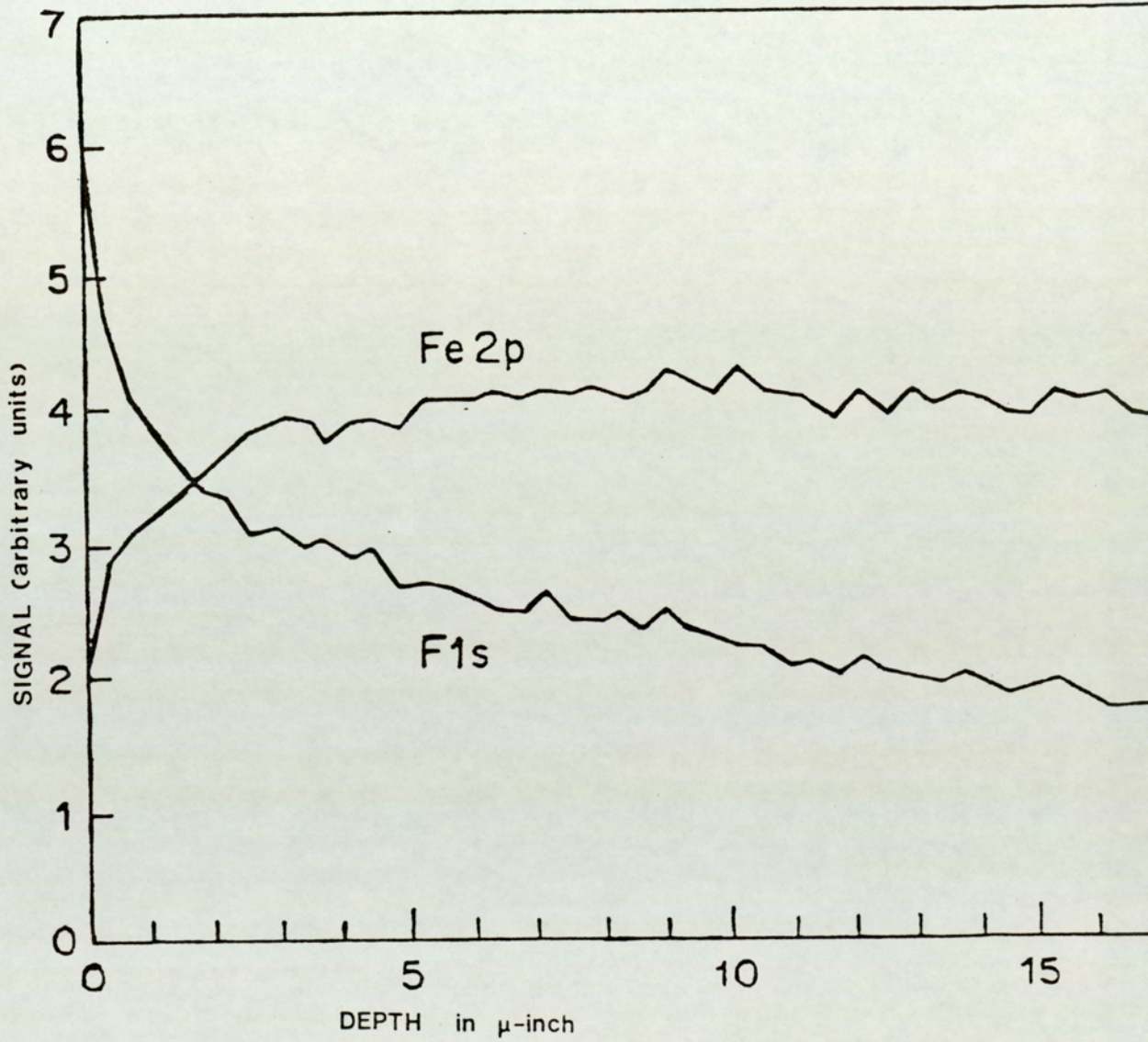


Figure 3.8 Depth profile of the lubricant performed on a diskette sample by Chambers [75].

re-read and spikes and missing pulses in the data was considered to indicate stiction. This is not a good method, however, as the spikes and missing pulses may occur due to other causes.

One such cause may be the onset of wear rather than stiction. Such onset of wear may be expected to produce a sudden increase in friction as indicated earlier through, for example, ploughing wear. Since this wear may not be occurring due to lubricant pooling and stiction, the method cannot be said to identify stiction definitely. In fact, this implies that this method may equally well be employed in detecting wear in adequately lubricated diskettes, as the friction forces correlate well with wear initiation, and is to be discussed later. Thus, the method of detecting stiction suggested by Heinrich et al [77] may result in some confusion as to the cause of the missing pulses. These may be missing because of stiction or the onset of wear.

Other problems for lubrication are those inherent in the lubricating substances used rather than their distribution on the surface or in the bulk of the media. One key aspect is that the lubricant molecules must not interact chemically with the binder in such a way as to degrade it, that is they must be fairly inert. It would appear that materials such as the aluminium oxide, which is used as the HCA and as the load bearing particle material, in their action as Lewis acids, often degrade the commonly used perfluorinated alkyl polyesters by catalytic decomposition [78]. Although no such lubricants have been used in this study, a solution to the problem is required as perfluorinated alkyl polyesters are commonly used in this application. One solution may be not to use alumina, but Fe_2O_3 is also a Lewis acid and this obviously cannot be removed. The action of the Lewis acids is in their propensity to accept electrons from electron rich sources such as the carbonyl and carboxyl groups in the polymers which form the binder of the media and lubricate it. These chemical groups exist in the binders and lubricants considered in the present work.

One of the other problems that can occur is the plasticising of the binder by lubricating agents. This can cause creep in the surface structure resulting in smoothing of the surface through plastic yield. Yet another serious problem is that of the peeling off of the magnetic layer from the PET substrate due to the action of unsuitable lubricants and this in turn leads to deterioration in performance as the active magnetic layer is removed. This means that lubricants which do not interact with the magnetic layer, except in a positive sense, must be used.

Materials often used as surface lubricants, as indicated earlier, are of the perfluoro-polymer type and the perfluoropolyesters Fomblin Y (branched polymers) and Fomblin Z (linear polymers) reported by Bagatta [34] are an example of these. Although they have not been employed in this work, they typify the properties that surface lubricants should possess. For this reason, they may be discussed briefly here.

Tests show that the Fomblin polymers have very little tendency to react with a very large range of chemicals (acids, alkalis, oxidising agents, etc.) and show a thermal stability to about 260 °C in air. Furthermore, their interaction with PET, the substrate material for floppy diskettes, was found to be non-existent at temperatures up to 70 °C in 10^3 hours; no results are presented by Bagatta [34] for higher temperatures. One other fact is that they seem to have a favourable response in elasto-hydrodynamic lubrication applications. This is one of the lubrication regimes into which the diskettes can fall according to Skelcher [60]. It appears that the linear molecules (Fomblin Z) act better as a surface lubricant than the branched (Fomblin Y) version due to various properties, for example, viscosity relative to the molecular weight factor. Active forms of the Fomblin Z polymer, such as ester end termination, can give extra bonding to the surface for surface retention, especially when combined with their low vapour pressure. This property implies that they can produce improved lubrication by

staying on the surface.

Obviously, retention on the surface is an important property for surface lubricants. The residence of these molecules on the surface rather than penetration into the bulk may be enhanced by making the surface rougher. This creates natural pockets uniformly all over the surface where the surface lubricant may reside. A novel method for creating such a surface has been suggested by Lorentz et al [79]. They suggested that material is added to the surface during manufacture, for example thermally degradable polymers, which may be removed later. In the case of thermally degradable polymers, these may be converted into lighter fractions by heating. This may be done during the thermal curing process. The lighter fractions created then evaporate leaving holes or pits behind in the surface thus providing lubricant reservoirs. According to Kraus et al [80], some benefit is to be gained by the addition of surface lubricant and then curing the media at 150 °C as it causes the surface lubricant to penetrate into the surface to a depth of approximately 5 to 50 nm. This penetrated lubricant then, presumably acts in the same fashion as bulk lubricants such as the butoxyethyl stearate (BES) or Krytox which act by being squeezed out under the pressure of the head as it slides over the media. The advantage over conventional bulk lubricants is, of course, the very much reduced distance required to be travelled in order to reach the surface. The extent of successful migration of the bulk lubricant to the surface has been studied using XPS by Chambers [75] and Hamada et al [81] and the latter suggest a similar pore formation to that described above by Lorentz [79]. This would, it is suggested, aid the lubricant in its migration to the surface and its retention on that surface. Chambers [75] has suggested that migration can be controlled by the chemical "construction" of the molecule. An example of this is the use of ester links in a molecule. These ester links improve migration to the surface since they provide the ability to rotate about the ester links.

The concluding comments on this section can only be that, despite the fact that the magnetic hard discs and diskettes have been the subject of study, no systematic study has been carried out concerning the wear or wear resistance let alone a logical progression of experiments to conclude in a theory of the mechanisms of wear initiation or propositions for its progression. The only real studies have been made by Skelcher, [20] and [60], and Skelcher, Sullivan and Dirks [82]. All of these were done at 3M. Two of these investigations (Skelcher [20] and Skelcher, Sullivan and Dirks [82]) related polymer richness (or otherwise) of the surface, its roughness and magnetic particle dispersion to wear. The other (Skelcher [60]) has related the roughness to the "in-drive" friction measurements and the cause (adhesion) of the friction at the diskette surface. He has also looked at the lubrication regimes which apply to diskettes and related them to wear. Once again, no wear mechanism has been proposed and no real method of looking at the media with different lubrication conditions has been suggested. Rather, media have been studied to show the operation of different lubrication regimes in terms of "positions" on the Stribeck curve with changes in the media's rotational speed and with changes in the extent of side 0 head penetration into the plane of the media.

3.4 Tape.

The study of wear in magnetic tape is relevant to this project as many similarities exist between magnetic tape and floppy diskette media. The most obvious similarity is that they are both flexible media but a more detailed investigation reveals that similar binders, backing and lubricants are utilised in both systems. Of course, differences also exist such as the ability of tape to stand long term longitudinal (elongating) stress without creep of the surface asperities when the tape is wound, under tension, onto the reel. Also, deformation of the asperities on the surface occurs when the tape is wound onto a spool as successive layers

stress those below them. Bhushan [83] has studied the tape at the centre of such reels. He has concluded that deformation of the tape at the centre must substantially be of an elastic nature even after long term storage. This means that no calendering type effect occurs and good frictional properties are preserved by maintaining a rougher surface. Diskettes do not face either of these problems but they do face the problem of repeated and frequent stressing of the same point, for example the tracks containing the directory of the diskette; tapes being sequentially accessed do not have this problem. In terms of wear caused by the magnetic transducer, however, interactions of a similar nature can be expected for both since the binder, lubricant and backing materials are so similar. However, the effects of a rigidly fixed head in the case of tape drives means that some subtle differences may be expected to emerge.

A study of the durability as related to the chemical and physical properties of the materials used in tape manufacture was carried out and reported on by Hiratsuka et al [84]. The first relevant aspect of this study to diskettes is the adhesion quality of the tape. The adhesion of the tape being pulled off the reel with that still remaining on the spool on unwinding is discussed. This could be of relevance in adhesive friction at the head-media interface where increased adhesion leads to an increased coefficient of friction and hence an increased rate of wear (see later for the reasons for this relationship). The wear particles thus generated can cause spacing losses when they become trapped in between the media and the read/write head [85]. It was found that the adhesion was greater with soft non-cross-linked binders and with fatty acid lubricants. The reason for this is that these binders are softened by an increase in temperature. This could be important as it is believed that transient contact temperatures may reach values as high as 250 °C at repeatedly stressed points on a diskette surface and fatty acids are used in lubrication of the present samples. Also, the fatty acids have a hydrolytic nature. This means that they tend to absorb water from the

atmosphere, this can lead to plasticisation of the binder by the breakdown of the polymer through hydrolytic degradation. Fatty acid esters are far better (for example, butoxyethyl stearate) in this respect as they have a better mixing property with the binder and, consequently, a reduced tendency to react with airborne water to produce the products of degradation. This also reduces the problems of stiction as it is the products of hydrolytic degradation that cause stiction.

The other feature that tape and diskette media have in common which is discussed in literature is that of friction. Bhushan and his co-workers [23], [86] have used various specially formulated tape media including one with an increased proportion of hard phase in the binder. They found that frictional properties can be affected by the relative proportions of the hard and soft parts of the binder co-polymer. With an increase in the hard portion, the bulk modulus is increased. This would be expected to reduce the friction at the surface and is found to do so because it increases the melting point of the binder's soft portion. Increasing the melting point has the effect of reducing the tendency to produce an interface with increased real area of contact. Increased hardness also reduces the real area of contact. This results in reduced friction since frictional force is directly dependent on the real area of contact. If, however, the proportion of the hard phase is increased excessively, then the increased phase separation between the soft and hard components which results can cause the soft polyester part of the co-polymer to soften and melt at lower temperatures. This then leads to increased friction through plastic flow of the soft phase creating a larger real area of contact thereby producing a high friction interface [29]. These researchers have also observed that the softer binders tend to promote the movement of lubricant so that with lubricated media it may be inadvisable to increase the polyurethane hard phase to such a degree as to affect lubricant mobility. It is possible that the harder, more crystalline, binder can be more brittle and it can

shear at the crystalline boundary interfaces. This may then cause an avalanche effect and increased wear as well as data loss through wear particles separating the head and media [85]. The above observations have been confirmed by others such as Hiratsuka et al [87] who studied the effect on friction and wear of the physical and chemical properties. Hanabusa et al [88] have further noted that the adhesive components of friction in the system can lead to stick-slip motion creating read/write problems independent of wear. In fact, wear is probably enhanced by such a stick-slip motion through the increase and concentration of stresses at the points where the coefficient of friction is higher.

Another form of sticking which causes increased friction is that of stiction. This is distinguished from the stick-slip phenomenon by the fact that stiction is said to be observed when a normal force greater than the weight of the upper body is required to separate the mating surfaces. The cause of stiction is often the water from a humid environment causing the chemical degradation of the binder polymer [23], a fuller description of this phenomenon is given later.

Although, since it is the softer of the two, the media wears far more rapidly than the head, the head also wears. This is because at the tribological interface of two interacting bodies wear of both occurs, as can be found explained in general texts on tribology such as Bowden and Tabor [47], even if one material is considerably harder than the other. That this is true in magnetic recording as much as elsewhere was discussed by Kelly [89] who intimates that the polymeric binder would eventually lead to wear in the slider. Of course, magnetic media also contains alumina particles as the head cleaning agent and this is what causes most of the the damage to the head slider.

Wear of the slider and media can be reduced by the action of lubricants as already discussed and confirmed by Kelly [89], who has considered the effects of bulk lubricants (such as butoxyethyl stearate). He has put forward some advantages of using bulk lubricants and their migration to the surface when and

where required; revelation of new lubricant as the surface of the media is abraded. Disadvantages, of using bulk lubricants have also been discussed by Kelly [89]. One example of this is the migration of these lubricants towards the substrate/magnetic layer interface where they may adversely affect the bonding between the binder and substrate. Another example is the possible interference of the bulk lubricant with binder polymerisation. As these disadvantages imply that a minimum amount of bulk lubricant should be employed, suggestions are also discussed which concern the possibility of using surface lubricants. Lubrication using 0.05 μm to 0.5 μm sized particles of any of the common solid lubricants such as molybdenum disulphide, graphite and polytetrafluoroethane (PTFE) are considered but dismissed as these would tend to cause spacing losses because the media and head would be physically separated. This would result in a smaller amount of magnetic flux being linked by the air gap in the magnetic transducer thereby causing a reduction in read-back signal. Also, a smaller signal can be expected to be recorded during the writing process for the same reason. The degree of these losses are determined by the size of the particles used as:

$$\text{The Spacing Loss} \propto e^{-d/\lambda} \quad (3.4.1)$$

Where d = separation of the head and media

λ = the recorded wavelength = relative speed / recorded frequency

Of course, some three body interaction in the form of ploughing type wear may also be expected in flexible media with solid lubrication. In order to avoid these problems, the use of very thin films of liquid surface lubricants has been advocated.

A comprehensive study was made of the coefficient of friction of polymeric media (tapes in this case) by Bhushan [90]. It was concluded that, for low stresses (very much less than 100 MPa), the shear strength of polymers is constant and with multiple asperity contact occurring (the regime operating for magnetic recording on flexible media) the coefficient of friction is independent of normal stress. This is particularly true as only a few grammes load is used in loading the slider onto the diskette surface leading to normal stresses of the order of only 8 kPa, assuming a minimum slider area of $\sim 0.25 \text{ cm}^2$ and loading of 0.2 N. Both of these are reasonable for floppy diskettes. The speed dependence, however, is governed by the mechanical properties of the material such as its elastic modulus but no dependence was noticed in the range of speeds studied. Temperature and humidity, however, have been found here, by Bhushan [90], and elsewhere by Bradshaw and Bhushan [23] and Bhushan et al [86], to have a profound effect on the friction, and hence wear. An increase in either of these environmental parameters leads to increased friction. In the case of temperature, it must rise to beyond the softening temperature of the polymer [86] and this depends on the exact constituents of the binder with the soft portion of the copolymer affected first. The exact value of relative humidity which is detrimental to the binder also depends on the constitution of the binder and it can be detrimental at 50% according to Bradshaw and Bhushan [23] in some cases or may be unimportant until it reaches a value of 70% in other cases [90]. The effect of water is to cause hydrolysis of the binder copolymer with the polyester part of this copolymer being attacked. So the amount of humidity tolerated depends on the relative proportion of the two parts. The result of the hydrolysis is to produce smaller molecules from the polymer by division of the long polymeric chains. These smaller fragments are very adhesive in nature and tend to increase friction by introducing stiction [23]. However, another effect of the water is to compete for bonding sites with the polyurethane on the magnetic particles' surface [23] and this is obviously undesirable.

The friction coefficient's dependence on the properties of the binder material has also been studied by Miyoshi et al [91]. They noted that, of four different binder systems, the polyester-polyurethane system was not the best in terms of both magnetic particle enclosure and its coefficient of friction. The best binder system for one property, however, is the worst for the other and it was suggested that the present binder system was the best compromise. It was the best for particle enclosure and second best for frictional properties. The best for frictional properties, nitrocellulose, was the worst for enclosure. As discussed earlier, however, the properties of the system may be altered by changing the relative proportions of the hard and soft phase compounds. This gives rise to increased or reduced friction. Miyoshi et al [91] found that consistently lower coefficients of friction were obtained for more elastic contacts than for plastic contacts. The results obtained by Miyoshi et al [91] should only be taken in a general sense, however, as it was also concluded by them that morphology makes a difference and only one tape contains just $\gamma - \text{Fe}_2\text{O}_3$ as the sole magnetic particle. Others contain mixtures, with solely CrO_2 or with Cobalt doping being used in their other samples.

Important and relevant work has been presented in several reports where the friction interface of polymer media was studied (Bradshaw and Bhushan [23], Bhushan et al [29], Bhushan [83], Bhushan et al [86]) and these results must be considered. The various theories of friction, as discussed earlier in section 3.1, were considered in these studies with regard to flexible media. These are referred to, explicitly or implicitly, in the other works.

Bhushan [83] has defined the "plasticity index", Ψ_p , as:

$$\Psi_p = (E'/\sigma_y) \cdot (\sigma_p/\beta_p)^{1/2} \quad (3.4.2)$$

where, E' = complex elastic modulus

σ_y = the yield stress

σ_p = standard deviation of the asperity peak heights

β_p = mean radius of these peaks

with

$$(1/E') = (1 - \nu_1)^2/E_1 + (1 - \nu_2)^2/E_2 \quad (3.4.3)$$

where

ν_1, ν_2 = Poisson's ratios for the materials

E_1, E_2 = Moduli of elasticity (or complex modulus in the case of polymers) for the interacting bodies

This is the same quantity as defined in equation (3.1.1.9) with reference to Greenwood and Williamson [53] with (E' / σ_y) used here instead of (E / H) , the ratio of Young's modulus to the hardness of the polymer.

According to Bhushan [83] this quantity, Ψ_p , determines the elastic or plastic nature of the interactions at the asperities with $\Psi_p < 1.8$ implying elastic contact and $\Psi_p > 2.6$ implying purely plastic contact. In order to minimise wear, the real area of contact needs to be as small as possible. The reduced contact may be envisaged as leaving least "chances" for wear to occur. The least contact, in the short term, is obtained for plastic contact as illustrated by graphs used by Bhushan [83] to compare metals and polymers. However, this contact area is increased considerably after repeated plastic deformation of the asperities occurs. Thus the real area of contact will increase rapidly as this plastic deformation increases this area of contact at each traversal. Wear, like frictional force, is proportional to the real area of contact. Therefore, it is best to have an elastic contact situation whereby there is little if any increase in the real area of contact with time. Another fact to emerge is that, on examination of the tapes by XPS, it

was found that the surface was polymer rich. This implies that smearing, by plastic flow, of the asperities had taken place. This causes a reduction in the magnetic signal as the effective separation of the read/write head from the magnetic particles is increased. This further emphasises the need for elastic rather than plastic deformation of the asperities.

Bhushan et al [86] have considered the physical properties of the binder in computer tapes and their consequent effect on the coefficient of friction between head and tape. Properties which were found to have an influence were those such as the surface roughness, softening temperature of the binder and its complex elastic modulus. The main causes of friction in tapes are adhesion and hysteresis [30] of which the hysteresis contribution to the total is considered to be negligible [29],[86]. Adhesion is dependent on the real area of contact and the shear strength of the asperities with the real area of contact in turn depending on the complex modulus of the material. It has also been observed that the magnetic particles' distribution can have a very great effect on the coefficient of friction and how this is possible has been illustrated in Fig. 3.9. The ideal distribution is uniform, Fig. 3.9 (a), so that the properties, for example E' , remain constant throughout the layer ensuring that the stresses are distributed evenly. If the surface layer of the media is polymer-rich, as represented in Fig. 3.9 (b), then it deforms plastically relatively easily causing an increase in the coefficient of friction through smearing of the asperities and the consequential increase in the real area of contact. A polymer-rich surface will also experience a lower read/write signal due to spacing losses because of the increased distance between the magnetic particles and the magnetic transducer. If the surface is magnetic particle-rich, as in Fig. 3.9 (c), then, although wear of the media would be expected to be reduced, abnormally increased wear of the slider would be expected to occur due to abrasion by the acicular shape of the particles and their hardness. (In fact excessive slider wear caused by the acicular particles is one of

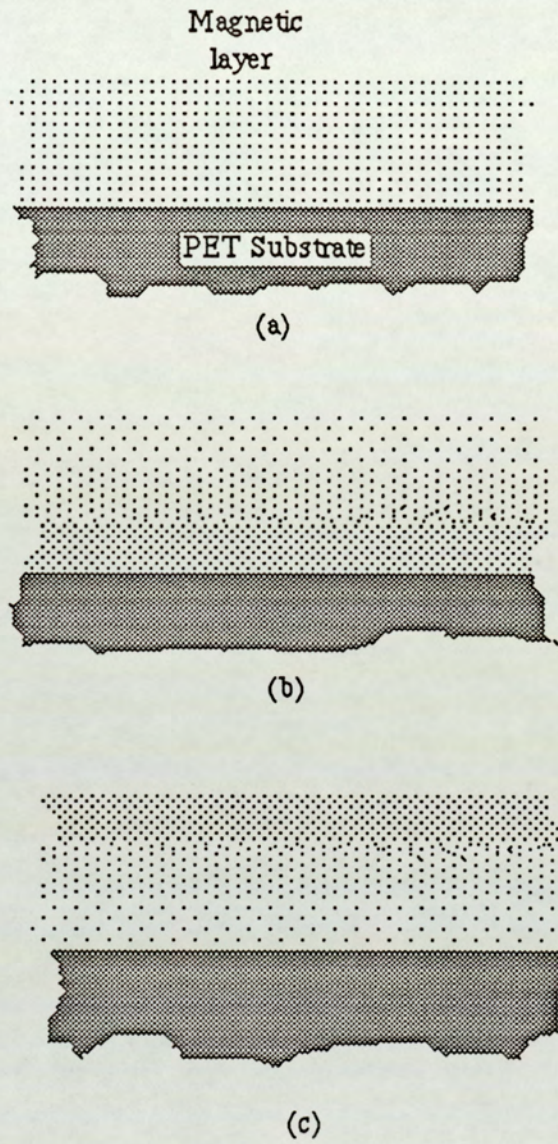
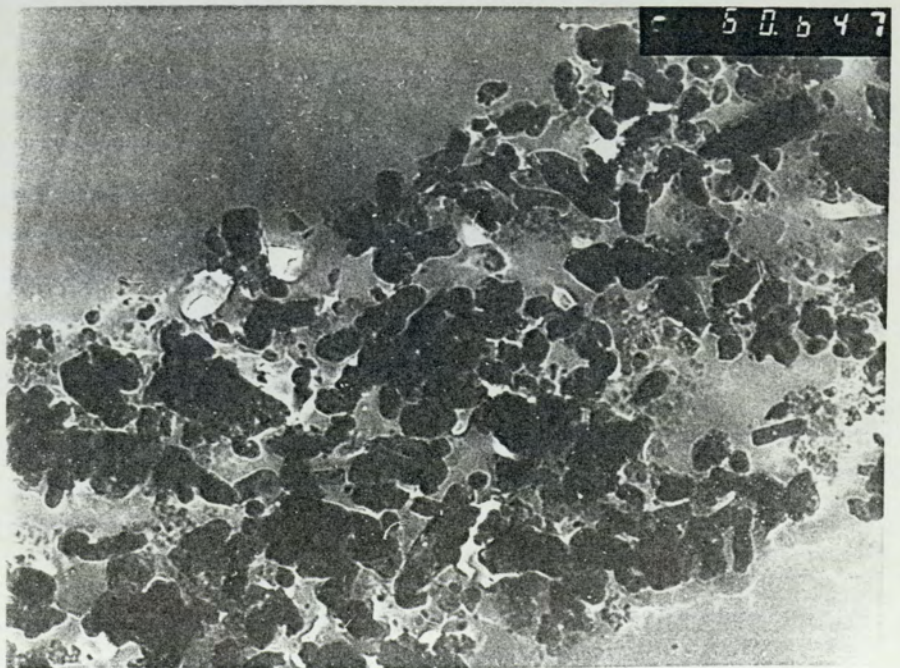
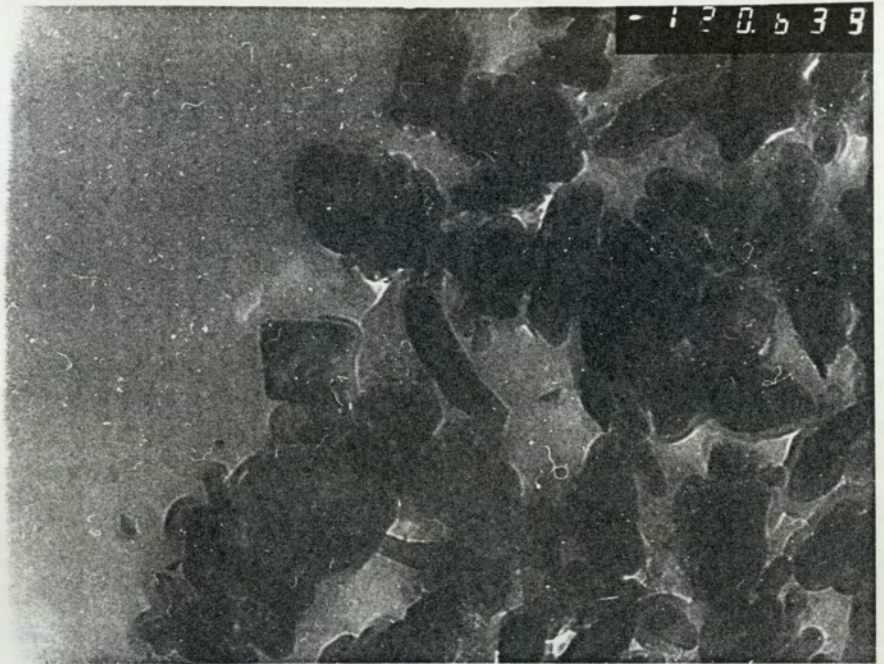


Figure 3.9 Schematic representation of magnetic particle distribution (a) The ideal magnetic particle distribution, (b) A polymer-rich magnetic layer and (c) A particle-rich magnetic layer.

the problems encountered in the production of perpendicular recording media. This is being developed by most manufacturers as it would enable greater data densities to be recorded as described in section 2.4 of Chapter 2). The magnetic layer would also be affected on its other interface, that with the PET substrate. At this interface, the reduced rigidity caused by the relative absence of magnetic particles could make shearing off of this top magnetic layer from the backing much easier. The ideal distribution is one where the magnetic particles are not aggregated in groups leaving sections devoid of magnetic particles. This is desirable both from the magnetic recording and tribological point of view. An example of the aggregation of particles leaving voids in the media's magnetic layer may be seen in the transmission electron micrograph of Fig. 3.10. This is a picture of a commercially available product. From a magnetic point of view, particles with an uneven distribution can lead to amplitude modulation of the magnetic signal. From a tribological point of view, such a distribution tends to produce a magnetic coating with non-uniform physical properties. Even if the distribution of the magnetic particles is very uniform, the surface topography is an important factor in slider wear: a rougher profile tends to enhance wear of the slider. The other problem to contend with, however, is that the smoother surface implies an increased real area of contact with this causing an increased coefficient of friction [29],[86] and, thereby, an increase in the rate of media wear. The best solution, considering roughness alone, would appear to be a compromise roughness to get the optimum performance from the media-slider combined system. It may be concluded, however, that it is probably better to design a binder with a higher value of E' so that no such compromises are necessary. This would be expected to show an improvement in the reduction of signal amplitude modulation as the read/write head could be closer to the bulk of the magnetic coating and the oxide particles that it encloses by using a smoother media surface. Furthermore, the enhanced wear which would be expected with

Figure 3.10 Transmission electron micrographs showing voids in the media in two separate samples, one (upper, SR2(4.5)) shown at 120 K \times and the other (lower, SR3(0)) at 60 K \times magnification.



an increase in the real area of contact for a smoother media surface may be countered by an increase in the complex elastic modulus, E' .

The chemical properties of the binder [29] affect the coefficients of friction through such aspects as the vulnerability of the constituent materials of the binder to hydrolytic attack. One candidate for such sites is the $-C(O)O-$ points on the Polyester and Polyurethane chains, Fig. 3.11.

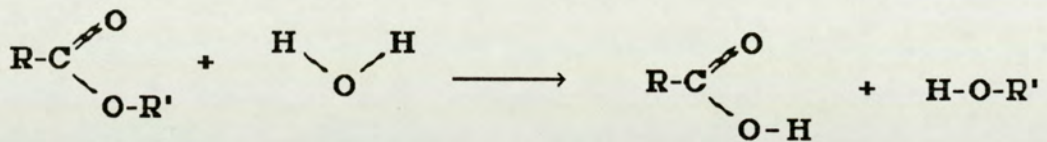


Figure 3.11 Hydrolytic degradation of an ester link to carboxylic acid and alcohol
(R and R' may be similar or different organic radicals).

Hydrolytic attack here causes the decomposition of the polymer into lower order molecules which can cause stiction as they form a more adhesive constitution and this is particularly prone to occur at high relative humidities (**RH**) as discussed earlier [23]. Another effect of increased RH is to prevent the formation of domains (by the hard, polyurethane sections of the binder) at elevated temperatures. This happens as a result of the fact that water hydrogen-bonds to the polyurethane rather than allowing two of these molecules to link up in the same fashion. Further, since the water molecule is more successful in the competition between it and the polyurethane in bonding to the surface groups of the magnetic particles [23], it reduces the ability of the the binder to enclose the magnetic particles of $\gamma - \text{Fe}_2\text{O}_3$. The hydrogen bonding effect of increased RH may be desirable to an extent. This is because it can prevent the binder from becoming too rigid at the expense of its elasticity. This elasticity is gained through the more flexible amorphous polyester sections of the binder structure.

So reducing the domain formation in the polyurethane can result in the more desirable elastic surface as briefly mentioned by Bhushan et al [86] and more fully described later in the context of the results obtained in this work. A similar effect to this may be seen by the use of lubricants which separate the polyurethane chains with the effect of reducing their interaction through hydrogen bonding. Interesting observations regarding the reaction to humidity have also been catalogued by Bradshaw and Bhushan [23] viz. that the hydrolytic reduction is only a surface phenomenon and if this layer is removed quickly enough, then further damage may be prevented as this is only plasticisation of the top layer which has absorbed the water. It is long term exposure to a humid environment which gives rise to a bulk change in properties as, even if the top layer is removed, more water from the environment then tends to produce further damage. This long term exposure damage would probably be aided and accelerated by the action of the alumina and iron oxide particles in, as intimated in an earlier section (section 3.3), their action as Lewis acid catalysts. As such, they help the water molecules in the hydration of the binder and the production of smaller molecules from the polymer creating the short chain length adhesive materials which cause stiction. This chemical reaction is understood to occur via a co-ordinated cationic mechanism. This results from the charges present on the surfaces of the metal oxides' surfaces which aid the removal of the -OH groups and finally lead to a severance of the ester bonds. This produces the original alcohol and acid. The mechanism is illustrated in Fig. 3.12.

Either of the Lewis acids (Fe_2O_3 or Al_2O_3) may be involved in the reaction although only Al_2O_3 is indicated in Fig. 3.12. These acids help by allowing easy severance of the initial C=O bond as their positively charged surface attracts the negatively charged oxygen atom.

Possibly one of the most important aspects of media degradation is that of thermally induced aging. In view of the temperatures that are thought to be reached at the head-media interface, this may occur during normal use. The

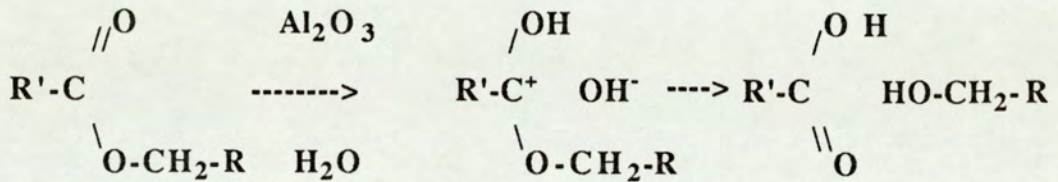


Figure 3.12 The hydrolytic degradation of the binder co-polymer with the aid of Lewis acids which are the Iron oxide and Aluminium oxide particles in the magnetic layer. (R and R' maybe similar or different organic entities).

problem is that the increase of temperature causes the greater phase separation of the two components of the binder co-polymer. Further, it also causes the softening of the hard phase which may be expected to flow more readily as a consequence and lead to an increased real area of contact. This produces greater friction resulting, ultimately, in reduced durability of the media.

Any effect which softens the magnetic layer is most significant as friction changes correlate well with changes in the bulk modulus of the magnetic layer. An increase in the former is seen if the latter is reduced and, as observed by Bhushan et al [86], a reduced E' leads to increased friction and wear. The addition of magnetic particles to the binder system has the effect of increasing the bulk modulus as the highly filled polymers of the magnetic media behave as rigid materials. But this is dependent on good adhesion between the magnetic particles and the polymeric binder as well as on the size of the particles [23].

One component of the binder discussed in item (2) of sub-section 2.2 in Chapter 2 was the cross linker which is used at the curing stage. The materials used are isocyanates and have the effect of causing phase separation of the soft and hard sections of the binder as they link the molecules of the hard phase together forming them into domains. Obviously, care must be taken to use the correct amount so that the physical properties of the binder are enhanced. An

alternative method of curing the binder to achieve the correct elasticity of the material was presented by Jurek and Keller [92]. According to them, the curing is better obtained by the use of electron beams rather than isocyanates. No firm conclusions can be formed on this as further reports on the subject were not obvious. However, electron damage to the media may be expected similar to that caused by the bombardment of any surface by energetic projectiles.

3.5 General Durability and Wear Considerations.

There has been much literature amassed which may in some way be related to this project. Of this collection, some concerns such areas as the techniques used in surface analysis, for example XPS, and some the wear properties of the magnetic heads and head materials (predominantly Ni-Zn or Mn-Zn Ferrite magnetic cores with a ceramic body) in forms other than usual head shape. The surface analysis techniques employed will be described in a later chapter, Chapter 5 where instrumentation is considered. The wear of the heads employed in floppy diskette drives has only been discussed in one report. In this Blevins et al [33] have looked more at the abrasivity of the media. A cursory study has been performed as part of this project and the results are presented in Chapter 6.

The main purpose of this section is to consider the literature concerning wear mechanisms. In particular, those mechanisms applicable to polymers and as a result to the magnetic media presently of concern. It is necessary to look at the mechanisms of wear reported for polymers because there appear to have been none reported directly for magnetic media. So it is necessary to study others and select the one which may apply to the present system. One point which leads in the direction of selection of the correct theory in that the diskette media's binder is constructed of elastomeric material, Bhushan et al [29]. In fact, the exact elasto-plastic properties of the polymer binder are determined by the actual nature of the

co-polymer employed but the addition of the magnetic particles produces a highly filled system which behaves more like a rigid body. However, because of the polymeric nature of the binder, it would be instructive to consider the wear of other elastic materials and the first to be considered is the wear of rubber.

One publication looking at the "roll formation wear" of rubber is by Reznikovskii and Brodskii [93]. It is suggested by them that this form of wear occurs with highly elastic materials interacting with very smooth abraders. Obvious similarities exist between this and the highly filled polymers of the diskette being abraded by the hard ceramic of the head which has a finely polished surface finish. The mechanism described by Reznikovskii and Brodskii [93] is shown in Fig. 3.13 (a) to (e). Referring to the stages of wear shown in that figure: basically the asperity is deformed in (a) and the real area of contact increases as in (b) leading to increased frictional forces and stresses on the asperity causing ripping to start at the point **P** shown in (c). The wear process then progresses with tearing occurring and continuing with the "to-be-wear-particle" rolling up in the fashion of (d). Further stressing causes this piece of material to become liberated from the bulk and to form an independent wear particle as shown in (e). This type of wear particle has been observed in the course of the author's investigation and photographs are presented later in this work. This particle may then cause further damage through three body interactions as described for abrasive wear earlier. According to Reznikovskii and Brodskii [93], this mechanism of wear is said to occur with high values of the coefficient of friction and may possibly be reduced by use of surface lubrication. Some similarities are pointed out between plastics and rubbers by Ratner [94]. He has suggested that, with both being polymers, some similarities in the wear mechanisms exist but more emphasis is laid on abrasive ploughing type wear as plastics are seen in their everyday form of being generally rigid and inflexible rather than elastic. In the case of diskette media, however, the

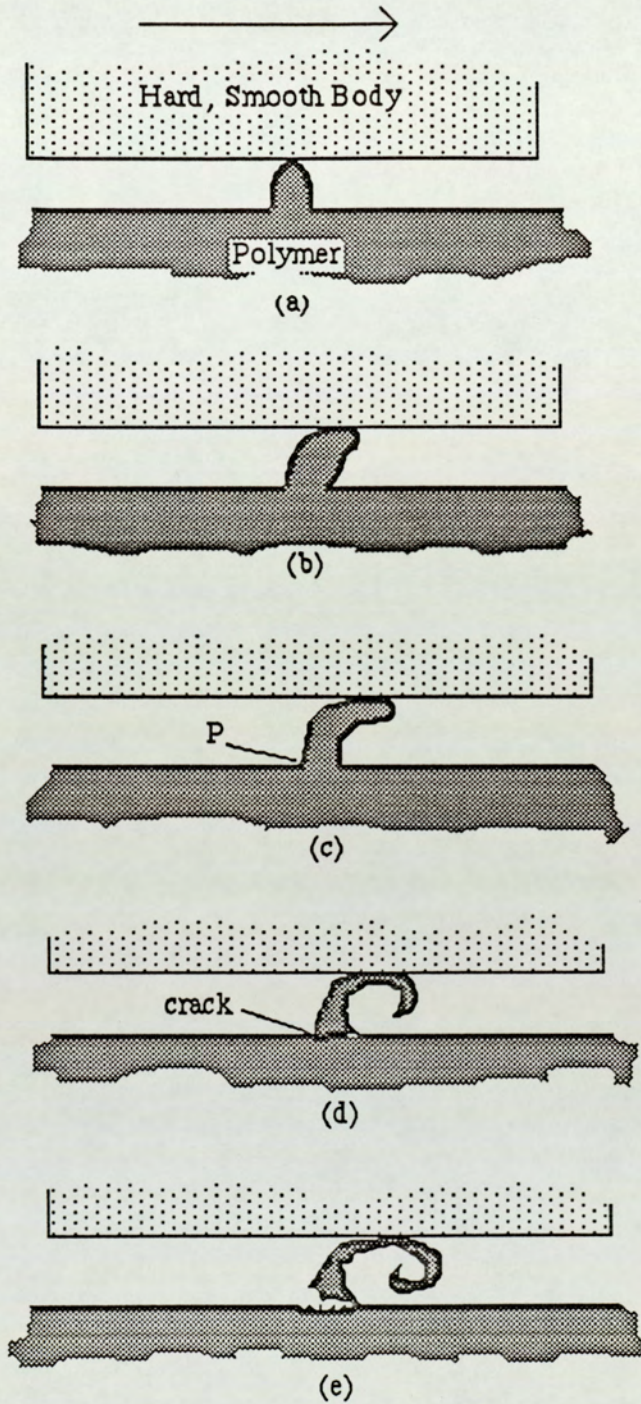


Figure 3.13 Wear of a highly elastic polymer by a hard and smooth abrader moving over it in a manner which causes cyclical stressing of the surface.

proposition of highly elastic surfaces may make the wear mechanism described by Reznikovskii and Brodskii [93] more relevant. Also, as related to their work, it is suggested by Ratner [94] that the rolling wear does not occur immediately but after a few passes. This may suggest a fatigue type process (possibly sub-surface fatigue), see the delamination theory of wear which is discussed later and in which sub-surface damage is of crucial importance. It is in the work of Ratner et al [55] that increases in wear for elastic materials has been reported for rises in the temperature. This is significant for floppy diskettes as the transitional temperatures at the interface are thought to reach values as high as 250 °C. The increase in wear is believed to occur due to the reduction in strength caused by partial or complete melting of the polymer at the surface. Bush [57] has reported dramatic decreases in the shear moduli of the crystalline and amorphous polymers as their temperature is raised. In particular, the amorphous polymers show decreases in the shear modulus even at relatively small rises in temperature and well before the glass transition is reached. Briscoe [51] has reported that deformation friction rises markedly with an increase in temperature as the polymer deformation losses increase.

Solidification of the melted polymer could leave a permanently smoothed surface if all of the molten material is not removed. This then leads to increased friction at such sites and an avalanche type effect can be expected to produce rapid deterioration of the surface. This high wear rate regime is preceded, however, by a period when the wear rate is very low because on crossing the glass transition temperature for a hard material, such as the polyurethane part of the binder, the breaking elongation is greatly increased. So, rather than producing wear, the frictional forces cause extension of the asperities as seen in Fig. 3.13 (c). Obviously, after a certain amount of extension, yield must occur. It is desirable, therefore, to avoid reaching a temperature such that the polymer is softened sufficiently to cause this plastic extension and eventual

breaking yield. So the temperature which should not be exceeded in frictional heating is the glass transition of the polyurethane. In the case of the diskette binder, the soft phase may already be well past its glass transition at room temperature which can be anywhere between -60 and +30 °C [23]. The polyurethane, which is bonded to the magnetic oxide particles' surface, needs to be kept below its glass transition so that the surface retains some rigidity.

The sub-surface activity of materials is obviously quite important in all forms of wear but, as suggested on the preceding page, from the work of Ratner [94], in the fatigue wear of elastic materials it may be even more important. A theory of wear (originally proposed for metals) is the delamination theory of wear as presented by Suh [95] in 1973. The original theory suggested the formation of a soft surface layer. This creates a discontinuity with the harder sub-surface. Dislocations in the metal then pile up at this discontinuity and ultimately cause delaminative wear. Later development of the theory led to suggestions concerning the sub-surface and surface cracking of the material caused by plastic flow around hard objects leading to sub-surface void formation and consequent weakening of the material. It was then suggested that metallic dislocations pile up against these hard particles in a similar fashion to that at the discontinuity described above. Suh [95] criticised the Archard theory of adhesion [96] for various reasons including not taking the physics of asperity deformation into account. The theory proposed by Suh [95] takes this into consideration and also includes such considerations as the removal of dislocations, in metals, which are close to the surface. In the case of polymeric materials, dislocations cannot form in the way that they do in metals. This is a result of the crystalline nature of metals where planes of atoms are able to slide with respect to each other if sufficient stresses are applied. Despite this the filled polymers used in the polymeric media present sites where sub-surface cracking can be initiated. In order to appreciate the role of such sites, the theory of delamination as described

by Suh [95] for metals may be considered

In metals the dislocations which are close and parallel to the surface are removed by the "image force". This is a concept whereby a dislocation of the opposite sense is pictured to be situated at a similar distance from the surface, but on the opposite side of that surface, as the actual dislocation which is inside the material under consideration; the image is outside it. The stress field of the real dislocation must be zero at the surface and this would be the case if it is combined at the surface with the field of an equivalent but opposite dislocation in the position of the image dislocation as described above and if the material was to be extended infinitely. The apparent attraction between the real dislocation and its image causes the former to migrate towards the surface where it disappears. In reality, motion towards the surface reduces the strain energy of the dislocation as there is no bulk beyond the surface to make it rigid [97],[98]. In the case of oxides on the surfaces of metals, however, the hard oxide causes a higher stress at the surface than is to be found lower into the material. This has the effect of repelling the dislocations close and parallel to the surface away from this surface and into the material [96],[98]. This is akin to a dislocation in the image position which is of the same sense as the real dislocation. In this case the energy stress field can be reduced by the two dislocations moving apart. In either case, the top layer becomes deficient in dislocations and much more prone to plastic deformation. The removed dislocations are replaced by new ones being formed through this plastic flow of the material immediately below the surface, produced by the slider imposed stresses at the surface. These are then in their turn also repelled from, or attracted to, the surface.

Another method of propagation of dislocations, whether parallel to the surface or not, is by the stress caused by the sliding due to the fact that only a fraction of the theoretical stress is required to move the dislocations [99],[100], the "Peierls stress" (or latterly "Peierls-Nabarro stress"); a further reduction of this

stress has been noted as dislocations do not necessarily lie in the lowest energy states in the lattice but rather across them [101]. These mobile, sub-surface dislocations then pile up against hard particles in the bulk and, once pinned at these points, cracks can be nucleated and caused to grow.

Further evidence in support of delamination wear in metals was presented by Suh et al [102] for various metals. Some key aspects were discussed by Suh [103] in an overview presentation of the theory. Of course, the nucleation and propagation of sub-surface cracks lays at the centre of the whole concept of delamination as presented in Suh's theory and was discussed by him elsewhere [103] but was more fully covered by Jahanmir and Suh [104] where it has been noted that nucleation occurs around included particles. It was also noted that nucleation may be retarded by the particle if that particle to surrounding matrix adhesion can be increased. Some mention was also made of the values of the coefficients of friction but all the work was for metals and not directly applicable to the polymeric surfaces encountered in the work involved in this project. What was relevant, however, was that the included particles are larger than $0.5 \mu\text{m}$ in size (the magnetic particles in floppy diskettes are about $0.5 \mu\text{m}$ long by about $0.1 \mu\text{m}$ in diameter). In this case the elastic energy released by decohesion to produce a crack must be enough to overcome the surface energy of the two free surfaces created as the material separates to form a crack [103].

When free surfaces are created in void formation in the sub-surface region, the crack created can be propagated. This can lead to the crack getting large enough to effect delamination or it can cause the crack to coalesce with other nearby ones as it grows and thus also leading to delamination. The critical aspect here is the rate determining step. Fleming and Suh [105] have discussed the mechanisms of crack propagation and how the crack propagation relate to wear rates for metals [106]. It is necessary to find out, for metallic wear, whether the wear rate is determined by the void nucleation process with crack propagation following relatively rapidly to delamination or whether a slow propagation of the

crack is preceded by the process of ready nucleation of voids. In polymers it would be expected that rupture of bonds would occur rather than void creation in the metallic sense as described in the above referenced works.

Jahanmir and Suh [104] have reported that if a large number of inclusions exist, as is the case here with magnetic media having some 70% by weight and 50% by volume of magnetic particles [23], then the nucleation of cracks will not be the rate determining step. This may almost be put down to probability theory whereby nucleation is "bound to occur somewhere" with so many potential sites available. It is felt that the rate of propagation of cracks determines the rate of wear.

The mechanisms of the propagation of sub-surface cracks and the nature of the distribution of stresses was investigated by Fleming and Suh [105]. The material in front of the asperity being deformed by the slider is plastically deformed but that behind it is under tension and elastically deformed in a shearing action. This means that any part of the crack in the plastic region is compressed together with the two free surfaces of the crack also pushed together which will not cause crack growth (but see later for the possible effect of the bulk lubricant in magnetic media). The part in the elastically deformed region, however, is under tension and the two separate surfaces created on crack nucleation are pulled apart. It is when the leading tip of the crack is in this elastic region that it is encouraged to grow. The wear particle lamina is created when the length of the crack is such that the shear stresses in the material still in contact with the bulk are sufficient to overcome the yield stress. At this point severing of the lamina from the bulk occurs.

The analysis of Fleming and Suh [105] is that of a linear elastic fracture mechanics and only the tip of the crack is involved which means that the length of the crack has no bearing on its propagation speed. The stresses at the surface combine such that the resultant stress reaches a maximum at some distance below

the surface from the point of contact. It is at this point that the crack propagation rate is maximised. The stress is intensified at the crack tip and the stress intensity factor falls as $1/r$, the distance from the crack tip. Its value depends on the coefficient of friction to the extent that as this coefficient increases, the depth at which the crack propagation rate is greatest increases leading to greater wear particle thickness for larger coefficients of friction and hence more rapid wear. The stress intensity factor is discussed further in Chapter 7. Also, since the coefficient of friction is defined by:

$$\mu = F/N \quad (3.5.1)$$

where F = frictional force

N = force normal to surface

The increases in the coefficient of friction implies an increase in F if the normal force remains constant, as it does in this case. The stresses propagating the sub-surface cracks can be expected to be greater and the rate of crack propagation can thus be expected to be increased also leading to a further increase in the rate of wear as the frictional force increases. A similar increase in the stresses would occur in the case of an increase in the normal load applied, for a given μ , and a similar increase in the wear could be expected to be noted.

The fact that the frictional coefficient for polymers is often related to the roughness of the surface (and asperity elasticity) [60], [86] means that this factor affects the thickness of the wear lamina particle created. The other effect of roughness may be that, as observed by Jahanmir and Suh [105] the size of the asperity contact determines the depth at which the stress field is maximum, and so the region in which the crack growth is maximum. This may lead to the thought of having a large range of asperity sizes so that for each one this factor is

maximised at different depths leading to less coalescing of cracks. This is not the case, however, as intuitive considerations tend to suggest that the largest asperities will be relatively few in number and, as a consequence, likely to yield plastically until they are all approximately the same size thus returning the situation to the point where most of the asperities support the load applied with each one being slightly deformed. The stress fields caused by the loaded abrader in the sub-surface regions of the media are not so easy to visualise as may be imagined [107].

Several points, though, need to be noted which show that the analysis of Jahanmir and Suh [105] is by no means the ultimate one: the work has been done only for a coefficient of friction greater than 0.5 and a mechanism other than linear elastic fracture mechanics may be required to explain crack elongation for lower values of the coefficient of friction. Although Cummings [36] has indicated that the friction coefficient is consistently in this range for the floppy diskettes that have been studied, some provisional work suggests that lower friction media tends to last longer in tests [36]. This indicates that the requirement for lower friction is paramount and then this model using linear fracture mechanics may not apply to diskette media either. Furthermore, many factors have been excluded from the analysis, such as the fact that sliding has a tendency to cause the existing cracks to link up which speeds up the elongation process and causes more rapid wear than is predicted by Jahanmir and Suh [105].

As mentioned above, the rate of progression of the sub-surface cracks is probably the factor which determines the rate of wear. The relationship between the two phenomena was studied by Fleming and Suh [106] for aluminium alloys. No final conclusions were reached but it was felt that correlation of wear rates with crack propagation rates was a strong possibility in light of the fact that the other factors played an equal part since they were the same for both of the samples tested there. The part played by the propagation rate and depth of sub-

surface cracks in determining wear coefficients was investigated by Suh and Sin [108]. The role of the stress intensity factor was also revisited and it was reported that using a finite element analysis method, the values obtained were closer to the actual wear rate when compared to Jahanmir and Suh [105] whose values were too small. The new values were still on the small side, however. It was found that the maximum value of the stress intensity factor increased as the cracks closer to the surface were analysed. Also described was the fact that the cracks which were very close to the surface tended to behave in such a way that the linear elastic fracture mechanics was not applicable [108]. This was because the crack tip was no longer ever in a region of elastic deformation but rather always in an environment of plastic deformation. This meant that the crack was not propagated through shearing of the top layer across the bottom one in a plastic fashion and, thus, a change in the rate of increase in the crack length occurred.

The conclusions reached by Suh and Sin [108] were that the rate of wear was proportional to the real area of contact of the two interacting surfaces; the depth of the crack relative to the surface; average growth of the crack per N passes of the abrader in cyclic stressing; and to the inter-asperity spacing and inversely proportional to the inter-crack spacing between adjacent cracks. It was also noted by others (such as Bhushan and co-workers [23], [83], [86]) that the total number of asperities in contact increases, rather than the real area of contact for each asperity when the normal loading is increased. In view of this, Suh and Sin [108] also showed that wear rate depended directly on the quotient L/H where L is the normal load and H the hardness of the abraded material. The expression obtained for the wear rate showed that the hardness, a measure of the resistance to deformation of the surface, reduces the crack nucleation rate. Increased plasticity (ductility) also reduces the crack growth. As these parameters are both desirable but do not exist together in a material, a compromise needs to be struck between them to provide the greatest wear resistance.

In the above discussion the crystallinity inherent in normal metallic

structures has been cited as being disturbed and dislocations formed in the material. This is the form of the theory of delamination as originally presented by Suh [95]. It would be correct, of course, to say that the surface layers of the magnetic medium do not contain crystalline lattices and hence no dislocations in the metallic sense can be present.

However, all particulate media contains hard particles in the form of the magnetic particles employed, but their analogy to hard sites in metals can only be used to a limited extent since there are no crystalline dislocations of the metallic nature in the present material.

In concluding this chapter, it may be noted that the studies on tape and diskette media materials have not revealed any hints as to the mechanisms of wear of the media although the consequences (spacing losses etc.) are clearly observed and understood. The delamination theory of wear which was originally proposed for metals, however, appears to fit the criteria well as the highly filled polymers of the magnetic media surface provide good inherent crack nucleation sites as well as the ease of propagation in view of the binders used for the magnetic layer. This warranted further investigation for confirmation of delamination as the mechanism of wear in diskettes: this has been one of the investigations made here and the results presented appear to be promising.

Chapter 4

Experimental Rigs and Rig Development

Chapter 4.

Experimental Rigs and Rig Development.

Introduction.

There have been five different rigs used in this project. This has been essential because, as mentioned in the introductory chapter, the field is a very much unresearched one. As a result the rigs described here have been used to investigate different aspects of the wear process and the effects of various parameters on durability.

The rigs are described more fully below but they are:

- (i) Model TM100-2A Tandon double sided 48 TPI 5.25 inch diskette drives;
- (ii) a supported sample simulation rig
- (iii) an unsupported sample simulation rig
- (iv) an in-situ friction testing device
- (v) bit analysis apparatus.

This chapter describes these rigs and the modifications that were necessary before they could be used to obtain reliable data.

The reason for using such a variety of configurations was so that the different aspects of wear might be isolated. The Tandon drives were used to enable the investigation of the in-situ wear experienced by the diskette media under normal use. As such, the drives' hardware has not been modified. Furthermore, they were expected to produce data relating to durability for each of the different samples employed. The two simulation rigs were designed to

simulate the conditions encountered at the two head-media interfaces in a double-sided diskette drive. Each one simulates these conditions such that the effects of the other head are removed. This enables study of the contribution of selected parameters to the wear process. Data relating to the durability of samples under these conditions was also expected to be generated so that it could be compared to the "in-situ" data in order to determine any correlations.

4.1 Tandon TM100-2A Diskette Drives.

These are commercially available diskette drives (Model TM100-2A) and are manufactured by the Tandon Corporation in California. They are designed to read 40 concentric tracks per surface at a track density of 48 tracks per inch (48 TPI). Any four of these drives may be connected to a single diskette drive exerciser or tester [109] and in this study eight drives were connected to two such testers. These testers were connected so that the drives are "daisy-chained" and any one of the four is capable of being accessed via the same flat ribbon cable at any one time. The four drives are fixed within a common housing and each of these drives consumes 15 W of power at maximum. They have been connected to the tester via a specially designed hardware interface circuit (Fig. 4.1) so that the drive motors may either be gated with the drive select lines, or not, as required. This means that the circuit of Fig. 4.1 allows individual drive motors to be turned on when that drive is selected. However, it is possible to turn on all of the drive motors by altering the position of the four-pole-two-way switch (Fig. 4.1). The reason for using the gating circuit was that if all of the drives were required for a test then this could be done. If only one drive was required, then gating reduced the heating effect and saved on power as well as extending the life of the drive motors. The latter was probably the most important factor as the louvered top of the enclosure ensured adequate ventilation and prevented

overheating. It was necessary not to run the drive motors unnecessarily in order to maximise their life. This was important because the drives needed to be run continuously for long periods for some tests as will be observed from the data presented in chapter 6.

The drive testers are capable of performing many tasks but the devices have not been used to their ultimate capability and were used only for the following functions:

- (a) setting the drives on the track to be tested
- (b) formatting and reading back to ensure the diskette to be tested was not

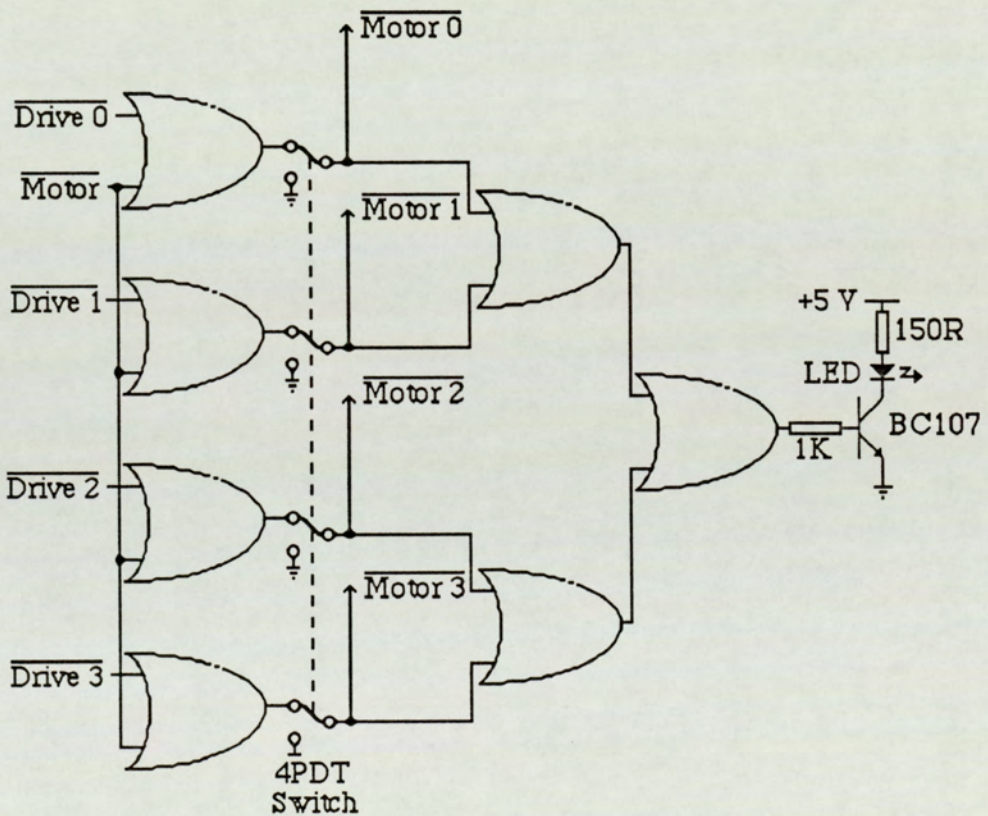


Figure 4.1 The circuit enabling gating of the drives' motors to their drive select lines. The circuit is shown in the "gated" mode. All lines are active at a logic LOW.

- faulty before testing
- (c) writing and reading back the "worst possible recovery pattern" (see later for details) to test suspect diskettes
 - (d) to check drive alignment with respect to reference tracks on a special diskette

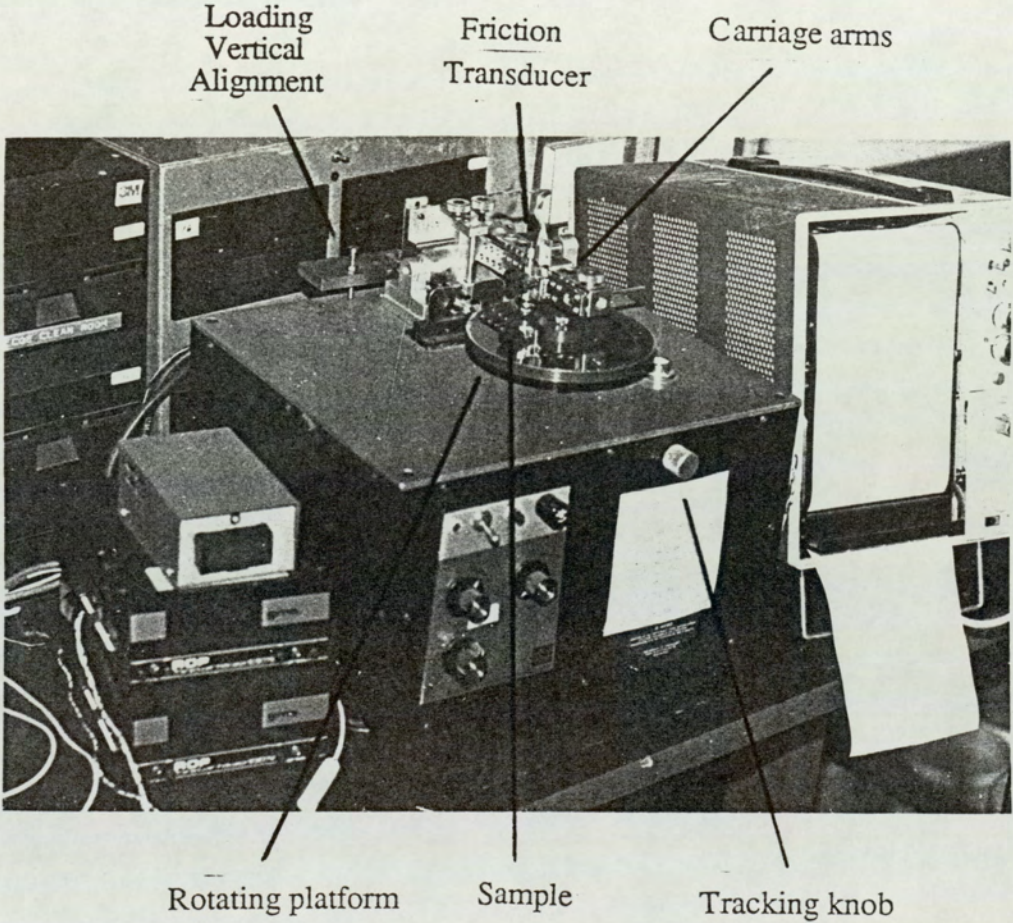
The only modification made to the drives has been the interface circuit of Fig. 4.1 as mentioned above and the changing of heads as and when required. The gating circuit was designed and built especially for this work.

4.2 Supported Sample Simulation Rig.

This rig is illustrated in Fig. 4.2. It was designed for conducting wear tests where the diskette is fully supported from the underside while an abrader is loaded from above onto the upper side. This rig is similar to the one used by von Behren [64] with test-tubes loaded onto the media as described earlier in Chapter 3. As received, the rig consisted of a rotating metal disc support for the diskette driven, through a belt drive mechanism, by a DC motor monitored by a servo-control mechanism. The abraders were loaded vertically onto the media by being attached to the carriage arm protruding radially across the sample support disc. A force measuring transducer was loaded on a parallel arm with the detector touching the abrader carriage assembly. The loading of the abrader onto the media surface, as originally designed, was achieved by a counter-balance arrangement.

Under this regime, the arm holding the abrader was set off balance by counterweighting until the required loading force was obtained at the radial position of the head holder. The problem with this system was that it provided high inertial loading, as described in Chapter 3, and it has been altered (see

Figure 4.2 The supported sample simulation rig.



Loading
Vertical
Alignment

Friction
Transducer

Carriage arms

Rotating platform

Sample

Tracking knob

below). The loaded abrader could be placed anywhere along the head carriage arm and was held in place by screws. The position on the diskette supporting platform could be fine tuned by the use of the tracking knob indicated in the Fig. 4.2. This works through a standard screw to linear motion mechanism. As mentioned above, another arm runs parallel to the head carriage arm which bears a friction force measuring transducer mounting. This transducer could be clamped anywhere on its carriage arm alongside the head holding mechanism mounted on its carriage arm (described below). It was possible to rotate both of these arms in a vertical plane about a pivot so that the abrader could be accurately loaded in a true vertical direction. In addition to this, the head carrying arm could also swing in a horizontal plane so that the frictional force would be translated to the transducer. The transducer output goes via a type 17403 AC carrier amplifier plug-in in a Hewlett-Packard 7402A chart recorder to a YEW type 3057 Portable Chart Recorder. The calibration of the transducer has been presented in Appendix A.

This rig was meant to simulate the stressing of the media which occurs without penetration into the plane of the diskette as is found at the side 1 interface inside a diskette drive. It provides a method for studying wear without flexing the media. This study was necessary because it was felt at the beginning of the project that the continual flexing of the media could lead to fatigue fracture of the diskette.

In order for the servo control to stabilise, it was necessary to run the rig for 15 minutes prior to the start of each experiment. With this control it is possible to vary the speed continuously between zero and over 400 rev.min^{-1} , although at speeds below 10 rev.min^{-1} the motion is in discrete and uneven steps. The calibration of speed is given in Appendix A for the rig after it has been running for a while (operating calibration). The rig was operated at drive speed, that is 300 rev.min^{-1} .

Several modifications have been made to this rig. One was for the purpose of counting the number of revolutions made in a particular run in order to enable the total number of traversals over the same point to be known, if required. A completely new apparatus for loading the abrader onto the media has been designed and implemented. This was necessary as the old method, briefly

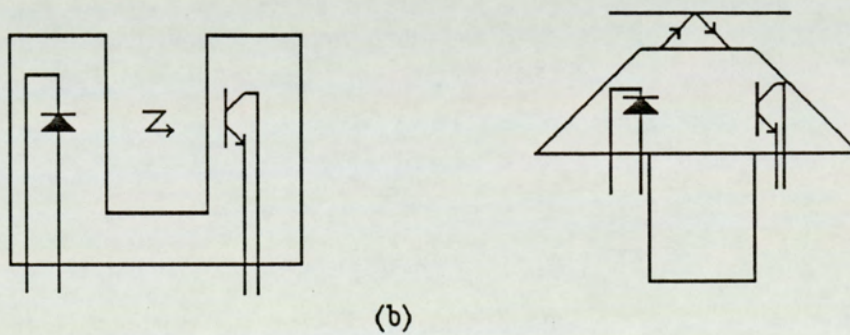
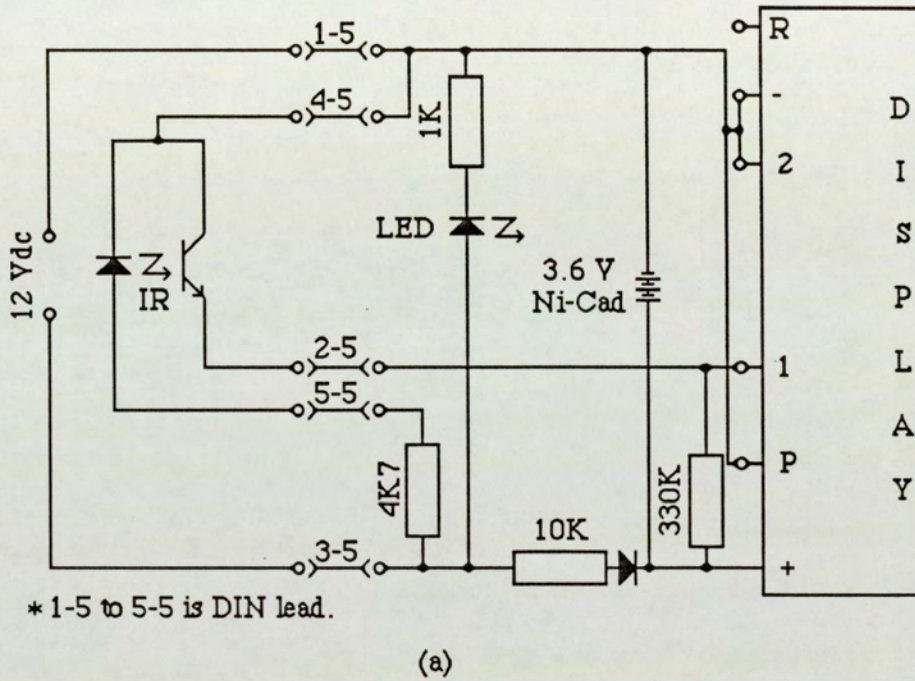


Figure 4.3 (a) The circuit diagram for the counter constructed to count the total number of passes made by the media and (b) the sensors used on either simulation rig.

described above, meant that the inertia of the loading arm was so high as to prevent the movement of the abrader in sympathy with the topography of the diskette surface. The supporting plate of the rig has also been modified as it had a peak-to-peak vertical run out of some 40 μm . The glass abrasers used by von Behren have been replaced. Heads from production model drives have been employed. These modifications are to be discussed individually below.

The circuit for the counter is given in Fig. 4.3 most of the work in which is done by the integrated circuit contained within the commercially available display module with the rest of the (discrete) circuitry relaying the positive going pulses for the counter enclosed there. Part of the discrete circuitry also maintains a back up Nickel-Cadmium rechargeable battery at full charge. The ultimate source of the pulses is the interruption in the reflection of the infra-red beam from the rotating shaft by a piece of black tape. The infra-red source and detector composite unit has been mounted inside the casing of the rig in order to prevent interference from background infra-red radiation. It was found that the unit could not be operated without this shielding as the background was so high as to swamp the detector.

The other modification is shown in Fig. 4.4(a) and concerns the fact that the wear of the samples was very severe on this rig as initially designed. This was due to the fact that the inertia of the loading arm was so high that it did not enable the test head to naturally follow the undulations of the diskette surface. Of course, inside the drive the diskette is somewhat more free to move but that is through it flexing and the supported sample rig is designed to eliminate that particular variable. The original high inertia loading caused massive plastic flow even when the nominal loading was similar to that in the drives. The device of Fig. 4.4 (a) was produced to overcome this problem. It enables the loading of a production head onto the media for the correct material interface. In the present case, the test head used was a side 1 head as removed from the head assembly in

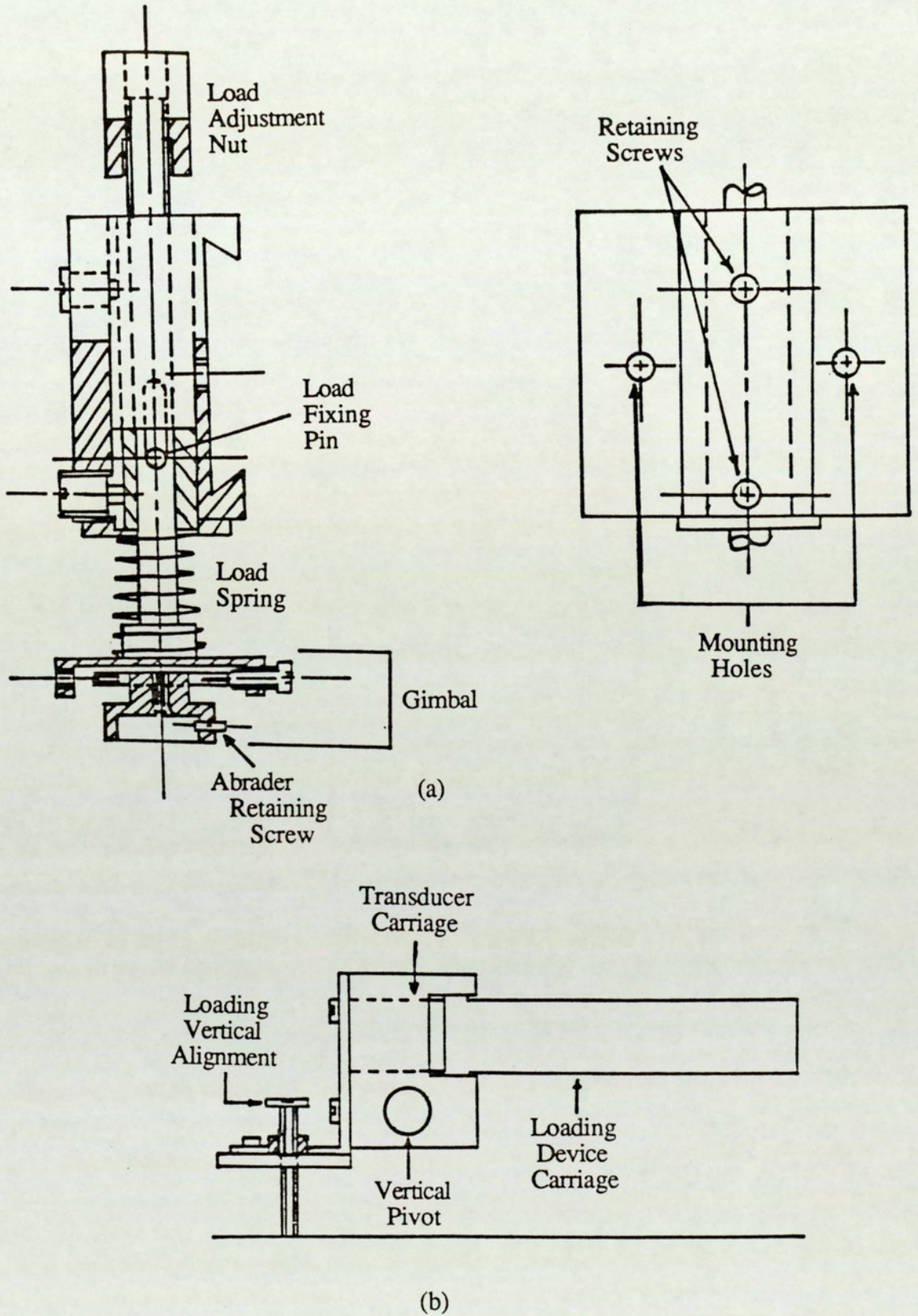


Figure 4.4 (a) The low inertia head loading device for the simulation rigs and (b) the carriage arm onto which it is mounted.

a 5.25 inch diskette drive so that a realistic head-media material interface was created.

The device illustrated in Fig. 4.4(a) works by eliminating any movement in the arm by fixing it horizontally. The arm is fixed horizontally with the aid of a spirit level using a screw as shown in Fig. 4.4(b). The nominal loading then comes only from this new, specially designed device for housing and loading the head and is achieved by the use of a very soft spring. This is done by adjusting the compression in the phosphor-bronze spring using the loading adjustment nut. At minimum compression of the spring, the loading on the gimball arrangement is 0.1 N and at maximum compression it is 0.2 N. The loading may be set to any value between these extremes but has been fixed for the purpose of this investigation at 0.2 N in order to reflect as accurately as possible the situation prevailing in the diskette drive. The way to use the device is to lift the gimball arrangement housing the test head up through the part fixed to the carriage arm. This may be done by lifting the inner pin attached to it. The test head may then be retained in this non-contact position by securing the position of the inner pin with the retaining screws. The original carriage arm attached to this assembly is then set horizontal using a spirit level before the test head is loaded onto the media by releasing the retaining screws. This releases the test head and permits it to make contact with the diskette on the rig's rotating platform. Re-tightening the retaining screws enables the preset loading to operate with an inertia comparable to the head assembly in the drive.

It was because the inertia problem had been solved that a hitherto unknown problem came to light. This concerned the run-out of the platform as shown in the Fig. 4.5 overleaf.

The value of the run-out was about $40\ \mu\text{m}$ (peak to peak) as measured with a clock gauge, which is small by engineering tolerances, but in a study concerning the wear of the magnetic layer, which can be as little as $1\ \mu\text{m}$ thick for

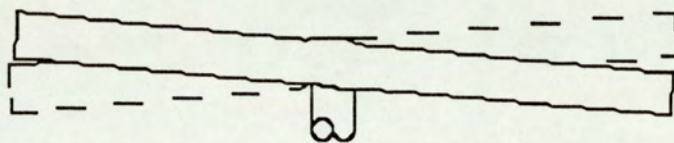


Figure 4.5 The run-out in the supported sample rig.

the "hi-density" diskettes now available, it can be appreciated as being extremely significant. In fact, it is of the order of half of the thickness of the whole diskette at a nominal $79\ \mu\text{m}$! Machining the rotating platform in-situ was attempted to solve the problem. In-situ machining was attempted as an error of this magnitude may be produced when mounting the platform onto the drive shaft. Although this improved the situation considerably, the final run-out at $12\ \mu\text{m}$ (peak to peak) is still quite serious compared to the thickness of the magnetic layer. A further incidental improvement has been achieved with the new low inertia loading mechanism allowing the head assembly to follow the run-out. A better solution to the run out problem would have been to use a bearing in the drive mechanism of the platform instead of the bush employed in the original design. It was not possible to implement this because of financial considerations.

4.3 Unsupported Sample Simulation Rig.

The purpose of the unsupported sample rig was to study the effect of flexing of the media as well as the simple wear found on the supported sample rig. The formation of the so called side 0 "bubble" as described by Skelcher [60], and discussed in Chapter 3, could also be studied. Obviously, any other contributions could also be considered. This includes factors such as the run-out

on the supported sample rig. In this case, however, the particular problem of run-out was not considered to be significant as the side 0 head actually intrudes into the plane of the media. How this happens is made clear later on.

The initial idea was to use this arrangement to study the contribution to wear due to fatigue in the material of the media as the diskette flexes and unflexes. This happens as the media passes over the side 0 head and forms the stationary wave pattern of the side 0 "bubble" referred to in Fig. 2.9 of Chapter 2. It was considered that the flexing which occurs due to this standing wave pattern, may cause damage akin to the repeated bending of a metal wire and, in a similar fashion to such a wire, ultimate failure of the diskette. This could be failure either in the magnetic layer or in the backing material, polyethylene terephthalate. This rig was intended to provide a situation intermediate between the simple wear of the media caused on the supported sample rig and that encountered in the drives.

The study of the penetration of the test head into the diskette plane was achieved by the use of a similar rig to that of section 4.2 with the exception of the groove in the platform. This enables the diskette to flex under the loading offered by the head's own weight and its loading mechanism. The form of the rotating platform used in this case is illustrated in Fig. 4.6 below.

There is one important factor: the form in which this rig has been manufactured, the annular groove produced in the platform is much too deep.

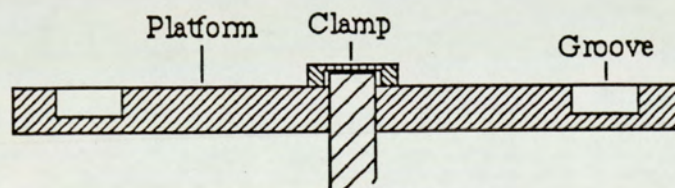
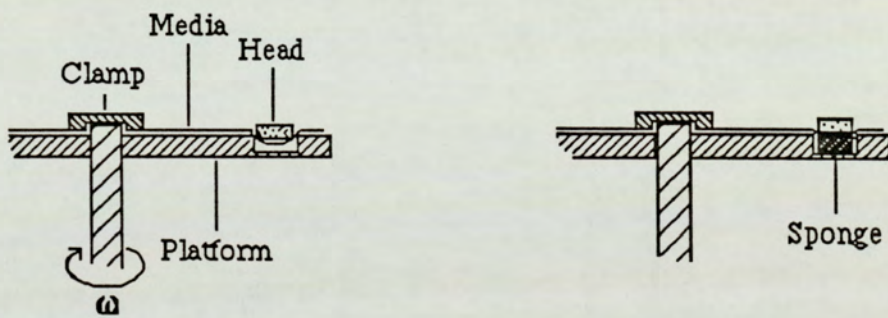


Figure 4.6 The rotating platform used in the flexing sample rig.

Although this depth was unimportant in the rig's original use with glass test-tube abraders, with real heads being used in this study it is very significant. This has made a modification necessary whereby a piece of sponge provides a very slight support for the media so that flexing of it still occurs when loaded with the head. The reason for this is that in the absence of the sponge an unrealistically small flexing radius is produced which results in the edges of the magnetic transducer causing ploughing wear to occur as these edges score the surface of the media and the rest of the head does not make contact with the media at all. This is a mode of wear which does not occur in practice. Fig. 4.7 below shows the situation before and after the insertion of the sponge.



(a) Without the sponge ...

(b) ...and with it.

Figure 4.7. The role of the supportive sponge in the flexing wear studies.

The other modifications to this rig are the addition of a counter of the same type as fitted to the supported sample rig, in this case the detector is of the beam interruption type as illustrated in Fig. 4.3 rather than of the reflection type. Also, a holder of similar design to the low inertia device of Fig. 4.4 (a), as has been used for the supported sample rig, has been employed on this rig. The head used on this rig is a side 0 head as removed from a production diskette drive's

head assembly. This enables not only the correct material interface to be established, but also reflects more accurately the conditions leading to the formation of the side 0 bubble.

4.4 In-situ Friction Testing Device.

The friction testing apparatus has been produced to investigate the in-situ frictional forces that are experienced at the head-media interface. As is discussed in Chapter 3, the real area of contact between the head and media is expected to be of critical importance in friction and wear. This is because for polymers in general, and for magnetic media in particular, the friction appears to be intimately related to wear. It is for this reason that the measurement of the frictional forces at the head-media interface is of paramount importance. Another point to note is that most of the in-situ tested samples using the drives have shown that it is the side 0 of the media which is damaged first. Of course, it would be expected from the above theory that the frictional force at this head would be higher. The supporting evidence for this is that the side 0 bubble leads to there being more head-media contact at the side 0 head as compared to the side 1 head. This rig can directly measure the force at both heads and confirm or deny these speculations.

The friction tester has been constructed such that the two heads are free to move in a horizontal plane parallel to the diskette surface and independently of each other, unlike the situation prevailing in the drives. The fact that the heads can move independently of each other, means that independent measurement of the frictional force experienced at either interface may be made. The forces are detected directly by two sub-miniature load cells. The cells which are used are Model 31 (side 1) and Model 33 (side 0) and are manufactured by Sensotec, USA. These devices, which are situated on a specially constructed mounting,

are powered by separate devices described by their manufacturers (RDP Electronics Ltd., Wolverhampton, England) as "Model E307-2 Transducer Indicators". The cells output a voltage, which is linearly dependent on the friction force measured, to their individual E307-2 devices. These serve a second purpose in that they amplify this signal and display it on a digital display incorporated into them. As a result, it is possible to get a direct numerical reading of the instantaneous frictional force (in grammes equivalent) at any time. The analogue output from these E307-2 amplifiers is fed into a dual pen chart recorder which records the frictional force at each head as an ink trace. The arrangement, which is based on that used by Skelcher [110], is illustrated in Fig. 4.8. The whole device is carefully fitted onto a purpose made bracket and into a custom-modified diskette drive unit and aligned in every direction using vernier linear and rotational micrometers. This enables the heads' penetration etc. to be set as required. Furthermore, the arrangement also enables the "angle of attack" of the head as seen from the diskette's frame of reference, to be modified both in the direction of rotational motion of the diskette and in the direction of the motion of the heads on tracking motion that is, both circumferentially and radially. That is to say that, the pitch and roll can be independently adjusted. Diskette penetration and angles of approach similar to those found in the commercial drives have been used here as far as possible. This means that the side 0 head has been aligned flat using eye judgement and a spirit level. The gimball flexural arrangement which accompanies the Side 1 head enables it to conform to the side 0 alignment under "rest" conditions. The penetration of the side 0 head, which helps in the stabilisation of the media as it passes over this head [33],[60], has been set at 0.635 mm. This is similar to that found in the commercial drives being used [60] to study in-situ wear.

The major problem that needed to be overcome with this apparatus was that of the thermal instability of the output from the load cells as the voltage

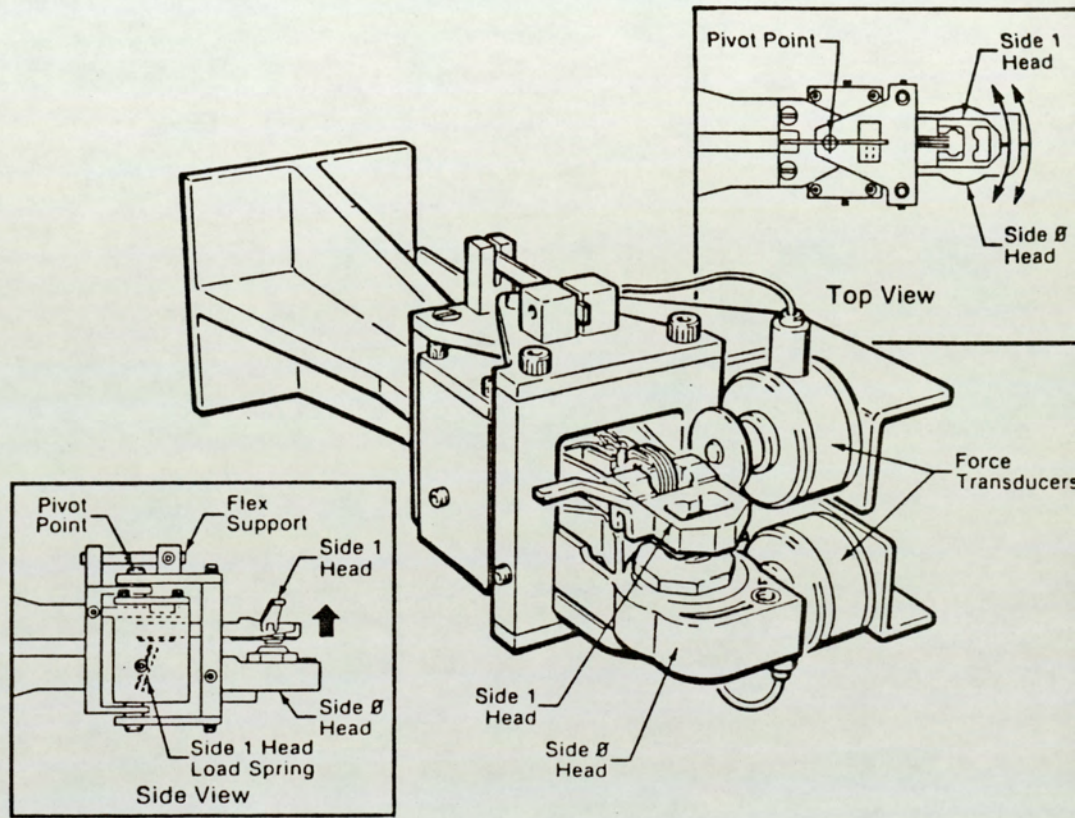


Figure 4.8 Heads and transducer arrangement in the in-situ friction tester.

appeared to vary considerably. The nature of this problem is illustrated in the graph of Fig. 4.9 below. This shows that the voltage output by the load cells varies in a linear fashion with temperature if the loading on the cells is kept constant. In the case illustrated in Fig. 4.9, all stressing was removed. The fact that one cell appears to have a negative temperature coefficient and the other a positive coefficient, has been resolved by simply reversing the signal polarity into the relevant amplifier by interchanging the wires. The method by which the underlying problem of thermal instability has been solved is through the use of a thermostatically controlled heater circuit which maintains the temperature of the

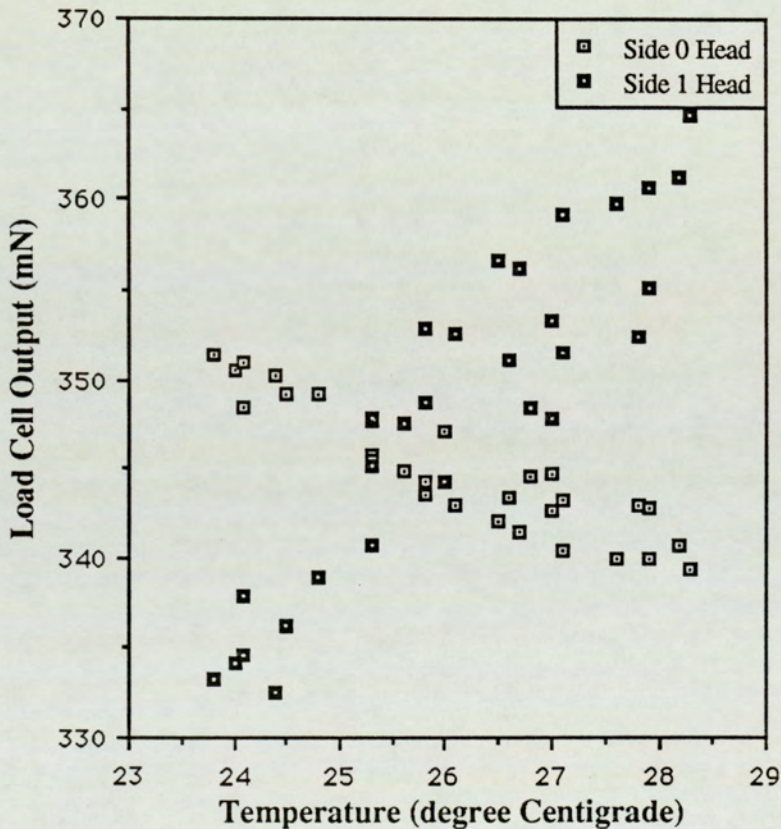


Figure 4.9 The variation of the output of the load cells before compensation due to changes in the ambient temperature; this output has been taken under zero load conditions.

load cells at some preset value. It not important what this value is as long as it is well below the maximum recommended for the load cells and above any temperature that is likely to be attained by the surroundings; a temperature of about 35 °C has been selected. The electronic circuit designed for this purpose is given in Fig. 4.10. It should be made clear that the two cells' temperatures are monitored independently of each other by separate thermistor detectors and also independently heated by independent heating coils. In fact, each cell has been provided with a total of two coils of approximately 25 Ω each. One of these is used to heat the load cell itself while the other is employed in heating its mounting bracket near to where it is mounted as it was discovered that a temperature gradient developed across the cells if this was not done.

Further measures which have been implemented have been in consideration of the fact that the load cells, whose maximum loading is only 0.5 N, are very sensitive to external vibration. In order to reduce this extraneous "pick-up" the whole device has been mounted on a platform and placed on anti-vibration rubber. The author's intuitive feeling is that further improvements to the apparatus may be made by the mechanical isolation of the drive motor from the rest of the rig. However, as this is a far from trivial task, it has not, unfortunately, been possible to implement this modification here.

4.5 Bit Analysis Software.

This software was meant to be used to test individual data bits of the tracks on the media so as to determine whether failure occurs preferentially at any particular point on any particular track. If this was the case, then it was intended to identify these areas of initial failure so that the physical methods of analysis described in chapter 5 may be employed to study these mechanisms of initial failure.

Some initial software for the purpose of this investigation has been

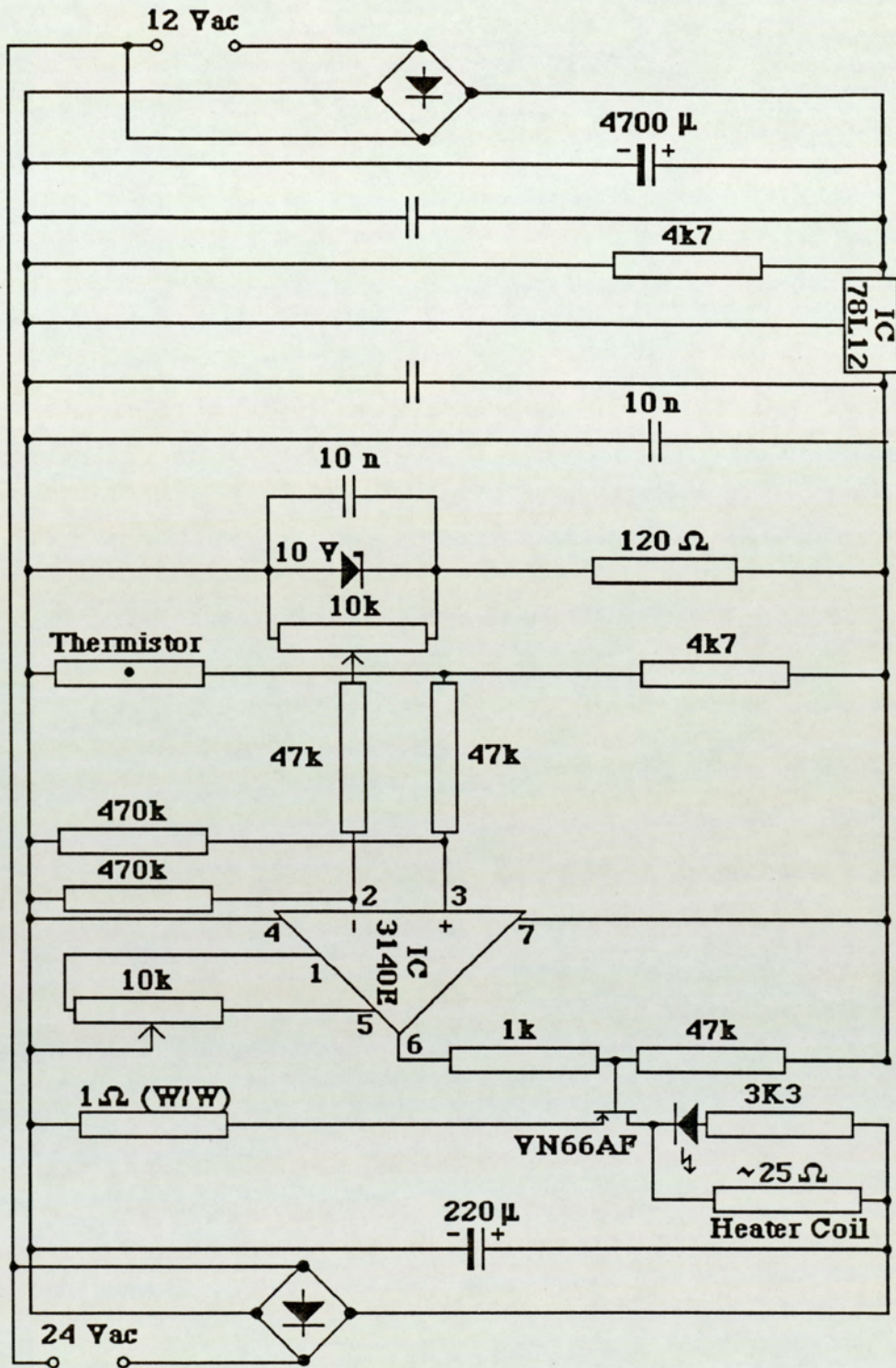


Figure 4.10 Circuit used to achieve temperature stabilisation of load cells.

developed by Pendergrass [111] and it includes routines to control certain of the drives operations such as seeking to a particular track. It does not, however, contain any means to identify which part of the diskette records a failure. Further development of this software obviously needed to be made in this direction as well as towards the production of controlling software and a master control main programme to acquire the data and record it onto data diskettes and a printer for instant reference.

The routine required most urgently was one to read data. This has been done and the full utilities package of routines used has been listed in Appendix B as well as the control routine. The working of the master programme and these subroutines are described below. The original software and the modifications are outlined in brief as the software is quite involved and complex. It has been written in 6502 assembly language which has been considered in detail in the text by Andrews [112] and reports by Crossley [113], Uhley [114] and Bongers [115]. They have also considered the special hardware and software features of the Apple machines. Since the software has been designed completely using the Apple® //e® microcomputer, further detailed information concerning its programming language [116], the Disk Operating System [117] and Machine Operation [118] has been used.

The main programme has been designed to enable as many or as few of the six drives employed to be tested at any one time. In order to understand the first lines of the master programme, it is necessary to consider the hardware of the Apple //e. The selection of head and track is possible individually on each drive so that the drives may all be testing on different tracks, and on different surfaces, of the media in each drive. The hardware arrangement of the Apple //e is such that the auxiliary slot and the slot 3 may not be used simultaneously. The slot 3 has been employed here for a timer using a circuit and software originally produced elsewhere [119]. It has been necessary to modify that software for

employment here. This limits the number of slots which may be employed for test drives' interfaces in the form of "Disk II Cards". These are described in the Apple //e User Manuals and are used to control the functions of two attached diskette drives per card either through a disk operating system or, as in this application, by machine code programme manipulation of these cards. The slots have been allocated as follows:

- Slot 1: Printer interface (Parallel/Centronics card)
- Slot 2: Test drives 1 and 2 (Disk II card)
- Slot 3: Real-time clock card
- Slot 4: Test drives 5 and 6 (Disk II card)
- Slot 5: Test drives 7 and 8 (Disk II card)
- Slot 6: Data drives 1 and 2 (Disk II card)
- Slot 7: Analogue-to-Digital + Digital-to-Analogue Converter (ADC + DAC) card
- Auxiliary: Unused (as Slot 3 is in use)

Considering the programme now, it requires input of certain parameters: whether the prompted drive is to be used; if so, then the track to test, the head to be used, datafile to which all the information for that test drive is to be directed; the code-name of the sample to be tested; the factor by which to reduce the head read signal (see later). This information is then recorded in the named file on the diskette in the data drive 2. The next operation reads the current (real) time from a real time clock card in the slot 3 of the computer which is constructed in accordance with the details given for the original design [119]. This clock is read using a substantially modified version of the routine also presented there for this purpose. This new clock read routine starts at line 1200 of the main programme; the clock is set up between lines 250 and 450 also in the main programme.

On execution, with all parameters entered and confirmed, the program locates the R/W head to the correct track using the machine code routine "SKSET" between lines 348 and 396 of the assembly language as originally provided by Pendergrass [111]. This routine also checks if a Slot or drive number has been selected which is disallowed for the reasons described above in the outline of the Apple //e hardware. If such an illegal quantity is detected, then an appropriate error message is issued and execution of the programme is terminated.

The machine code section starting at the label "WRITE", between lines 153 and 239, is called to write a full track (in fact, just over to make certain) of binary "1" data bits. Pendergrass [111] has provided at this point for the diskette to be checked for "Write protection" and an "Index pulse". If the diskette is write protected (that is it is not meant to be re-written over), an appropriate error message is issued and the user given a choice between terminating the programme and restarting or continuing with the next test drive in the sequence. The index pulse is read, for the purposes described in chapter 2, via the ADC + DAC card in slot 7. If the pulse is not present because, for example, the diskette does not rotate or the drive's front latch (Fig. 2.12, Chapter 2) is not closed, then an appropriate error message is issued and execution termination choice is offered as previously for write protection. If the results of the write protection and index pulse checks are both satisfactory, then the write operation proceeds. This procedure is repeated for all of the drives selected at line 90 of the main programme for testing.

The data is then re-read from each drive in sequence to test for failure. The index pulse check is made each time to ensure that the drive is still operating properly. The index pulse is also used to detect the point at which to start the read operation so that accurate reference may be made to where any failure is detected. The way in which this is done is to use the trailing edge of the index

pulse, which is an average of 4 mSec. duration [62], to start the read operation. The read routine has been modified from that originally used by Pendergrass [111] as it did not allow for immediate checking of the data read in or for recording the point at which any detected failure had occurred. In the present routine, labelled "READ" (lines 252 to 292 of the machine code, Appendix B), provision has been made for both of these by considering the number of clock cycles taken by the 65C02 Central Processing Unit (CPU) to execute each of the machine code instructions and the amount of time taken to read the data and process it via the hardware.

The details of the routine are such that after the usual index pulse checks, between lines 252 and 266, the routine sets up two counters between the labels "RDNOW" (at assembly language line 269) and "READBYT" (at Assembly Language line 275) to identify the sector and the byte in that sector which is being processed. After the data has been read, it is compared to the byte (in binary) "11111111" (or Hexadecimal \$FF). If the comparison reveals no differences, that is, no errors, the routine is exited, after the whole track has been compared, at assembly language line 287 and the next drive is prepared for a read operation. If, however, the comparison does reveal an error, then the routine is terminated at that point after the counters containing the identities of the sector and byte as well as the value of the bad byte have been stored in memory (assembly language lines 288 to 292); an error detected flag is also set. Control is then returned to line 870 of the main programme. The stored values are then compared to the values of the same parameters for the same drive for previous read errors, if any. If this results in a total of three consecutive errors at the same sector and byte in that sector, and the bad byte has the same value each time then the same bit is in error each time. This results in the drive being de-selected and the read failure data being recorded on an on-line linked printer and on to data diskette in data drive 2. However, if any of the sector identity, byte identity or bad byte value are not the same as previously, then the error is recorded as a

"soft" (that is, recoverable) error and the drive continues to be tested in sequence. The real time (from the real time clock card in slot 3) is also recorded for consistent "hard" (or non-recoverable) errors. This, in conjunction with the time recorded at the start of the tests, enables the total test time for a particular sample in a drive to be established. Once a drive has produced a consistent hard error, and its de-select flag has been set, its activity indicator LED (Fig. 2.12) is extinguished by software control in the programme and that drive is not read again. When all of the drives' de-select flags are detected as set by the main programme, it stops execution after displaying an appropriate exiting message.

One extra point which should be mentioned here is that the drive to computer interface is obtained via a custom designed electronic device. The circuit diagram for this is reproduced in Fig. 4.11. This essentially interfaces the 20 pin header of the Apple //e microcomputer to the 34 Pin header of the Tandon drives. This circuit has been taken from part of Pendergrass's original interface [111] which reads the analogue signal from the drives.

The final point to consider is that the read-back amplitude has been tailored in all tests to be 50% of that normally detected. This has been done in the analogue part of the logic control board of the diskette drives by tapping a voltage from an externally connected potentiometer. The reason for doing this is that it is not expected to change the durability of the samples relative to each other but can be expected to increase the data acquisition rate as the threshold for the readback circuits is reached with less wear on the media. Even in the present case, the media has to be worn until the backing is visible in certain parts before any losses can be detected. Details of this are considered in the results chapter. A further reduction in the signal was attempted by reducing the value of the active arm of the potentiometer employed such that the signal read-back from a standard alignment test diskette [120] was only $1/3$ of its maximum value but this produced failure to read conditions on the first attempt and had to be abandoned as a result!

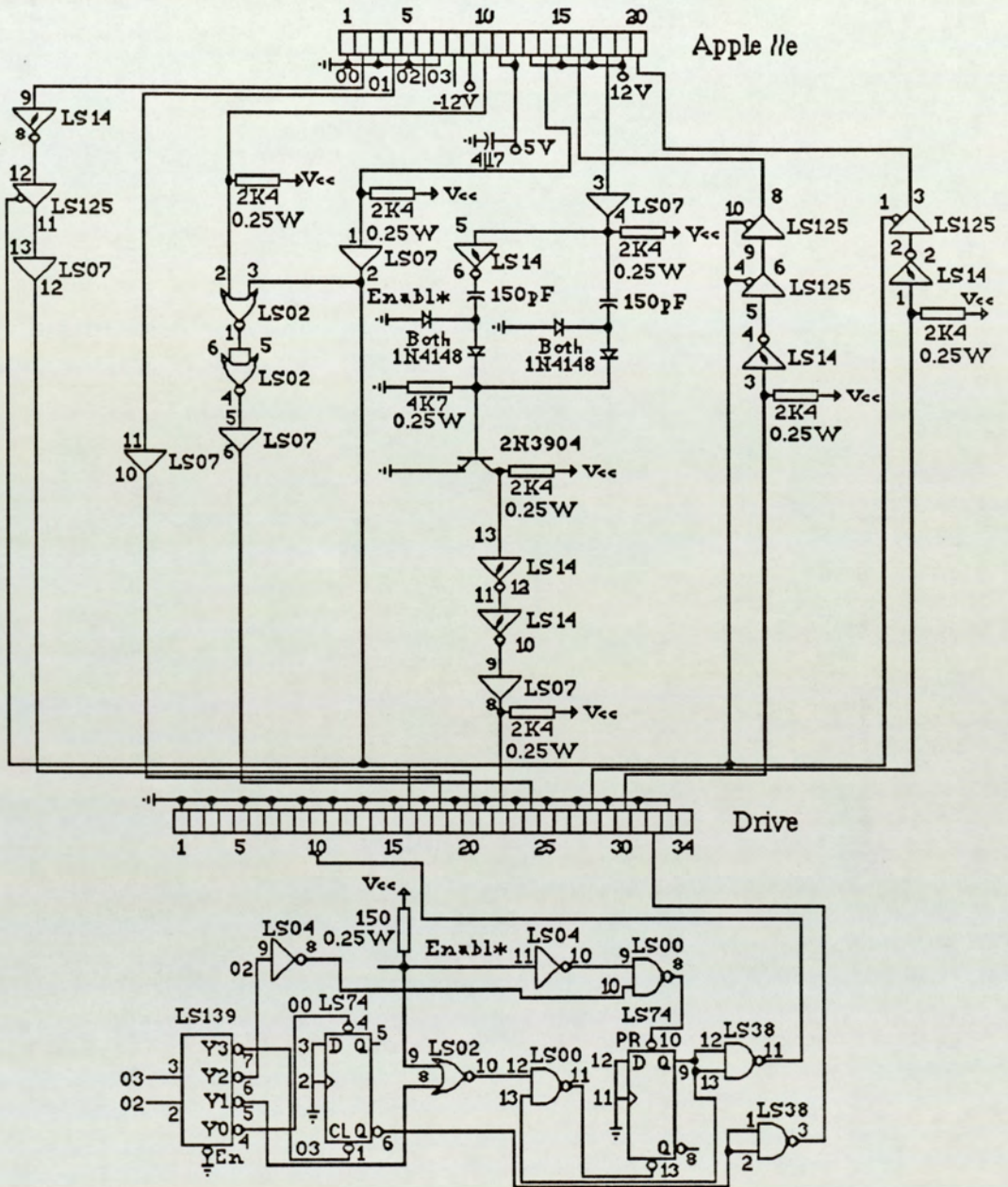


Figure 4.11 The circuit diagram of the interface used to communicate between the computer and diskette drives for the bit analysis tests.

In concluding this chapter, it has to be said that the rigs used here are not standard laboratory equipment and some significant improvements have been necessary to those made available in order to carry out the investigations which lead to the achievement of the aims originally outlined. These have been time consuming but, it was felt necessary, and the modifications were implemented before data was acquired from any of the rigs.

Chapter 5

Instrumentation and Techniques: **A Review**

Chapter 5.

Instrumentation and Techniques: A Review.

Introduction.

The instrumentation and methods of analysis that have been used are those of surface analysis. This is understandable as the friction and wear of materials in any sphere, including magnetic media, is essentially a surface phenomenon. There are very many instruments available, in theory, [121], but they all give different types of information. One key factor is, of course, the cost involved and the techniques readily available. Fortunately, those considered to be of most use are available in the department or within the locality and at reasonable cost. These have been described individually below in this chapter indicating what information is to be gained from each technique.

5.1 Optical Microscopic Analysis.

This technique is a familiar one and need not be described here in detail except to say that an Olympus Model BHC microscope fitted with a Model PM-6 camera

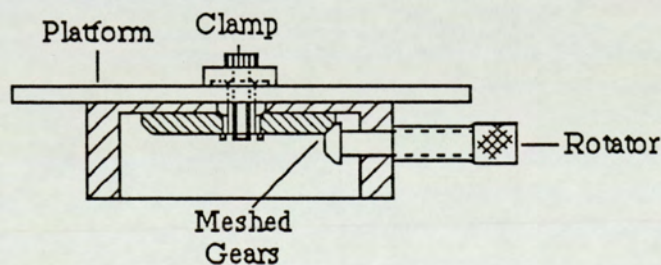


Figure 5.1 Specially constructed rotating platform for examining diskettes with the optical microscope.

has been used. Also, a special device has been produced, Fig. 5.1, which enables the examination of a diskette track as the media is rotated under the objective lens of the microscope. This device had to be produced in order that the flexible media would remain steady while being examined and so that the wear track could be easily examined without unnecessary movement of the media. The device simply allows any part of the track to be positioned under the microscope after which the rotator turns the diskette such that different sections of the track come into view.

5.2 Scanning Electron Microscopy.

The Scanning Electron Microscope (SEM) is now a familiar instrument which is in common use. It is of great use in looking at the surface of the media before and after testing has taken place. It works in a similar way to a reflection optical microscope except that the radiation used is a beam of electrons rather than light. These are focussed with electromagnetic, rather than optical, lenses. The details of the machine are both unnecessary and readily available in text books and will not be described here in any detail but, basically, an electron gun in a cathode ray tube scans a television monitor screen in synchrony with the beam scanning the sample using the intensity of reflected electrons as the signal. Magnification of 5 K and 10K are sufficient for this work although up to 100 K (*albeit* with poor signal to noise ratio, that is, picture quality) are potentially available on most simple machines.

This technique shows visible contrast between worn and unworn areas. Also, the appearance of wear sites and debris can be seen and interpreted as well as the structure (roughness, micropores etc.) of the surface of the magnetic layer. The use of a back scattered electron detector can often facilitate better contrast and has been used in some of the investigations that have been made on heads.

5.3 X-ray Photoelectron Spectroscopy.

X-ray Photoelectron Spectroscopy (XPS) is a surface analytical technique which was first used by Siegbahn in Sweden in 1954. The atomic processes involved has been illustrated in Fig. 5.2 and described below where the energetics of the process are considered. This technique is often used to identify the chemical state of atomic species on the surface. This is possible because the chemical environment of an element determines its atomic energy levels' arrangement. So, it is possible to use the characteristic spectra of the atomic species to identify the components of the surface as well as the chemical states of these components. When chemical states are identified, the technique is often referred to as Electron Spectroscopy for Chemical Analysis (ESCA).

The technique is meant to produce data spectra that may be relatively easily processed showing the chemical states of the atomic species identified by other methods such as Auger Electron Spectroscopy (AES) and Scanning Auger Microprobes (SAM) as well as confirming this identification. Also, with the use of different anodes in the X-ray gun, it is possible to extract further information. Spectrum interpretation is considered later. In the case of polymers, XPS can have an analysis depth of between 40 and 100 Å [122]. A definite advantage is that it is not inherently surface destructive as other techniques, such as Auger analysis [123], may be. With soft plastic surfaces being studied in the analysis of flexible magnetic media, it therefore provides a method for looking repeatedly at the same surface. The actual energetics of the process are presented in Fig. 5.2 and a description of this is necessary.

The surface sensitivity of this technique arises from the fact that the photo-electrons liberated by the X-ray photons below the surface suffer collisions with atoms in travelling to the surface. This inelastic scattering leads to a loss of kinetic energy and the electrons originally much further than about 100 Å below

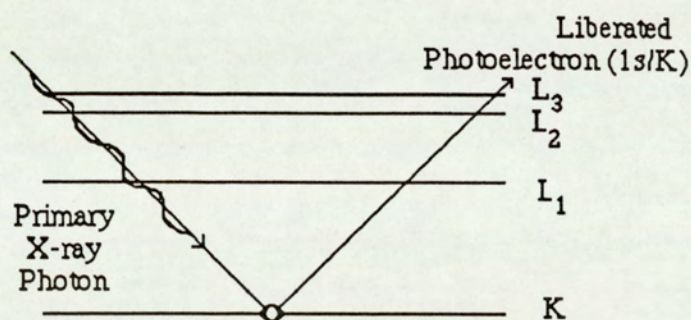


Figure 5.2 Mechanism for producing the photoelectrons detected in XPS.

the surface tend to contribute to the background rather than the characteristic peak.

If the energy of the exciting X-ray photon is designated $E_x = h\nu$; and that of the inner atomic energy level (the "K-shell", or "1s energy level", in the lighter elements has the highest probability) is designated E_K ; the kinetic energy of the photoelectron detected at the analyser = E_e , then the energetics of Fig. 5.2 are described by the equation:

$$E_x = (E_K + \phi_S) + E_e + (\phi_A - \phi_S) \quad (5.3.1)$$

or,

$$E_e = h\nu - E_K - \phi_A \quad (5.3.2)$$

Where, ϕ_A and ϕ_S are the work functions of the analyser and sample respectively

Clearly the full photon energy is involved for the XPS process in determining the kinetic energy of the ejected electron.

The output spectra from the XPS analysis can give semi-quantitative as well as qualitative information on the chemical elements present on the surface in addition to the chemical state of these elements: a typical XPS spectrum is

shown in Fig. 5.3. The information is only semi-quantitative as the efficiency of absorption of X-rays is different for different elements, as reported by Wagner [124], since each element will have a different cross-section of interaction. The relative sensitivities of the technique to many elements is also presented by Wagner [124]. All of the sensitivities are presented relative to that of Fluorine which is assigned a sensitivity of 1. It should be noted that the sensitivity increases with atomic number to the point where the cross-section for X-ray absorption becomes greater for the next energy level up [124]. As an example of this phenomenon, Magnesium (atomic number = 12) may be considered for which this step-wise fall in sensitivity occurs for the 1s level to 2p level. The fall for Magnesium then presents a new series of increases in the cross-section. The sensitivity is such that atomic concentrations of as little as 0.1% may be detected, *albeit* with long data acquisition times; in the case of high sensitivity to an element, fine tuning of detection equipment, low background noise, etc. it may be possible to detect elemental presence at concentrations of 10 parts per million. Sensitivities of this order are not possible in practice.

A further complication, in addition to sensitivity, is that due to the masking effect of the lower atomic layers by the ones above them. This effect is due to the inelastic scattering of the electrons produced lower down in the sample by the upper mono-layers and has the effect of reducing the signal from these lower layers. Obviously, the deeper the penetration, the more masked the signal tends to become. This makes it necessary to allow for this masking effect in the data before any quantitative analysis can take place.

The greatest advantage of XPS is its presentation of different peaks for different chemical states of the same element. Any energy peak shifts detected due to the chemical environment can be seen using XPS and an example is given in Fig. 5.3 where polyethylene terephthalate (PET: which is often used as a backing, or substrate, material for flexible magnetic media and is employed for

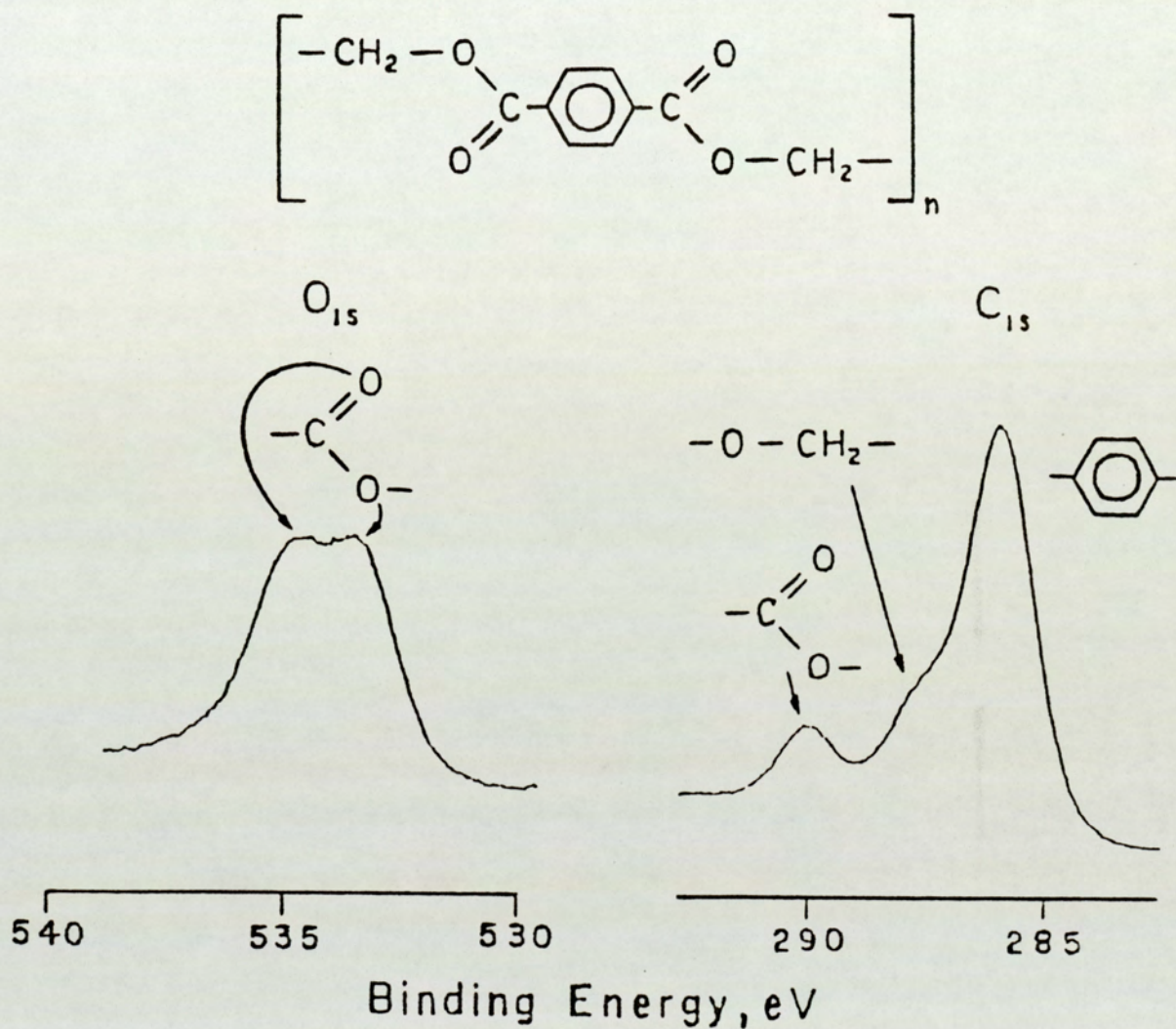


Figure 5.3 An example XPS spectrum of PET [122].

the diskette samples used here) has been analysed. The shift occurs due to the different electronegativities of elements and the consequent polarisation of the chemical co-valent bond between them. Thus it is most pronounced between highly electronegative elements on the one side bonded to very much less electronegative elements. Examples of such bonds are C-F, C-O, C-N, C-Cl (Fluorine is the most electronegative element of all).

The chemical shift occurs because the highly electronegative element polarises the bond between itself and the atom of a different element. This causes dipole separation of charge along the bond. The remaining core electrons on the resultant positively charged species at the other end of the bond are more tightly bound to their nucleus. This is a similar effect to that seen in the case of full ionisation where the electrons remaining after ionisation become more tightly bound. Here, however, this tighter binding occurs to a lesser, but easily detectable, extent. The charge polarisation that differences in electronegativity produces is observed in the XPS spectra as a shift in binding energies. This is a shift towards higher binding energy for positively charged species and towards lower binding energies for negatively charged species. An example of this is the C-O bond which is clearly labelled in Fig. 5.3. Experience shows that there is usually a shift of about 1.5 eV per C-O bond in the spectrum. Care must be taken in interpreting spectra, however. As an illustration, the carboxyl structure (C=O(O)) of Fig. 5.3 may be considered. By the above rule, the Oxygen atom which has a double bond with the Carbon atom should show a binding energy ~3 eV lower than for an Oxygen bonded to another Oxygen atom. Similarly, the Oxygen attached to the Carbon atom by a single bond, should be shifted towards lower binding energy by 1.5 eV. This means that the doubly bonded Oxygen atom should appear at a lower binding energy in the XPS spectrum. This does not happen, however. The reason for this becomes clear when the PET molecule in Fig. 5.3 is studied as a complete unit. It then becomes apparent that the singly

bonded Oxygen atom is bonded on both sides by large numbers of Carbon atoms. As a result, it is able to attract more of the bonding electrons through delocalisation along the whole chain. The doubly bonded Oxygen atom then appears at a higher binding energy. This shows that the spectra need to be analysed very carefully before any conclusions can be drawn concerning the species present and their bonding energies.

It is theoretically possible to detect chemical shifts using other techniques (such as Auger Electron Spectroscopy spectra) also as, again, the energy levels will shift in response to the chemical environment in which the analysed element is found. This is difficult to detect, however, because the signal to noise ratio in Auger techniques is very much poorer than for XPS. This may be as a result of the fact that the Auger electrons from the lower layers are inelastically scattered forming some background. Also, the primary electrons used to excite the sample become inelastically scattered and contribute to the background.

XPS studies of polymers have also been carried out by Briggs [125] and by Dwight and Riggs [126]. Among other polymers, PET is again studied by Briggs [125] with similar conclusions to those obtained by Wagner [124]. Fluoropolymers were studied by Dwight and Riggs [126] showing large chemical shifts as are to be expected for the atom with the highest electronegativity.

Although these will not be immediately obvious from Fig. 5.3 where small energy scan windows have been employed to ascertain individual peak structure details, there are other interesting general features to any XPS spectrum [127], [128], [129], which are more obvious from the data obtained and described in the results chapter of this work. These other features are as follows:

- (1) X-ray satellites: These arise from the non-monochromatic nature of the source used. As an example, the Magnesium source may be studied.

In this case the principal $K_{\alpha 1,2}$ unresolved doublet in the X-ray spectrum of Mg, at a photon energy of 1253.6 eV, is accompanied by the slightly more energetic $K_{\alpha 3,4}$ doublet line which leads to a satellite peak approximately 10% of the height of the main peak and removed from this main peak towards the higher kinetic energy end by about 9 eV, these being the differences in the two photons' relative emission intensity ratio and energy of the two doublet lines respectively.

- (2) Ghosts: These appear from several sources but are often the result of impurities in the anode material and can (in the case of multiple anode source guns) arise due to the misalignment of the different anodes. The Aluminium K_{α} principal line can often be seen with the Mg source in use because of the electrons exciting the Al foil screen used to prevent these electrons from entering the main specimen chamber. A further ghost can appear from the Copper L_{α} line when sources become aged due to a great degree as Cu is the base material used for the anodes.
- (3) Shake-up satellites: These are produced, in contrast to X-ray satellites (1), on the lower kinetic energy side of the main peak. They appear because the loss of an outer electron appears as an increased nuclear charge for the remaining outer electrons. The re-organisation in the subsequent atomic electron relaxation can lead to the excitation of one of these valence electrons to a higher energy level. The energy used for this process is no longer available to the principal transition in the form of kinetic energy and hence a lower kinetic energy electron is emitted. This results in a lower kinetic energy satellite being detected.
- (4) Shake-off satellites: These occur when, instead of the promotion of a valence electron to a higher energy level as happens in the shake-up process described in (3) above, this electron is removed completely from the atom. Obviously, this may be expected to correspond to a

peak at an even lower kinetic energy than the shake-up peak in the energy spectrum. In fact, these serve merely to broaden the main peak rather than to show up as discrete peaks in their own right.

- (5) Other loss peaks: inelastic scattering of electrons, particularly those generated well below the surface, can lose much of their energy before escaping at the surface. These electrons contribute to the tail on the low binding energy side of the peak.
- (6) Multiple Splitting: These separate lines often serve to further broaden existing peaks rather than to create distinct new peaks especially with low resolution equipment. They are caused by the degeneracy of levels being split by, for example, quantum mechanical spin - orbit splitting, or, in the presence of magnetic fields, the Zeeman effect.
- (7) Auger peaks: These peaks are produced by the X-ray excitation of the atoms which relax by emitting Auger electrons by the familiar Auger effect as described by many authors, such as Joshi et al [123]. The peaks corresponding to these transitions are superimposed on a high background and tend to be very much less prominent than the photoelectric peaks when a wide energy window is scanned. Auger peaks may be clearly distinguished when two different X-ray lines are used for the exciting radiation by changing the source anode for the same detection energy window scan. The fact that the XPS peaks' positions are dependent on the energy of the exciting photon energy (see equation (5.3.2)), they will shift by an amount equal to the difference in the energy of the incoming radiations. Since the Auger peaks are independent of the incoming energy but depend on the difference between energy levels in the particular atom, these will not shift and will remain at the same kinetic energy [128], [129].

The above peaks are all superimposed on a total shift of the whole

spectrum which is unavoidable in the case of non-conducting polymer samples. Although the magnetic layer of diskettes contains the electrically conducting amorphous C-black, as explained in Chapter 2, it only prevents local charging of the sample and does not prevent the whole sample from charging up. This has the effect of causing the whole spectrum to be shifted towards higher binding energies (that is, lower kinetic energies) as the positively charged sample attracts back, and thus retards, the secondary electrons emitted. This then shows a similar effect to a higher binding energy but for the whole spectrum rather than only certain peaks.

There are various remedies but none are completely successful and the normal solution to this positive charge accumulation due to loss of electrons is to define the Carbon 1s main peak (caused by Carbon in the symmetric C-C chemical environment) as being at a binding energy of 284.6 eV and then to measure the other peak energies relative to this.

In concluding this section it may be noted that XPS is a technique which is very powerful and readily available. Use has been made of it in attempts to look at both the media and the surface of used heads removed from drives. Clearly, care must be taken in interpreting the spectra and the processes involved in data acquisition have to be properly understood before meaningful results may be obtained. It has been used to great effect by Skelcher [20] and Skelcher, Sullivan and Dirks [82] in the analysis of 3M special formulation high density diskettes. One other aspect of XPS contrasted to techniques such as Auger analysis, which often use charged particles as the exciting radiation, is that the former technique is not inherently surface destructive. This does not, however, allow for the inherent possibility of the surface being changed by the Ultra High Vacuum (UHV) used. In the case of magnetic media, surface lubricant can evaporate from the surface at typical UHV pressure of 10^{-8} Torr. This is despite

the polar nature of the surface lubricant and its consequent low vapour pressure characteristics. This can lead to the possibility of incorrect quantity analysis, for example. It is expected that this will not be a serious problem in the relatively short time that the present samples need to be exposed to these low pressures.

5.4 Transmission Electron Microscopy.

The final analytical technique to be discussed is that of **transmission electron microscopy (TEM)**. This is a fairly well established technique [130], [131] but has not been used very much for the study of magnetic media. It has been used to some extent by Bhushan et al [86] for magnetic tape and with great effect by Skelcher, Sullivan and Dirks [82] on 3M diskettes. In each case, it is the dispersion of the magnetic particles which is observed. The biggest hurdle to overcome in TEM is the specimen preparation on the microtome both in the author's opinion and as is confirmed by Bhushan et al [86].

The transmission electron microscope works in a similar way to the SEM except that the beam of electrons passes through the specimen and forms an image of the magnetic particles on a fluorescent screen, the polymer being transparent at the beam energies used, hence the need for ultra thin specimens with a typical thickness less than 500 Å.

The key aspects of TEM specimen preparation is that the sample needs to be stiff in order that it may be sliced into thin sections. In the case of metals, for instance, this is quite simple but floppy diskettes have to be pre-treated in some way. There are many options open of which the most common are probably cryogenic and embedding methods. The easier option of these is embedding as the samples used are quite small and they must not be allowed to warm up if the cryogenic method is used. The cryogenic technique, therefore, requires specialist equipment which is not readily available.

The embedding technique involves the preparation of a mixture of organic resins which are poured into moulds. The samples of floppy diskette are placed in the moulds prior to the resin being poured. Care has to be taken to leave the samples flat as the resin is poured. After curing for approximately 24 hours at 60 °C a block of resin with the embedded sample is produced and has approximate dimensions 15 mm × 5 mm × 5 mm. The block is illustrated in Fig. 5.4 (a) including the sample. This block then needs to be trimmed to produce the shape shown in Fig. 5.4 (b) so that the diskette sample is held rigidly at the point to be sectioned on a microtome. In fact, the process of trimming the sample block involves trimming with scalpel; filing the rough edges; fine trimming with a glass knife on the microtome; final trimming of the block with a diamond knife prior to sectioning.

Sectioning of the sample involves mounting the sample onto the microtome (LKB Model 4801A, in this case) and filling the trough attached to the diamond knife (Fig. 5.4 (c)) with a de-ionised water and acetone mixture. The process of sectioning then produces the ultra thin slices of the sample as shown in Fig. 5.4 (d). The colour of the sections is determined by their thickness; silver or grey samples ($\leq 600 \text{ \AA}$ thick) samples are acceptable. A train of such slices are allowed to form on the liquid surface before being relaxed by heating with a special tool by warming the air above the samples. The relaxed samples are lifted off using a copper grid using the surface tension of the liquid. The samples are then permitted to dry in air before being carbon coated prior to being inserted into the TEM for inspection. The form of the sample on a copper grid is illustrated in Fig. 5.4 (e).

Each stage of the sample preparation is important and must be carried out with great care as the process determines the final quality of the samples produced.

It has been found that polymer rich surfaces, as seen by TEM, lead to a

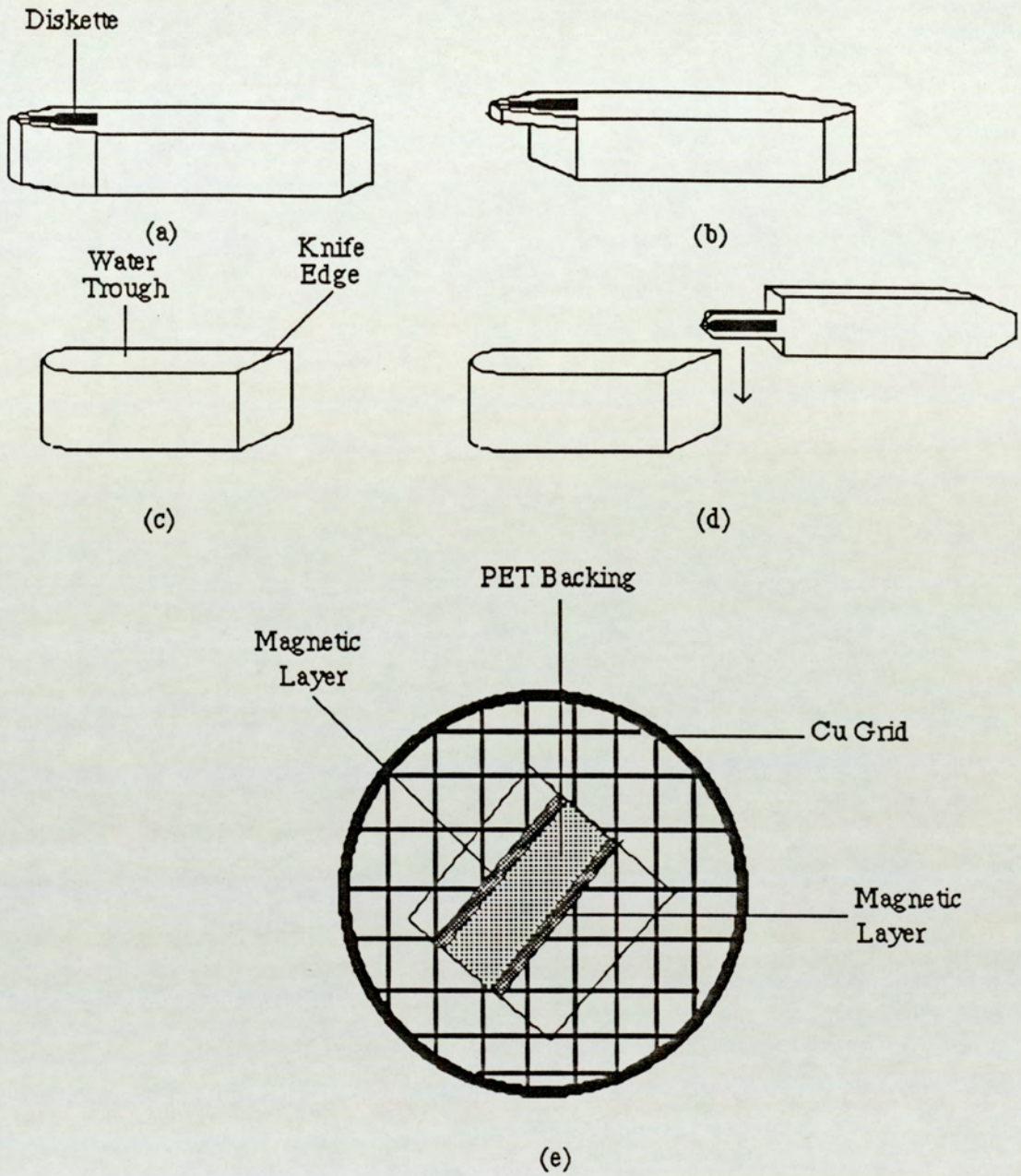


Figure 5.4 TEM sample preparation (a) Cured resin block with diskette sample embedded in it (b) The roughly trimmed block (c) The diamond knife and trough (d) How the sample is sectioned (e) The section of diskette on the Copper grid.

loss of magnetic signal and increased friction [86] and badly dispersed, or agglomerations of, particles leads to uneven stress distribution [82], [86]. It is felt that the movement of particles can occur in the sub-surface region as the polymer in this area is caused to flow plastically by the stresses imposed on it by the head. This can aid the sub-surface crack nucleation and propagation.

5.5 Computer Analysed Optical Interferometry.

The technique employed for determining the degree of roughness of the surface of the samples used in this study is that of computer analysed optical interferometry.

This has been possible using the facility available at 3M (UK) plc., Swansea. The apparatus used scans a small area of the sample (typically a few hundred micro-metres square) and produces a map of the heights of the surface features, including the asperities of the surface.

The technique involves the use of a light beam split up to form a reference beam and one reflected off the sample. The fundamentals of the system are illustrated in Fig. 5.5 [132]. Here the original illuminating beam is reflected

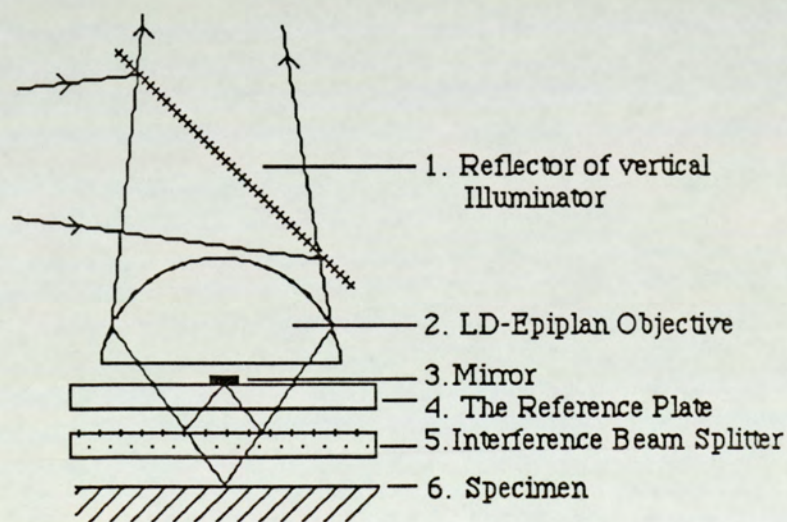


Figure 5.5 Schematic beam path of the Mirau interference system.

towards the specimen by the mirror (1) and focussed by the objective lens (2) of the microscope used. The mirror (3) mounted as an integral part of the reference plate (4), reflects the reference beam provided by the beam splitter (5) while the specimen beam progresses towards the specimen (6). The light returning from the reference plate mirror (3) and the specimen can clearly have different path lengths. In the case of the reference beam, this is determined by the separation of the reference plate and beam splitter. In the case of the specimen beam, the specimen and beam splitter separation determines this path length. Clearly if this separation is equal, and the specimen perfectly smooth, then the two beams will emerge towards the objective in perfect phase. However, if the specimen beam should encounter an imperfection on the surface, the two beams will not emerge exactly in phase. The difference in phase will be governed by the vertical height (or depth) of the imperfection as it will determine the relative reduction (or increase) in the path length of the specimen beam.

In order to measure the height or depth of the surface feature, the optics of the situation may be analysed. Considering some random point on the surface of the specimen, the intensity of the combined reference and specimen beams detected at the objective will be I where:

$$I = I_0 [1 + \gamma \cdot \cos(\phi)] \quad (5.4.1)$$

where I_0 = Intensity at objective with constructive interference
 γ = Interference contrast for that point: $0 \leq \gamma \leq 1$
 ϕ = Phase difference between specimen and reference beams

Different intensities may be calculated for phase shifts of the specimen beam by increments of $\pi/2$. This gives for:

(a) reference beam phase shift = 0:

$$A = I_0 [1 + \gamma \cdot \text{Cos} (\phi + 0)] = I_0 [1 + \gamma \cdot \text{Cos} (\phi)] \quad (5.4.2)$$

(b) reference beam phase shift = $\pi/2$:

$$B = I_0 [1 + \gamma \cdot \text{Cos} (\phi + \pi/2)] = I_0 [1 - \gamma \cdot \text{Sin} (\phi)] \quad (5.4.3)$$

(c) reference beam phase shift = π :

$$C = I_0 [1 + \gamma \cdot \text{Cos} (\phi + \pi)] = I_0 [1 - \gamma \cdot \text{Cos} (\phi)] \quad (5.4.4)$$

(d) reference beam phase shift = $3\pi/2$:

$$D = I_0 [1 + \gamma \cdot \text{Cos} (\phi + 3\pi/2)] = I_0 [1 + \gamma \cdot \text{Sin} (\phi)] \quad (5.4.5)$$

Rearranging equations (5.4.2) and (5.4.4) gives:

$$I_0 = A - I_0 \cdot \gamma \cdot \text{Cos} (\phi) = C + I_0 \cdot \gamma \cdot \text{Cos} (\phi) \quad (5.4.6)$$

$$\Rightarrow \text{Cos} (\phi) = (A - C) / (2I_0 \cdot \gamma) \quad (5.4.7)$$

and similarly with equations (5.4.3) and (5.4.5):

$$I_0 = B + I_0 \cdot \gamma \cdot \text{Sin} (\phi) = D - I_0 \cdot \gamma \cdot \text{Sin} (\phi) \quad (5.4.8)$$

$$\Rightarrow \text{Sin} (\phi) = (D - B) / (2I_0 \cdot \gamma) \quad (5.4.9)$$

Also, from equations (5.4.2), (5.4.3) and (5.4.4):

$$A + C - 2B = 2I_0 - 2I_0.[1 - \gamma.\text{Sin}(\phi)] \quad (5.4.10)$$

$$\Rightarrow \text{Sin}(\phi) = (A + C - 2B) / (2I_0.\gamma) \quad (5.4.11)$$

Thus, using equations (5.4.7), (5.4.9) and (5.4.11):

$$\text{Tan}(\phi) = \text{Sin}(\phi) / \text{Cos}(\phi) = (D - B) / (A - C) \quad (5.4.12)$$

or
$$\text{Tan}(\phi) = (A + C - 2B) / (A - C) \quad (5.4.13)$$

This then gives:

$$\phi = \text{Tan}^{-1} [(D - B) / (A - C)] \quad (5.4.14)$$

or
$$\phi = \text{Tan}^{-1} [(A + C - 2B) / (A - C)] \quad (5.4.15)$$

So, the phase of the reflected wavefront may be determined by measurement of three or all of the parameters A, B, C and D.

Clearly a maximum phase shift of 2π corresponds to a difference in path length of λ , the wavelength of the light used, and an imperfection of height or depth of $\lambda / 2$. Thus, a maximum deviation from the surface of $\lambda / 2$ may be measured. Any intermediate phase ϕ then corresponds to a deviation from the surface of z where:

$$z = (1 / 4\pi).\phi.\lambda \quad (5.4.16)$$

A pit in the surface will be characterised by $\phi < 0$ and a raised area by $\phi > 0$.

It should be noted that data acquisition and processing is performed by computer. Also the size of the area scanned is usually very much bigger than the asperity height or pit depths. This means that the z - direction is plotted magnified by a factor known as the "Depth Scale" which is quoted at the bottom of each scan plot output; the average deviation from the surface ($\phi = 0$ point), R_a , and root mean square deviation, R_Q , are also quoted.

The technique has been extensively developed at 3M and now involves the use of lasers to provide a monochromatic beam. It has been employed on stationary magnetic media and heads [133] [134] as well as on moving media [135] [136].

Chapter 6

Presentation of Results

Chapter 6.

Presentation of Results.

Introduction.

This chapter presents the results obtained using samples which were specifically prepared for this project. The sample specifications are obviously important and have been described first. The full discussion of these results is left until the next chapter, but it is felt that in order to understand the reasons for performing the tests described it is necessary to briefly discuss some aspects here.

The results obtained can be split into several sections, that is, those relating to the separate rigs, and this has been done for ease of analysis. One further point to note is that some work was initially carried out on samples with the identification codes CN20714 and CN20718 and some of these results have also been presented in this chapter even though they were merely used for the purposes of establishing techniques before the samples finally used had been prepared. The results, however, were meaningful and some are used in illustration of the wear mechanism of the media where they produced the same information as the present specimens.

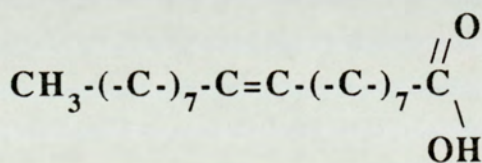
6.1 The Samples Coded 58759-4.

All of the samples used in this project were produced and supplied by 3M. In the case of those identified by the code "58759-4", these were specially produced for this investigation by 3M, St. Paul, Minnesota, USA on their Pilot Plant. They have been designed to enable the investigation of certain, controllable, parameters on the durability of the media. It was also intended to study the effect of

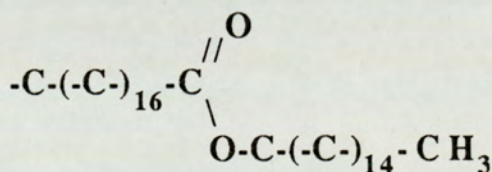
changing these parameters on the mechanisms of wear, and to isolate these mechanisms. An understanding of these mechanisms should lead to the development of a better product. Progress has been made in both areas and the results are presented here.

It is essential, however, to look first at the differences in the sixteen samples that have been utilised in this investigation. These samples fall into four major categories, Stock Roll numbers SR1 to SR4, each with a different lubrication status and each category splitting into four further roughness groups. It is obvious that the effectiveness of the two lubricants used in the media should be established so that the best possible combinations can be used. Indeed, the necessity of the lubricants needs to be established. To this end, the samples include unlubricated, surface only lubricated, bulk only lubricated and both surface and bulk lubricated. The details regarding these categories are as follows:

- (a) SR1: These samples contain only the surface lubricant, or top coat, which consists of a mixture of oleic acid and hexadecyl stearate in the ratio 3:1. The chemical structures of these are given in Fig. 6.1.



- (a) Oleic acid, bulk and part of the surface lubricant.



- (b) Hexadecyl stearate, part of the surface lubricant.

Figure 6.1. The skeletal structures of the bulk and surface lubricant molecules.

- (b) SR2: These are completely unlubricated.
- (c) SR3: These samples most closely resemble the commercially available media in the respect that the SR3 samples contain both surface and bulk lubricants. The only way in which they differ from the commercially marketed product is in the quantity of each "ingredient" utilised. The top coat is similar to that used in SR1, that is, hexadecyl stearate and oleic acid mixture, and the bulk lubricant is oleic acid only.
- (b) SR4: These samples contain only the bulk lubricant which is present in the form of oleic acid as is used in the SR3 samples.

As mentioned above, each of the sample types occurs in four different roughnesses. This has been done to fully determine the effects of surface topography on durability and wear. It has been found from earlier studies that the roughness of the surface of magnetic media determines its durability as has been reported for diskette media by Chambers [75] and for tapes by Bhushan [90]. Early tests were carried out using samples JLS01 and JLS02. These show only slightly different roughnesses as shown in the interferometric scans of Fig. 6.2. These correspond to the samples CN20714 and CN20718 used by Skelcher, Sullivan and Dirks [82] in their investigations. They also used other samples to give a wider range of roughnesses. It was for the same reason that four different roughnesses were used in each of the samples SR1 to SR4. Some of these samples have been supplied in their "as produced" form after cutting with the 5.25 inch die from the relevant stock roll and are completely unburnished; others have been burnished for 1.5, 3.0 and 4.5 seconds. Clearly, the unburnished media is the roughest and that burnished for 4.5 seconds is the smoothest with the other two lying in between. The details are presented in Table 6.1. This roughness has been determined using the facility at 3M (United Kingdom), Swansea, Wales. Some typical samples are shown in Fig. 6.3 and

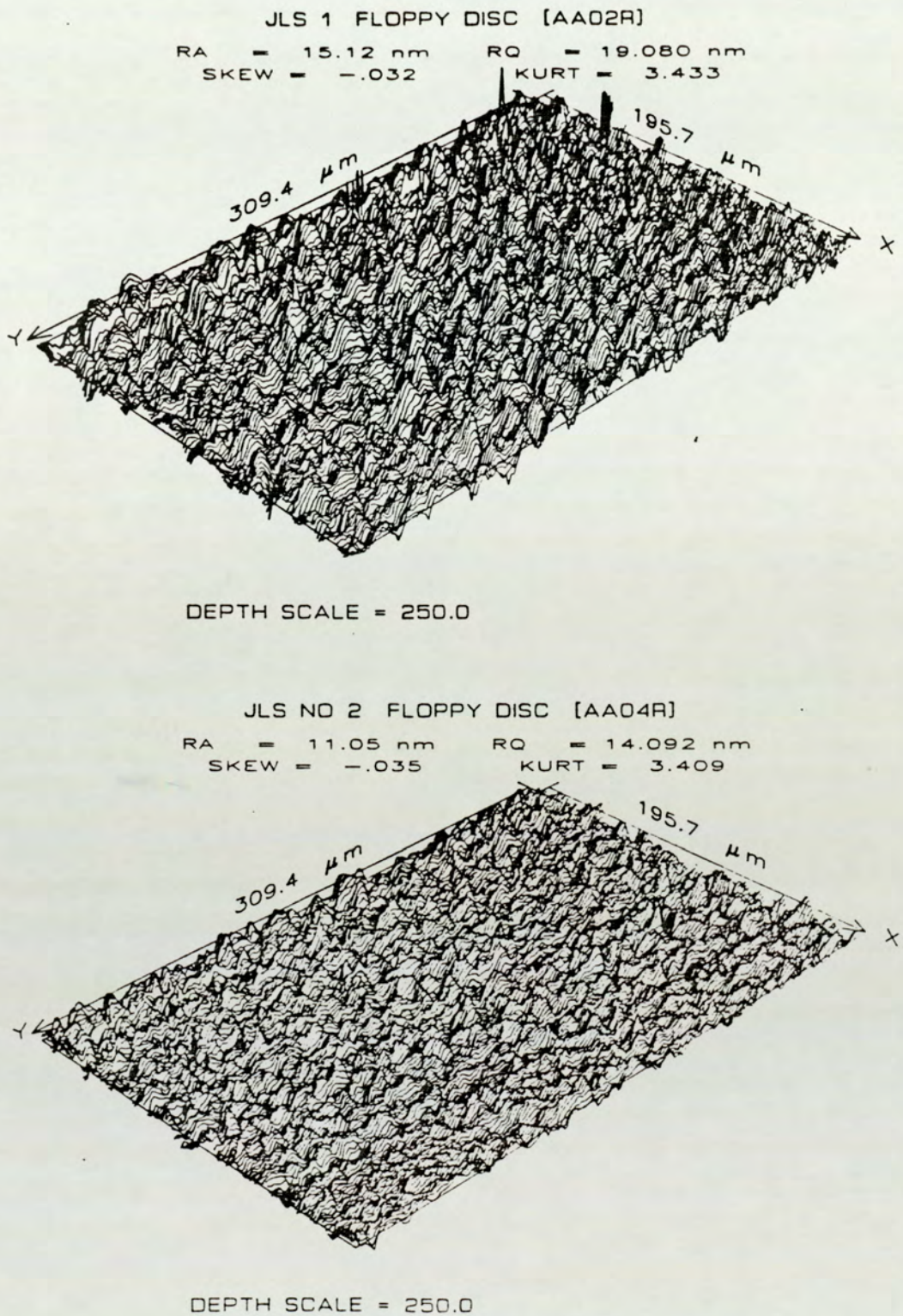


Figure 6.2 Interferometric scans showing the surface of samples JLS01 and JLS02 corresponding to the samples CN20714 and CN20718 respectively.

	Burnish Time (Seconds)			
	0	1.5	3.0	4.5
SR1	46.73 nm	22.01 nm	16.33 nm	14.94 nm
SR2	45.29 nm	27.20 nm	23.04 nm	19.49 nm
SR3	43.99 nm	20.07 nm	17.24 nm	13.26 nm
SR4	31.94 nm	16.75 nm	14.84 nm	18.41 nm

Table 6.1 The values of surface roughness (RA) of sample 58759-4 SR1 to SR4.

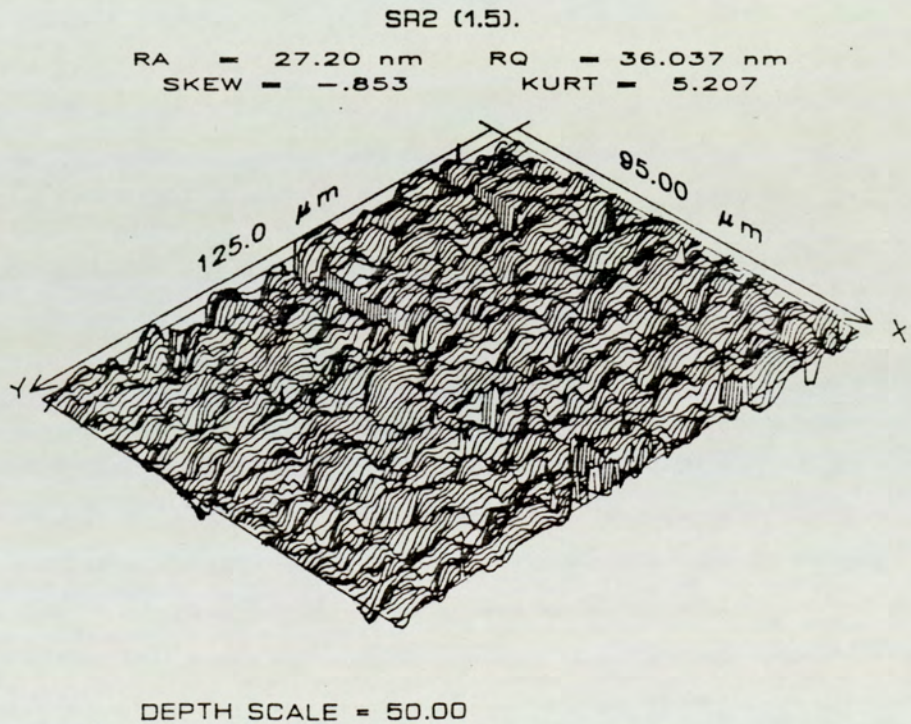
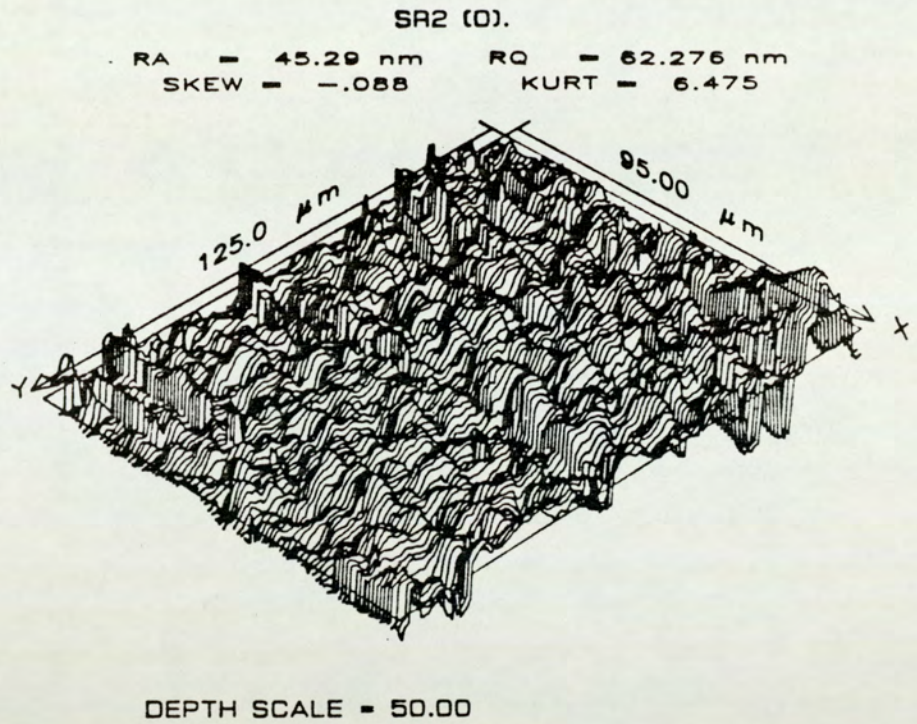


Figure 6.3 Interferometric scans of samples (a) SR2(0) and (b) SR2(1.5).

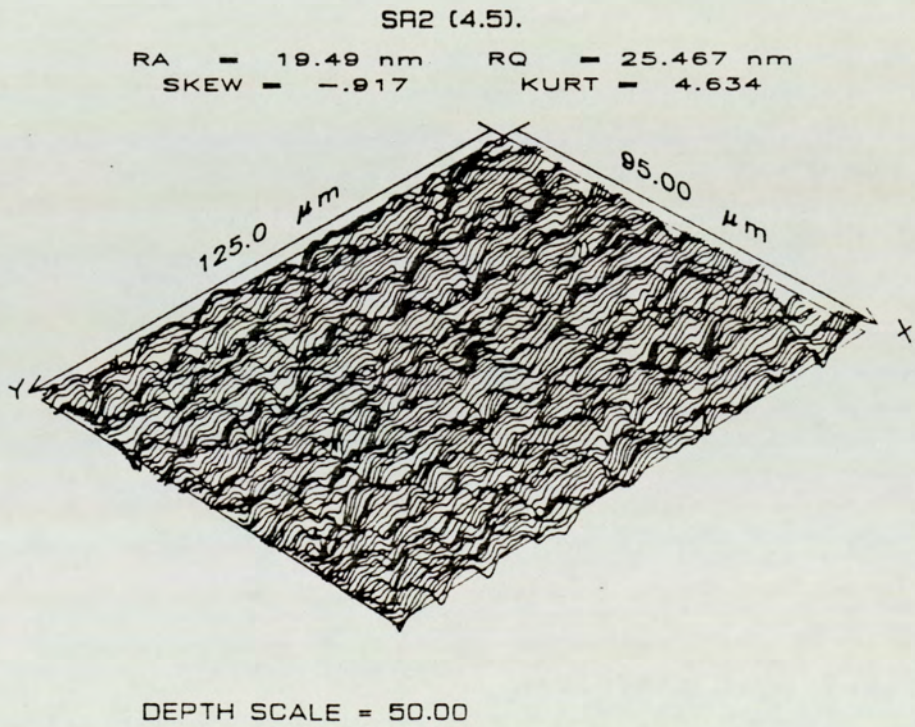
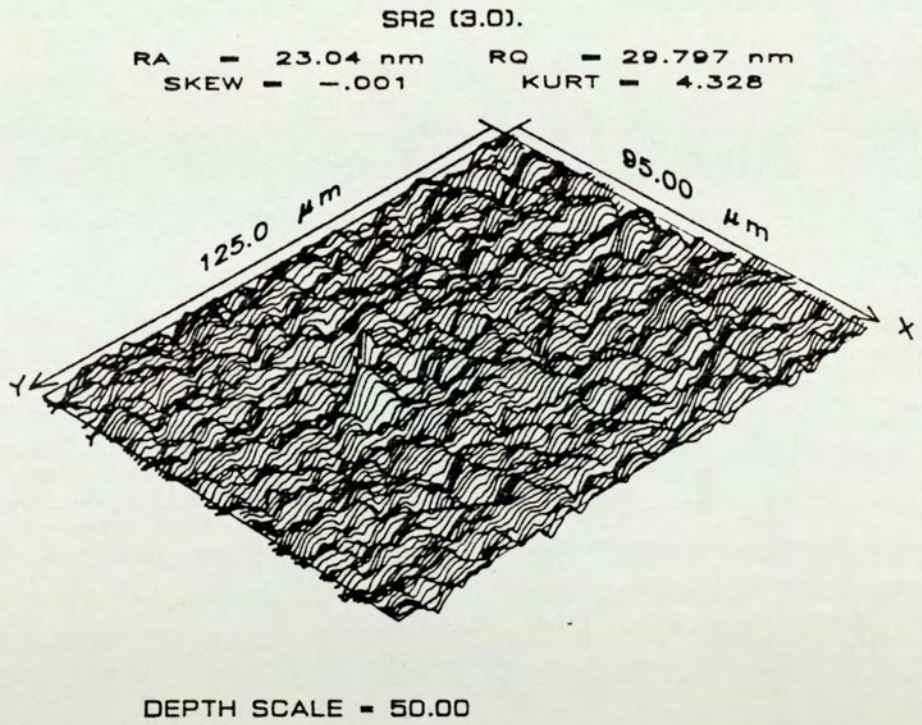


Figure 6.3 Interferometric scans of samples (c) SR2(3) and (d) SR2(4.5).

relevant comments will be made later, in Chapter 7, where the significance of the roughness will be discussed. However, it may be mentioned here that burnishing has a profound effect on the media surface quite separate from making it smoother. It is, in fact, the first stage in the wear process.

6.2 Experimental Procedures and Criteria for Wear.

The tests were performed using the rigs which have been described in Chapter 4, that is, using the drives of section 4.1 and the simulation rigs of sections 4.2 and 4.3. As described in those sections, this leaves the sample under test either fully supported from below at the head-media interface or allowed to flex out of the diskette plane at that point. Thus the latter situation provides for flexing of the media whereas the former does not. These rigs are designed to simulate the side 1 and side 0 head-media interfaces respectively with each one removing the variable of the other head's influence. Moreover, the rig providing for media flexing was expected to reveal the effects of this flexing, if any, on the fatigue wear of the diskettes. These rigs were also intended to investigate methods of providing accelerated testing of samples. Diagrams and a full description relating to these two rigs have been presented in previous sections.

The criteria used to determine wear have been defined depending on what information has been sought from a particular run. For the purpose of durability tests, that is how long a sample appears to last, this status was defined as the appearance of any damage which was easily visible to the naked eye, perhaps equivalent to grade 2 damage status as defined by 3M. The reason for this being that the user might be expected to discard the media at this stage. The key point to note here is that such apparent initial damage is not, in fact, wear but merely plastic flow of the surface asperities similar to that encountered during the burnishing process.

This is a very subjective criterion which not only depends on the observer, but also on external factors such as the ambient lighting available at the time of the observation. However, the subjectivity of this criterion can, perhaps, be said to be less pronounced on a statistical basis, especially in light of the fact that the user would, presumably, have similar ambient lighting etc. conditions.

For the purpose of establishing wear mechanisms, it was found to be far more instructive to leave the sample to run, regardless of which rig was being used to perform the test, until the scar was very much more obvious, that is, when it reaches between a grade 3 and 4 failure. Although these gradings have been described elsewhere by Skelcher et al [82], this has only been done briefly. It would be useful to define these gradings as interpreted for this project.

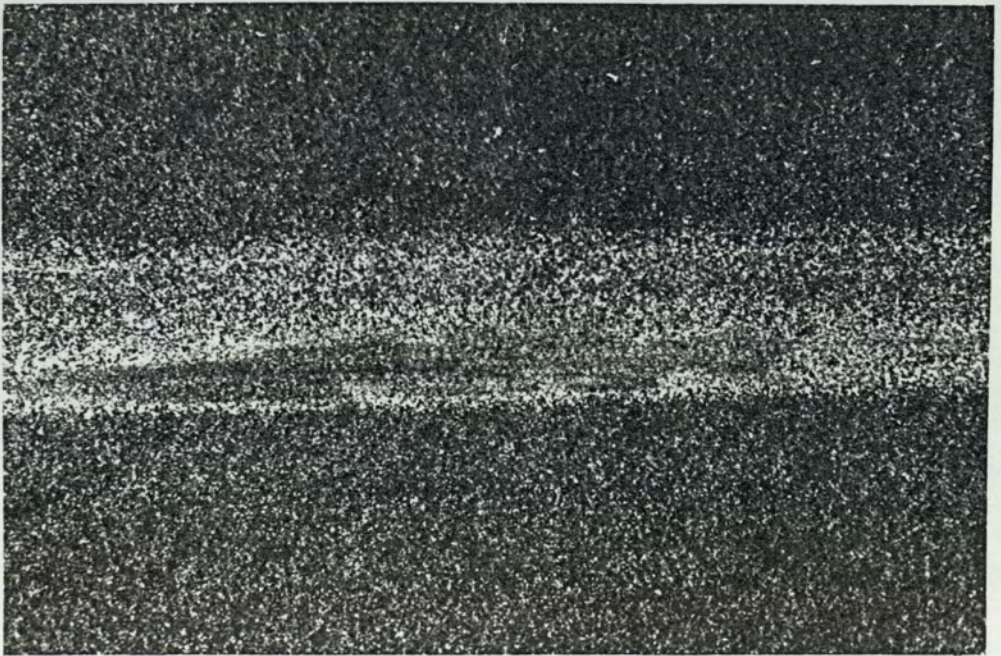
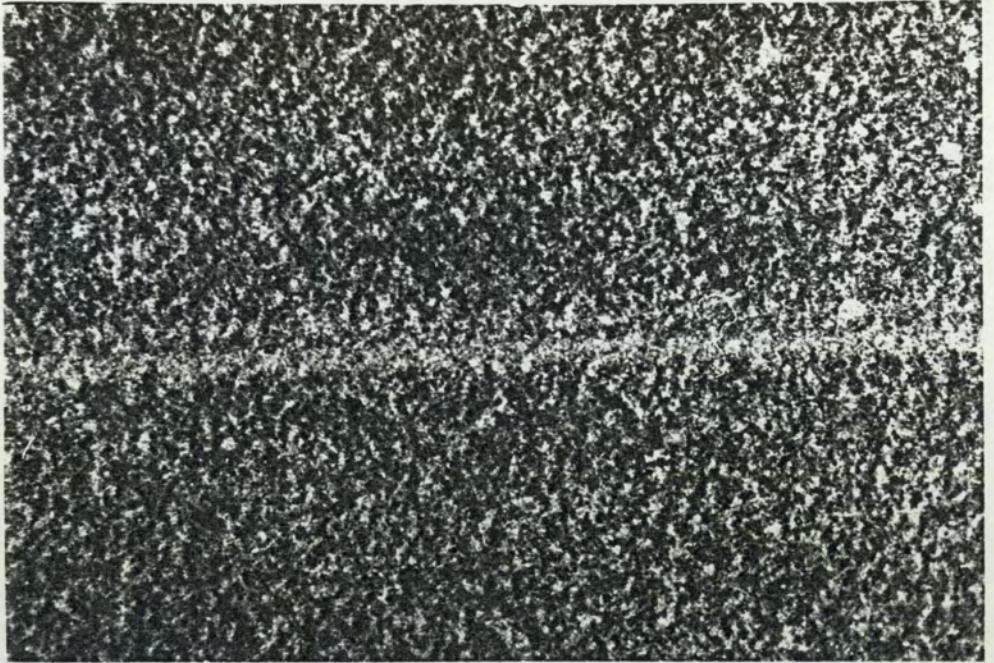
Grade 1 failure is deemed to have occurred when a scar is just visible on the surface. It is not important how this scar has been formed. At this stage, the largest asperities have experienced plastic flow forming a very slightly shiny surface in the region where the head has traversed the media. In fact it is not possible to detect grade 1 failure with instrumentation. Samples showing grade 1 failure to the naked eye appeared to be undamaged when inspected by optical and scanning electron microscopy. Good lighting is essential to detect grade 1 failure.

When plastic flow of the surface is much more obvious, grade 2 failure is said to have occurred. At this point, wear of the surface has still not taken place, but the plastic flow should be seen to be extensive. This grade of failure is associated with the production of a very shiny scar due to "polishing" of the surface. An example of grade 2 failure, is illustrated in Fig. 6.4 (a). It is highly probable that this type of damage occurs during the burnishing process.

When grade 3 failure occurs, the surface shows a wider scar than under the above gradings with considerable plastic flow having occurred. However, real damage to the surface can also be detected by using microscopic inspection.

Figure 6.4 (a) A typical example of grade 2 failure seen on a sample examined by optical microscopy (200 \times).

Figure 6.4 (b) A typical example of grade 3 failure seen on a sample examined by optical microscopy (200 \times).



A typical example of this damage is illustrated in Fig. 6.4 (b). Wear of the media has been initiated at this stage and material has been removed from the surface.

Grade 4 failure is characterised by catastrophic damage to the surface. Under this category plastic flow of the material may often be obscured by extensive material removal from the media surface. It may not be possible to usefully employ this grade of failure to study the mechanisms of wear as all of the events associated with the wear process have already occurred by this point. The damage is so extensive that material has been removed to a very large depth compared to the thickness of the magnetic coating. Media used in the bit analysis tests (as described in section 4.5, Chapter 4) were found to reach this stage of damage before data read errors were detected.

Although grade 2 failure was to be sufficient for ranking durability of samples as may be done by the customer, grade 3 was the minimum used for studying wear mechanisms. At this stage the scar is often wider than those found using the durability criterion, grade 2 failure, above. This means that the central part of the wear track is "well worn" and little information can be gained from this particular area because extensive plastic flow obscures any other occurrences. The region either side of this part, however, at greater and lesser radius as measured from the centre of the diskette, is much more informative. This tends to show all stages of the wear process. These range from the very initiation of the sequence of events concerned with wear to the final event where actual removal of material has occurred and consequential pits formed in the surface. Typical debris has also been observed and is illustrated later in this chapter. This debris helps in identifying the mechanisms of wear. These observations have enabled a wear mechanism to be proposed. Full discussion of this mechanism has been left until Chapter 7 where these observations have been explained. Optical and scanning electron micrographs of the samples shown in the figures which follow in the later sections of this chapter illustrate the

observations made. The mechanisms of wear are similar regardless of whether the tests take place on the rigs or whether they were conducted in the drives. They show a similar sequence of events and very similar final consequences for both the rigs and the drives.

As far as the in-situ friction tester apparatus is concerned, the data obtained is affected by the fact that the more durable samples have been studied for a limited period and not to their ultimate failure. The less durable ones have been studied to their ultimate failure and this highlights the enormous differences between them. The details of this work are discussed below.

6.3 Mechanical Measurements: Friction and Wear.

This section presents the data obtained pertaining to the friction and wear of the samples. Clearly, as discussed in Chapter 3, the friction in polymeric materials can be closely related to wear. Thus, it was felt that in order to establish the processes involved in the wear of magnetic media, it was essential that the friction forces encountered at the head-media interface be measured. This can be done under the different conditions provided by the rigs described in Chapter 4, sections 4.2 to 4.4. Wear of media has also been studied, although no wear rates (for example, volumetric removal of material as a function of the number of revolutions) can be determined in this case since the amount of material removed is negligibly small and cannot be measured. It is, therefore necessary to assess wear in some other way. It is for this reason that the criteria defined above have been employed. The mechanisms of wear have been determined by terminating tests at the initiation of wear. This enables the initial causes of wear to be ascertained.

The wear aspect has been dealt with first in this present section and is followed by the friction aspect as this offers better continuity.

6.3.1 Drives.

The initial tests were terminated on the first appearance of a scar on the tested media surface showing surface changes, a grade 1 failure [82]. But, since the durability trends were not different from the samples tested to a grade 2 to grade 3 failure criterion (which present a more obvious wear scar), the results for the latter criterion have been presented here. The reason for this is that initial samples tested to grade 1 failure, when examined later, showed that some of the scar had disappeared. This was an example of visco-elastic recovery by the material. Visco-elastic recovery of a material is said to have taken place when the surface exhibits elastic recovery over an extended period of time.

In relation to the results for the drives, presented in Fig. 6.5, it must be noted that an important observation has been made which relates to wear of the media by the side 0 and side 1 heads of the drive: the side 0 interface consistently shows greater wear and testing was terminated when the relevant grade of scar had appeared on side 0. It was found that when this condition was satisfied, the side 1 interface either exhibited no visible damage, or a lower grade of failure. The explanation for this concerns the difference in the side 0 and side 1 interface as illustrated in Fig. 2.9 of Chapter 2 and as further considered in Chapter 3.

The results in the graphs of Fig. 6.5 relate to the drives and have been set out so that each shows the effect of the burnish time on durability for a particular stock roll number. This means that the effect of burnish time (conversely the roughness of the surface) on durability may be assessed. Each graph only shows the effect of burnish time as the lubrication is a constant factor for each stock roll number. The effects of changing the lubrication parameter may be seen simply by comparing the units on the co-ordinate axes of each graph.

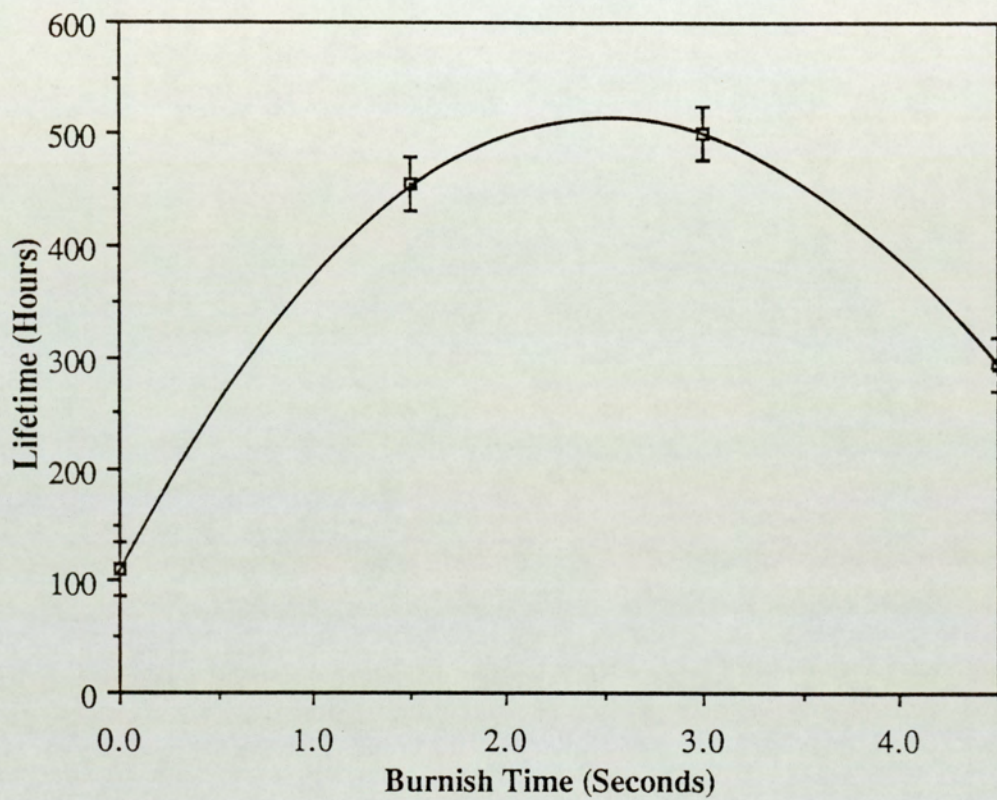


Figure 6.5 (a) Durability of differently burnished SR1 samples in the drives.

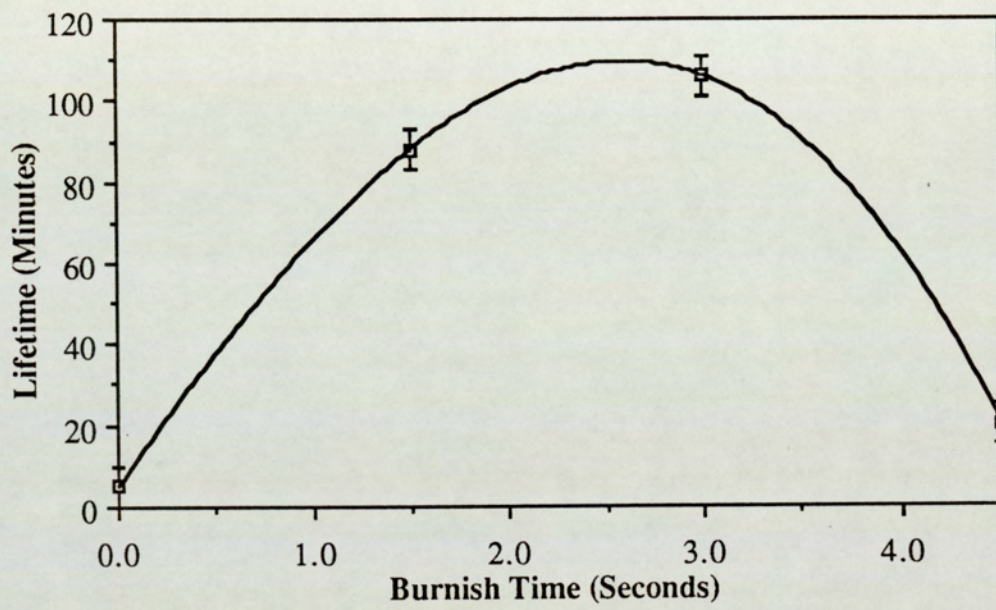


Figure 6.5 (b) Durability of differently burnished SR2 samples in the drives.

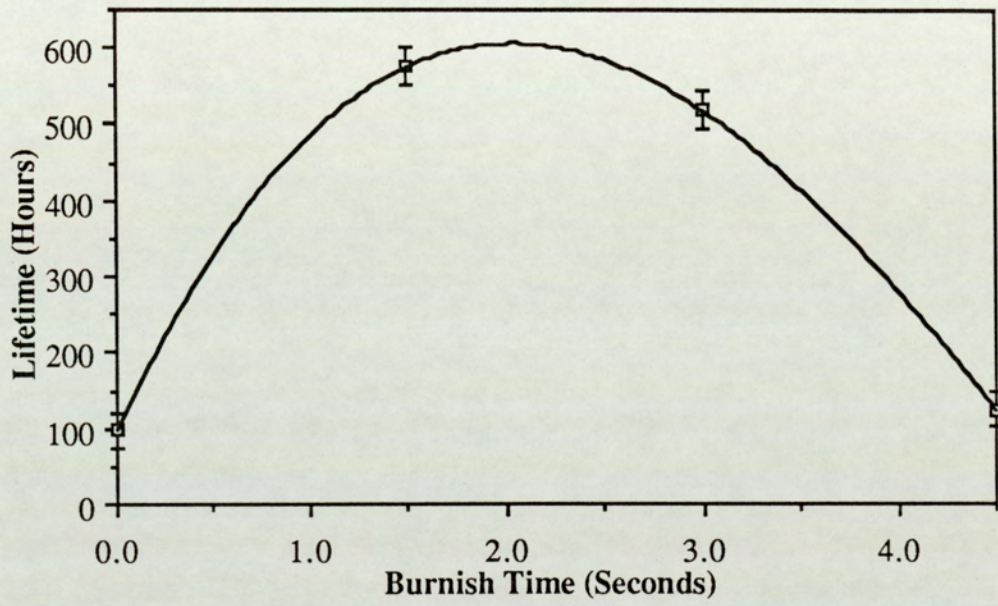


Figure 6.5 (c) Durability of differently burnished samples SR3 in the drives.

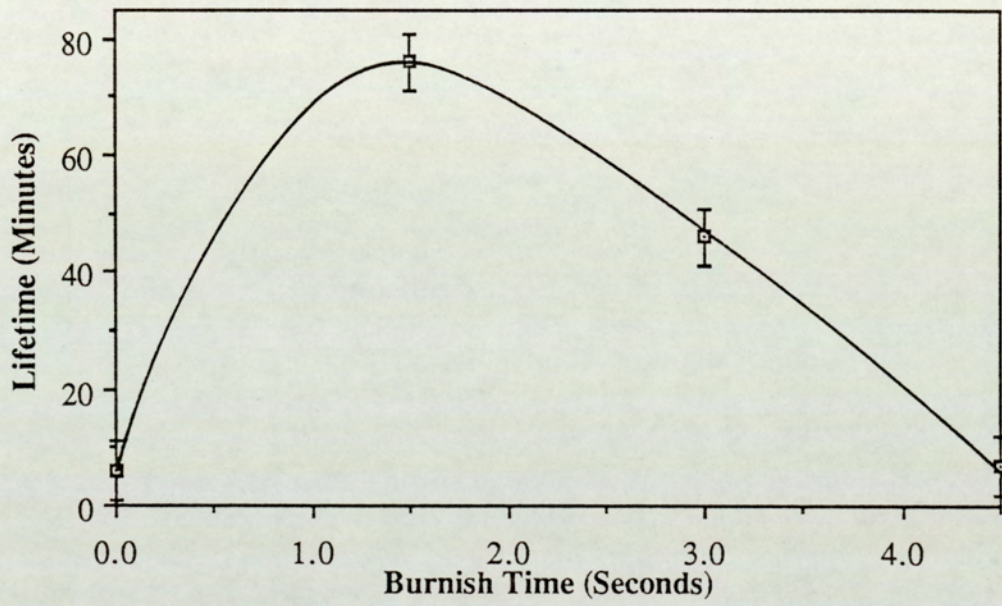


Figure 6.5 (d) Durability of differently burnished SR4 samples in the drives.

Before discussing the effects of lubrication and burnish time on durability, some discussion on the production of this data is necessary. Each of the data points on the graphs is a result of averaging many trials. For example, those presented in Fig. 6.5, pertaining just to the in-situ lifetime measurements in the drives, are a result over 125 separate experiments. It was found necessary to perform extra experiments on the less durable samples to reduce the errors. A comment on these errors is also necessary here.

These errors are introduced primarily and substantially at the observation stage. This is because of the necessarily subjective nature of the criteria employed in this work. This subjectivity has been discussed earlier. Each rig has different errors and it has been found easiest to present the errors relating to a certain set of results with that set.

As an example, the drives may be considered as these results are presented first. In this case, the absolute magnitude of the errors on the highest durability media are larger but not in per centage terms. This is so because the lower durability media was observed more frequently to check for signs of damage, as dictated by the earlier criteria. This means that reasonable errors to quote for the lower durability media, which appears to last of the order of an hour, would be ± 5 minutes. A reasonable quote for the more durable media, which can last over 500 hours in the drives, would be ± 24 hours. There are further complications, in fact, caused by lubrication with transferred layers; drive-to-drive variation and head assembly alignment; and state of wear of the heads. These effects all introduce further errors into the data which are difficult to quantify. All of these sources of error have been allowed for in the estimates of the errors, but data which was obviously affected by one or more of these effects was discarded. Details of the parameters have been left to the discussion in the chapters that follow.

Considering the results from the drives now, it may be seen from Fig.

6.5 that the roughest samples (see Table 6.1 presented earlier), as a general trend, exhibit the lowest durability as defined by the usual grading criteria. This is true for each of the particular stock roll samples, that is, a particular state of lubrication. The reasons for this are concerned with the type of damage seen in these tests. Although the exact nature of the damage will be discussed in the following chapter, it must be mentioned here that the damage consists mainly of plastic flow of the surface leading to a smoother (and more reflective) surface being formed. This is easily detected by the eye, though not so easily by the optical or scanning electron microscopy techniques used. However, a typical example obtained by SEM showing obvious plastic flow of the surface is shown in Fig. 6.6 (a) and a picture showing actual wear is presented in Fig. 6.6 (b).

A further observation to be made is that the most burnished samples also appear to show a lower durability than the intermediate burnished media samples, in general. This is to be expected because of the smoother surface being detrimental to wear through increased real area of contact. The details of this are considered in the discussion pertaining to these results but it is worth noting the shape of the curve. This shape appears to suggest an optimum burnish time between 1.5 and 3.0 seconds.

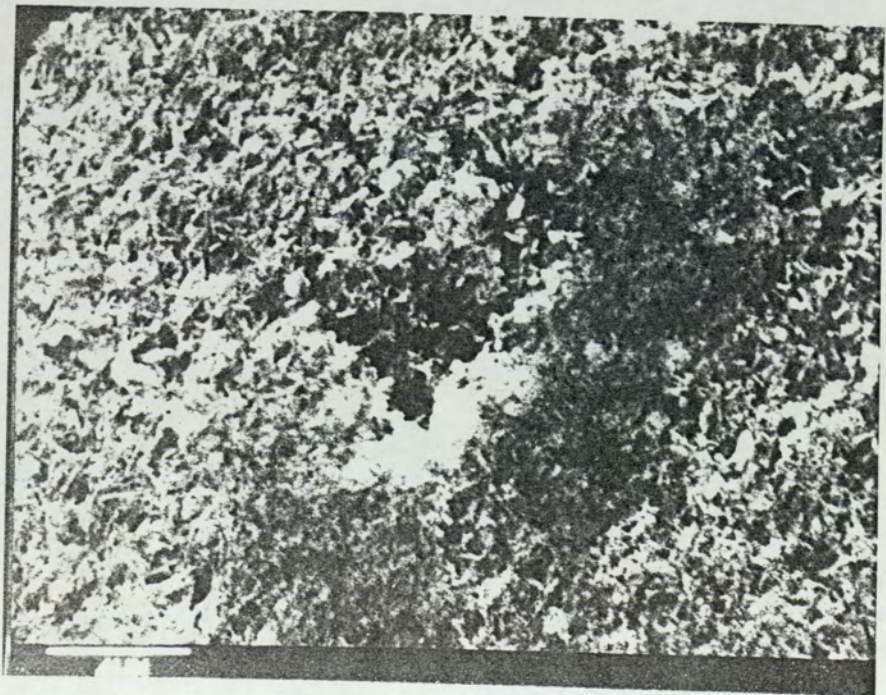
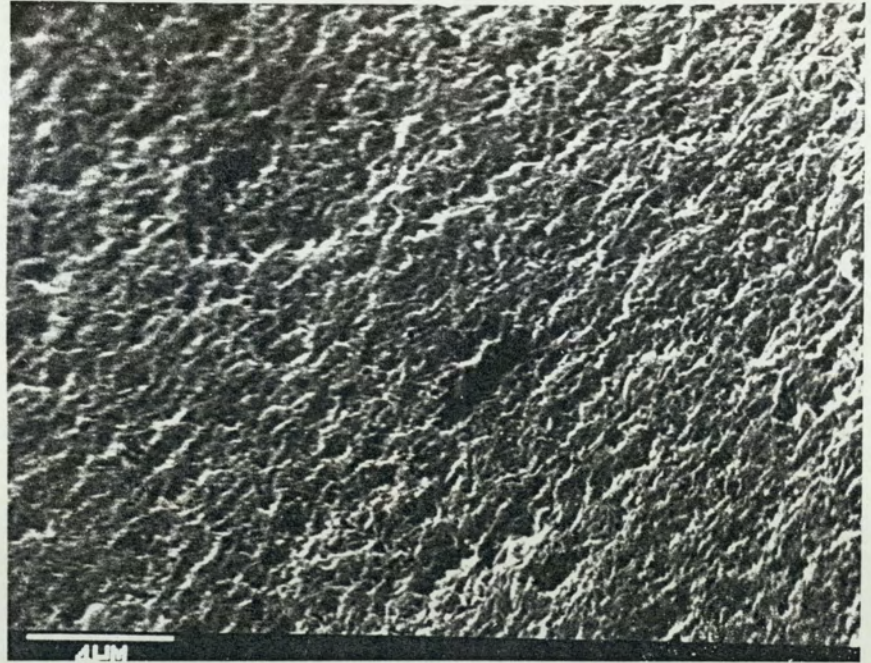
6.3.2 In-situ Friction Tester.

It is clear that friction cannot be measured directly inside the standard drives used in this part of the investigation. This problem has been overcome by the use of the novel design of the in-situ friction testing device described in section 4.4 of Chapter 4. The in-situ friction measurements have been made using this apparatus and the data presented below.

The friction tester has enabled a study to be made of the friction encountered at the head - media interfaces inside a modified diskette drive. It has

Figure 6.6 (a) A typical example of plastic flow on the surface of a diskette sample seen under SEM examination.

Figure 6.6 (b) A wear site on the media showing the edges of the damaged area lifting up around a void.



enabled the acquisition of data relating to the magnitude of the friction forces encountered at both of the head-media interfaces so that the differences between them may be readily seen. The difference in the side 0 and side 1 durability observed in the drives and the friction relating to both head - media interfaces can be seen from the friction traces obtained. Typical traces for all of the samples are presented here in Fig. 6.7. The traces relating to different burnish times for the SR2 media samples have been shown. Similarly, so have the ones for the SR4 media samples. The reason for this is that both of these samples have a low durability and produce short traces. Presenting them enables easy comparison between the different burnish times with constant lubrication parameter. The samples SR1 and SR3 produce such long traces that it is necessary to reduce them. Otherwise, this makes it impossible to present all of the traces for any particular one of these samples on one sheet.

This study has enabled the effects of the burnishing of the media surface and lubrication of that surface to be considered. In fact, it is possible to isolate the effects of each of these variables and consider them independently using the data that has been obtained. Before making the specific observations from the data relating to these separate conditions, some general points pertaining to all of the friction traces may be noted:

- (1) The friction traces show that the side 0 friction is consistently higher than the side 1 friction: this point is illustrated by the typical traces shown in Fig. 6.7.
- (2) One other point to be noted from Fig. 6.7 is that the widths of the friction traces for the two heads are different. This and the above observation, (1), may be due to the nature of the different head-media tribological interfaces at the two heads (refer to Fig. 2.9). The head at side 0 penetrates into the plane of the media in order that a better

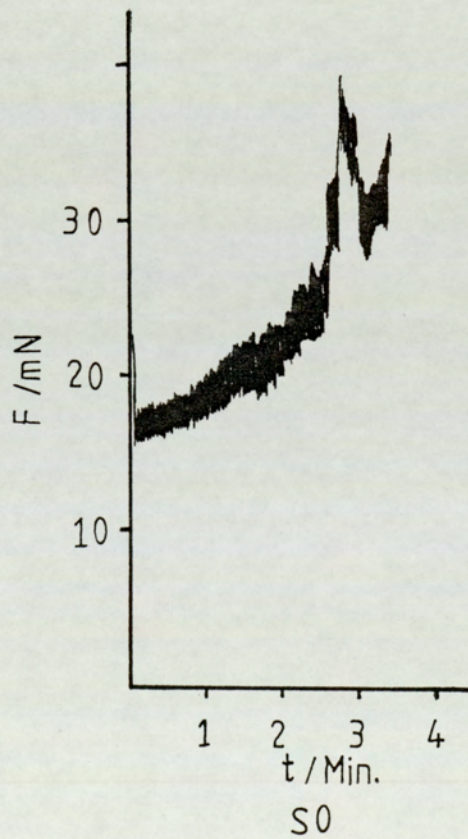
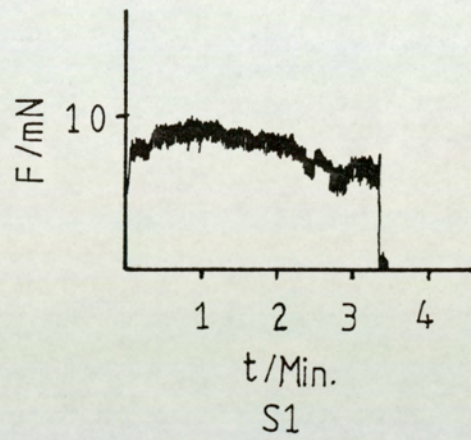


Figure 6.7 (a) Friction trace from the in-situ friction tester: SR2(0).

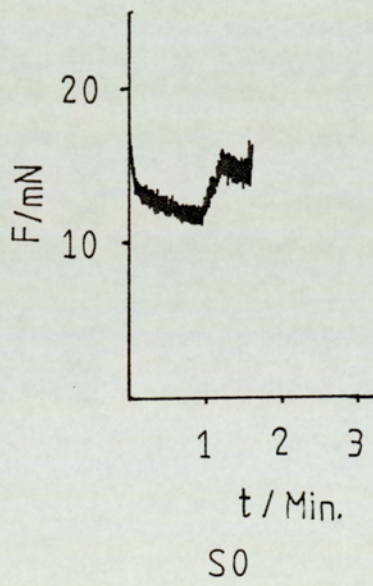
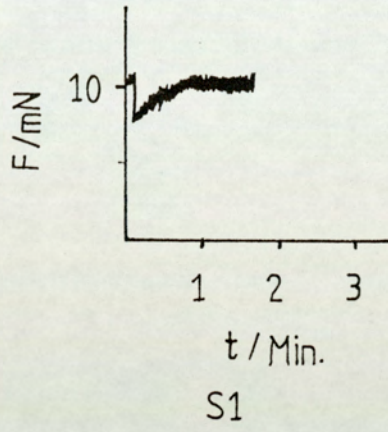


Figure 6.7 (b) Friction trace from the in-situ friction tester: SR2(1.5).

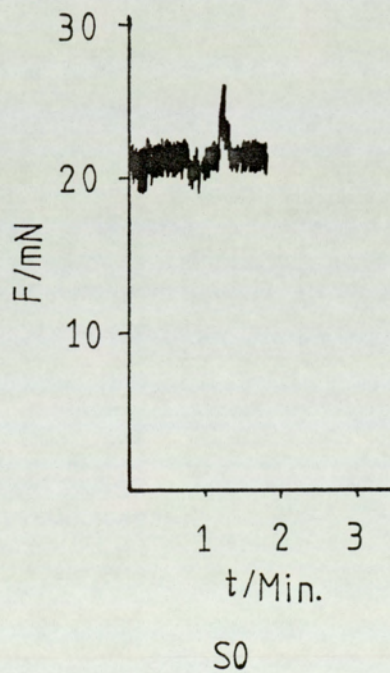
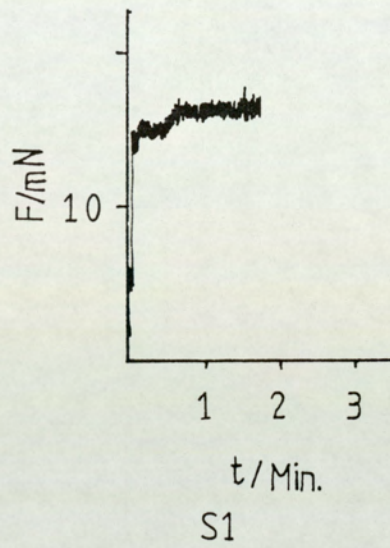


Figure 6.7 (c) Friction trace from the in-situ friction tester: SR2(3).

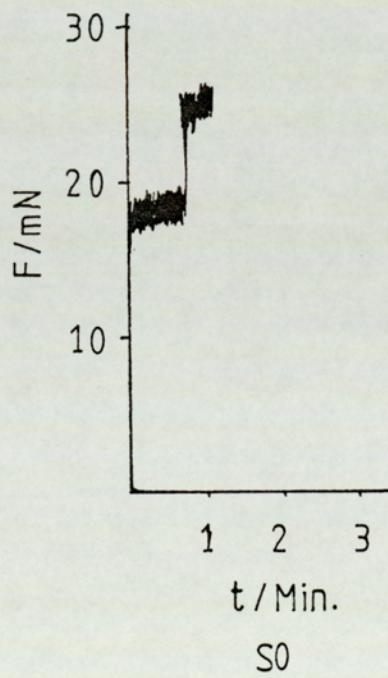
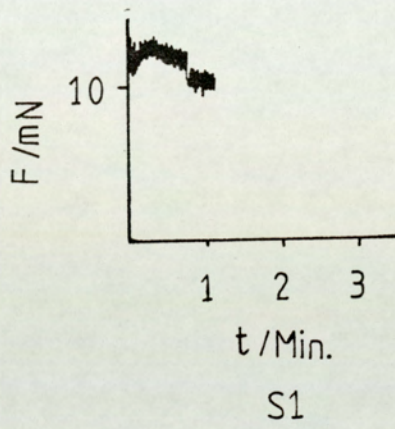


Figure 6.7 (d) Friction trace from the in-situ friction tester: SR2(4.5).

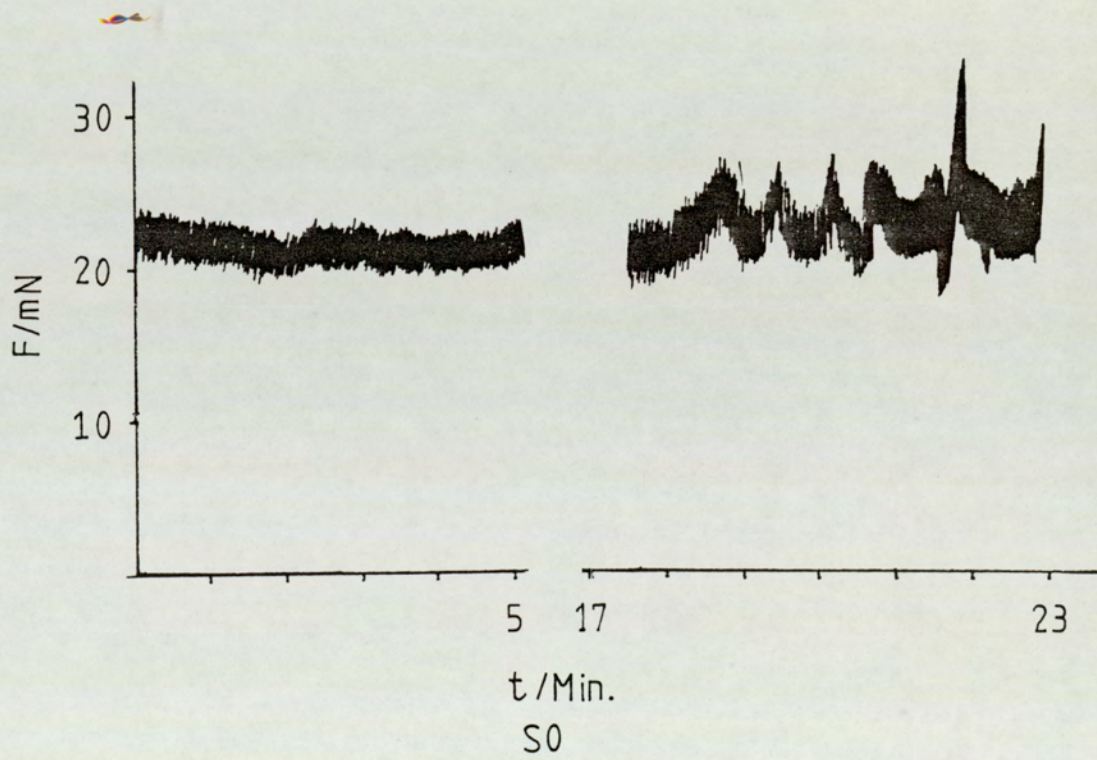
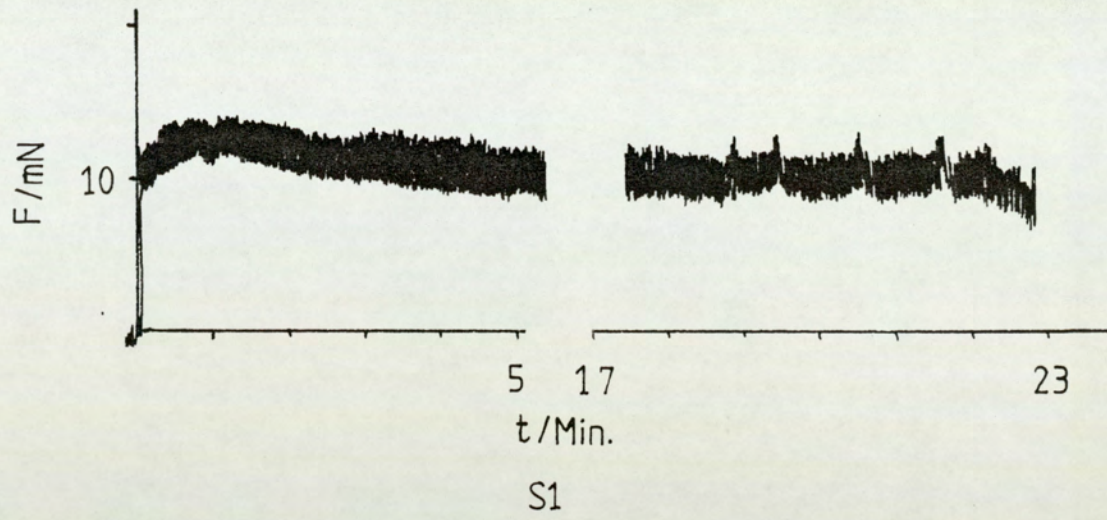


Figure 6.7 (e) Friction trace from the in-situ friction tester: SR4(0).

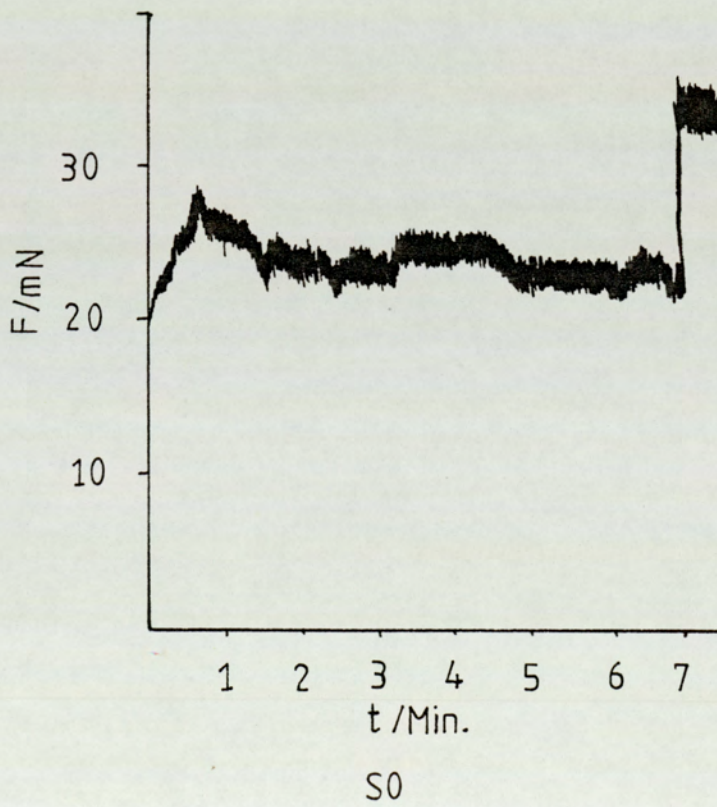
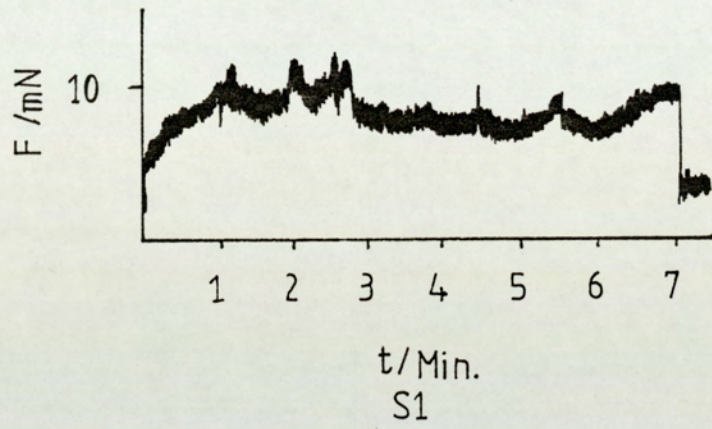


Figure 6.7 (f) Friction trace from the in-situ friction tester: SR4(1.5).

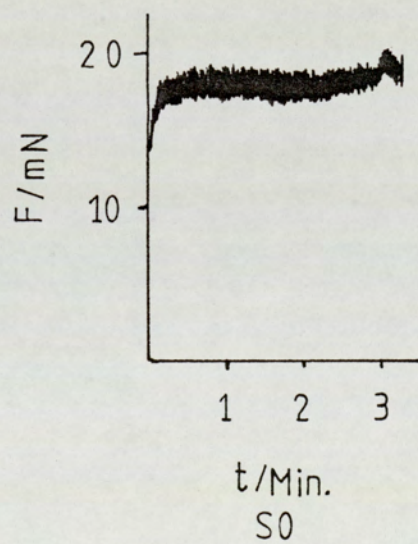
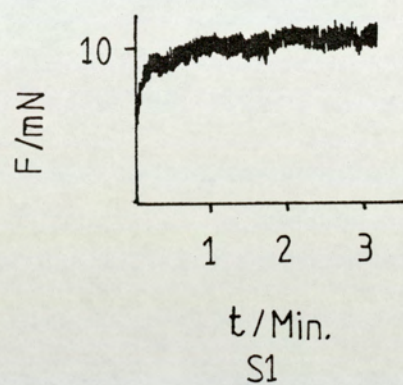


Figure 6.7 (g) Friction trace from the in-situ friction tester: SR4(3).

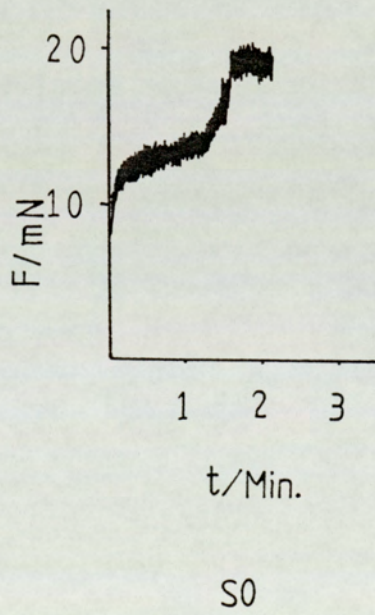
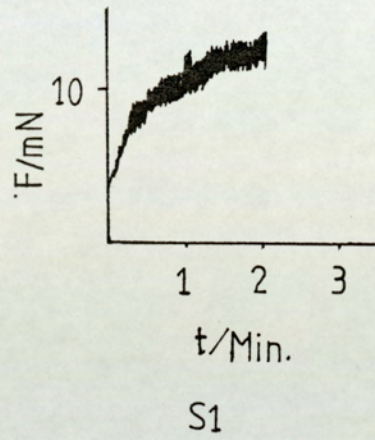


Figure 6.7 (h) Friction trace from the in-situ friction tester: SR4(4.5).

interface for the purposes of the read/write operation may be obtained [60] and this results in greater media contact with the side 0 head compared to that suffered by the side 1 head.

- (3) All traces show a general rise in friction as the test progresses except at the start of the test where the heads "settle into position". This effect being very much less pronounced in surface lubricated media, as will be seen from the typical friction traces shown in Fig. 6.8 and discussed later.

(a) Effects of Burnishing.

Considering the effects of the surface burnishing of media, Figs. 6.7(a) to (h) show typical traces for the samples without any lubricant present at all, SR2, (Figs. 6.7(a) to (d)) and those with only the bulk lubricant present, SR4 (Figs. 6.7(e) to (h)). Each of the two sets of figures shows the effect of burnishing on the different samples. It is clear that the more burnished samples exhibit a reduced durability in terms of real damage to the surface. This may be seen from the fact that the unburnished samples show the longest trace before a sudden rise in friction. This rise in friction occurs as the media sample begins to wear, as shown by the ends of all of the traces of Fig. 6.7. All of the traces are on the same time scale and show a slightly different trend to that observed in the drives. The drives data for SR2 and SR4 (Figs. 6.5(b) and 6.5(d) respectively) show that the unburnished samples exhibit the lowest durability. They show the optimum burnish time to be between 1.5 and 3 seconds. However, the present data from the friction tester (Fig. 6.7(a) to (d) and Fig. 6.7(e) to (h)) shows that durability decreases with increased burnish time. The unburnished media shows greatest durability.

The apparent contradiction in the data that this highlights may be

resolved by more careful consideration. This comes from the fact that the samples may be removed from and re-inserted into the drives during a test if a wear scar has not been formed. In the case of the friction tester, however, the setting up procedure is intricate and precarious. This forbids removal of the sample "mid - test" for examination. This, in turn, results in the friction variable being used to signify the end of a test. In fact, the friction tester probably constitutes a better scientific test as a consequence because the damage is no longer purely superficial but possibly more real. The gradual increase in the friction during a test indicates increasing plastic flow and so real area of contact. The grade 2 failure detected in the drives is considered to have occurred at this stage. The sudden increase in the friction at the end of friction tester experiments indicates real wear. The mechanisms of this real wear are discussed in Chapter 7. It is worth noting, however, that, despite the scientific superiority of the friction criterion, the question of customer acceptability is considered more important by media manufacturers. Hence the present criteria.

One of the key points to be noted here from all of these traces is the sharp upward transition in the magnitude of the friction force which has been observed at the end of the tests on the friction tester. This clearly demonstrates, together with the relative magnitudes of the side 0 and side 1 friction forces and their respective durabilities, that friction and wear are intimately related in the case of magnetic media.

Another observation to be made here is that there is no obvious difference in the initial frictional forces exhibited for the different samples. However, it is clear that the side 0 friction is consistently higher than the side 1 friction.

The effects of burnishing on the samples SR1 and SR3 is difficult to assess from the relevant friction traces as they show a very high durability. Each of these samples was only tested for a period of approximately two hours. The

justification for using such a test is that a media sample under normal use would probably not subject a single track to such a long period of use in the entire lifetime of that sample. As such, the samples have probably been tested beyond the requirements under normal use. Furthermore, to test these samples to failure, would probably have shown durability periods exhibited in Figs. 6.5(a) and (c). So, in the time available, it was not possible to test these samples to failure using the friction tester. The tests on these samples do show, however, that the friction does rise, in general, but only very slightly even after a relatively long time. At the end of these two hour tests no wear scar of any description can be observed as such. Some very small wear patches can be seen, however, on careful scrutiny. These friction observations seem to indicate that the same processes are occurring in the surface lubricated samples as those without this lubricant, but over a much longer period of time. In fact, had these tests been taken to their logical conclusion, the steady increase in friction seen in the cases of the supported sample and the unsupported sample accelerated testing rigs would be expected. The data from these rigs is presented in section 6.3.3 for comparison. In the case of the friction tester, longer term tests were not possible because of the time constraints mentioned above. Also, one further reason for not performing long term tests on this rig is that this study has discovered that the zero-stability of this rig is quite poor. The tendency of the zero to drift randomly, is probably due to the difficulty in mechanical isolation of the whole rig from external vibration, despite the considerable precautions taken, and the sensitivity of the delicate load cells employed to detect the small forces encountered. Further steps to eliminate this problem can be taken, but require development of the instrumentation and since these were the last set tests to be performed for this work, this has not been possible in the allotted time. It is recommended, however, that before any more meaningful data can be acquired with long term tests some redesign is necessary. Skelcher [110] used a similar rig to the friction tester in its present form. He

used it to measure the initial friction of the diskette media. It would appear that no long term tests have been performed on this rig before and no investigation of its stability have been made [137]. Another reason for the length of these tests being limited is that, since this rig is a "one-off" specially produced at 3M, there are no spare parts readily available. The heads employed in the rig have been taken from production diskette drive units and as such are prone to similar wear. Long term tests in the drives have necessitated replacement of heads but this was not possible here. Obviously the wearing of heads prevents any more meaningful data acquisition as worn heads merely cause the media to wear immediately after insertion by a ploughing mechanism. Furthermore, long term tests would be expected to last as long in the In-situ friction tester as they do in the drives as it resembles them very accurately. This, as can be seen from the data of Fig. 6.5, would take an excessively long time to complete. In fact, this would be a very useful study as the present data suggests. One test was performed on SR1(3) media and was selected as a typical representative of the more durable media. It has shown a similar rise in the friction to that observed for the less durable media when wear is initiated. This occurred for the SR1(3) media after some eight days and may, it is suspected, have been accelerated by the removal of the media in mid-test for examination. This examination was necessary in order to confirm that the rise in friction was a true indicator of the onset of wear.

The frictional forces encountered at the two heads in the friction tester are presented in Fig. 6.9 after the effects of lubrication have been considered.

(b) Effects of Lubrication.

As has been discussed above, the samples SR1 and SR3 show a very high durability in the drives. The results of applying a surface lubricant, whether in conjunction with (SR3) or without (SR1) a bulk lubricant, has been found to be

to increase the durability lifetime of the media dramatically. The friction trace produced on the friction tester shown in Fig. 6.8 illustrates the situation and is typical of the traces obtained for the SR1 and SR3 media. This has been reduced to fit. It is instructive to note, however, that in this case, as in every other case, the side 0 friction is higher than that at the side 1. Also there is no significant change in the friction at either head.

Produced in Fig. 6.9 are the averaged friction results obtained on the friction tester for each of the samples SR1 to SR4 with their four sub-divisions regarding the extent of burnishing experienced. These forces represent the initial friction at the start of each test. The averages have been obtained by performing many tests on each sample. The number of tests performed is shown in brackets for each sample by each point on the graph.

A comment on the errors to be quoted for this is necessary. The errors arise from the widths of the traces. The frictional forces for any particular trace has been quoted as the mean of the two extremes formed by the width of the trace. The error on the value of the frictional force can be quoted as $\pm 0.5 \times (\text{width of trace})$. This leads to an error of $\pm 10^{-3}$ N on both side 0 and the side 1 traces. The reason is that these values are, generally, more than or of the order of the statistical spread. Although the side 1 traces appear to be narrower than the side 0 traces, they also show less stability. Further, both sides show a similar statistical spread.

Looking at the data, some points are particularly obvious from it. One such observation is that, in general, the surface lubricated samples (SR1 and SR3) have lower friction than the samples SR2 and SR4 which do not have the surface lubricant added to them. Also it can be seen that the side 0 friction is, in all cases, greater than the side 1 friction. The higher friction in the roughest samples (0 second burnish) may be explained by, in the case of surface lubricated media, the consideration that the frictional force merely serves to deform the

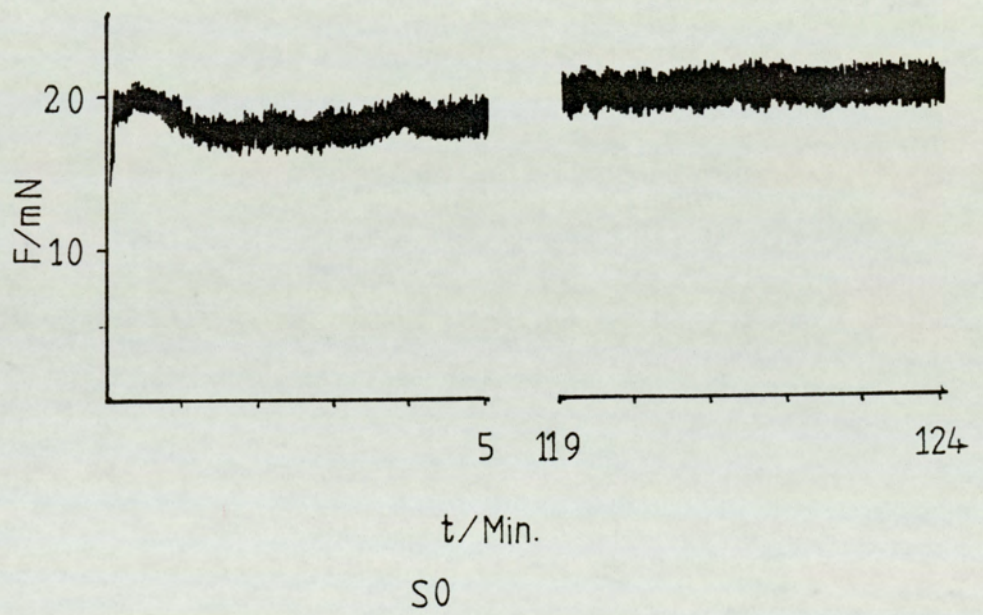
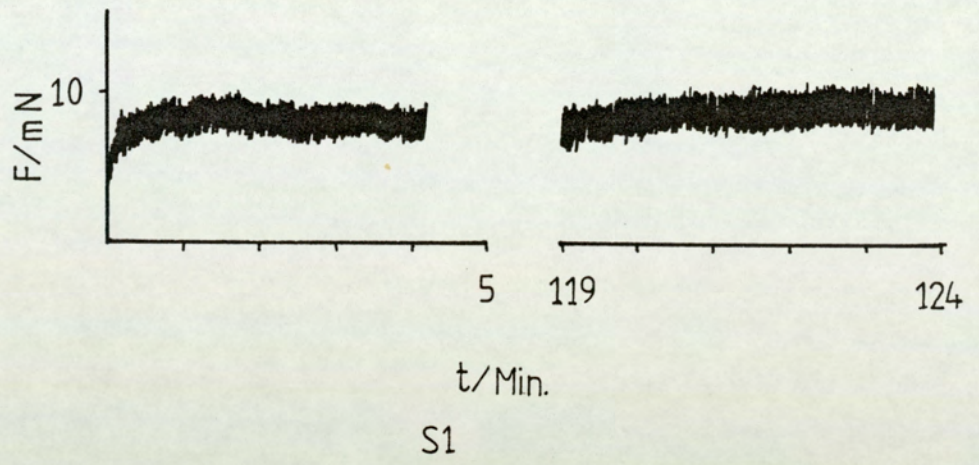


Figure 6.8 Friction trace for a sample with surface lubrication applied: note the time scale shown.

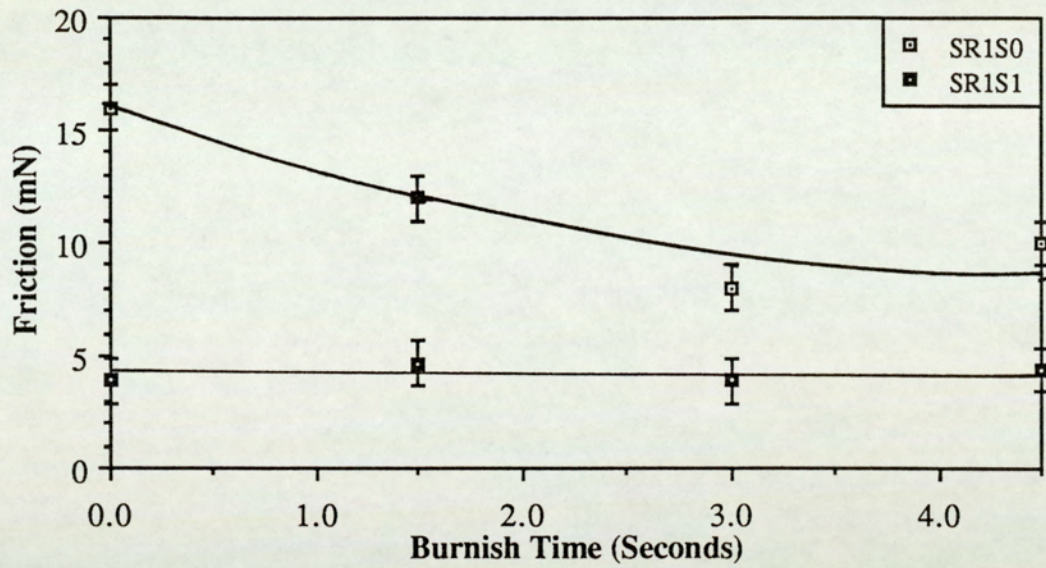


Figure 6.9 (a) How initial friction varies with burnish time for Samples SR1 in the in-situ friction tester.

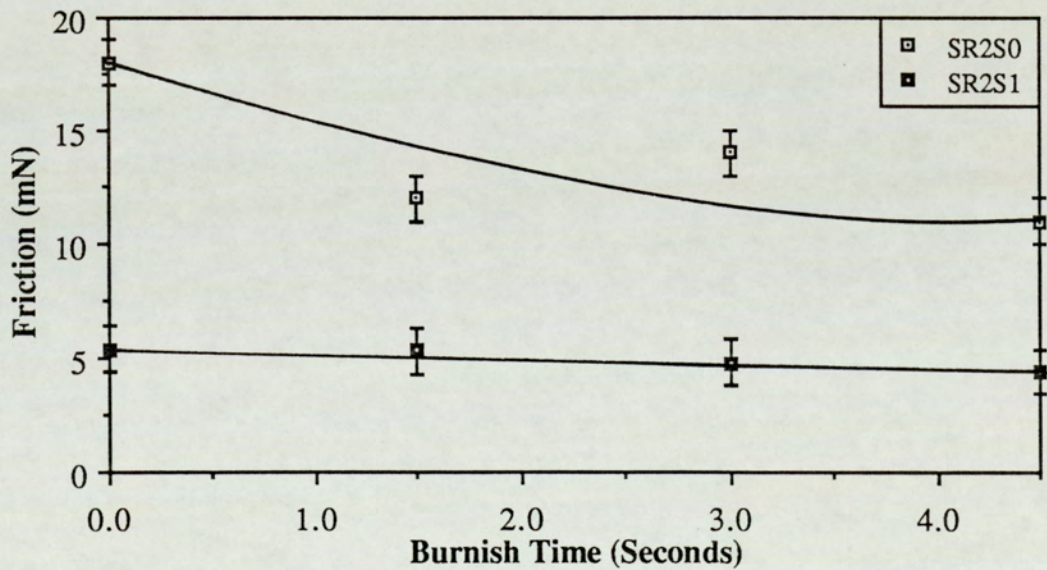


Figure 6.9 (b) How initial friction varies with burnish time for samples SR2 in the in-situ friction tester.

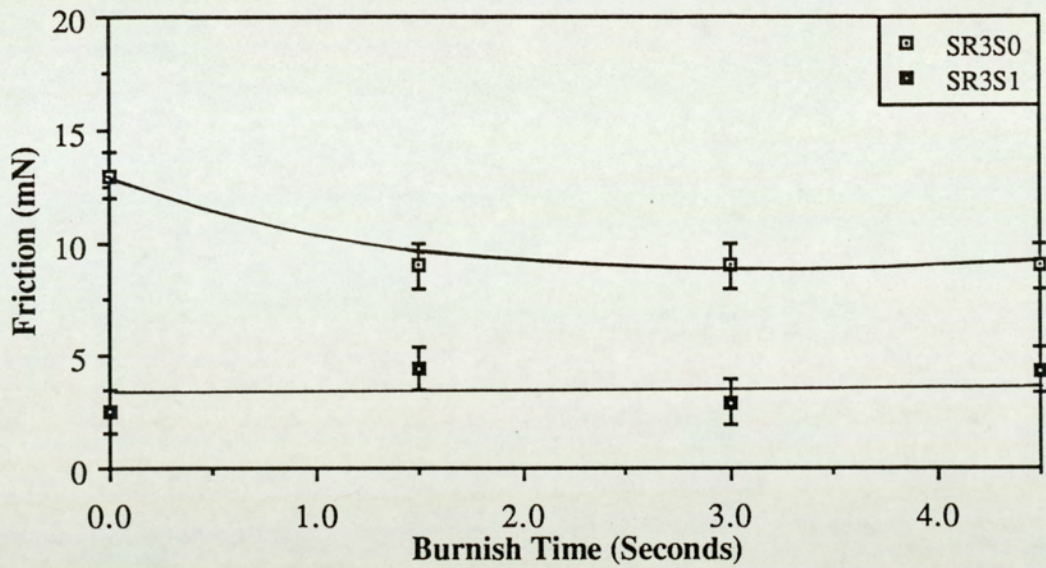


Figure 6.9 (c) How initial friction varies with burnish time for samples SR3 in the in-situ friction tester.

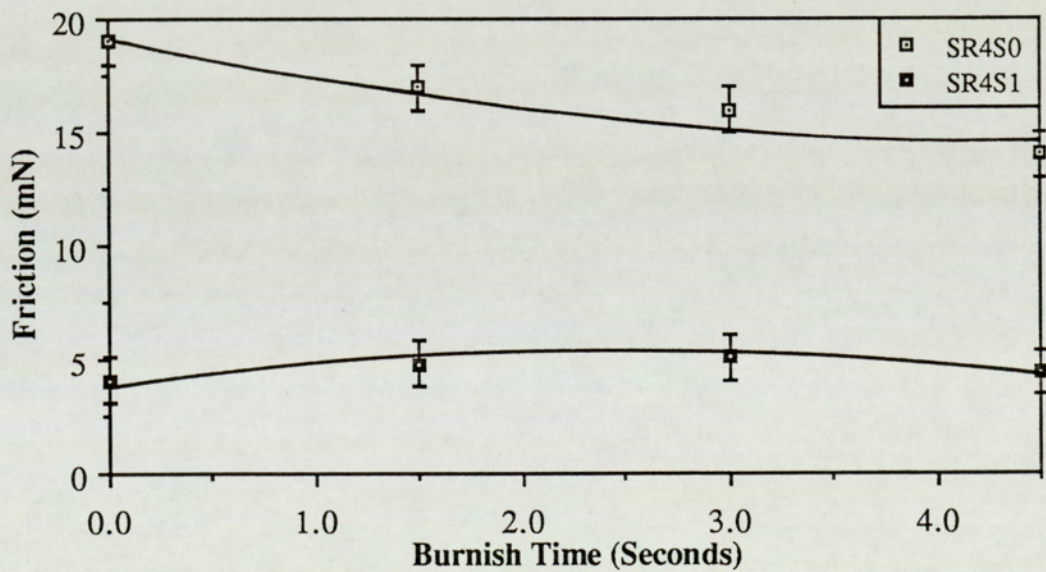


Figure 6.9 (d) How initial friction varies with burnish time for samples SR4 in the in-situ friction tester.

asperities and produces a smooth surface with little surface lubrication. The surface lubricant may physically combine with the deformed asperities. With smoother samples, the surface lubricant still exists on the surface affording less real contact. In the case of the samples without surface lubrication (SR2 and SR4), the plastic flow of the larger asperities produces an environment of increased real area of contact as no surface lubricant is present to limit this contact. Further, the bulk lubricant in the samples SR4 appears to have no appreciable beneficial effects with the samples burnished for 3.0 and 4.5 seconds. Similarly burnished samples in the SR2 (completely unlubricated) category show a lower friction than for the bulk lubricated SR4 samples.

6.3.3 The Simulation Rigs.

The samples tested on the simulation rigs, both supported (side 1 simulator) and the unsupported (side 0 simulator), are considered in this sub-section. The durability results are presented in Figs. 6.10 and 6.11 for the supported and unsupported sample rigs respectively. These can be seen to show broadly similar trends in durability for the samples as have been found earlier for the drives and for the friction tester apparatus with the surface lubricated media showing much greater durability than those samples without the surface lubricant.

One particular point which needs to be considered here is that which concerns the actual durability of the samples. It can be seen that all of the samples produce wear scars more rapidly on the two simulation rigs when using the same grading for terminating tests as was used for the drives and the friction tester, that is, a grade 2 to 3 failure status. The shape of the durability curve is similar to that for the drives and this will be discussed in Chapter 7. However, as will also be discussed more fully in that chapter, the justification for using these rigs as accelerated testing rigs needs to be confirmed. The fact that they

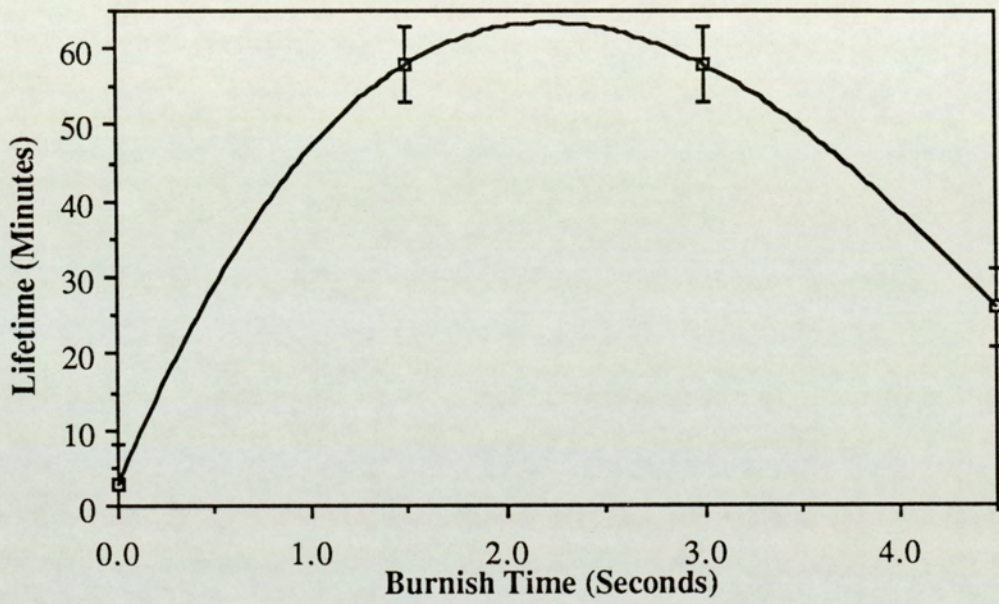


Figure 6.10 (a) Durability of differently burnished SR1 samples on the supported sample simulation rig.

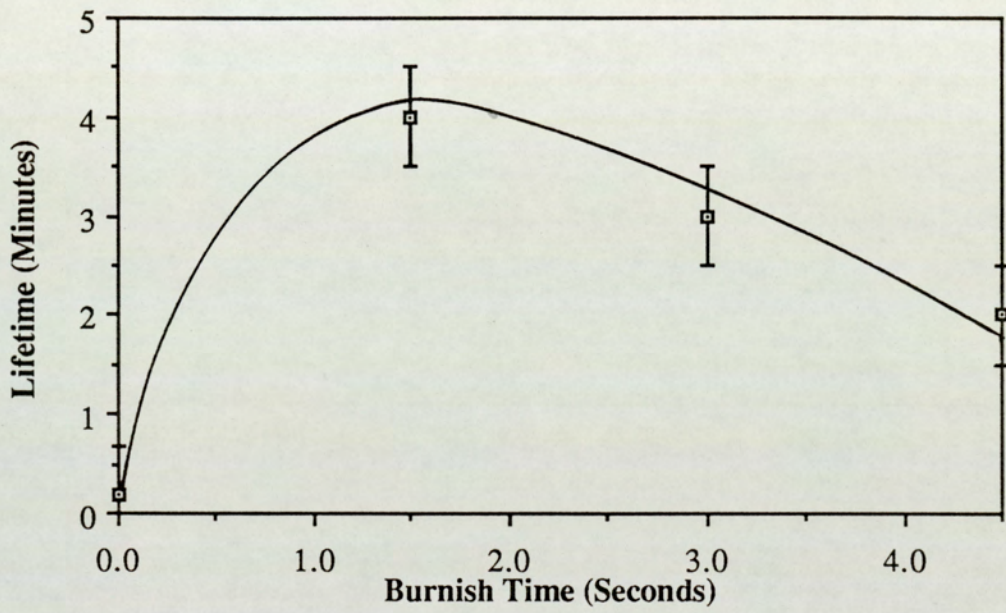


Figure 6.10 (b) Durability of differently burnished SR2 samples on the supported sample simulation rig.

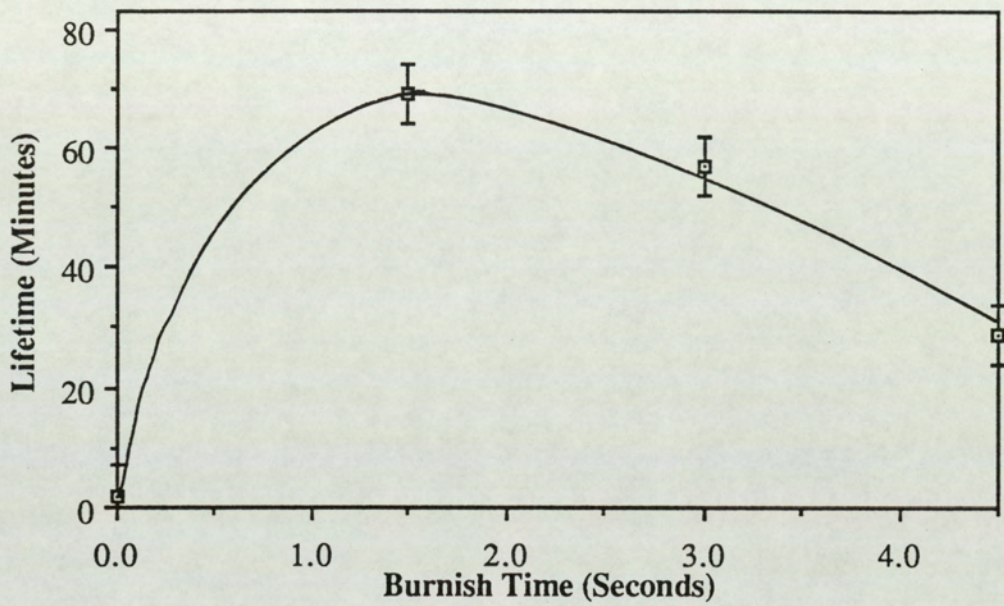


Figure 6.10 (c) Durability of differently burnished SR3 samples on the supported sample simulation rig.

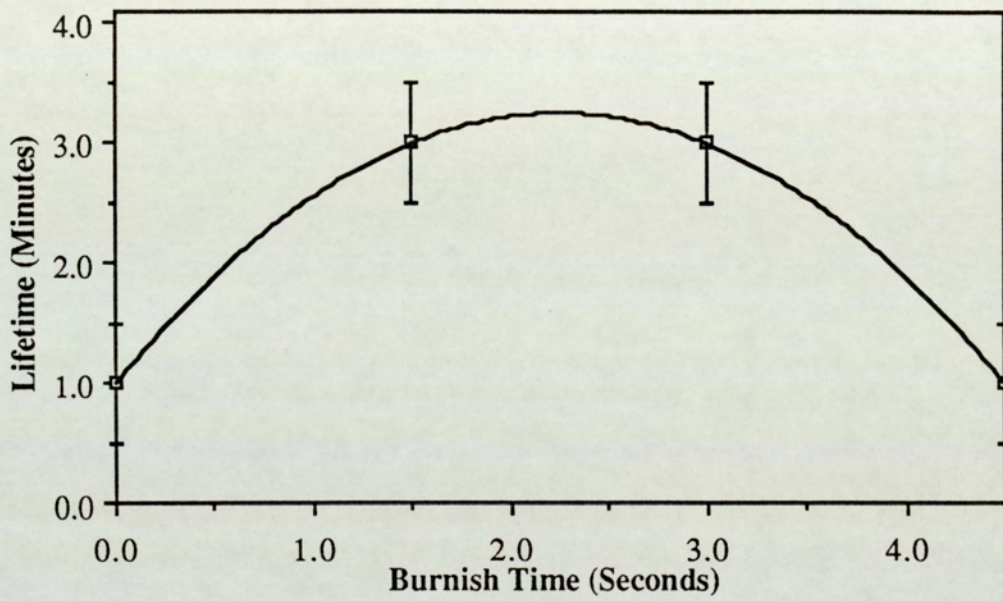


Figure 6.10 (d) Durability of differently burnished SR4 samples on the supported sample simulation rig.

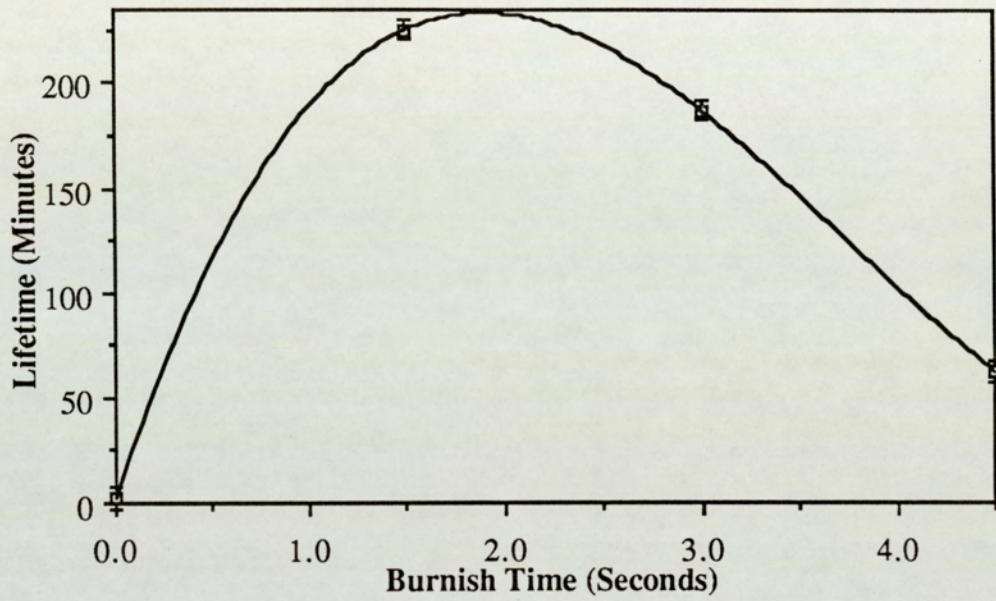


Figure 6.11 (a) Durability of differently burnished SR1 samples on the unsupported sample simulation rig.

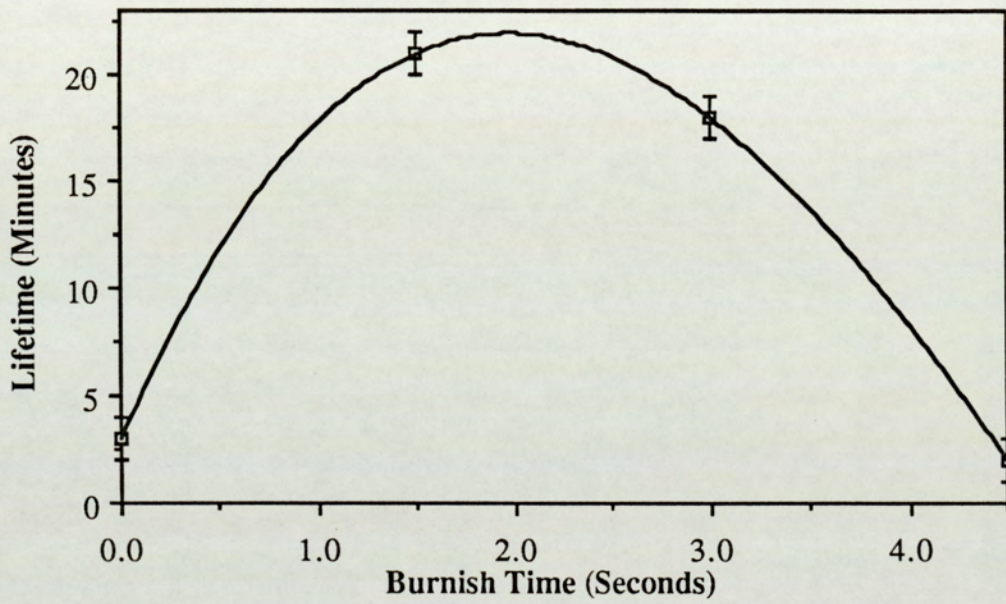


Figure 6.11 (b) Durability of differently burnished SR2 samples on the unsupported sample simulation rig.

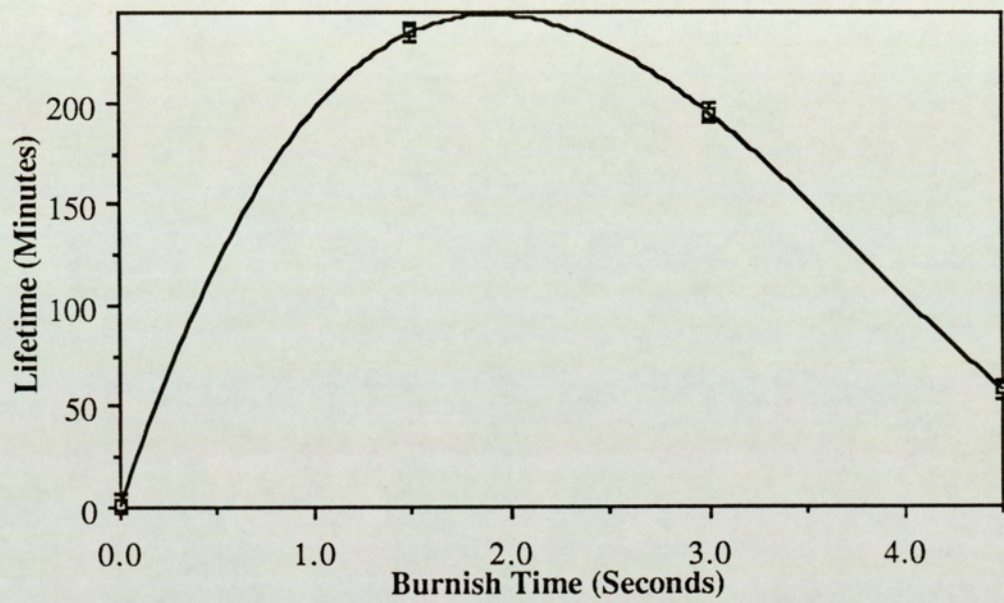


Figure 6.11 (c) Durability of differently burnished SR3 samples on the unsupported sample simulation rig.

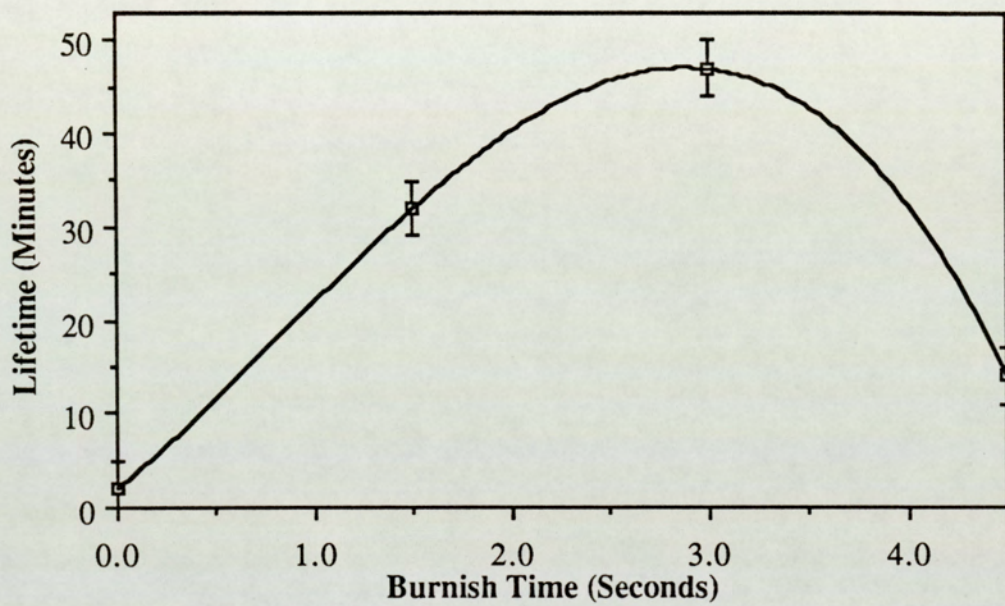


Figure 6.11 (d) Durability of differently burnished SR4 samples on the unsupported sample simulation rig.

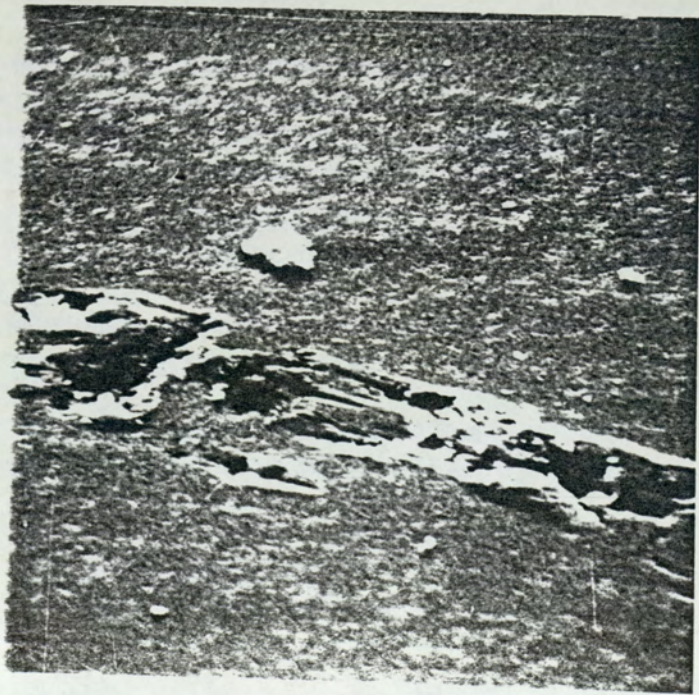
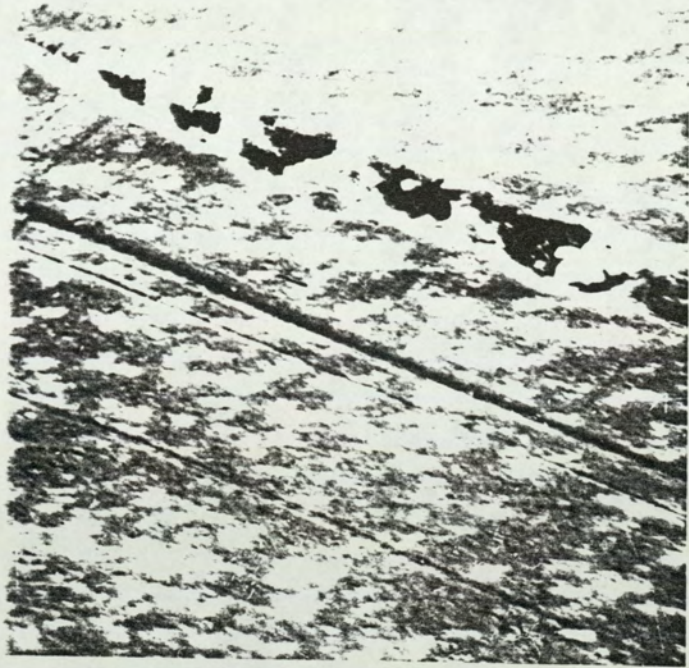
produce wear more rapidly is not sufficient, the type of wear must also be similar.

Once again, the detailed description of the wear process is left to the following chapter but it can be seen from the micrographs of Fig. 6.12 (a) and (b) that the two rigs do produce surface features which resemble very closely those found on the media tested in the drives. These features tend to be more pronounced in the case of the rigs and at a further stage of wear. This is probably because the wear progresses much more quickly and the tests could be stopped slightly earlier. It appears that genuine accelerated wear testing is achieved.

In considering the friction encountered at the head-media interfaces on the two simulation rigs, the data presented in Fig. 6.13 may be utilised. This data has been presented in a similar fashion to that of Fig. 6.8 earlier which showed the results obtained on the friction tester. In the present case, however, instead of using side 0 and side 1 friction, one arm of the graph represents the flexing sample case and the other arm the supported, non-flexing, sample case. These graphs may be compared to those of Fig. 6.8 where the side 0 friction and side 1 friction has been recorded. It can be clearly seen that the side 0 (Fig. 6.8) and the flexed sample simulation (Fig. 6.13) consistently show higher friction than the side 1 (Fig. 6.8) and the unflexed sample (Fig. 6.13). The rigs may very loosely be considered to represent the the side 0 and side 1 cases. In fact, what is undoubtedly achieved with the rigs is that the flexing variable is removed in the one case and inserted in the other. The similarity between the two sets of data is incredible and shows that the rigs appear to represent the processes occurring in the drives quite accurately. The reduction in friction with burnish time is a point very well worth noting. This appears to contradict the concept of burnishing producing smoother media with a larger real area of contact. In fact, the situation is much more complex and so its full consideration has been left until the discussion of the following chapter.

Figure 6.12(a) Catastrophic failure shown by a sample on the supported sample simulation rig with plastic flow and ploughing clearly visible (1 K \times).

Figure 6.12(b) Similar to the above but clear ploughing wear on the unsupported sample simulation rig (550 \times).



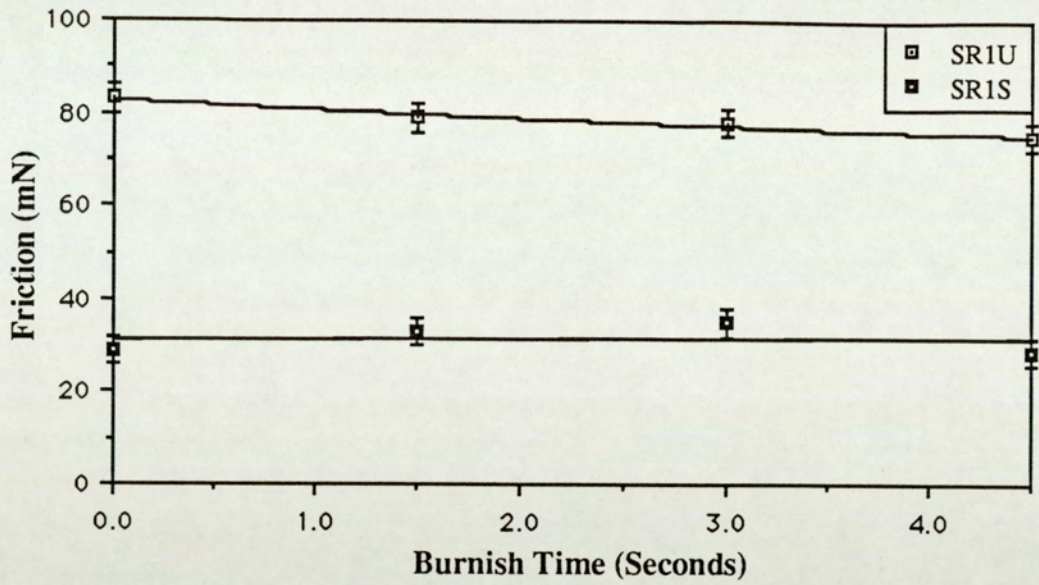


Figure 6.13 (a) How initial friction varies with burnish time for samples SR1 on the simulation rigs (U=unsupported, S=supported sample rig).

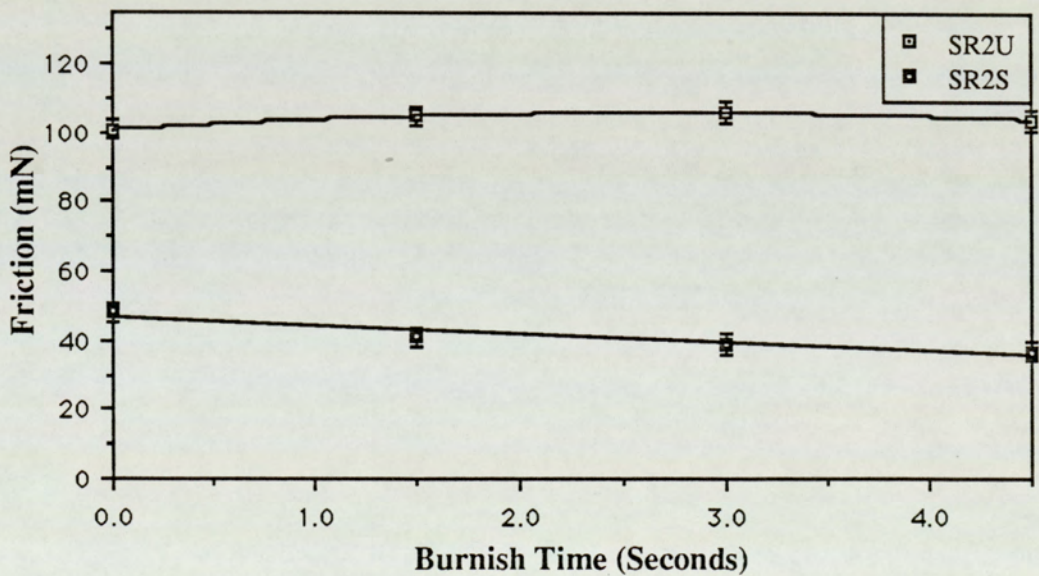


Figure 6.13 (b) How initial friction varies with burnish time for samples SR2 on the simulation rigs (U=unsupported, S=supported sample rig).

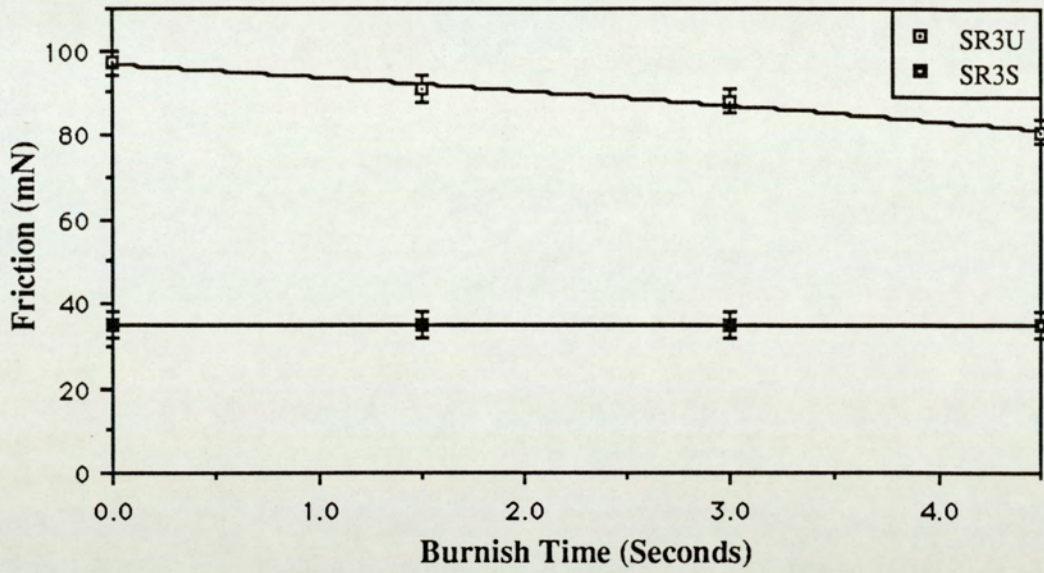


Figure 6.13 (c) How initial friction varies with burnish time for samples SR3 on the simulation rigs (U=unsupported, S=supported sample rig).

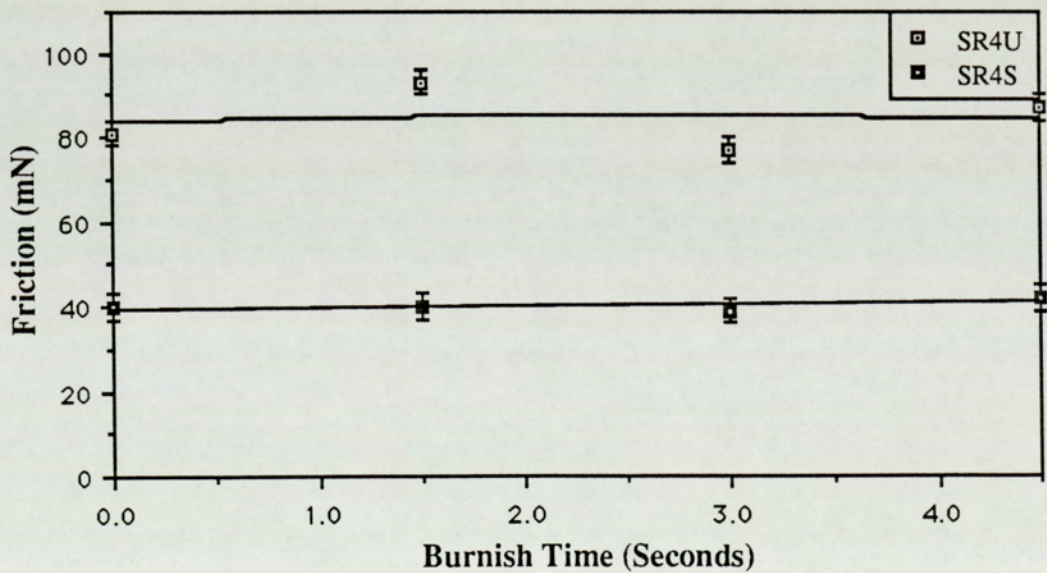


Figure 6.13 (d) How initial friction varies with burnish time for samples SR4 on the simulation rigs (U=unsupported, S=supported sample rig).

The accuracy of the results is obviously important and in this regard the errors on the friction measurements made on the simulation rigs need to be considered. The main error of measurement is due to the thickness of the pen and amounts to approximately $\pm 3 \times 10^{-3}$ N. In the case of the supported sample rig, the statistical spread is typically less than this. So, the error on the supported sample simulation rig friction measurements may be quoted as $\pm 3 \times 10^{-3}$ N. In the case of the unsupported sample rig results, some complications arise from loading of the head onto the media. These arise due the sample causing the head to twist slightly on its gimball flexure. The overall consequence of this is that the quoted error is somewhat higher. The size of the error for this rig may be quoted as 8×10^{-3} N. It may be noted that in per centage terms the errors on the two rigs are similar at $\sim \pm 10\%$.

The effects, as for the friction tester, of burnishing may now be considered.

(a) Effect of Burnishing

The effect of burnishing is, once again, seen to show remarkably similar trends to those found in the drives in both the supported sample rig and the unsupported one. Clearly the completely unburnished samples show a very low durability probably for the same reasons as mentioned earlier concerning plastic deformation of the larger asperities. The effect of burnishing the samples, as found in the drives' data, appears to be initially beneficial. However, further burnishing shows an adverse effect. Reasons for this could be related to the effect that the burnishing process has on the fundamental constitution of the surface layer. It is possible that initial burnishing has an effect on the crystallinity of the surface leaving it relatively hard. Clearly, this would improve durability as the harder material would be less prone to plastic flow. Since the durability criterion entails

detection of this plastic flow, as discussed earlier, an improvement may be observed in this case. Further burnishing, however, may then cause sub-surface damage at the interface of this harder surface and the material in the sub-surface region. This would be the initiation of the wear process and is considered more fully in the discussion of these results later in Chapter 7.

In considering the friction traces obtained from the supported sample and unsupported sample rigs, some important observations may be made. Figs. 6.14 to 6.17 illustrate the effects of the different burnishing times for the samples SR2, SR4, SR1 and SR3. Each figure shows (a) the unsupported sample and (b) supported sample rig data. It is clear from these that the friction value is higher by approximately an order of magnitude for these rigs when compared to the friction tester data. Also, a general rise in the friction similar to the friction tester data may be observed as the test progresses in each of the cases. This is far more pronounced here than in the case of the friction tester where it is noticeable only on close scrutiny. However, although there appears to be some evidence for a sudden increase in the the friction at the end of tests, this is not as pronounced in the present case as for the friction tester. The reason for this may be that the friction tester is much more sensitive than the simulation rigs.

One further observation is that there is consistency between the friction tester and simulation rigs' data in that both show higher friction - time gradients for the SR2 and SR4 media samples than for the more durable SR1 and SR3 samples.

(b) Effects of Lubrication.

Once again the value of the surface lubricant is highlighted with the samples SR1 and SR3 showing far greater durability than the samples SR2 and SR4.

One point which comes out very clearly is that regarding the burnishing

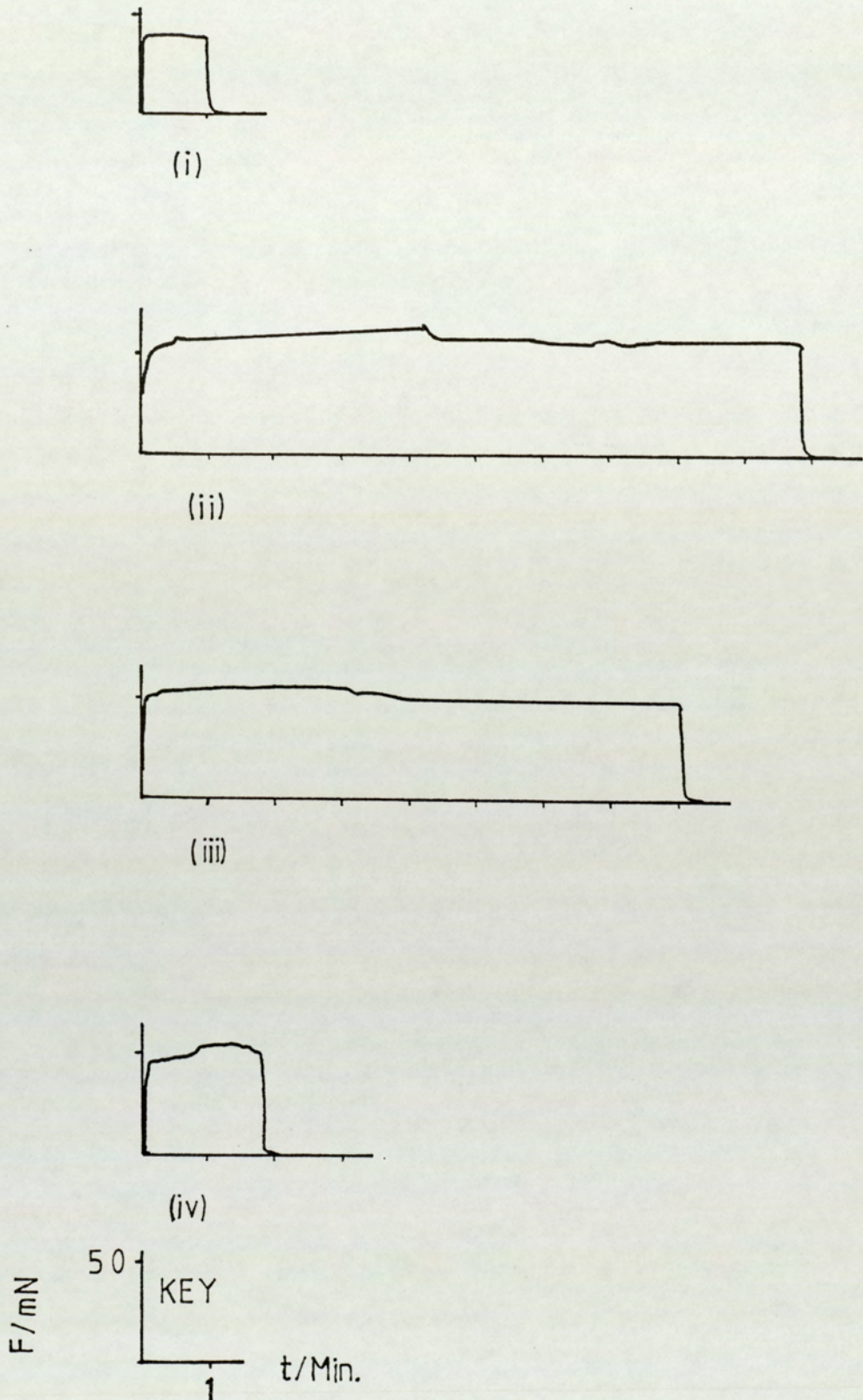


Figure 6.14 (a) Friction for the sample SR2 on the unsupported sample rig showing (i) SR2(0), (ii) SR2(1.5), (iii) SR2(3), (iv) SR2(4.5).

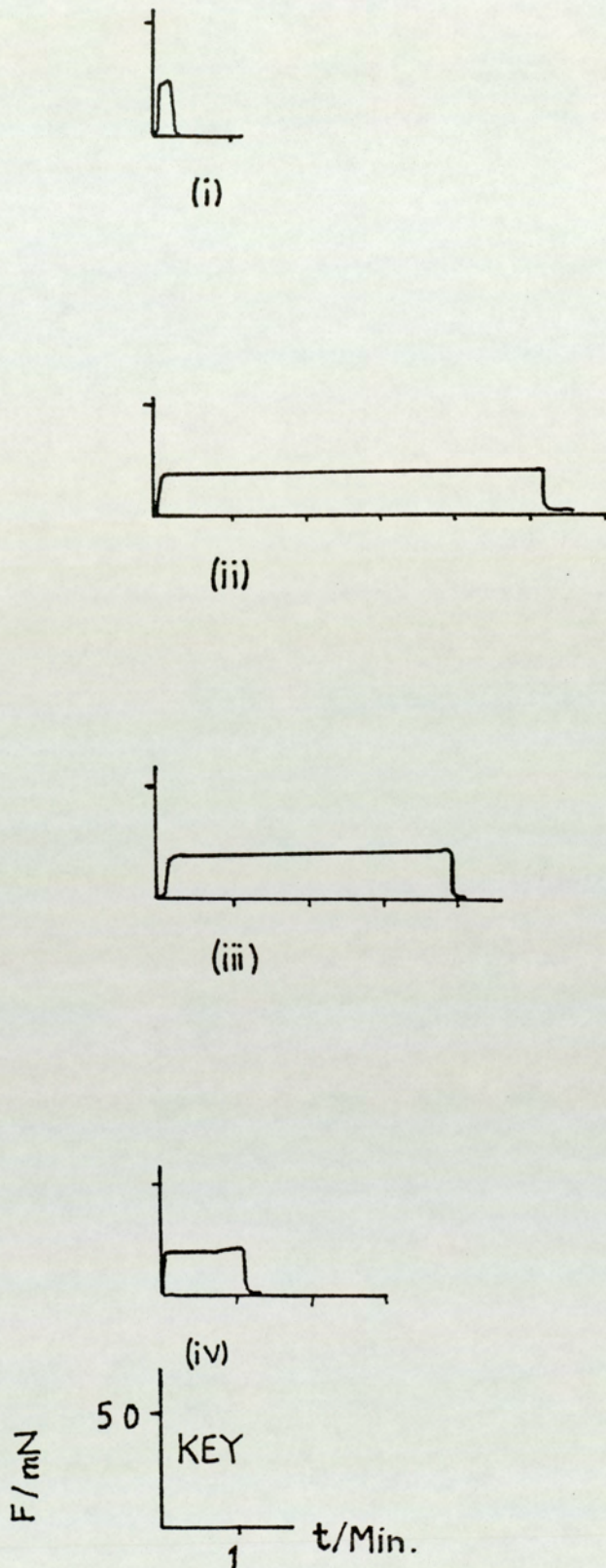


Figure 6.14 (b) Friction for the sample SR2 on the supported sample rig showing (i) SR2(0), (ii) SR2(1.5), (iii) SR2(3), (iv) SR2(4.5).

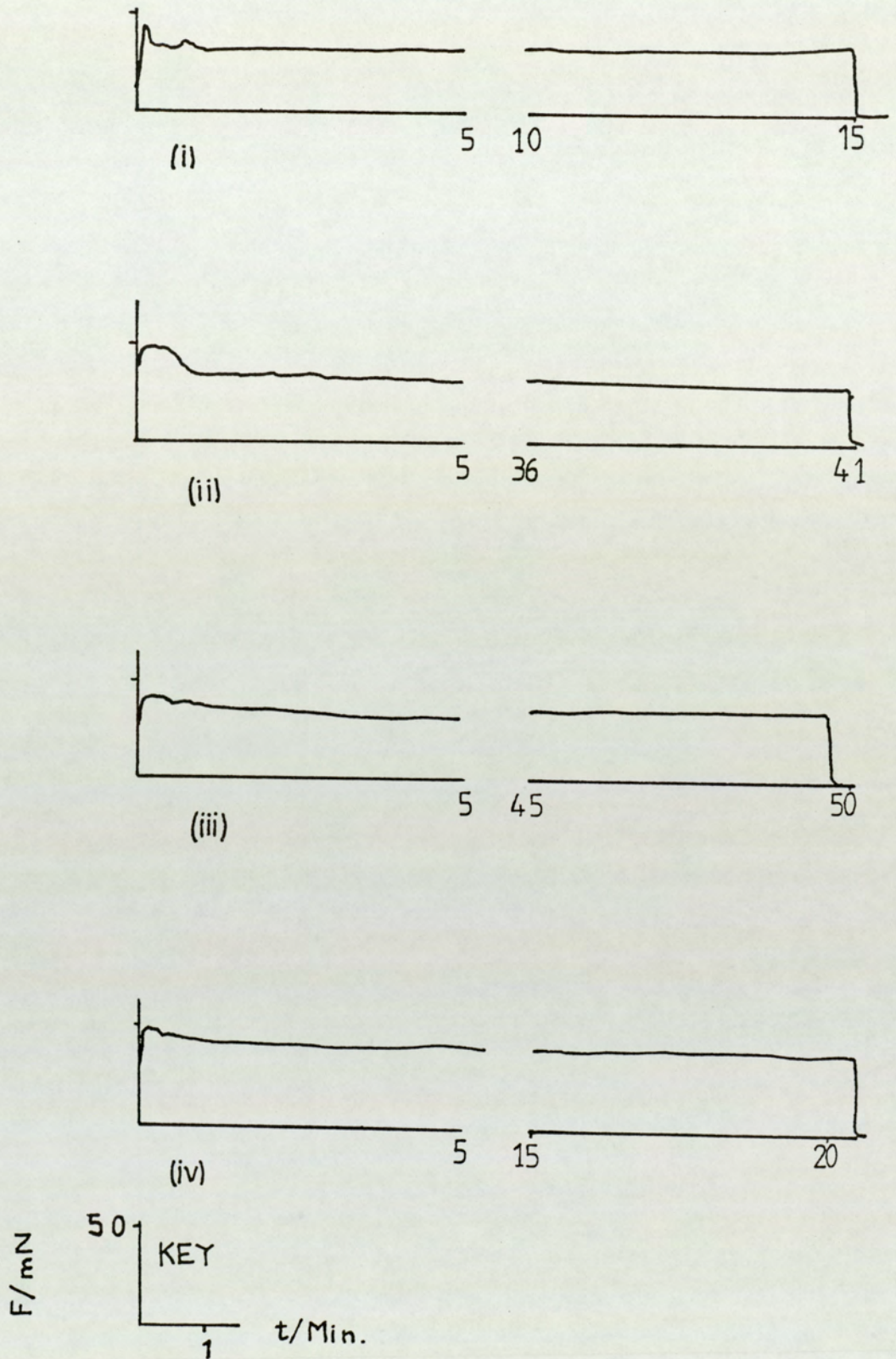


Figure 6.15 (a) Friction for the sample SR4 on the unsupported sample rig showing (i) SR4(0), (ii) SR4(1.5), (iii) SR4(3), (iv) SR4(4.5).

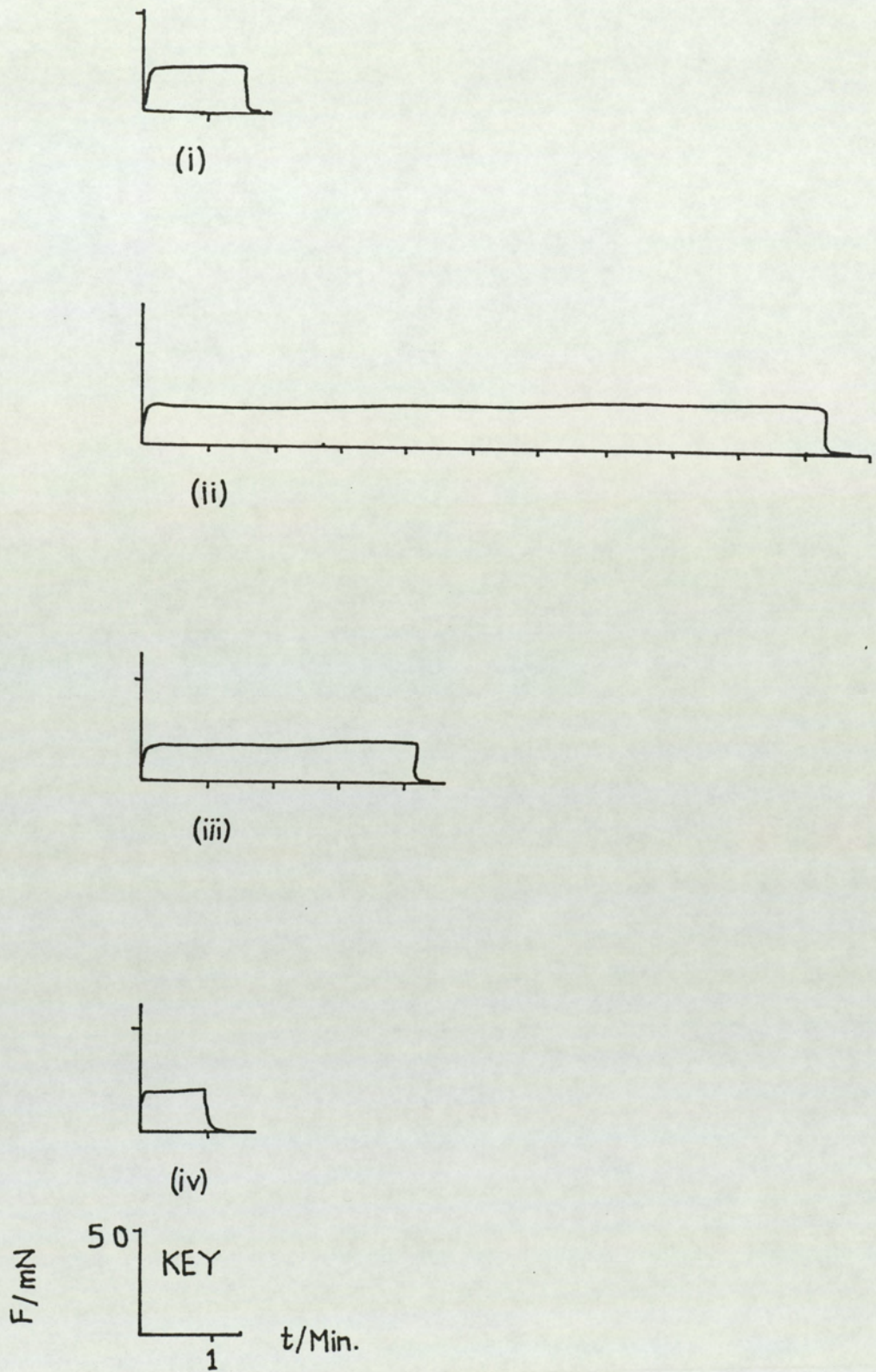


Figure 6.15 (b) Friction for the sample SR4 on the supported sample rig showing (i) SR4(0), (ii) SR4(1.5), (iii) SR4(3), (iv) SR4(4.5).

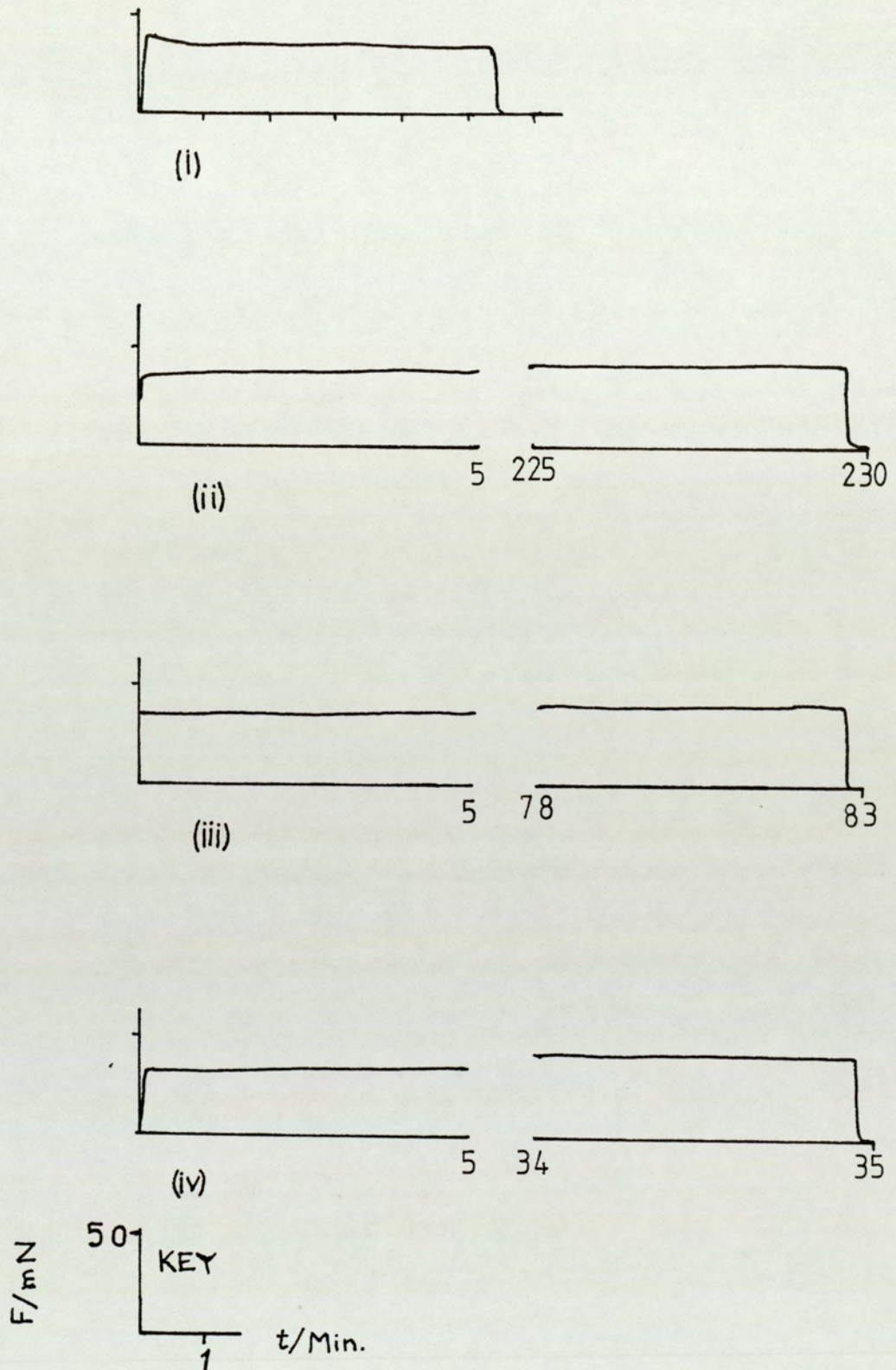


Figure 6.16 (a) Friction for the sample SR1 on the unsupported sample rig showing (i) SR1(0), (ii) SR1(1.5), (iii) SR1(3), (iv) SR1(4.5).

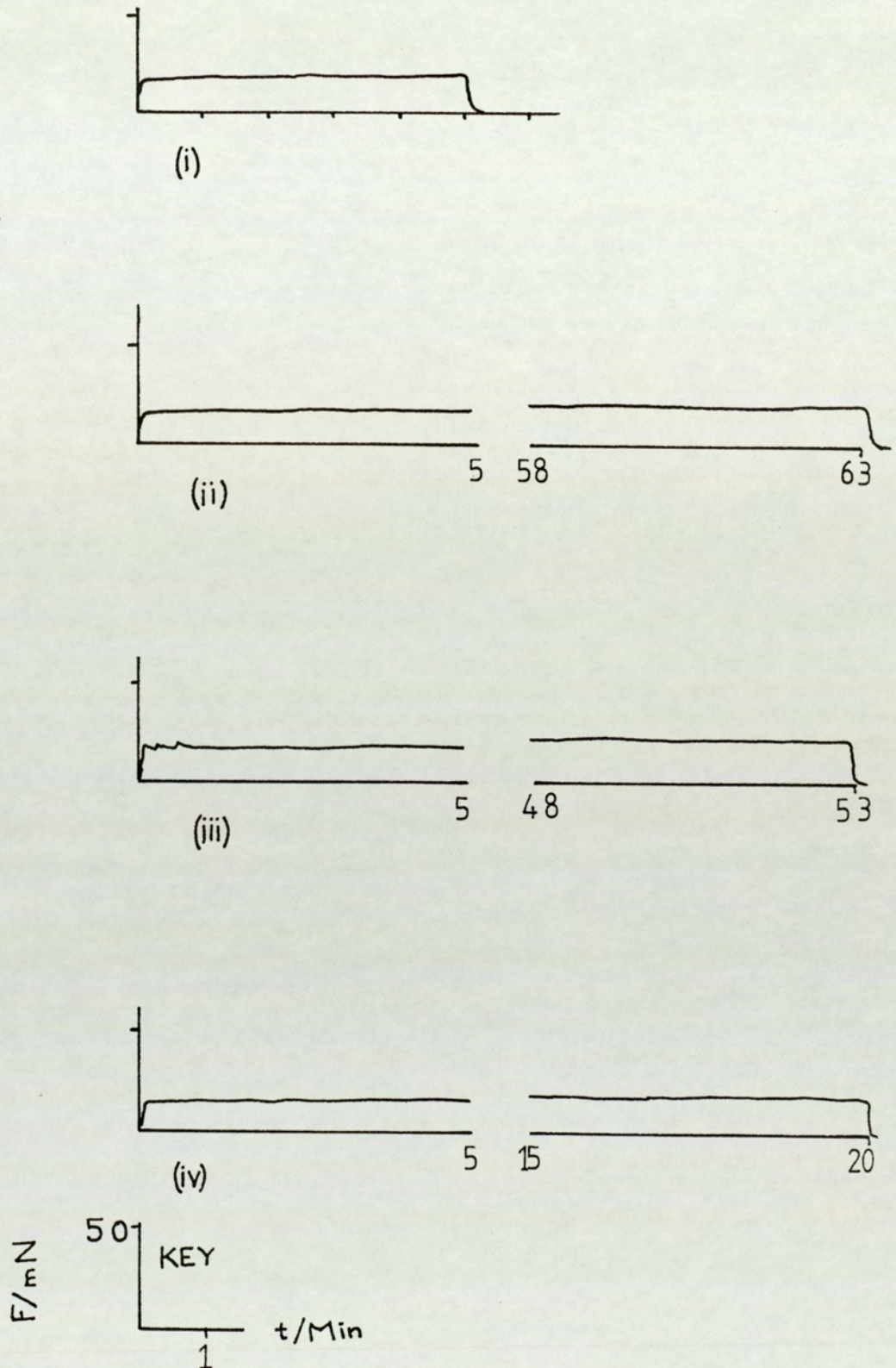


Figure 6.16 (b) Friction for the sample SR1 on the supported sample rig showing
 (i) SR1(0), (ii) SR1(1.5), (iii) SR1(3), (iv) SR1(4.5).

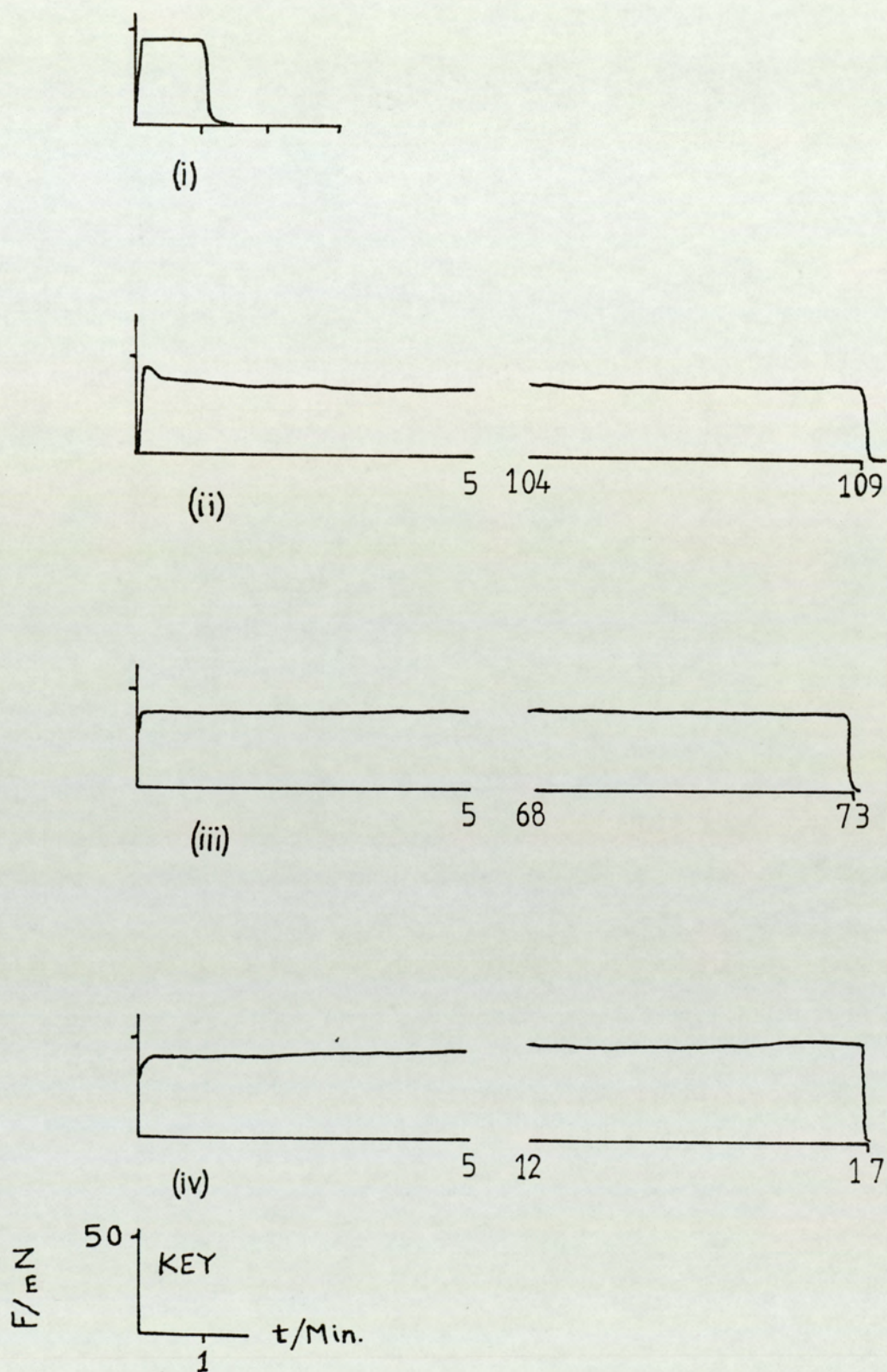


Figure 6.17 (a) Friction for the sample SR3 on the unsupported sample rig showing (i) SR3(0), (ii) SR3(1.5), (iii) SR3(3), (iv) SR3(4.5).

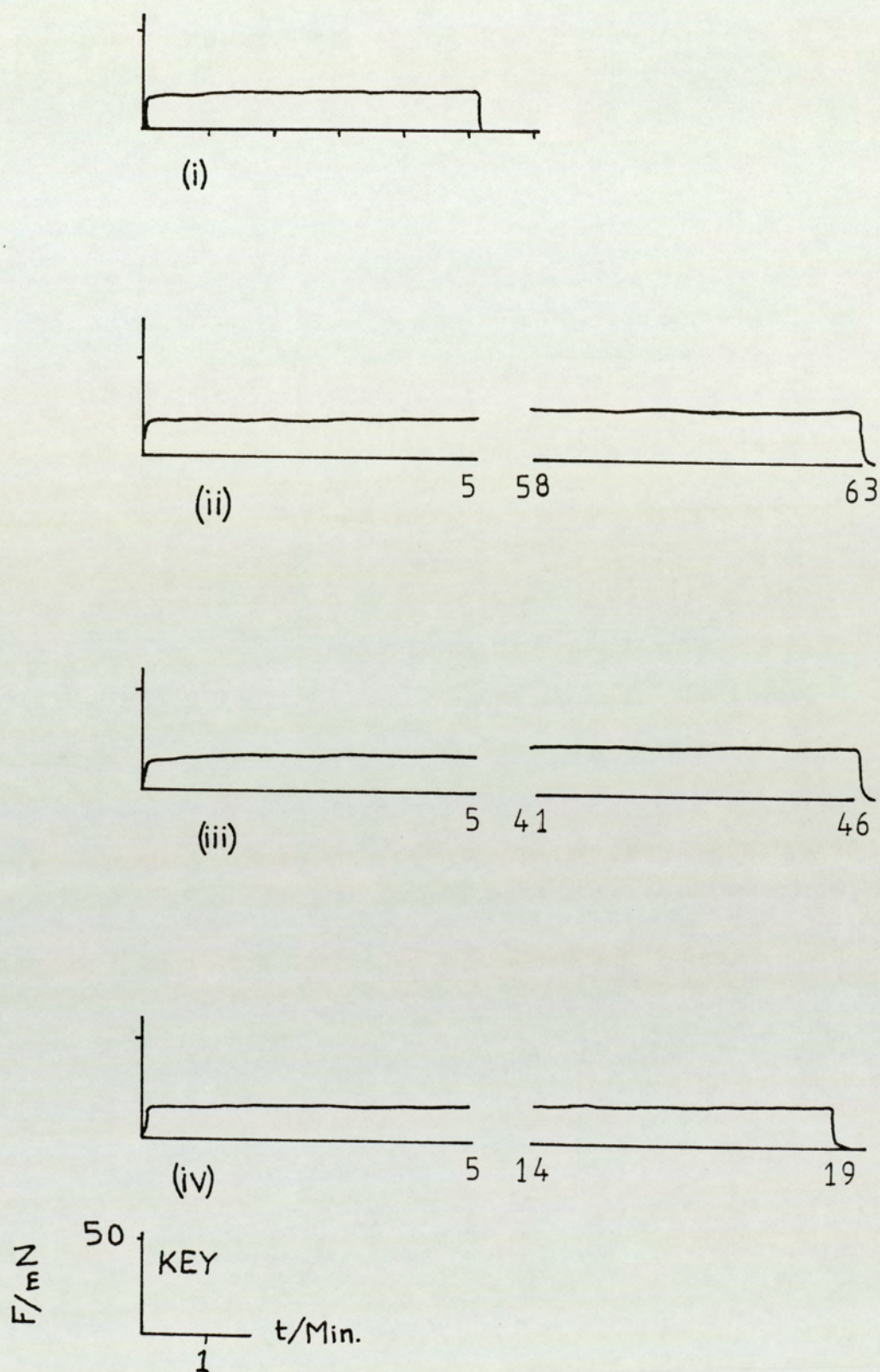


Figure 6.17 (b) Friction for the sample SR3 on the supported sample rig showing (i) SR3(0), (ii) SR3(1.5), (iii) SR3(3), (iv) SR3(4.5).

factor in the surface lubricated media whereby the smoother, that is more burnished, samples show lower friction. The significance of these results may be noted by considering the errors. The errors on the higher durability samples' results may be quoted as ± 5 minutes and arise mainly from the frequency of observation. The lowest durability samples (lasting only of the order of 2 to 3 minutes on these rigs) were continually observed and errors of only a few seconds can be quoted.

Once again it is felt that the primary source of friction in the surface lubricated and burnished media samples is that due to asperity deformation. However, the surface lubricant helps in load bearing and reduces this deformation leading to lower friction. In the roughest, unburnished samples, some penetration of this lubricant by the largest asperities of the media would be expected to increase the friction through easy plastic deformation of these asperities. This creates a larger real area of contact not covered by the surface lubricant resulting in higher friction. The value of the friction coefficient is too high to represent classical boundary lubrication as described in Chapter 3.

A very important point to note is that the friction forces in general here are very much higher in magnitude than those measured for the friction tester and it is possible that the accelerated wear is produced through the increased real area of contact represented by this increase in the frictional forces. There is a complication, however, in the flexing sample case. In this case, some of the input energy, through the work done by the friction force, may be expended in the process of flexing. This observation would appear to give credence to the notion that in the case of magnetic media, unlike the majority of cases in tribology, the friction and wear are intimately linked.

Finally, it is interesting to note that the frictional forces in the bulk only lubricated media, SR4, are, both here and in the friction tester data, slightly lower than in the completely unlubricated samples, SR2. It is possible that the bulk

lubricant may be more effective if a different substance is employed, see the discussion in Chapter 7 for further details.

6.4 Electrical measurements in the Drives.

It was only possible to perform a limited amount of electrical measurement on the drives. The main problem arises from the high durability of the surface lubricated samples in the drives. The fact that each of these samples has a lifetime of several hundred hours, on average, as shown by the graphs of Fig. 6.5, means that testing all of these samples would have taken longer than the time available for this project. This is especially true in light of the fact that several tests need to be performed on each of the samples in order that a representative average value of any set of data may be obtained. Further, the samples tested show that the situation, from the point of view of time, is even worse than that portrayed by the above arguments. This becomes clear when typical data is considered in relation to the media samples which do not have the surface lubricant added.

The key point to note is that, despite the fact that the signal has been reduced by a factor of 2 by employing a potentiometer as described in Chapter 4, the drive electronics which converts the analogue voltage signal read from the diskette require only a small transition to decode data. This means that the data read errors as detected by the software do not appear until virtually all of the magnetic layer has been removed. In fact, some places on the wear track, show that complete penetration of the magnetic coating has taken place on both sides of the media. Although it seems unreasonable that all of the magnetic layer needs to be removed before read errors occur, this becomes more acceptable on careful examination of the samples. This reveals that samples have become completely worn only at the edges of the tracks so that magnetic material still remains where

the read/write ferrite loop contacts the media surface. Nevertheless, even this situation only occurs after a long time. Hence the employment of the above method for reducing the signal. Also, in order to minimise the time taken to accumulate this data, the facts established so far concerning the greater wear at the side 0 head-media interface, were profitably employed and data loss on side 0 was sought.

Typical data from the samples SR2 and SR4 is present in Fig. 6.18 from where it may be seen that these samples show duration lifetimes of many hours when consistent data loss is used as a criterion to determine the end of a test. In fact, the SR4 samples burnished for 1.5 seconds and those of SR4 that have not been burnished (SR4(1.5) and SR4(0) respectively) exhibit durabilities of several days. In view of the fact that all samples showing read errors showed a similar amount of wear, projected wear durabilities for the SR1 and SR3 samples, considering the data acquired so far, would probably be of the order of several weeks per sample. Of course, when such long tests have to be carried out, the state of the heads becomes important and these would need to be replaced more frequently making the process expensive. The reason for replacing the heads is that once they become worn, the data acquired is not determined by the media samples' attributes and any sample, no matter what the state of lubrication or burnish, is worn catastrophically instantly after insertion through what appears to be a ploughing type wear; a picture of a worn head is presented in Fig. 6.19. Typically worn media samples are shown in the optical micrographs of Figs. 6.20(b) to 6.20(d) and may be compared to the unworn sample illustrated in Fig. 6.20 (a) and the relatively mild scars formed for grade 3 to 4 failure presented in the next section.

Sample used = 58759-4 SR2(0)
Drive = 1 Track = 20 Head = 0
Test started at = Sunday 27 March 01:36:54
Test ended at = Sunday 27 March 17:34:41
Bad byte at 0th Sector, 0th Byte; Bad byte = 11011111
Total soft read errors = 2248
Signal reduced to 0.5 * head read signal
Data file = D1SR2-0-0-20-A

Sample used = 58759-4 SR2(1.5)
Drive = 5 Track = 20 Head = 0
Test started at = Sunday 27 March 01:36:54
Test ended at = Sunday 27 March 08:45:47
Bad byte at 0th Sector, 59th Byte; Bad byte = 11011111
Total soft read errors = 5810
Signal reduced to 0.5 * head read signal
Data file = D5SR2-1-0-20-A

Sample used = 58759-4 SR2(1.5)
Drive = 6 Track = 20 Head = 0
Test started at = Sunday 27 March 01:36:54
Test ended at = Sunday 28 March 10:53:41
Bad byte at 3th Sector, 247th Byte; Bad byte = 11101111
Total soft read errors = 12258
Signal reduced to 0.5 * head read signal
Data file = D6SR2-1-0-20-A

Sample used = 58759-4 SR2(3.0)
Drive = 7 Track = 20 Head = 0
Test started at = Sunday 27 March 01:36:54
Test ended at = Sunday 27 March 19:16:39
Bad byte at 2th Sector, 77th Byte; Bad byte = 11111011
Total soft read errors = 11090
Signal reduced to 0.5 * head read signal
Data file = D7SR2-3-0-20-A

Sample used = 58759-4 SR2(4.5)
Drive = 1 Track = 20 Head = 0
Test started at = Monday 28 March 18:04:37
Test ended at = Monday 28 March 19:42:51
Bad byte at 0th Sector, 0th Byte; Bad byte = 11001110
Total soft read errors = 1179
Signal reduced to 0.5 * head read signal
Data file = D1SR2-4-0-20

Sample used = 58759-4 SR4(0)
Drive = 6 Track = 20 Head = 0
Test started at = Monday 28 March 18:04:37
Test ended at = Friday 08 April 06:17:37
Bad byte at 3th Sector, 75th Byte; Bad byte = 11110111
Total soft read errors = 188118
Signal reduced to 0.5 * head read signal
Data file = D6SR4-0-0-20

Continued on following page

Sample used = 58759-4 SR4(0)
 Drive = 6 Track = 20 Head = 0
 Test started at = Monday 28 March 18:04:37
 Test ended at = Wednesday 06 April 21:47:01
 Bad byte at 1th Sector, 177th Byte; Bad byte = 11111110
 Total soft read errors = 217251
 Signal reduced to 0.5 * head read signal
 Data file = D5SR4-0-0-20

Sample used = 58759-4 SR4(1.5)
 Drive = 8 Track = 20 Head = 0
 Test started at = Monday 28 March 18:04:37
 Test ended at = Sunday 03 April 08:29:07
 Bad byte at 0th Sector, 172th Byte; Bad byte = 11111011
 Total soft read errors = 36782
 Signal reduced to 0.5 * head read signal
 Data file = D8SR4-1-0-20

Sample used = 58759-4 SR4(1.5)
 Drive = 7 Track = 20 Head = 0
 Test started at = Monday 28 March 18:04:37
 Test ended at = Wednesday 30 March 17:11:44
 Bad byte at 10th Sector, 59th Byte; Bad byte = 11110111
 Total soft read errors = 188118
 Signal reduced to 0.5 * head read signal
 Data file = D6SR4-0-0-20

Sample used = 58759-4 SR4(3.0)
 Drive = 1 Track = 20 Head = 0
 Test started at = Friday 08 April 10:15:32
 Test ended at = Friday 08 April 13:55:10
 Bad byte at 0th Sector, 2th Byte; Bad byte = 11011111
 Total soft read errors = 2774
 Signal reduced to 0.5 * head read signal
 Data file = D1SR4-3-0-20

Sample used = 58759-4 SR4(4.5)
 Drive = 5 Track = 20 Head = 0
 Test started at = Friday 08 April 10:15:32
 Test ended at = Monday 11 April 10:33:58
 Bad byte at 3th Sector, 75th Byte; Bad byte = 11111110
 Total soft read errors = 6945
 Signal reduced to 0.5 * head read signal
 Data file = D5SR4-4-0-20

Sample used = 58759-4 SR4(4.5)
 Drive = 6 Track = 20 Head = 0
 Test started at = Friday 08 April 10:15:32
 Test ended at = Thursday 14 April 02:36:21
 Bad byte at 0th Sector, 238th Byte; Bad byte = 11111011
 Total soft read errors = 69230
 Signal reduced to 0.5 * head read signal
 Data file = D6SR4-4-0-20

Figure 6.18 Bit analysis software durability data for the SR2 and SR4 samples.

Figure 6.19 The read/write gap in the ferrite loop of a typical M-R head. Wear of the glass bonding can be seen where the ferrite bonds to the ceramic pull-outs from the glass has left voids (100×).

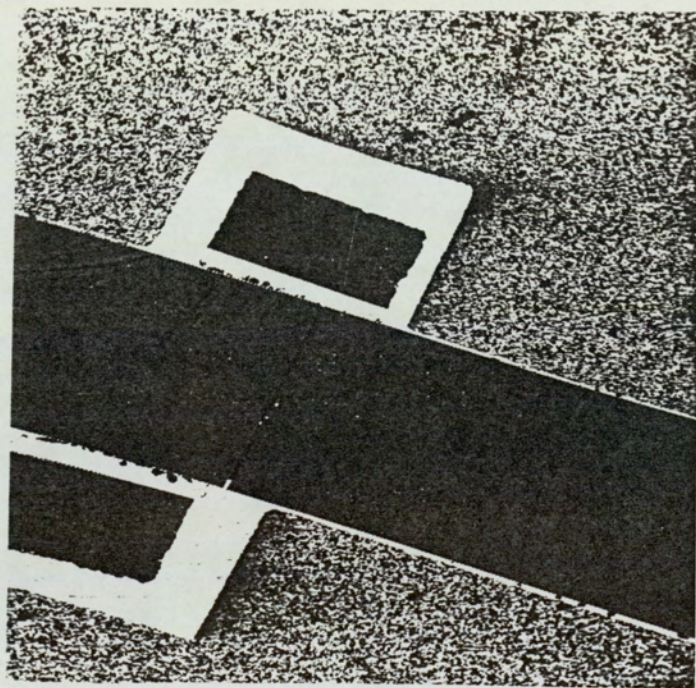


Figure 6.20 (a) The surface of SR2(0) media seen using optical microscopy before testing using the bit analysis software (50 ×).

Figure 6.20 (b) Typical optical micrograph of a sample after testing using the bit analysis software showing patches where the total removal of the magnetic layer has occurred (50 ×, SR2(0)).

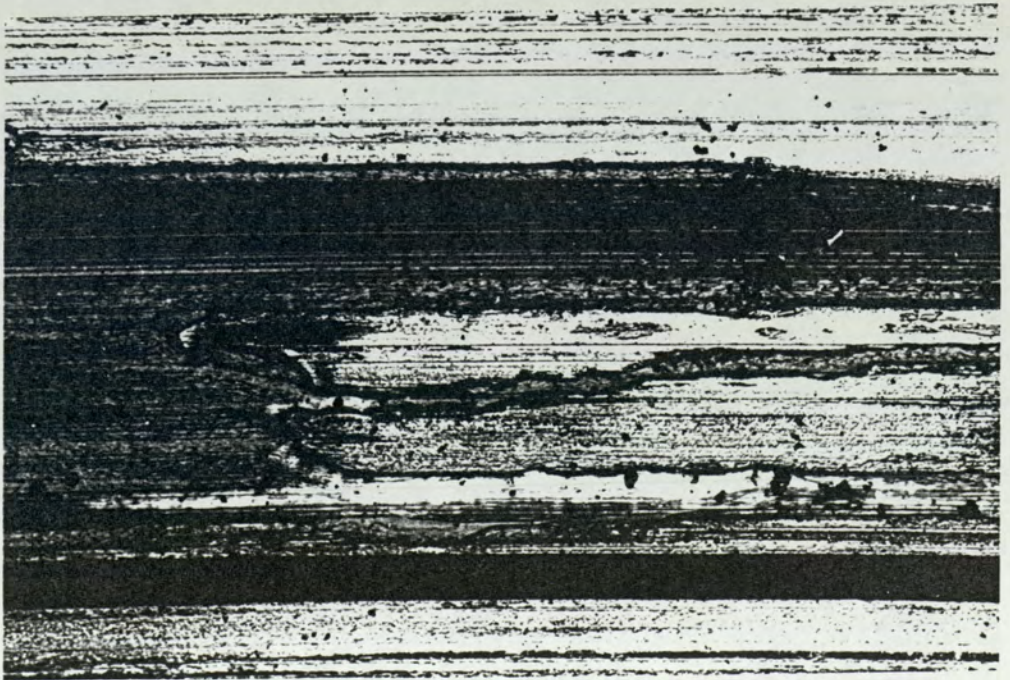
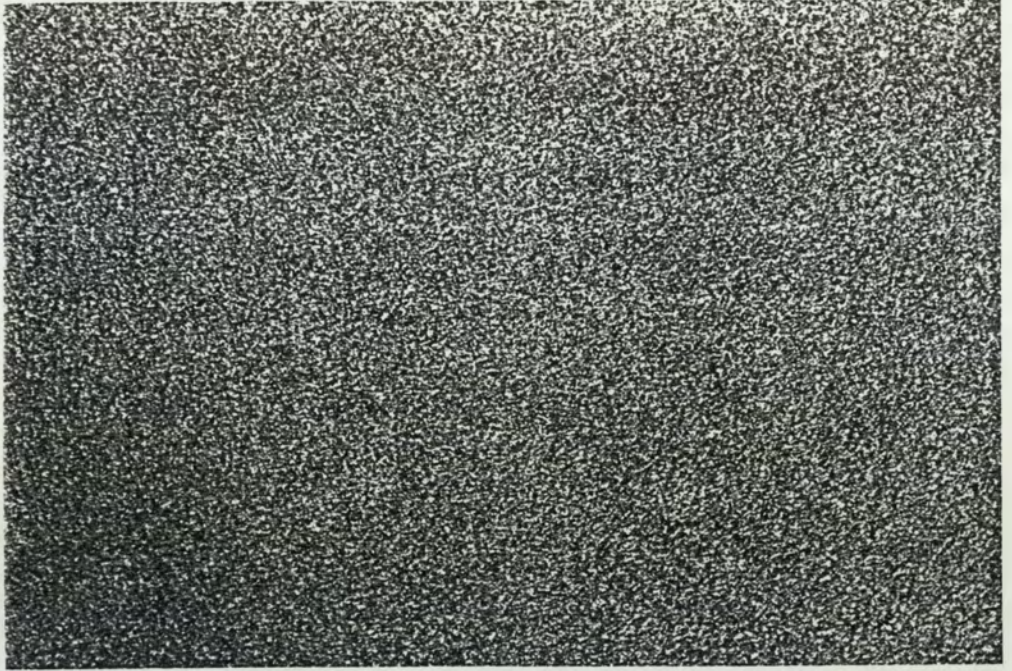
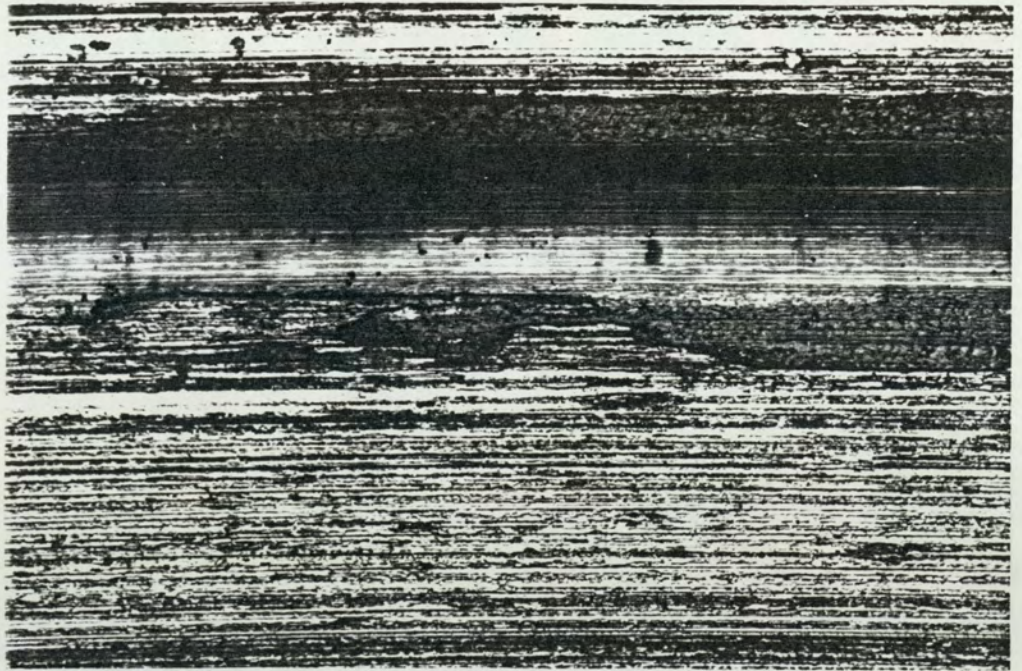


Figure 6.20 (c) Sample SR2(4.5) 50 ×.

Figure 6.20 (d) Sample SR4(0) 50 ×.



6.5 Physical Analysis of Samples.

In this section the results of employing the physical methods of analysis described in Chapter 5 are presented. The intention of this part of the study was to produce evidence which explained or complimented the observations already made regarding friction and wear of the media and of establishing the mechanisms of wear.

In order to achieve the aims briefly outlined above, it was decided to investigate any features which were different to the normal appearance of the surface. The nature of the damage which occurs can be seen from these alien features and this is important in establishing the mechanisms responsible for that damage. The other reason for looking at these surface features is that the damage to the media resulting from accelerated testing on the simulation rigs and the drives needs to be compared in order to determine whether these rigs do produce similar damage, that is, genuine accelerated wear testing with the same mechanisms of wear. Clearly, if the mechanisms of wear are different the employment of the simulation rigs for accelerated testing would be brought into question and could not be justified.

The final observation which needed to be made on the worn samples using the analysis methods was to systematically study the surface features created by wear. This was done to determine the common points in the wear sites so that the processes involved in producing them could be established.

6.5.1 Interferometry.

The samples as provided have all been subjected to surface profilometry monitoring by means of the facility provided by 3M (United Kingdom) plc., Swansea, Wales. The results of these scans have been presented earlier in Figs.

6.2 and 6.3. It is clear from these interferograms that burnishing produces smoother media, that is media with a surface having a smaller average asperity height. Another point worth noting is that burnishing can produce damaged media. In fact, it is probably impossible to avoid producing imperfections as the process of burnishing employs abrasive papers embedded with hard particles. These cause ploughing type wear of the soft media surface. Examples of this are presented in the damage seen as caused to the samples of Fig. 6.21, where grooving has been detected by the interferometer. The samples illustrated are SR1(3), Fig. 6.21 (a), and SR4(4.5), Fig. 6.21 (b) which both exhibit similar type of damage due to burnishing.

Further comments relating to this are reserved until Chapters 7 and 8 where the results are discussed and further recommendations for media improvement and better testing methods are made so that better media may be tested more effectively.

The data acquired by this technique may be used to relate and correlate the friction results to the wear of the media.

6.5.2 Transmission Electron Microscopy.

The intention of studying the media by TEM was to look at sub-surface activity in the magnetic layer. This was expected to provide indicators to the mechanisms of wear involved. However, this had to be limited somewhat in light of the difficulty of producing suitable samples for use with this technique. As observed earlier when describing this method of analysis in Chapter 5 (and by Bhushan et al [86]), the main problems are encountered in the preparation of the extremely thin samples demanded by this technique. This prevents the samples from "burning" through absorption of the electron beam energy. One other problem is that of locating the part of the media to be examined: each section to be viewed

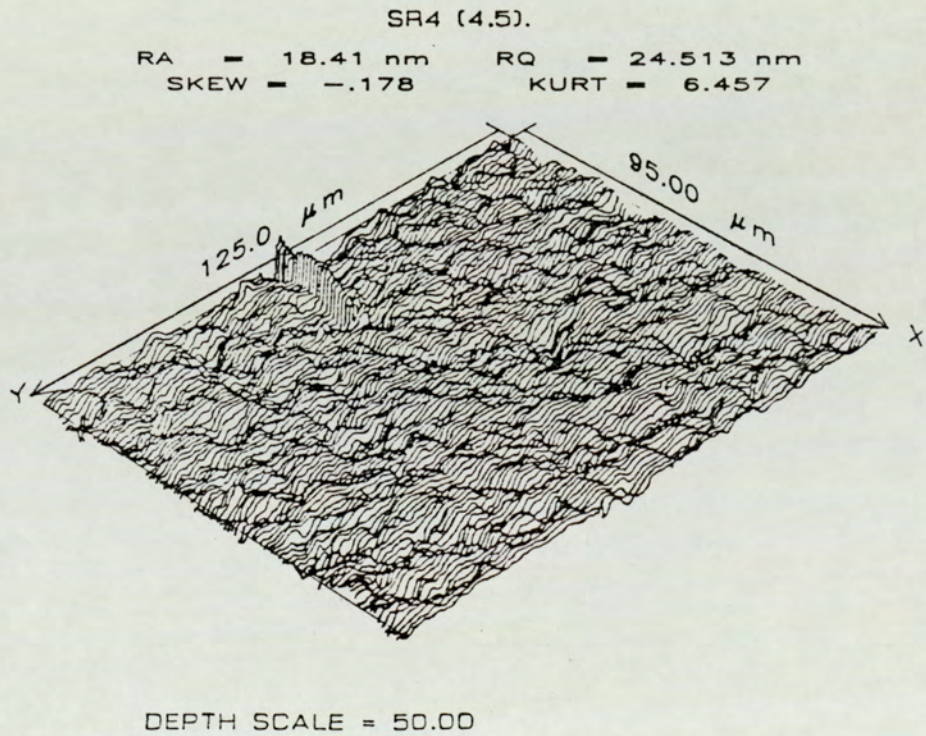
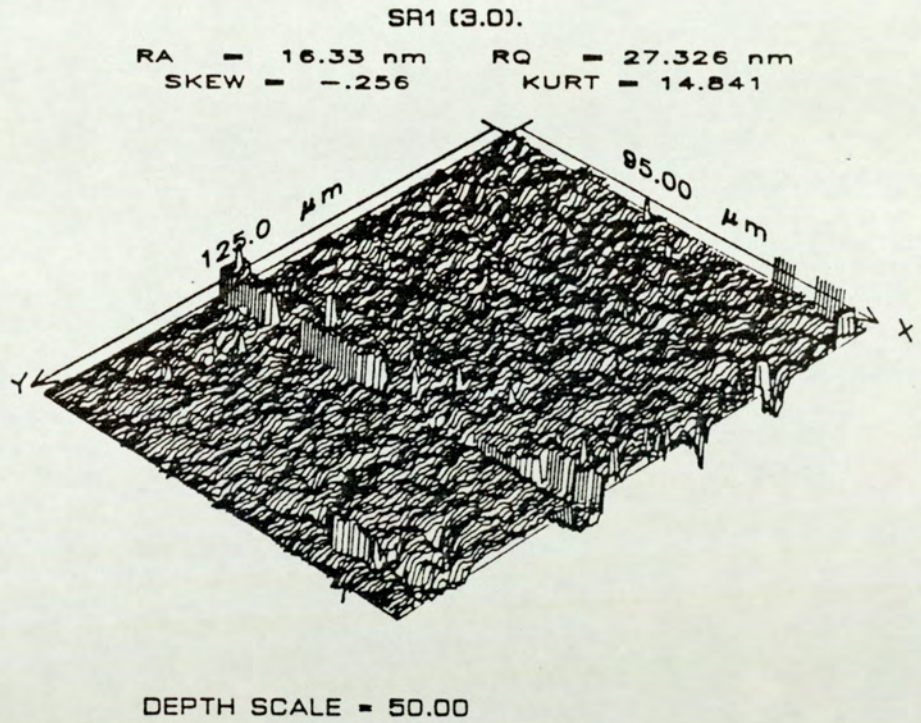


Figure 6.21 Examples of damage caused to the media surface during burnishing: illustrated here are sample (a) SR1(3) and (b) SR3(4.5).

has to be prepared to a "V" shape, as shown in Fig. 5.4, with the sharp end of this then being microtomed to produce the thin slices required. It is extremely difficult to locate the apex of the "V" at the position of a wear scar when the relatively soft media is embedded inside the cured resin block which supports it for microtoming.

As a result of all this, the media samples used for TEM were the fully lubricated and the completely unlubricated ones. Two of each group were used: those that were unburnished and those that were burnished for the maximum period of 4.5 seconds. In fact, as illustrated in the pictures of Fig. 6.22, there is little to be detected between the samples. However, one key point may be noted in the form of the dispersion of the magnetic particles. The dispersion of the magnetic particles, as discussed earlier in Chapter 3, is very important in giving the magnetic layer uniformity of mechanical properties. It can be seen that some polymer-rich areas exist where the magnetic particles' population is lower than the average. It would be expected that these areas would yield most readily under the imposition of external stresses causing local flow of material. These areas may be "balls" of polymer which have passed through the filtration process for removing the larger ones. Even the smaller particle deficient areas can be detrimental as they lead to non-uniformity of mechanical properties, particularly if they become agglomerated at local points. Another observation which may be readily made is that some samples show a lower particle density, Fig. 6.22 (a) to Fig. 6.22 (c). These would be expected to exhibit a lower rigidity and expected to show greater wear as a result.

6.5.3 Optical Microscopic examination.

In this sub-section the pictures presented are from the drives and the simulation rigs so that these may be compared directly. The two sets of micrographs need

Figure 6.22 (a) The polymer rich areas which may be seen in the samples using TEM: SR2(0) 60 K \times .

Figure 6.22 (b) Sample SR2(4.5) 60 K \times .

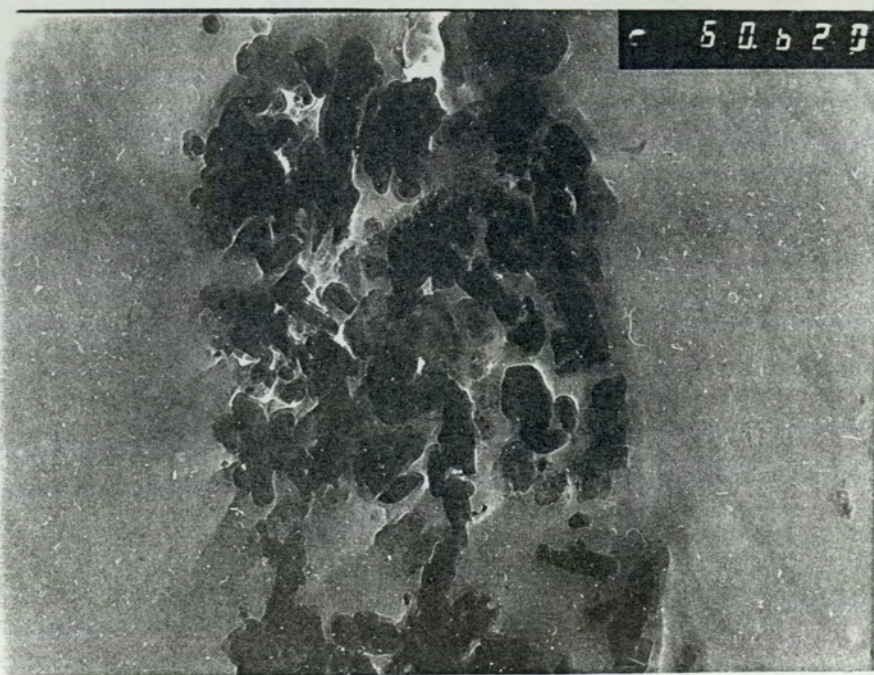
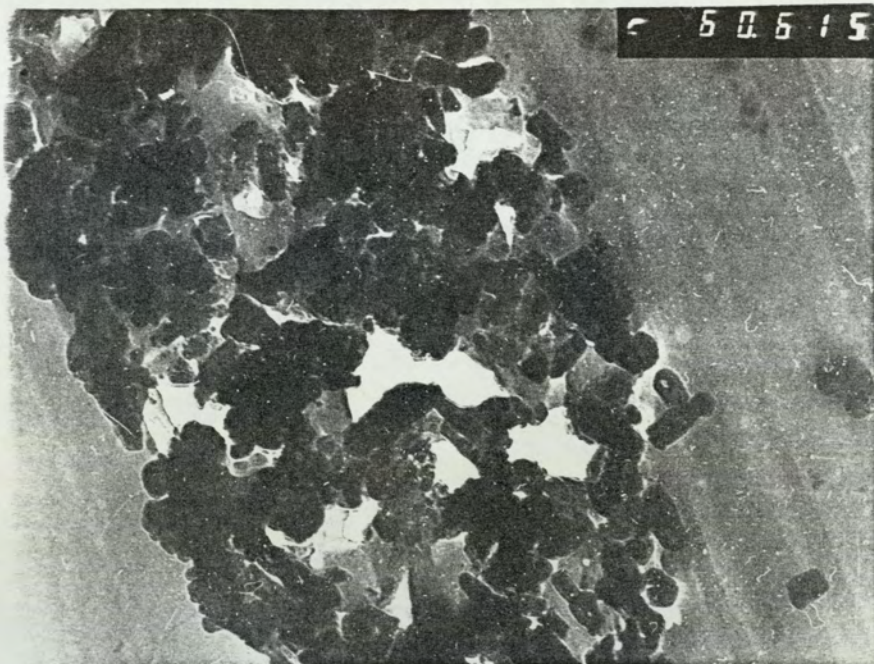


Figure 6.22 (c) Sample SR2(4.5) 80 K \times .

Figure 6.22 (d) Sample SR2(4.5) showing a crack in the magnetic layer which was probably produced during microtoming, 38 K \times .

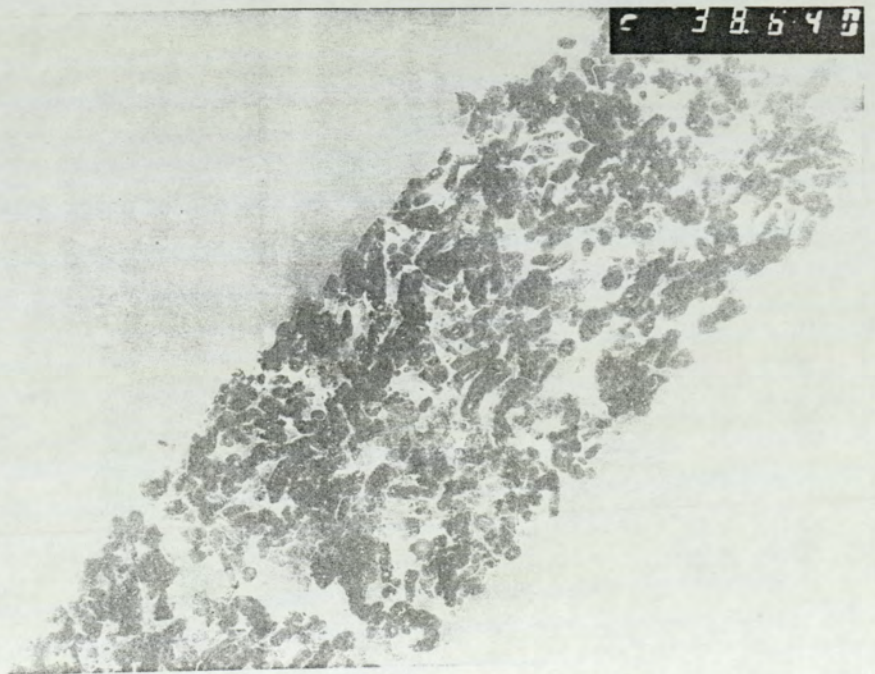
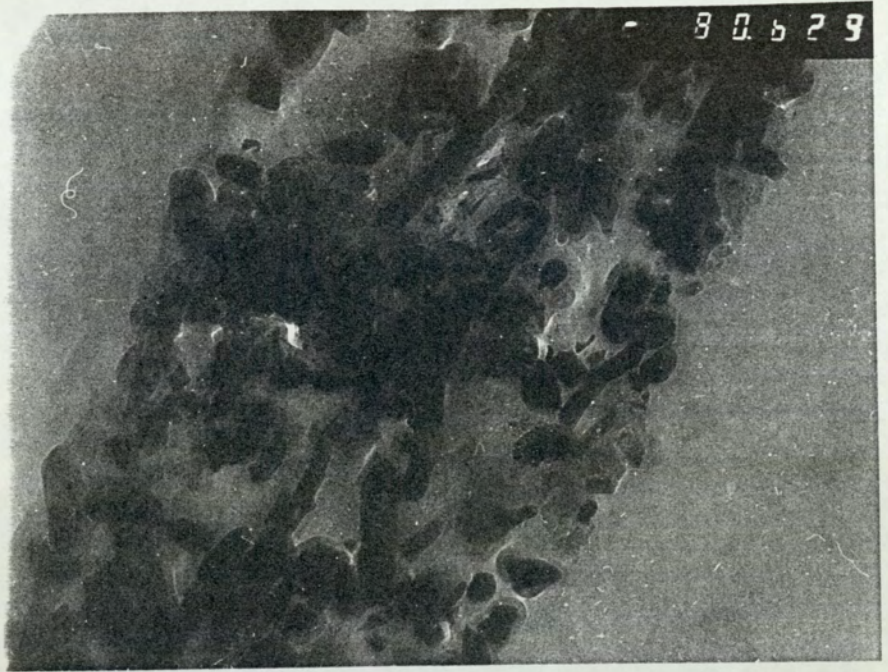
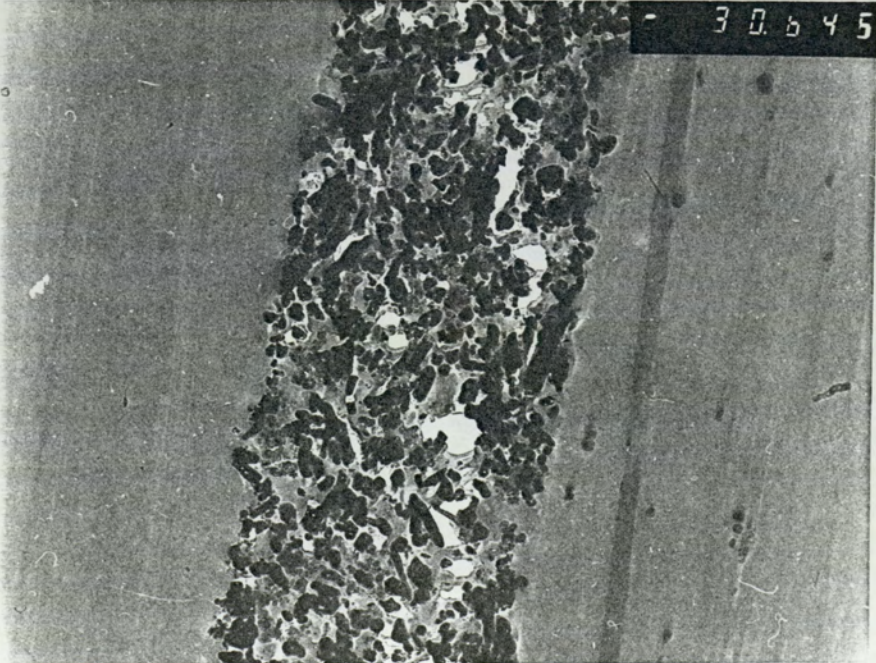


Figure 6.22 (e) Sample SR3(0) showing slightly more uniform particle distribution 35 K \times .

Figure 6.22 (f) Sample SR3(4.5) with particles protruding from the surface 30 K \times .



- 35.541



- 30.645

to be compared in order to establish any similarities and, if any, the degree of such similarities so that the use of the rigs as accelerated testing equipment can be validated or otherwise.

Optical pictures have been presented here so that typical examples are shown. This means that in the case of the drives, and the simulation rigs, SR2 and SR3 samples have been illustrated for the full burnishing range. This enables the unlubricated and fully lubricated samples to be compared. The partially lubricated samples are very similar. In the case of the friction tester, however, only the less durable samples have been tested. The reasons for this have been outlined earlier and need not be repeated here. As a result, only the pictures relating to the SR2 samples have been presented.

(a) Drives.

All of the pictures shown here are for the side 0 interface as this is the one showing damage first. Illustrated in Figs. 6.23 (a) to (h) are samples SR2 and SR3 burnished as follows: (a) and (b) 0 seconds; (c) and (d) 1.5 seconds; (e) and (f) 3 second; and (g) and (h) 4.5 seconds. The similarity in the surface features is evident. Both the unlubricated and fully lubricated media show similar patterns of plastic flow and areas where material appears to have been removed. The patches where material appears to be missing are an important observation as they indicate definite wear processes. It may also be noted that, despite the shorter lifetimes exhibited by the unburnished and most burnished samples, they still show similar surface features to the more durable 1.5 and 3 seconds burnished samples.

Figure 6.23 (a) Unlubricated sample tested in the drives: SR2(0), 200 ×.

Figure 6.23 (b) Lubricated sample tested in the drives: SR3(0), 100 ×.

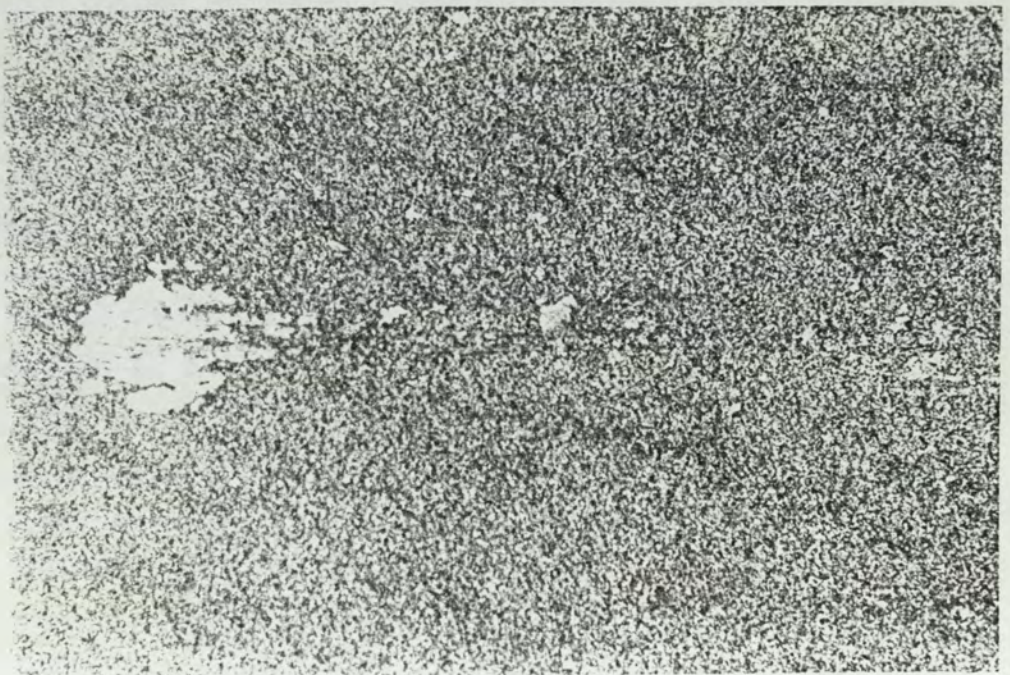
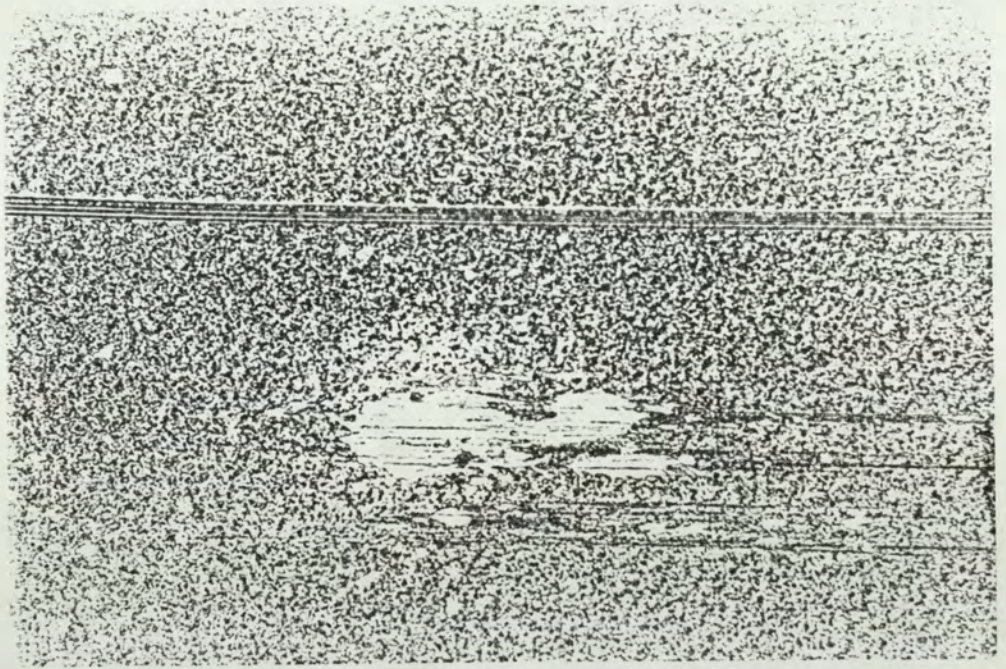


Figure 6.23 (c) Unlubricated sample tested in the drives: SR2(1.5), 400 ×.

Figure 6.23 (d) Lubricated sample tested in the drives: SR3(1.5), 400 ×.

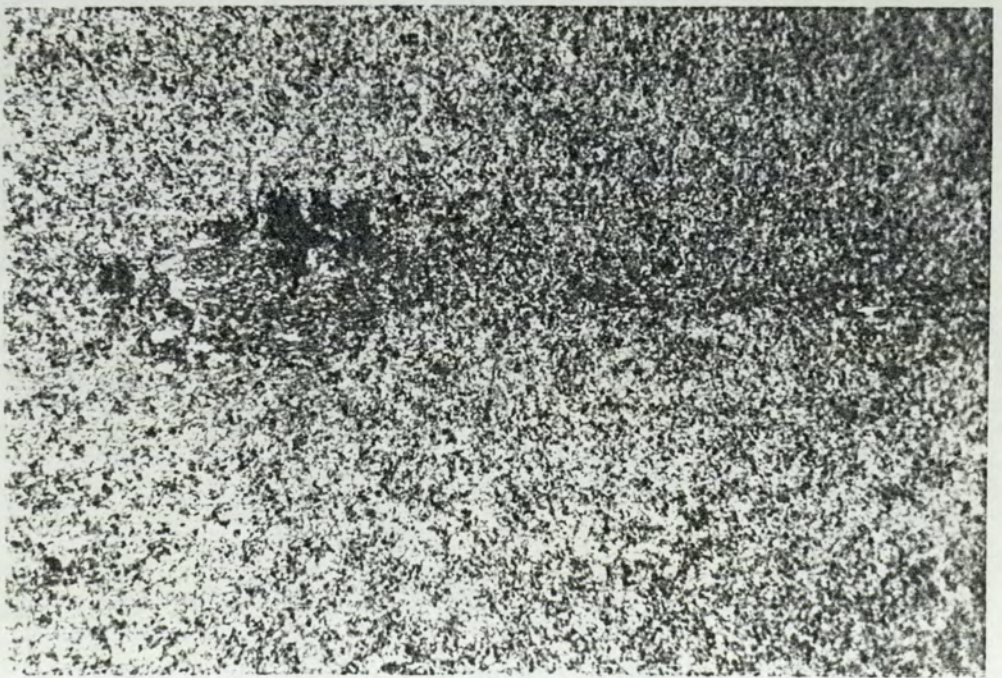
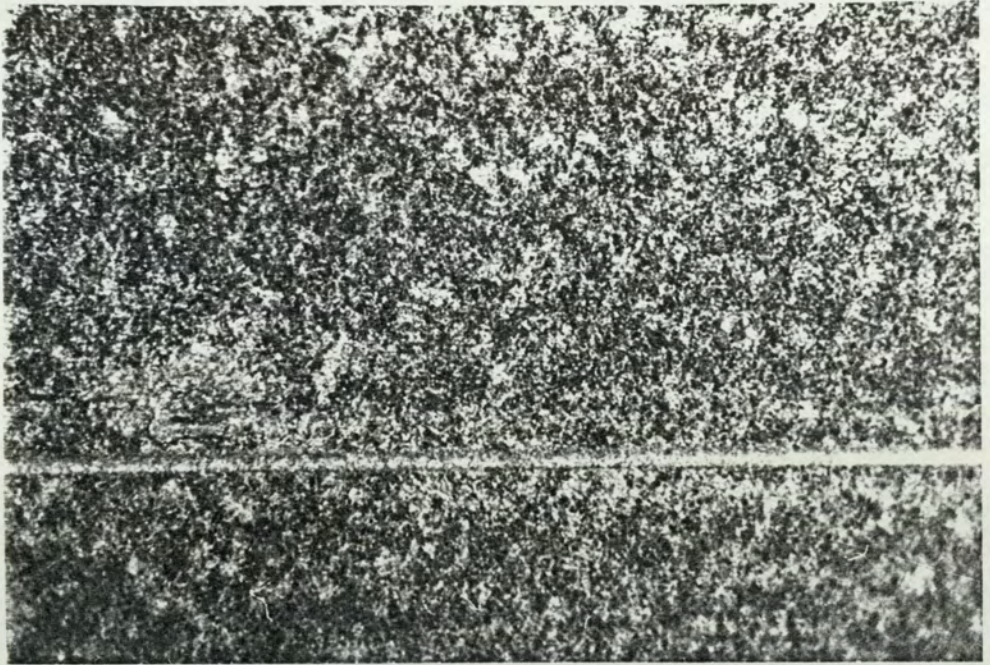


Figure 6.23 (e) Unlubricated sample tested in the drives: SR2(3), 400 ×.

Figure 6.23 (f) Lubricated sample tested in the drives: SR3(3), 400 ×.

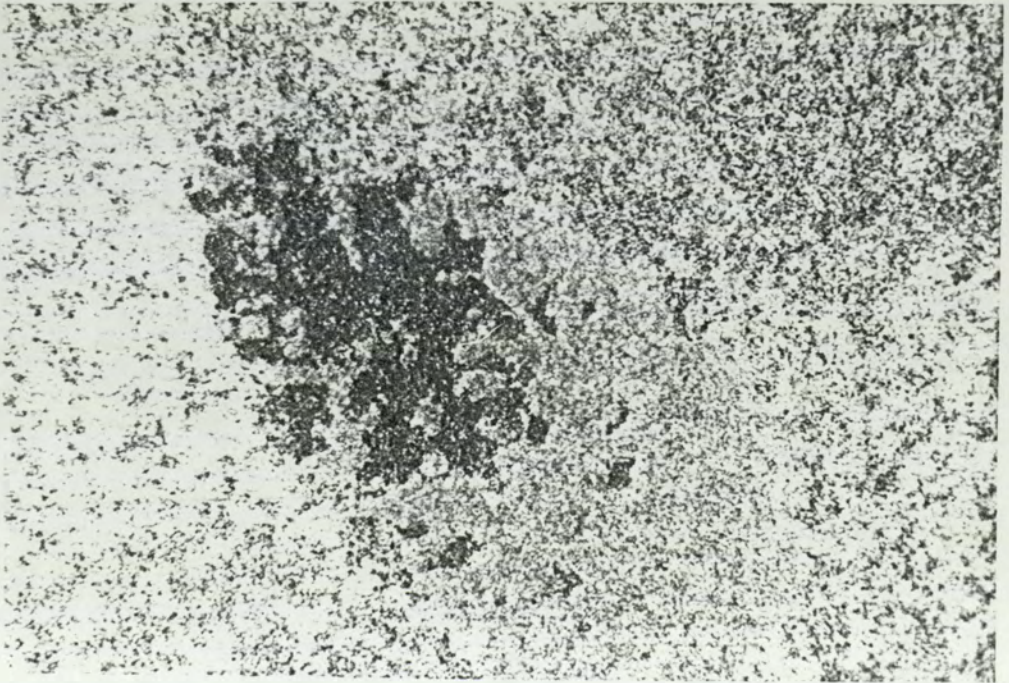
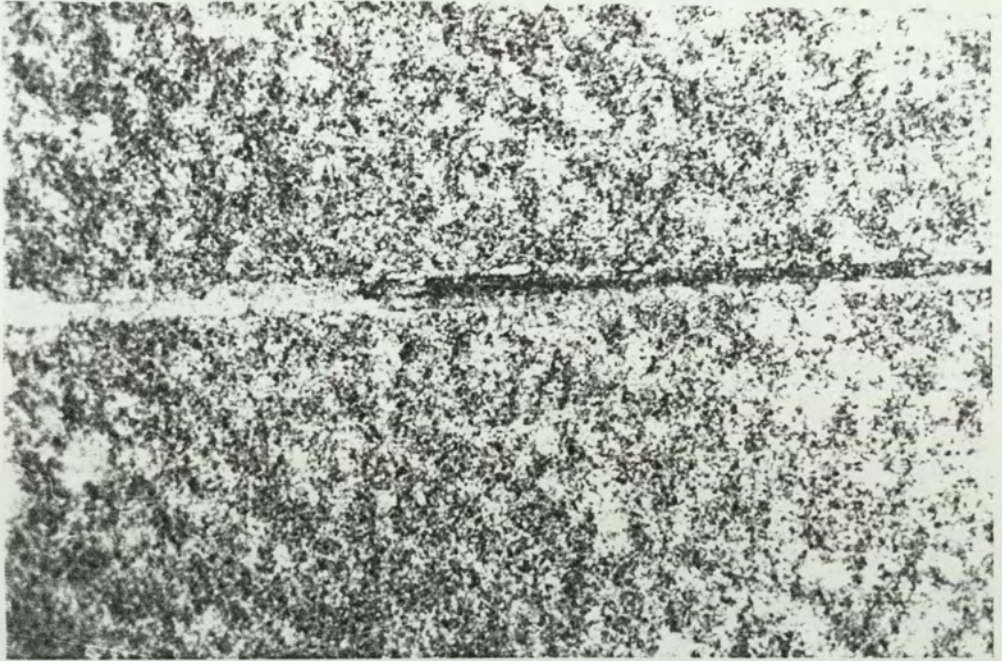
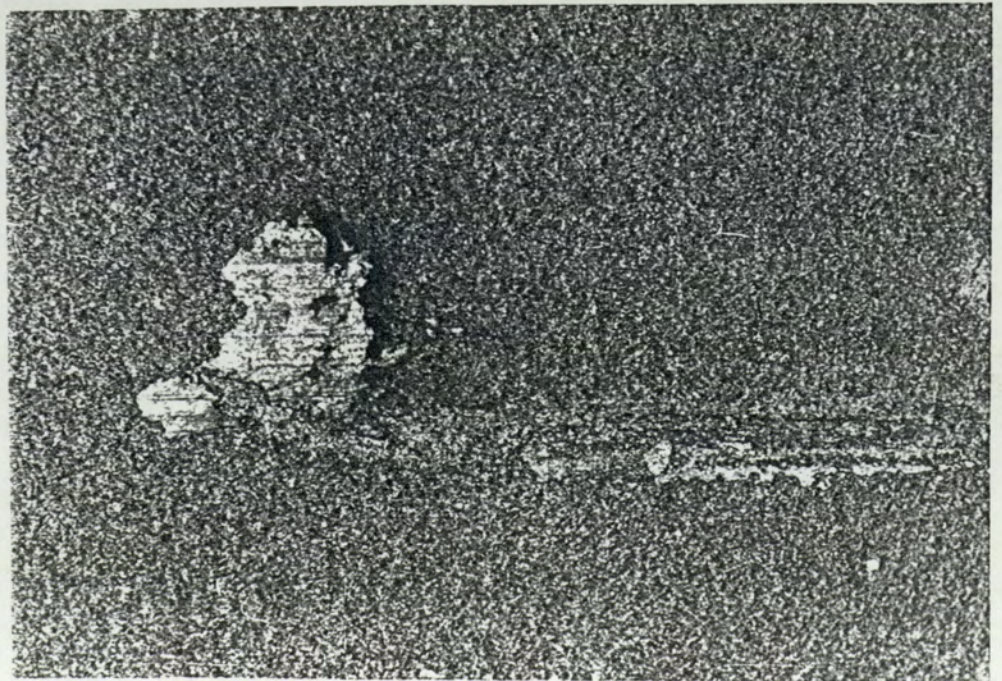
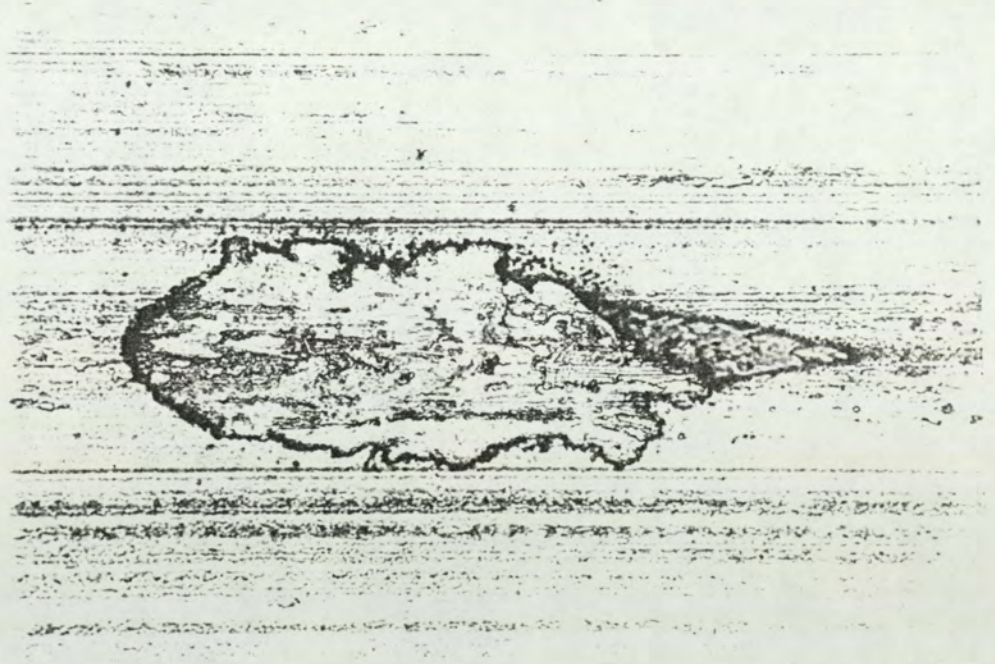


Figure 6.23 (g) Unlubricated sample tested in the drives: SR2(4.5), 200 ×.

Figure 6.23 (h) Lubricated sample tested in the drives: SR3(4.5), 200 ×.



(b) The Simulation Rigs.

The samples from the drives illustrated in Fig. 6.23 may be compared to the optical micrograph of Figs. 6.24 and 6.25 where the samples tested on the simulation rigs are shown. Fig. 6.24 shows samples from the unsupported sample rig and Fig. 6.25 samples from the supported sample rig. In both cases the samples are SR2 and SR3 and may be compared directly with the sample in Fig. 6.23 representing the drives.

Also, looking at these photographs, the similarity of the wear sites can be appreciated; with the differently lubricated samples showing similar surface damage. Also, the samples from the rigs tend to show similar features. Furthermore, these are similar to the features observed for the drives in Fig. 6.23.

One point which needs to be made here is that, as implied earlier in the description of the rigs in Chapter 4, the simulation rigs are not working optimally and some differences might be expected. As an example, the fact that the run-out on the supported sample rig tends to produce discontinuous wear scars should be noted. In fact, the pictures used for this work have not been taken at the edge of these discontinuities but at points where the stressing of the samples are expected to be relatively constant over a considerable distance. Further modifications recommended for this rig should improve its performance.

The key general points to note in all of the micrographs of Figs. 6.23 to 6.25 are as follows:

- (i) All show wear areas with distinct boundaries. This indicates that a section of material has been removed.
- (ii) All appear to show smoothed areas around the wear sites making these regions very distinctive. This may confirm the relationship between friction and wear described earlier.

Figure 6.24 (a) Unlubricated sample tested on the unsupported sample simulation
rig: SR2(0), 200 ×.

Figure 6.24 (b) Lubricated sample tested on the unsupported sample simulation
rig: SR3(0), 400 ×.

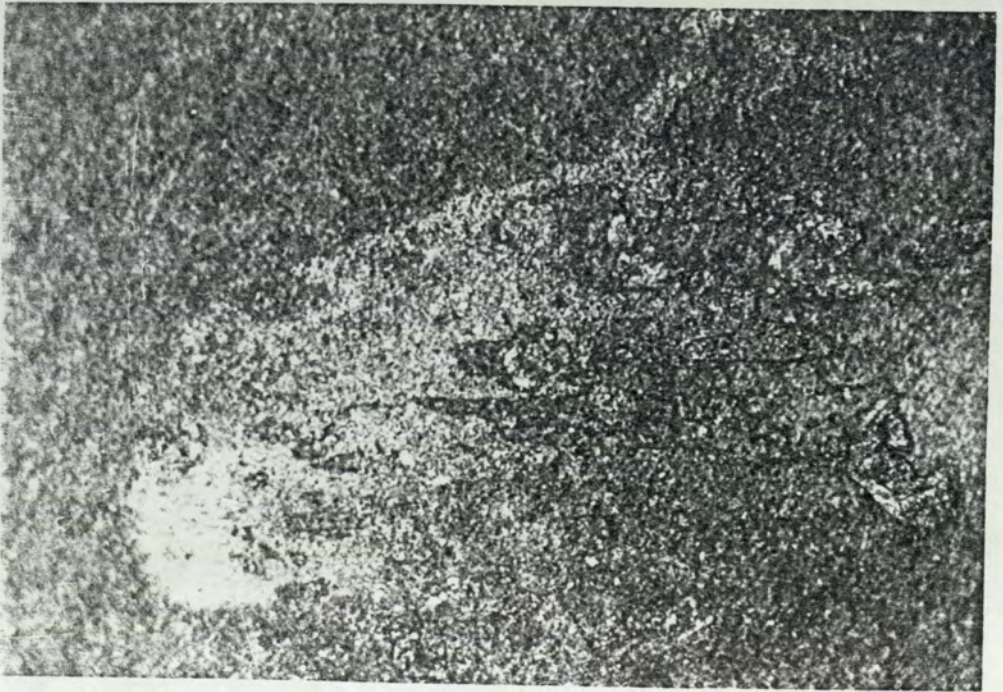
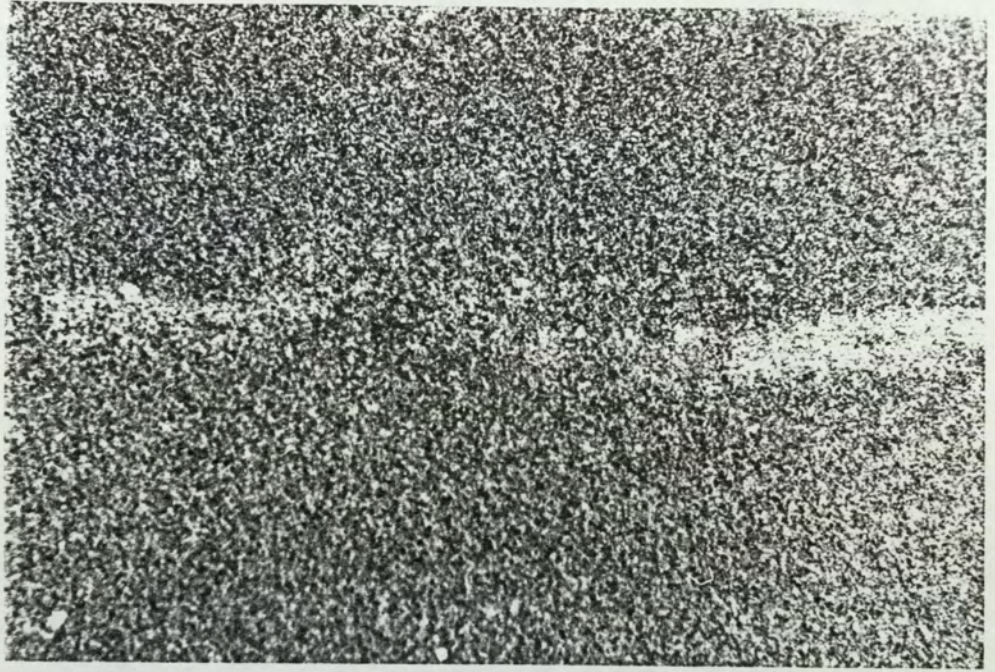


Figure 6.24 (c) Unlubricated sample tested on the unsupported sample simulation
rig: SR2(1.5), 400 ×.

Figure 6.24 (d) Lubricated sample tested on the unsupported sample simulation
rig: SR3(1.5), 400 ×.

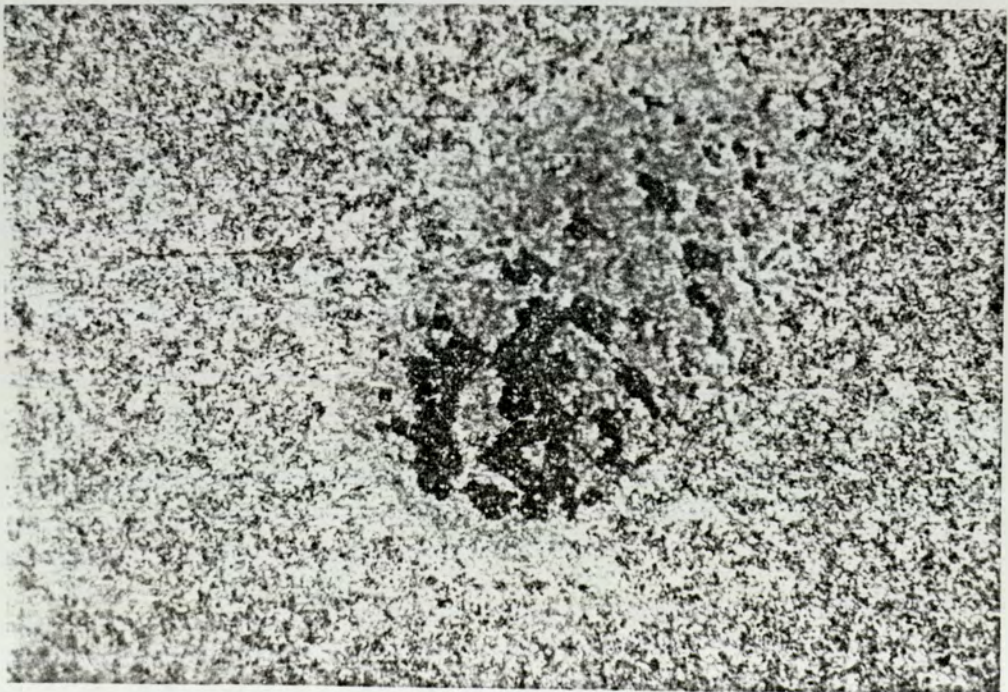
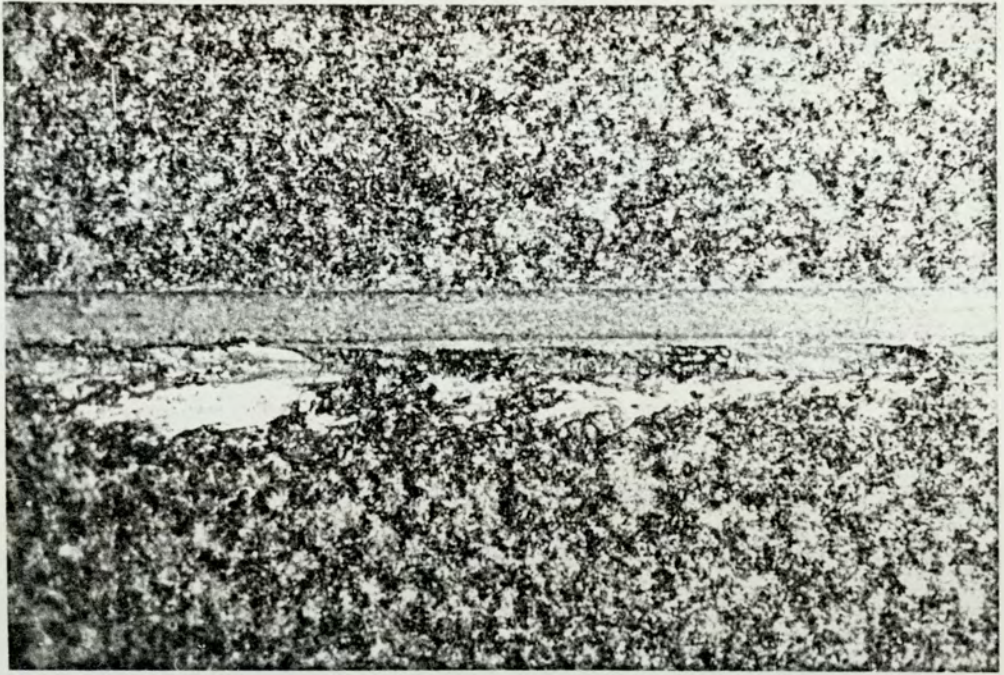


Figure 6.24 (e) Unlubricated sample tested on the unsupported sample simulation
rig: SR2(3), 400 ×.

Figure 6.24 (f) Lubricated sample tested on the unsupported sample simulation
rig: SR3(3), 400 ×.

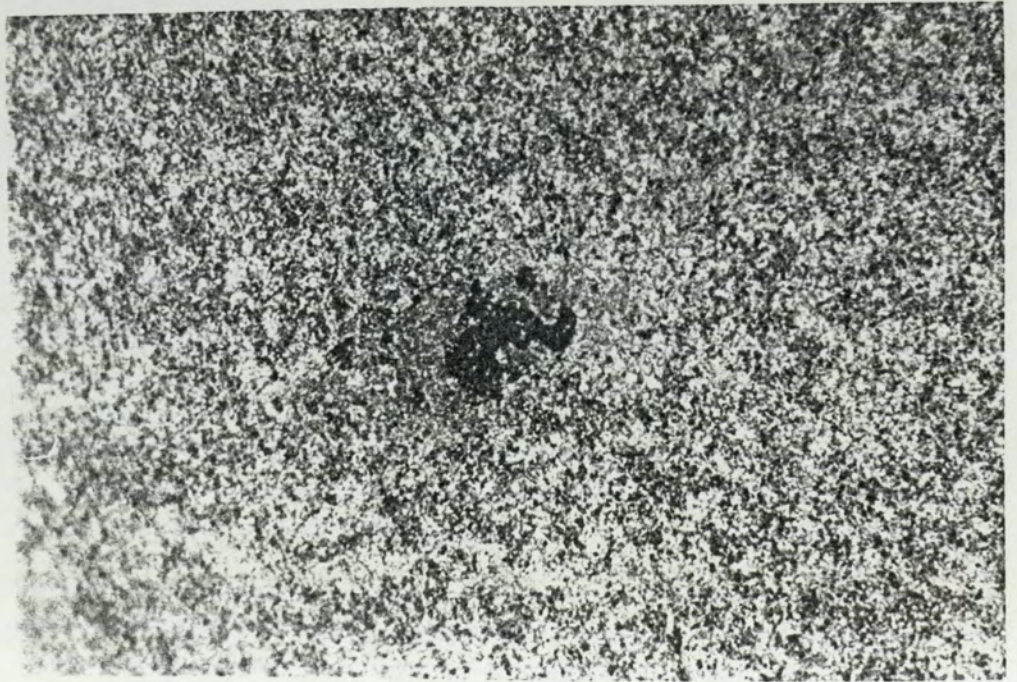
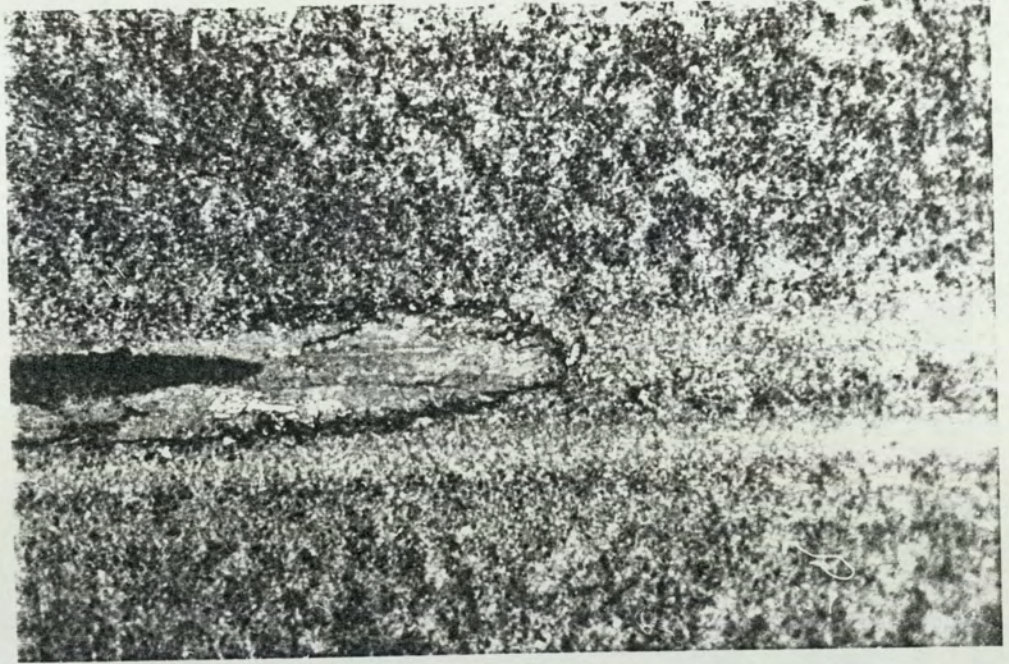


Figure 6.24 (g) Unlubricated sample tested on the unsupported sample simulation
rig: SR2(4.5), 400 ×.

Figure 6.24 (h) Lubricated sample tested on the unsupported sample simulation
rig: SR3(4.5), 400 ×.

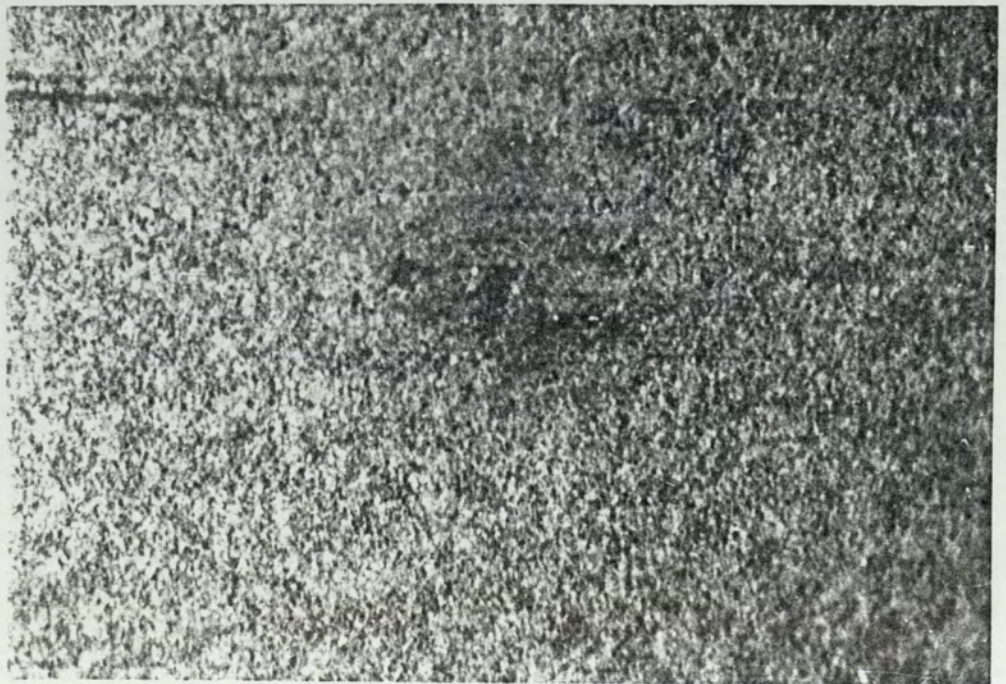
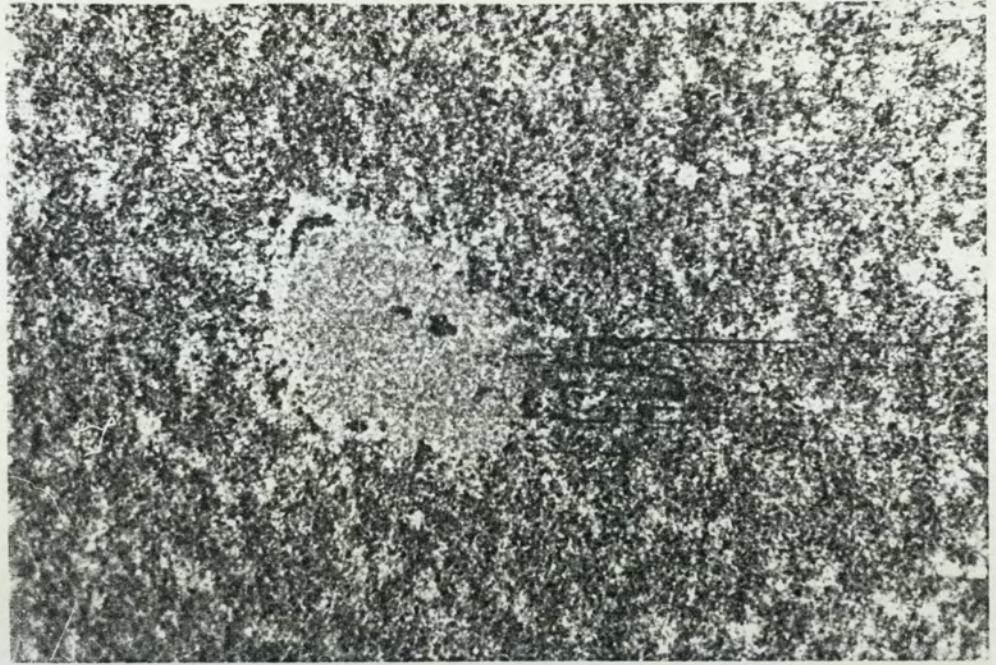


Figure 6.25 (a) Unlubricated sample tested on the supported sample simulation
rig: SR2(0), 400 ×.

Figure 6.25 (b) Lubricated sample tested on the supported sample simulation
rig: SR3(0), 400 ×.

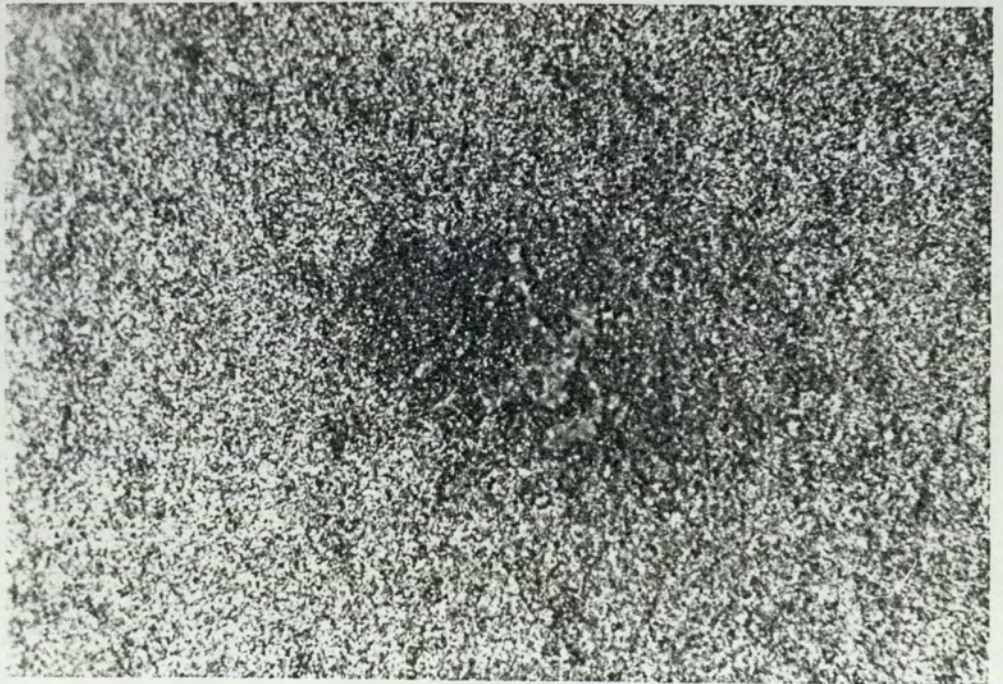


Figure 6.25 (c) Unlubricated sample tested on the supported sample simulation
rig: SR2(1.5), 200 ×.

Figure 6.25 (d) Lubricated sample tested on the supported sample simulation
rig: SR3(1.5), 400 ×.

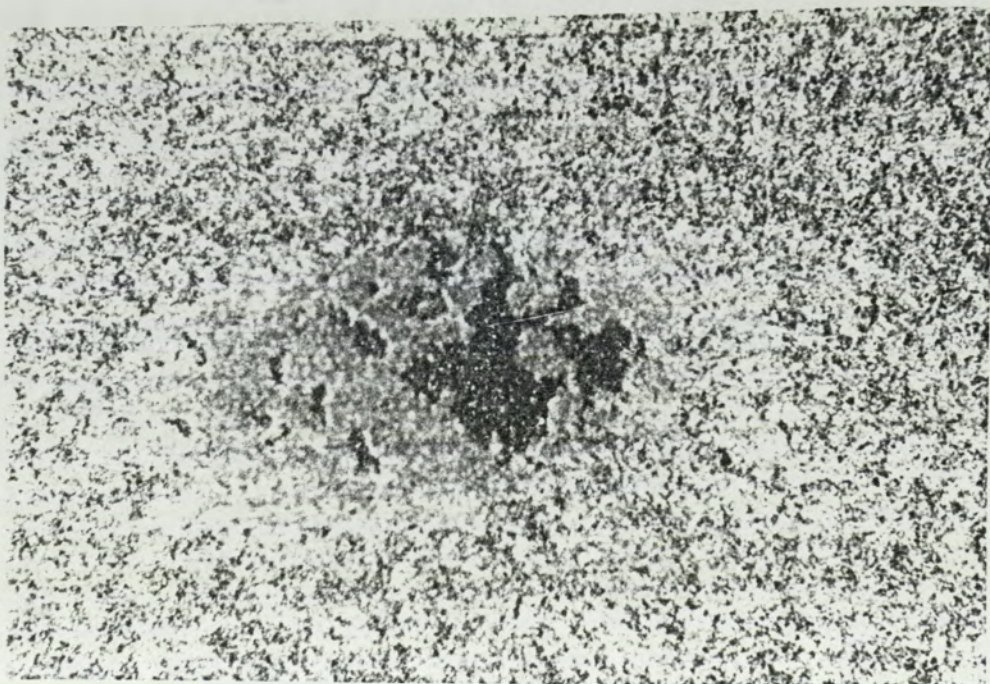
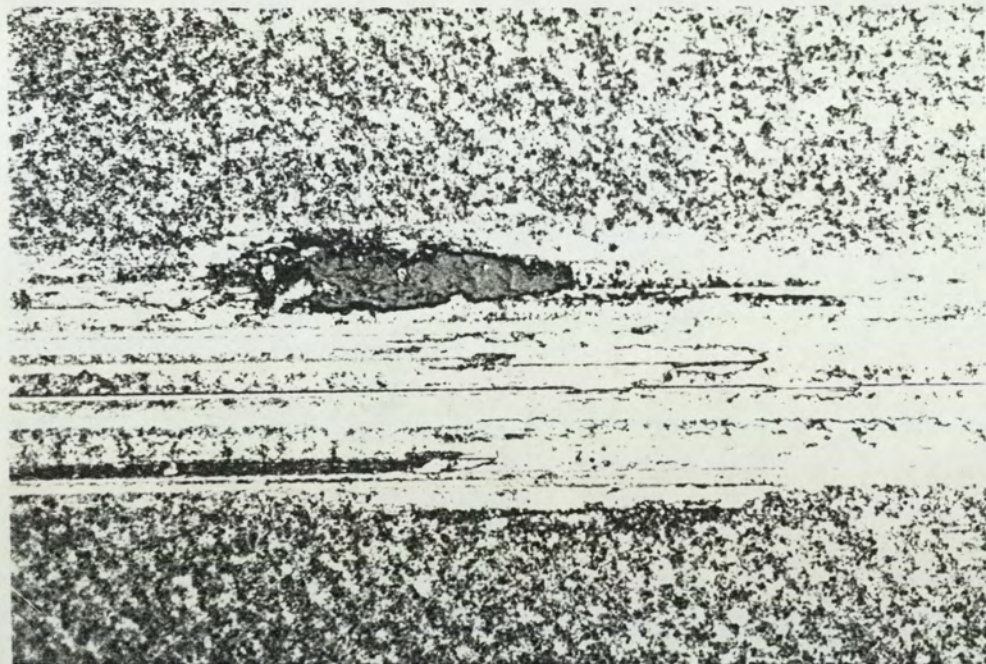


Figure 6.25 (e) Unlubricated sample tested on the supported sample simulation
rig: SR2(3), 200 ×.

Figure 6.25 (f) Lubricated sample tested on the supported sample simulation
rig: SR3(3), 200 ×.

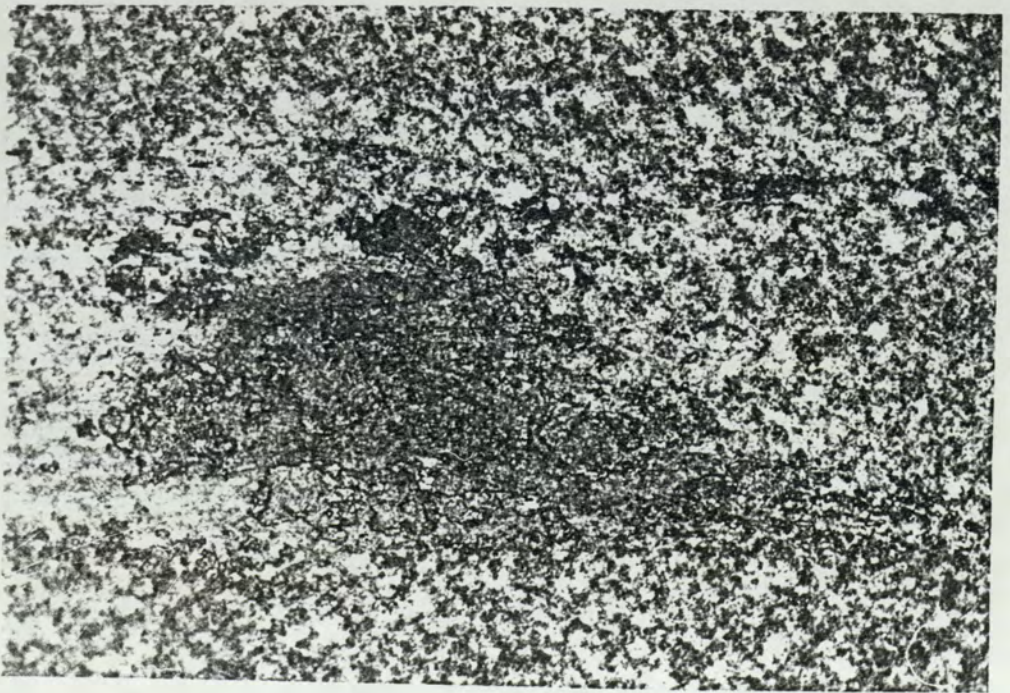
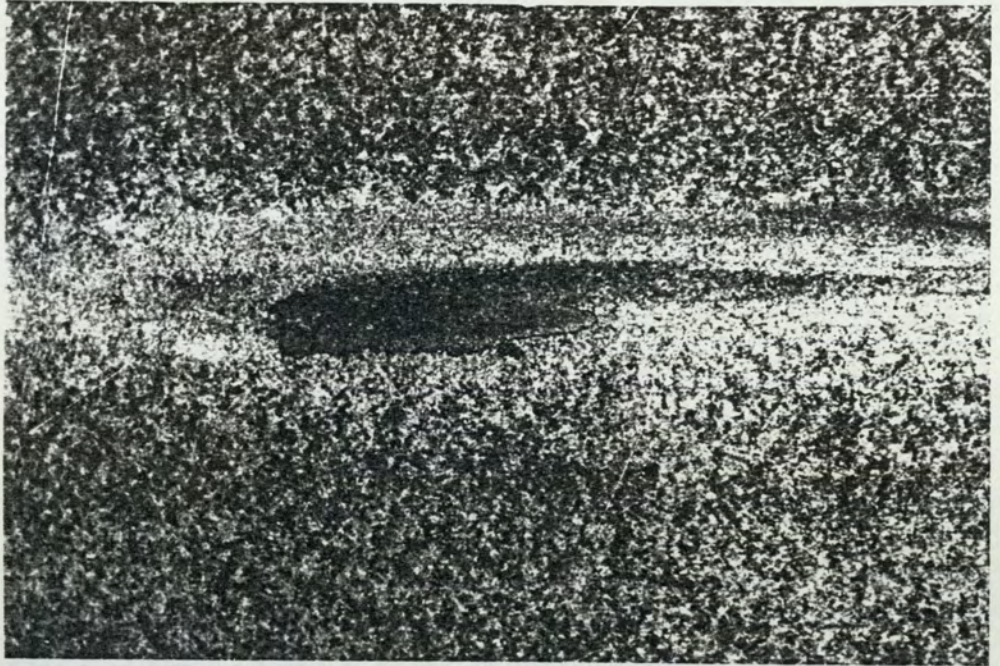
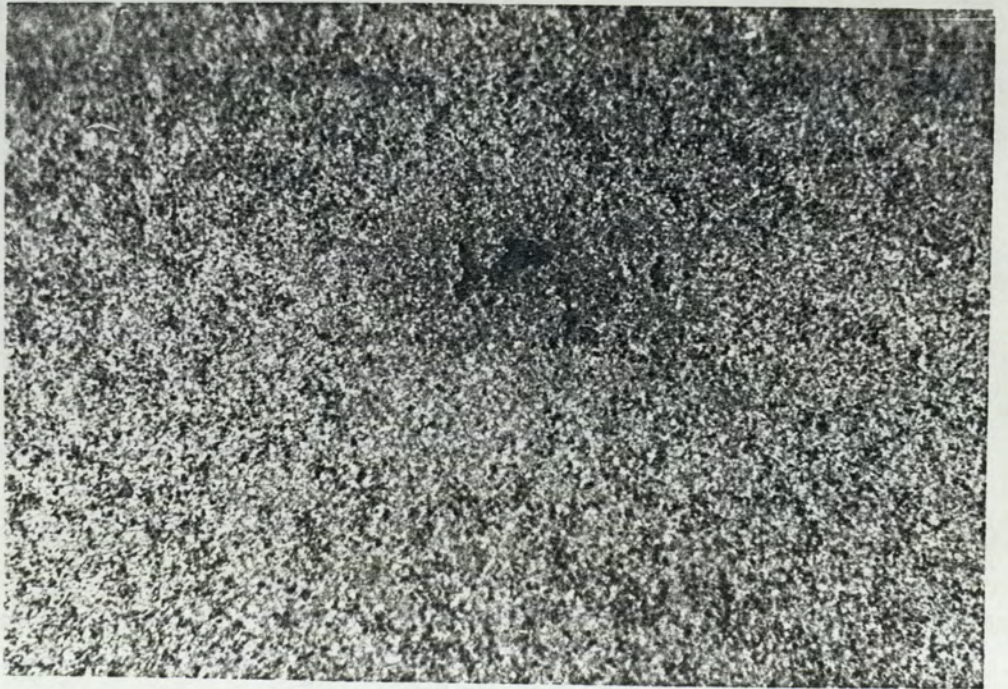
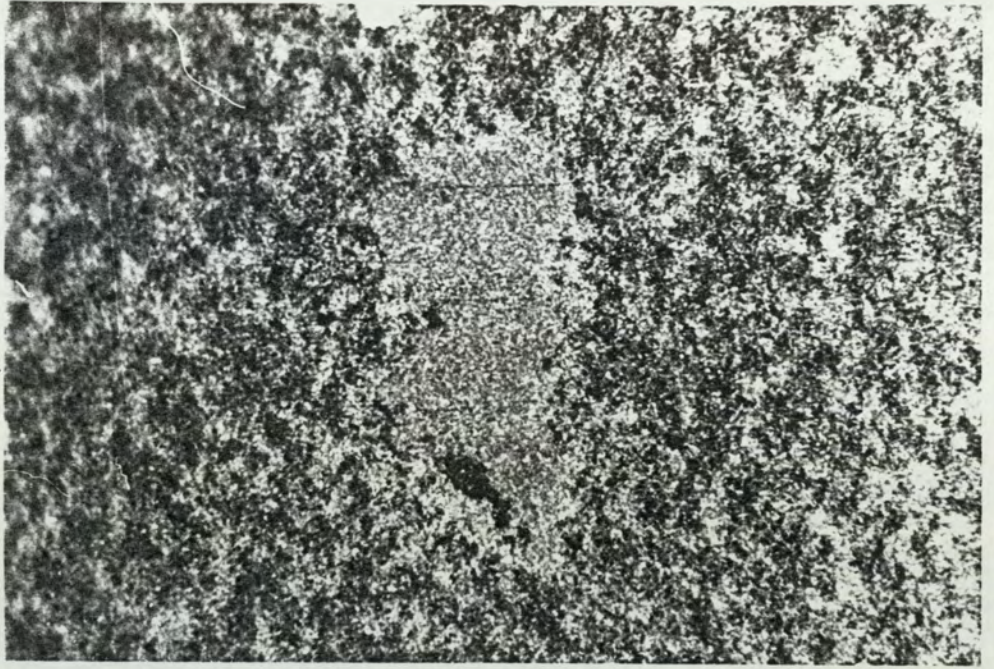


Figure 6.25 (g) Unlubricated sample tested on the supported sample simulation
rig: SR2(4.5), 400 ×.

Figure 6.25 (h) Lubricated sample tested on the supported sample simulation
rig: SR3(4.5), 400 ×.



(iii) All show that the edges of the wear sites are raised indicating that the wear particles produced were not in contact with the material immediately below them. The edges appear to have been the final points of contact and the last positions to sever before liberating the wear particles. The act of severance seems to have caused these edges to become raised. This indicates sub-surface failure prior to wear particle production.

More particular points to note are that some micrographs show "streaks" emanating from the wear sites. These are consistently in the direction of head travel. In fact, closer scrutiny shows them to be the results of ploughing wear and indicates a three-body interaction with wear particles. These features may be seen quite readily in Figs. 6.24 (e) and 6.24 (f); and Fig. 6.25 (c). These features are present regardless of which sample has been tested or which rig was used to perform the test.

One other interesting wear feature which has been optically observed is the debris produced as a consequence of wear. There is not very much debris generated but the particles that are produced are very distinctive and indicative of a particular process of wear, more discussion of this is presented in Chapter 7. Typical such particles are shown in Fig. 6.26. Typically observed debris is shown in this figure with several pictures (Figs. 6.26 (a), (b), (c) and (d)) illustrating the removed material laying on top of the wear track. It is highly likely that this material has been transported by the head to its final location from wherever it became detached. In all cases a laminar flake has been observed with this being curled up. The flakes normally show no repetition or regularity in shape but the curling is always evident. This curling is probably caused by the internal stresses remaining in it after severance from the surface.

Figure 6.26 (a) Typical fine debris found on wear tracks, 400 ×.

Figure 6.26 (b) Wear debris laying on a track with a wear patch visible in the background, 200 ×.

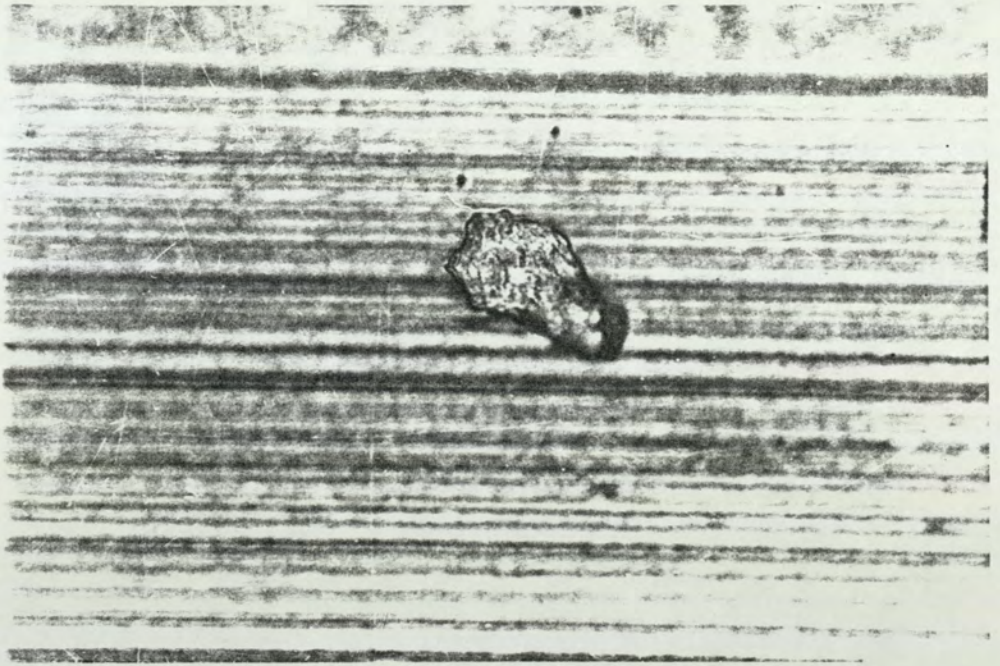
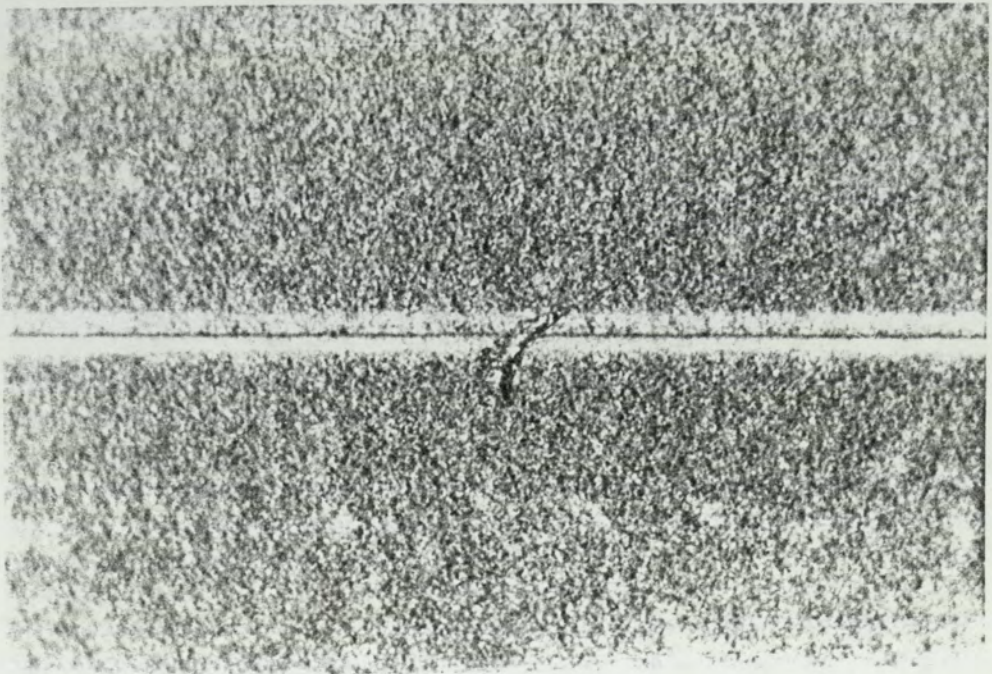
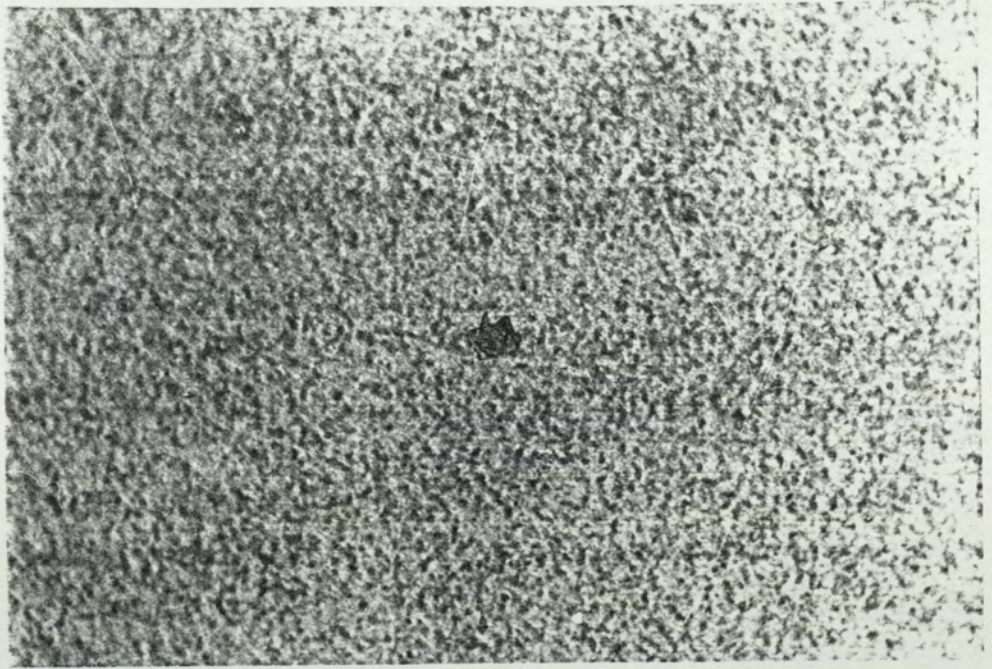


Figure 6.26 (c) More debris on a sample which shows only a little plastic flow of the surface, 50 \times .

Figure 6.26 (d) Debris particle which shows clear curling, 400 \times .



Another form of observed debris is shown in Fig. 6.27. Here large amounts of material, still in laminar form, can be seen. This appears to have been rolled up in the fashion of a scroll. This may have been formed by an extremely large wear particle being broken up or several particles being created separately. The curling of these is, nevertheless, still noticeable. Careful examination of the worn material shows that it has the form of polymeric laminae but which appear to have dark particles inside them. These particles are the magnetic $\gamma\text{-Fe}_2\text{O}_3$ acicular particles. This shows that the wear particles have come from the media surface.

(c) The Friction Tester.

As mentioned earlier, the friction tester rig was employed only to test the less durable media samples to full. Pictures from the rig are illustrated in Fig. 6.28. Here the samples illustrated are the samples SR2. The full burnishing range is illustrated and shows similar damage to that seen on the simulation rigs and in the drives.

6.5.4 Scanning Electron Microscopy.

Using the SEM, it is possible to detect smaller features on the media surface than is possible by optical means. The samples illustrated here, again, typifying the damage seen on or around the wear tracks where head-media contact has occurred but some different samples can be seen.

A similar approach to that of the optical microscopy sub-section above has been taken in the sense that typical damage is presented for each of the rigs showing the features on the surface of the tested media. Once again the samples have been shown after testing. The features seen and the type of damage caused

Figure 6.27 (a) Polymeric wear debris which has been rolled up, 50 ×.

Figure 6.27 (b) A close up of the largest features with extensive plastic flow visible on the wear track in the background, 100 ×.

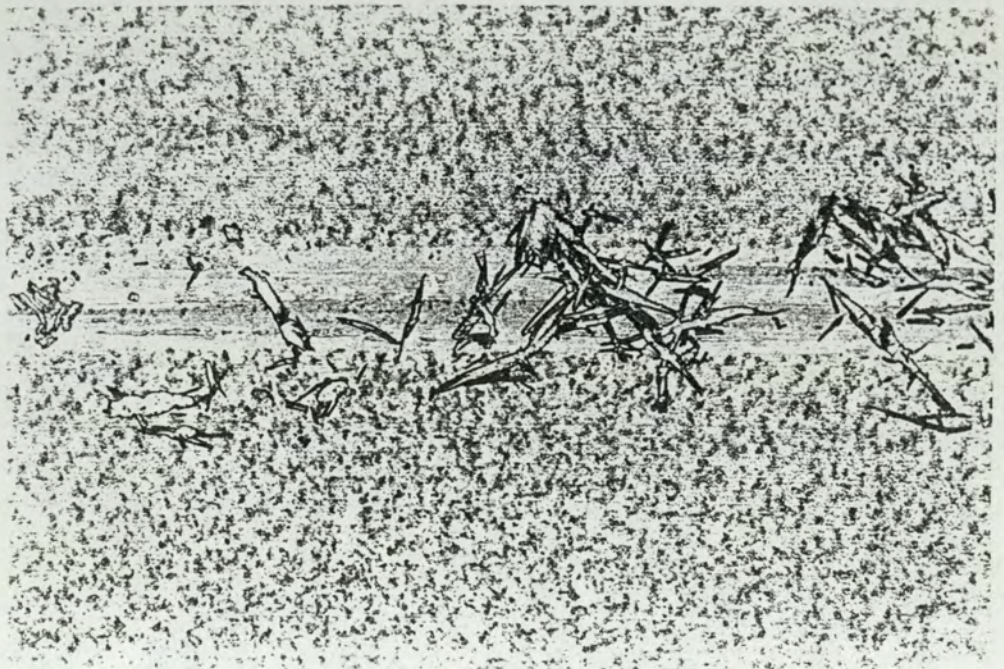
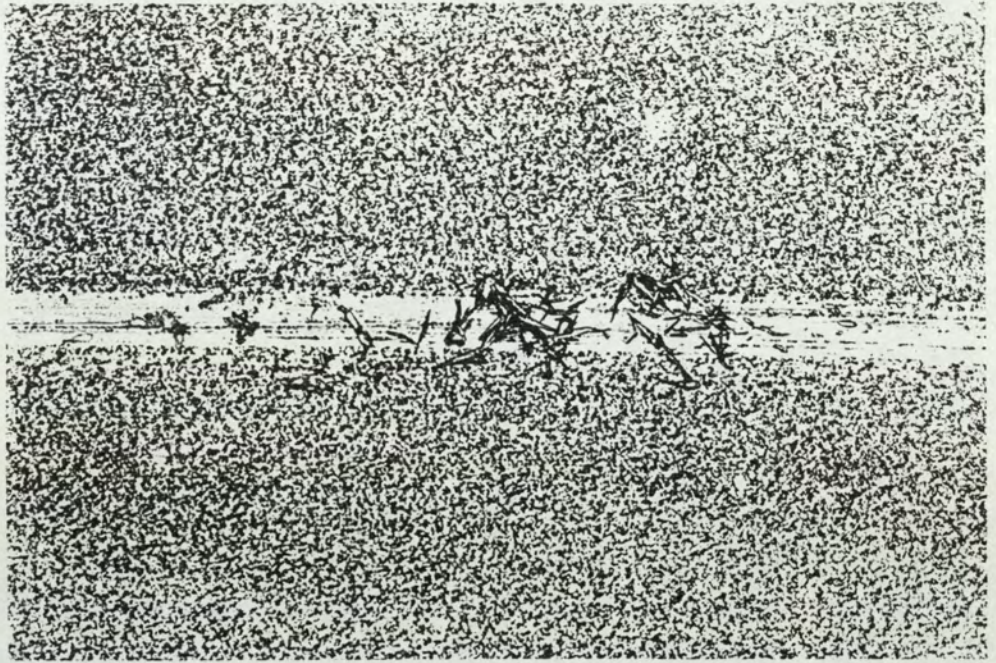


Figure 6.27 (c) Wear damage is visible in the middle of the plastic flow of the wear track in the background, 200 \times .

Figure 6.27 (d) The black specs visible in the rolled polymer debris are the acicular magnetic particles, 400 \times .



Figure 6.28 (a) Unlubricated sample tested on the in-situ friction tester showing wear sites as for the other rigs: SR2(0).

Figure 6.28 (b) Typical wear sites on the media tested on the friction tester SR2(1.5).

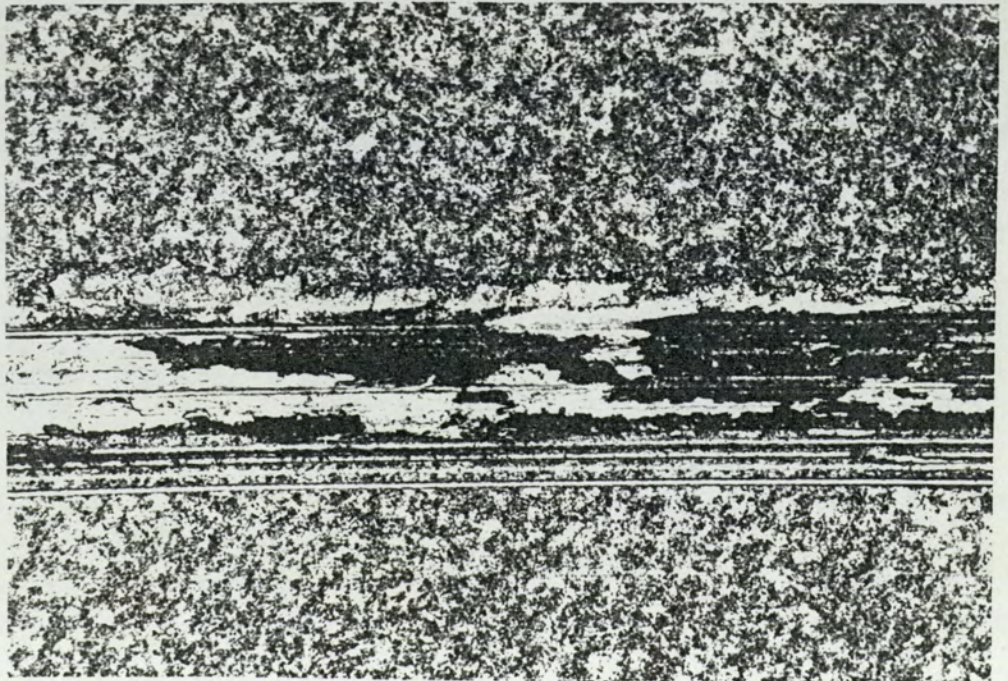
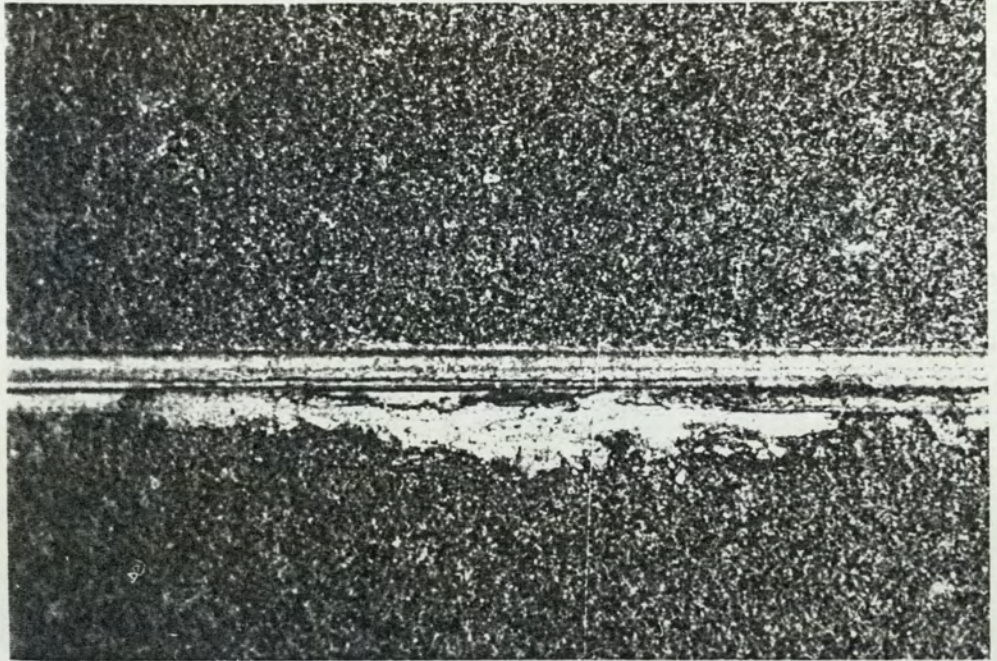
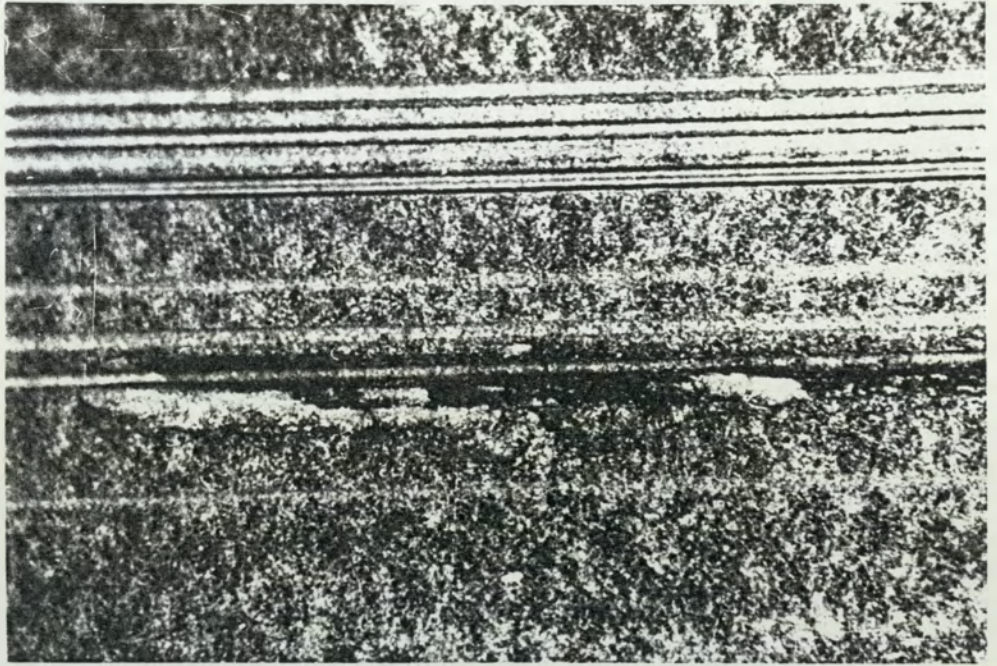


Figure 6.28 (c) SR2(3).

Figure 6.28 (d) SR2(4.5).



under the conditions imposed on the samples by the various test equipment have been illustrated. Some similarities in the surface features can again be noted. The examples presented in this section are typical of all of the media, regardless of the burnish time and lubrication, and this can be seen from the variety of samples used for illustrating the points made in this text. The reason for this is that the features studied using SEM show the microscopic changes caused in the surface leading to the initiation and propagation of the wear process and this was found to be similar in all samples and with all test rigs.

(a) Drives.

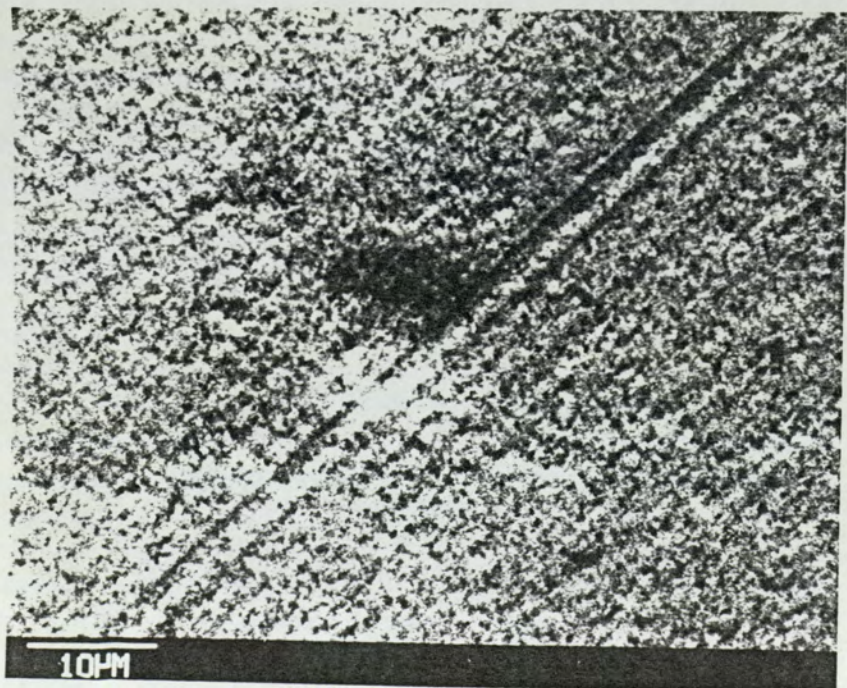
It was found that the SEM technique was not as successful as may be anticipated for looking at the examples of plastic flow selected by optical microscopy. It was found that the contrast between the adjacent areas at sites of plastic flow was not obvious. This is because of the small field of view as compared to optical techniques. However, the examples that were found show features which are different to those shown by the optical microscope. This can be attributed to the differences in the two techniques.

Unlike the optical microscope, where the reflective properties of the surface change due to plastic flow, the plastic flow seen under SEM shows more layering of the surface as if a viscous material has been forced to flow and examples may be seen in Fig. 6.29. The samples illustrated show fully lubricated media. In both of these cases the surrounding area may be used to compare the normal diskette surface to the area where plastic flow has taken place. Fig. 6.29 shows plastic flow of the material as caused by a ploughing deformation mechanism described in the Chapter 3.

Damage in terms of actual removal of material and sites where this material has either been removed or is in the process of being removed are far

Figure 6.29 (a) Typical plastic deformation of the type caused by a ploughing mechanism.

Figure 6.29 (b) As with the above micrograph, the plastic flow is clearly visible but this may be compared more easily to the surrounding surface.



more easily detected by SEM than by optical means. Several examples of this type of damage can be found in Fig. 6.30 where different media have been illustrated in each micrograph. It is instructive to note that the lifting areas of the media at the wear sites in each of the examples appears to be smoother than the surrounding, undamaged, surface and it is possible that these wear sites have been arrived at by increased local friction. Also common to the examples is the fact that there appears to be a small area lifted out. This may suggest that the area below the wear particle had become weakened. Looking closely at the pictures, such as Fig. 6.30 (a) top left hand corner, shows another commonly observed feature. This is a line like structure which appears to be a crack in the surface.

(c) The Simulation Rigs.

Similar damage to that described for the drives has been observed for the simulation rigs although it often tends to be more severe with more such wear sites being produced. The optical and SEM techniques, therefore, present similar wear sites for both the samples on the simulation rigs and in the in-situ tests of the drives. Plastic flow and wear scars found on samples tested on the rigs may be seen in Fig. 6.31. In both cases the surrounding area may be used to contrast with the damaged area in order to see the differences between the normal and damaged diskette surface. The plastic flow of Fig. 6.31 (a) once again shows the plastic deformation of the ploughing type with material displaced to both sides of the groove formed. The wear site in Fig. 6.31 (b) shows similar characteristics to that of Fig. 6.30 with evidence for small areas having been lifted out rather than ploughing out. The edges of the feature of Fig. 6.31 (b) suggest that the progression of wear is through some sub-surface mechanism as the edges appear to be lifting up from the surface.

Figure 6.30 (a) Typical wear site showing a void where material appears to have been removed leaving raised edges.

Figure 6.30 (b) An enlarged view of the feature showing clearly raised edges.

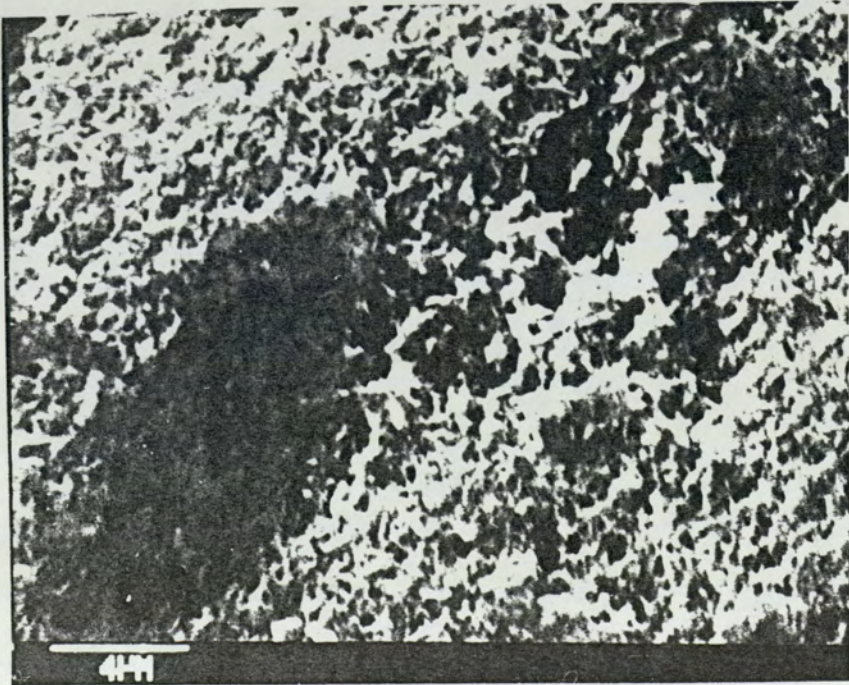
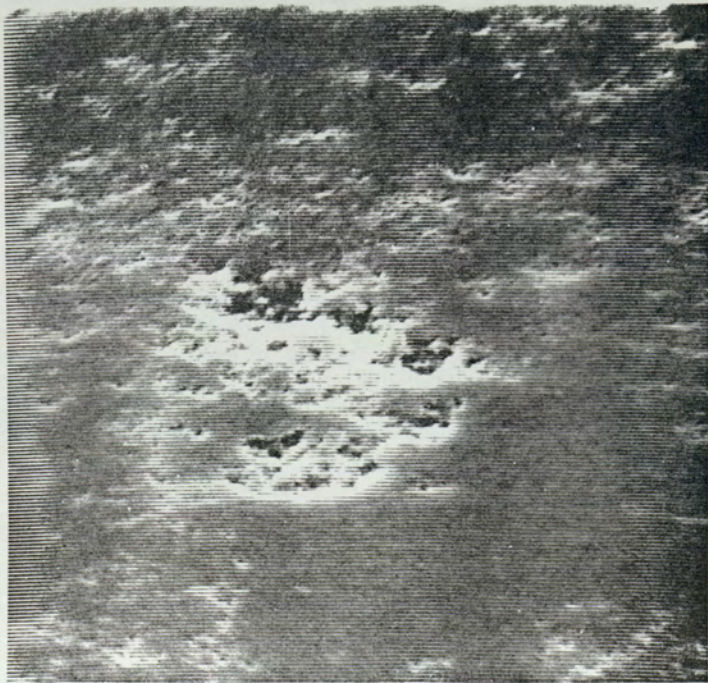


Figure 6.30 (c) Wear site showing smoothing in the area where material has been removed possibly suggesting that the high local friction led to wear.



Figure 6.31 (a) Clear ploughing type plastic deformation on a sample tested on the simulation rigs.

Figure 6.31 (b) Another typical wear site on the media surface with the remaining material showing raised edges; the edge of the feature appears to be raised suggesting it is only weakly in contact with the sub-surface material.



Once again the wear debris found on the media surface may also be examined and is similar to, though smaller than, the materials observed by optical methods and provides further evidence for the mechanism of wear proposed for magnetic media in the following chapter. Fig. 6.32 shows typical examples of such wear debris particles. The two pictures show the debris to be thin flakes with one on top of another in Fig. 6.32 (a). The particle of Fig. 6.32 (b) shows clear curling of the wear particle. The debris of Fig. 6.32 (a) does not show any curling probably because these particular particles are thicker, typical of the debris found on less durable media. More of the curled type debris is observed in general and another example of this is shown in the picture of Fig. 6.32 (c). Fig. 6.32 (d) shows surface cracking of the media before any surface material removal has occurred; the crack extends from about 25 mm away from the bottom left hand corner to just past the area where a small particle has been removed.

(c) Heads.

One other source of problems in the study of wear was mentioned earlier in this chapter when describing the electrical measurements made on the drives using the bit analysis software. This is the condition of the surface of the read/write heads. If the heads should become worn then the data reflects this fact through the rapid wear of the soft polymeric media by the hard materials constituting the head which are ceramic/ferrite structures. In order to determine what kind of wear this is, a cursory examination of the heads has been made using the SEM technique. Fig. 6.33 shows a typical used head (though not the type employed in the drives used here, the latter have three air gaps as has been discussed much earlier in this work, in Chapter 2). The picture in Fig. 6.33 (a) shows the read/write gap and Fig. 6.33 (b) a close up of the glass bonding the ferrite to the ceramic which has worn away with large particles of material having been removed. This has left

Figure 6.32 (a) A large particle which appears to be of the same constitution as the diskette surface.

Figure 6.32 (b) Another wear particle showing more typical curling and having a laminar appearance.



Figure 6.32 (c) Another wear particle which appears to be a curled lamina.

Figure 6.32 (d) A typical wear site with clear plastic flow around it in a direction from the bottom right hand corner to the top left hand corner.

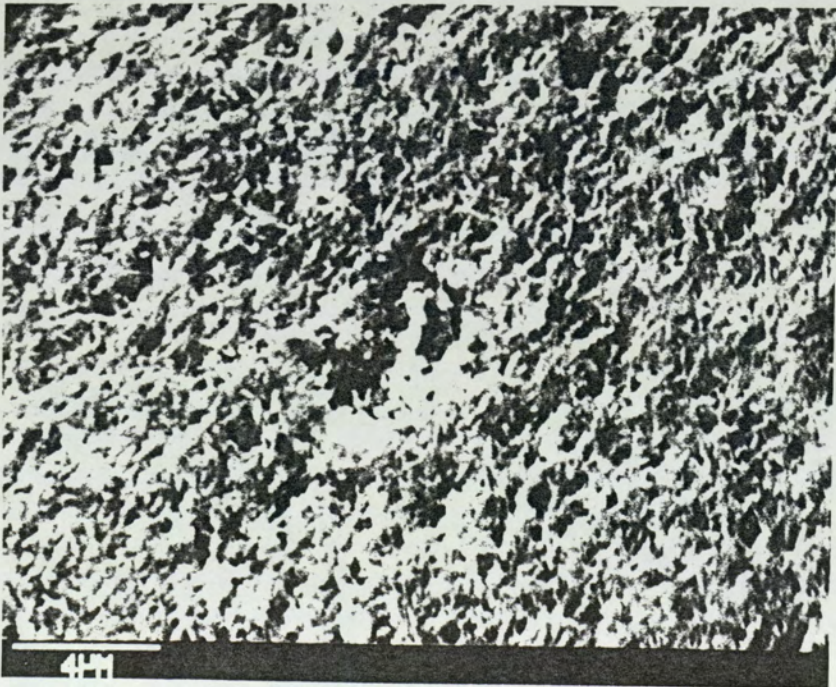
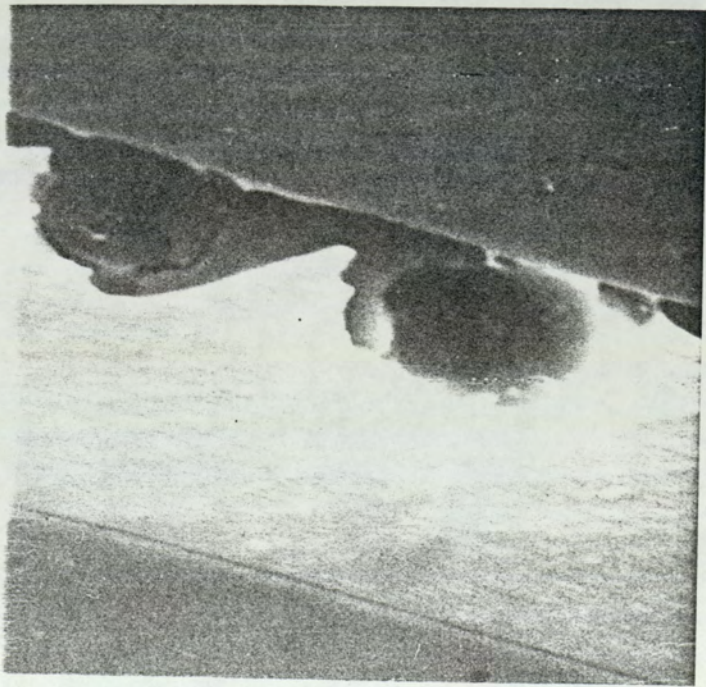
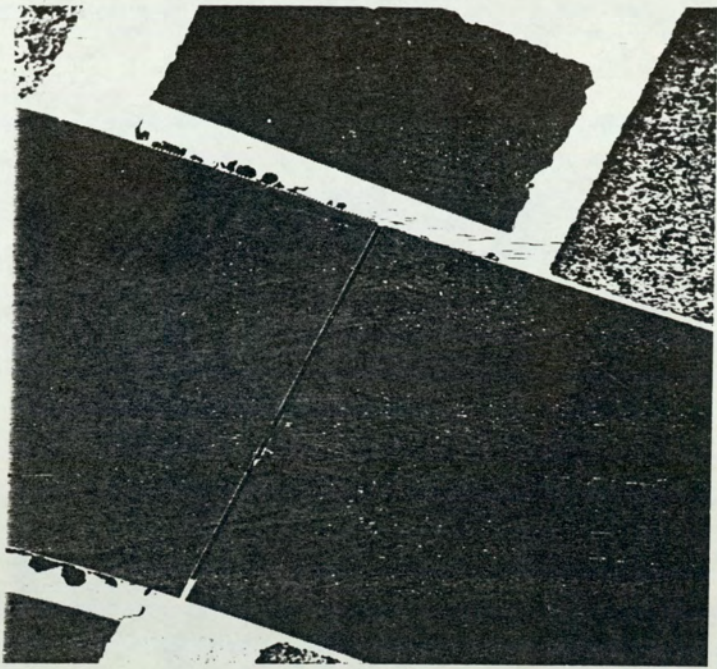


Figure 6.33 (a) Typical head R/W gap showing wear of head, 200 ×.

Figure 6.33 (b) A close up of one of the worn regions of the head showing material has been removed through "pull-outs"; this head has not been worn in the present tests, 2 K×.



behind pits where the material has been removed. This head has been illustrated to show that similar damage occurs in other drives to that detected here and that the present case is not a unique occurrence.

Fig. 6.34 shows a typical head as employed in the Tandon TM100-2A drives used in this work: Fig. 6.34 (a) shows one erase gap and Fig. 6.34 (b) the other with the two pictures showing either half of the read/write gap. It is clear from the two pictures that there has been substantial removal of material with the weak points for wear of the head being at the boundaries of the grains in the ceramic which appear to get pulled out. The situation is even worse at the edges of the heads as displayed by the picture in Fig. 6.35. Here, Fig. 6.35 (a) shows the edge of a used side 1 head with the ferrite being less worn than the ceramic around it. However, the ferrite has been pitted quite badly producing sharp edges at these points which can damage the media; a close up of the pits formed may be found illustrated in Fig. 6.35 (b). The situation is reversed for the side 0 head where the ferrite appears to wear more than the ceramic but pits are still formed in it as is shown in Fig. 6.36.

6.5.5 X-ray Photoelectron Spectroscopy.

XPS analysis was carried out on binder samples which were produced to establish the nature of the profile of each of the different binders used in magnetic media. It has also been performed on all sixteen of the samples SR1 to SR4 that have been used in this study. This enables comparison of the media samples used in tests to see whether the addition of the magnetic particles has any effect. However, this is an optimistic objective since the key chemical groups which are readily detectable and identifiable (such as the carbonyl, carboxyl, ester links and phenyl groups) are present in the binder systems of all the binder preparations and in the media samples used here. In fact, they are all present in

Figure 6.34 (a) Typical wear of the type of heads fitted in the drives used for this investigation showing the R/W gap and one erase gap.

Figure 6.34 (b) Similar damage at the other erase gap.



Figure 6.35 (a) The trailing edge of a side 1 head showing apparently preferential wear of the ceramic, 120 \times .

Figure 6.35 (b) A close up of the worn area shows pits left by material which has been pulled out, 600 \times .

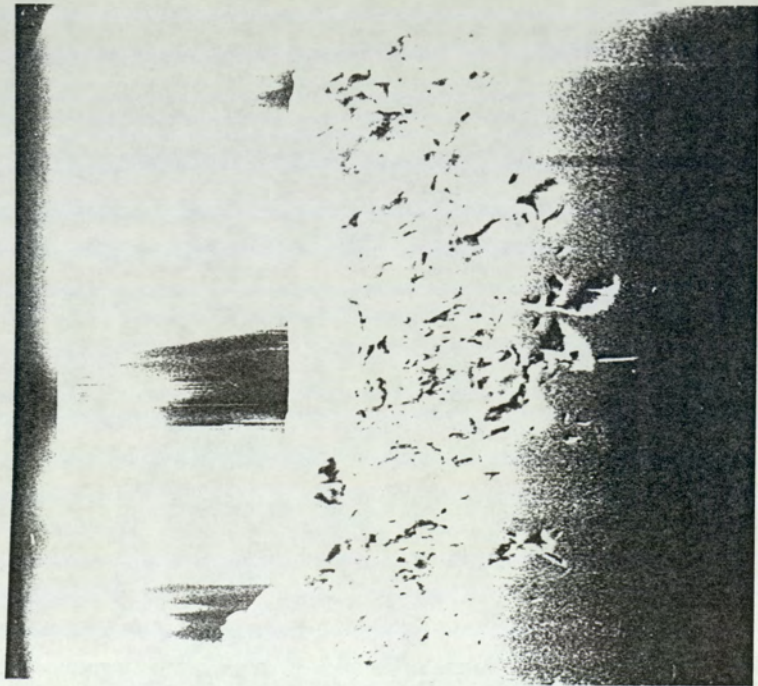
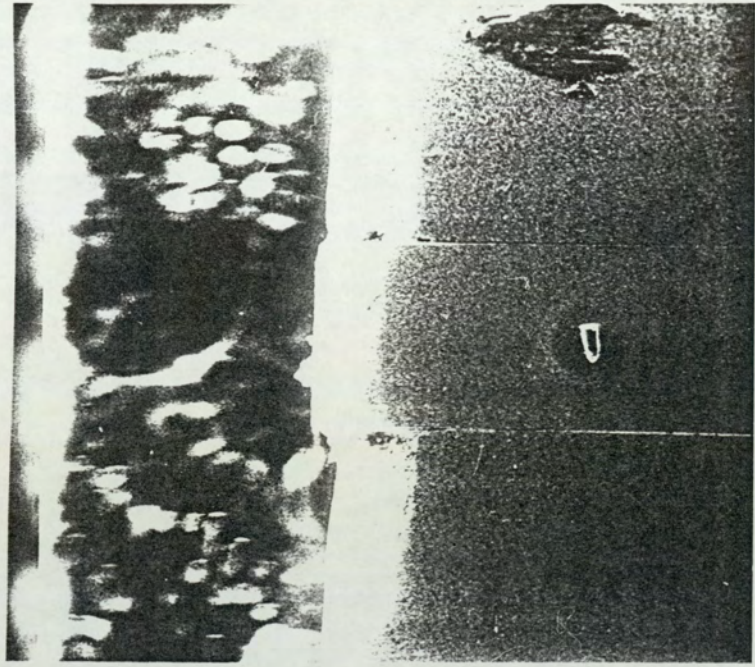
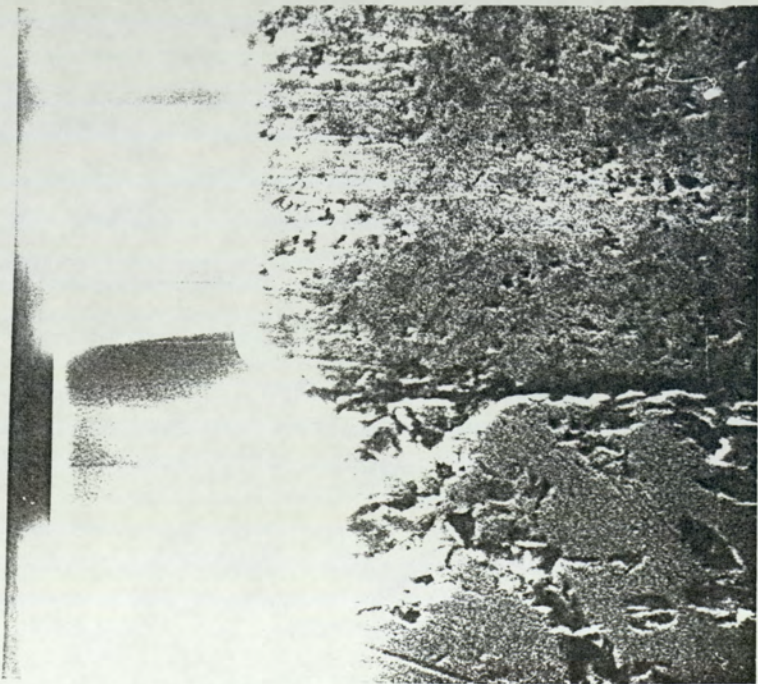
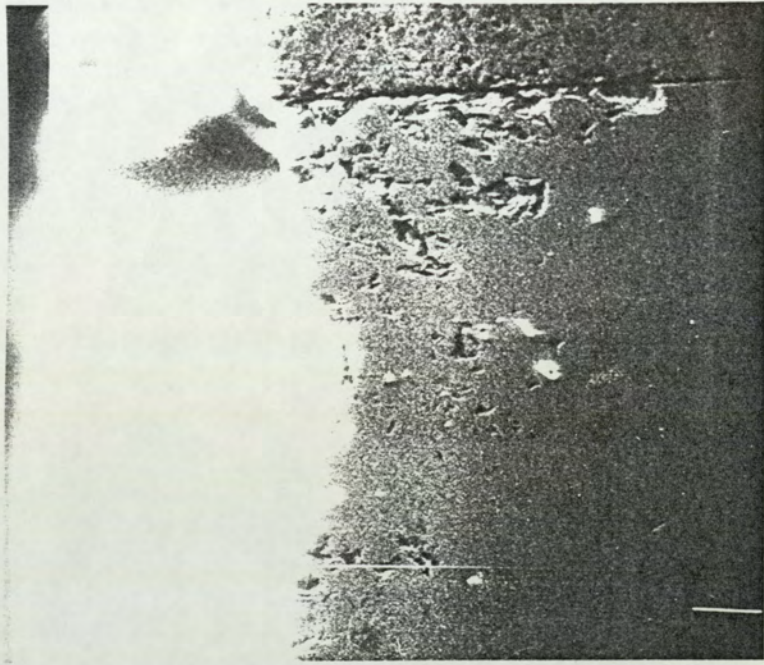


Figure 6.36 (a) A side 0 head shows greater wear of the ferrite, 600 \times .

Figure 6.36 (b) A close up shows the mechanism of wear appears to be the same as for the side 1 head, 1.2 K \times .



the different samples of binders and media in much the same chemical environments such as in the form of the binder co-polymers and the lubricating materials used.

One other objective was to look at the wear scars on the media with this techniques in order to establish whether, for instance, the wear scars with significant plastic flow being caused were more polymer rich than the rest of the surrounding media surface. Attempts were made to do this by looking at the strength of the signal obtained for the various elements but it was found that the size of the X-ray beam emitted by the X-ray gun, at approximately 24 mm^2 in cross-section ($6 \text{ mm} \times 4 \text{ mm}$) was much wider than the wear scars resulting in the signal coming not only from the wear scar but also from the surrounding region. In fact, under these conditions, the signal from the worn area becomes very much smaller than that from the surrounding area. Attempts to produce samples which had the surrounding areas shielded with materials which did not have characteristic features near to the Carbon and Oxygen to be studied, left so little of the sample visible, due to the scars being very thin, that the noise was overwhelming. It was concluded that the only method which could produce meaningful data on and off the wear scar would be one which employed "small spot" XPS techniques whereby a beam of very much smaller cross-section is produced by the X-ray gun.

One area in which XPS was successfully employed was in the analysis of the heads. This stems from the fact that the drives' data of Fig. 6.5 includes some durabilities data where samples SR2 (completely unlubricated) and SR4 (bulk only lubricated) have been affected by lubrication caused by the transferred layers left on the heads by previously tested, lubricated, samples from earlier trials providing surface lubrication. Evidence for this phenomenon which may be considered concerns tests which were carried out on samples SR4 in testing drives numbered 4, 5, 6 and 7 after SR3 samples. These appear to cause an

anomalous extension in the lifetime of the second series of samples. The original tests performed on SR4 at the beginning of this project, with new drive heads, indicated a lifetime of the order of minutes. The samples inserted in the drives after the SR3's produced lifetimes of over 12 hours and, in one case, over 39 hours! The removal of these transferred polymeric lubricating layers may be effected, however, by running the less lubricated samples. This is made clear by the fact that re-runs of the SR4 samples in the same drives produced a dramatic reduction in the lifetime to a range stretching from less than 2 hours to 1 minute. The final result can be brought down to the initial observation of lifetimes of the order of minutes rather than hours. This would suggest that something is indeed occurring which affects the drives' heads. Exactly what occurs, has been discovered through the use of XPS which has shown that there are indeed polymeric substances on the used heads.

The data presented here is for the Carbon signal from one unused and one used head, Figs. 6.37 and 6.38 respectively. In both cases the major part of the complex structure of the Carbon peak is due to the indistinguishable C-C and the C-H bonds found in the majority of organic molecules including all of the ones encountered in this study. The minor contribution, however, is of most interest here and is situated to the left of the main peak as presented here. Although the C-C and C-H bonds are present in airbourne dust, the C=O bonds are present, if at all, to a very small degree. Certainly, their contribution from the dust on the unused head would not be detectable. However, as may be recalled from the description of the nature of the materials of the magnetic media binder and lubricating substances, there are substantial numbers of such bonds present. So the fact that this contribution has increased in the spectrum of Fig. 6.38 compared to the spectrum of Fig. 6.37, provides very strong evidence for layers of the polymeric lubricant being transferred to the head from the media. Even small amounts of material (monomolecular layers are sufficient) can then provide

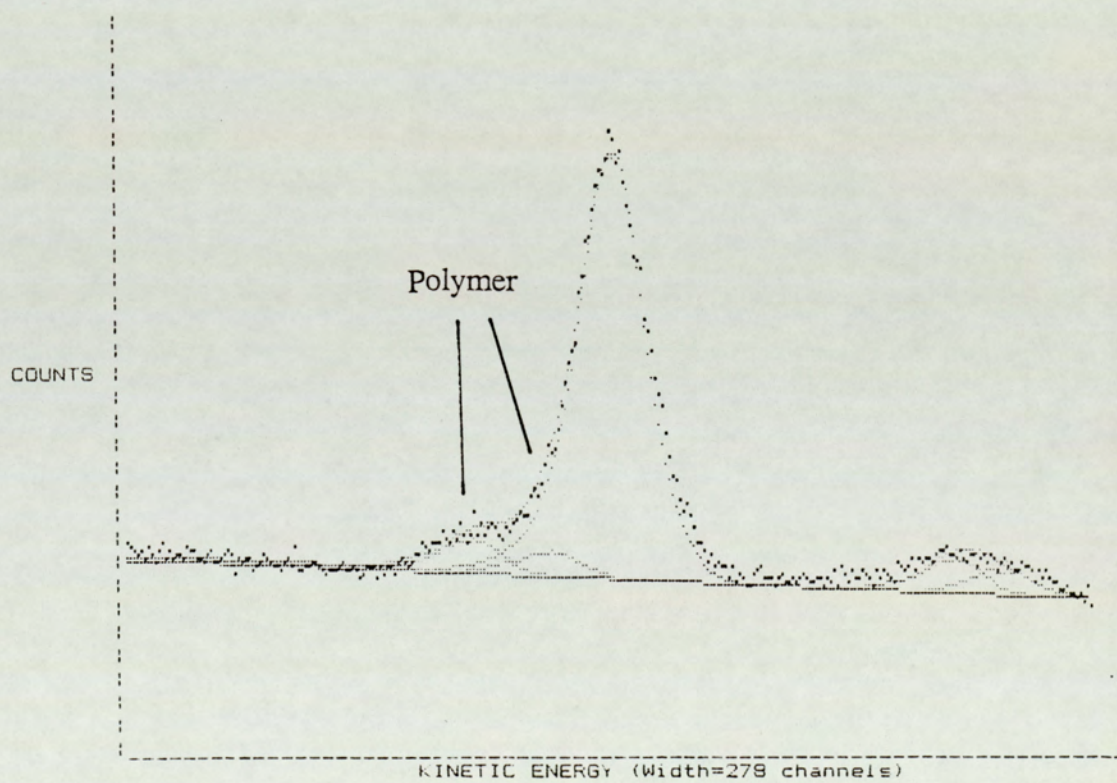
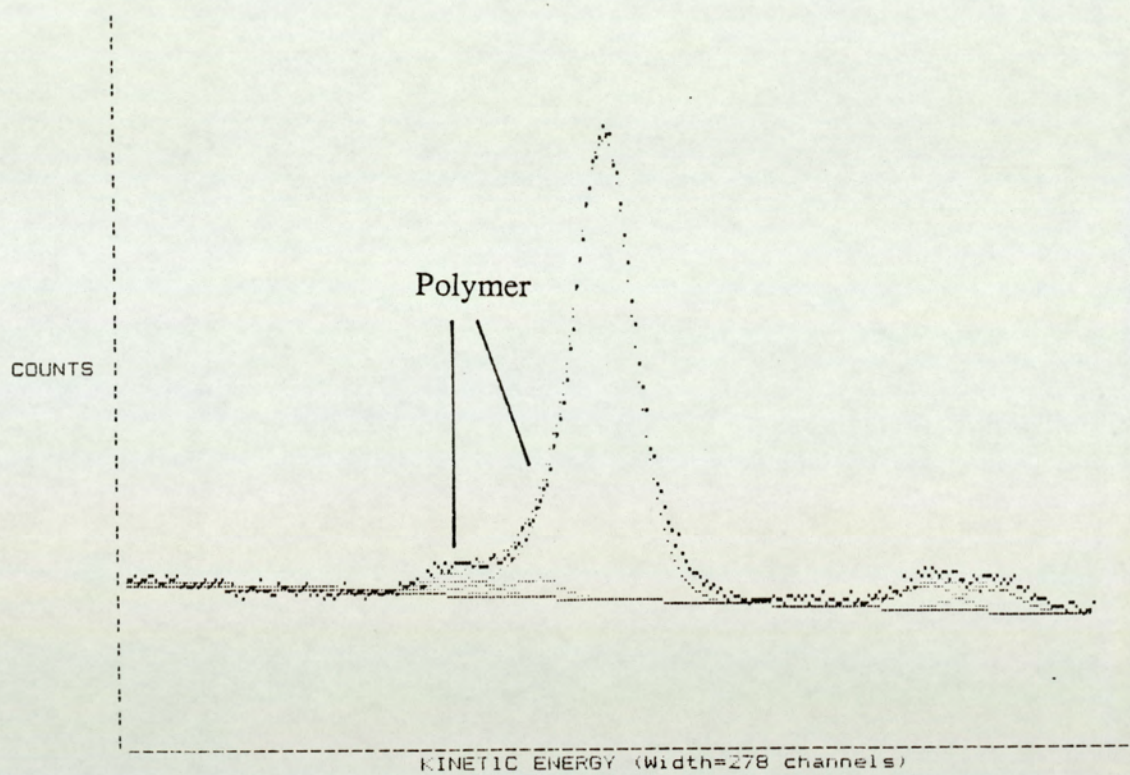


Figure 6.37 XPS scans for Carbon on (a) Unused side 0 head (b) Used side 0 head.

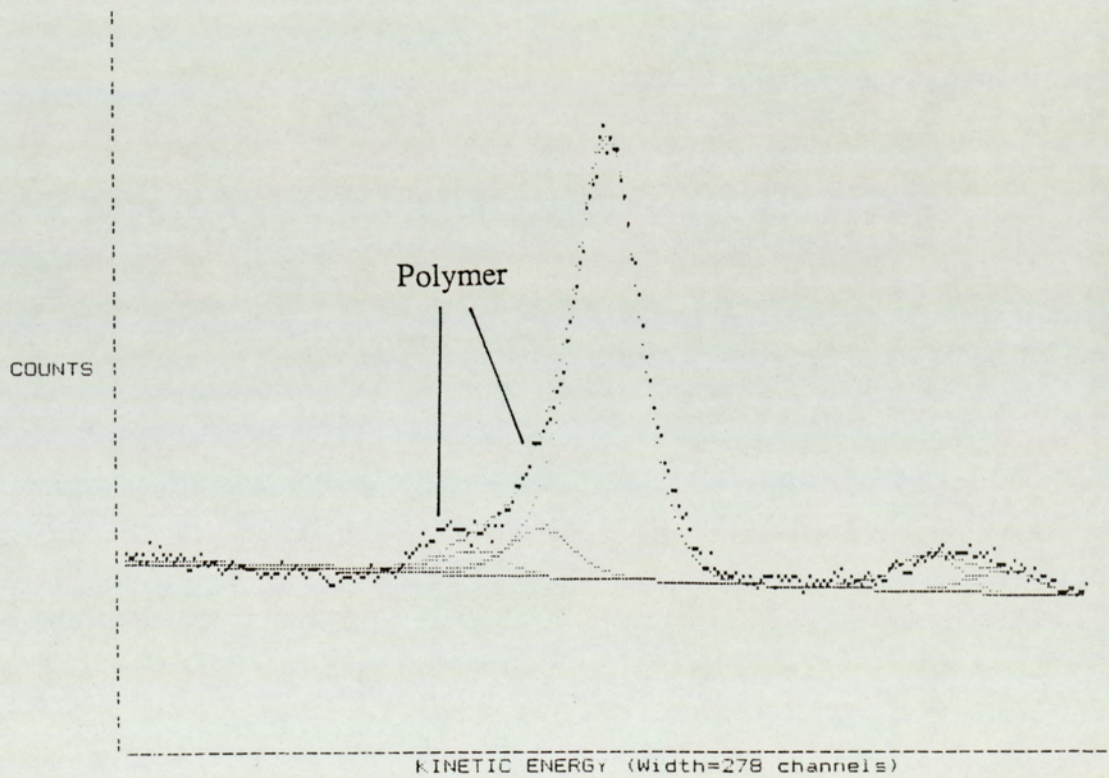
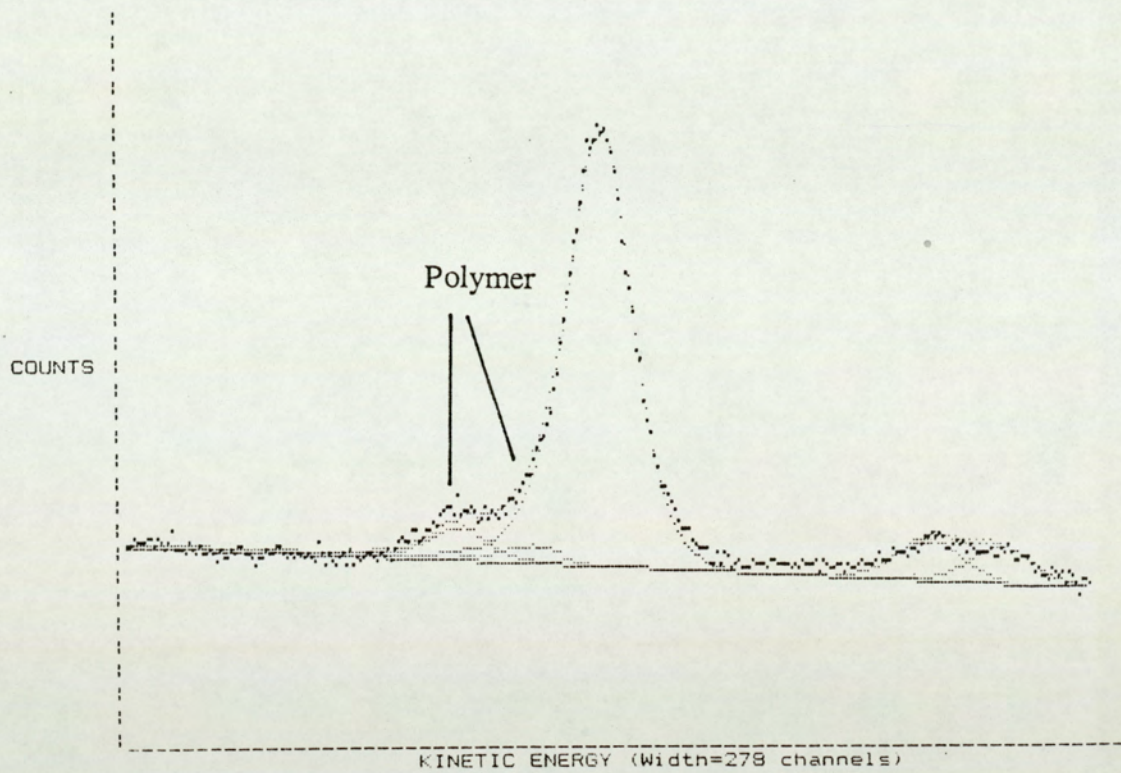


Figure 6.38 XPS Scans for Carbon on (a) Unused side 1 head (b) Used side 1 head.

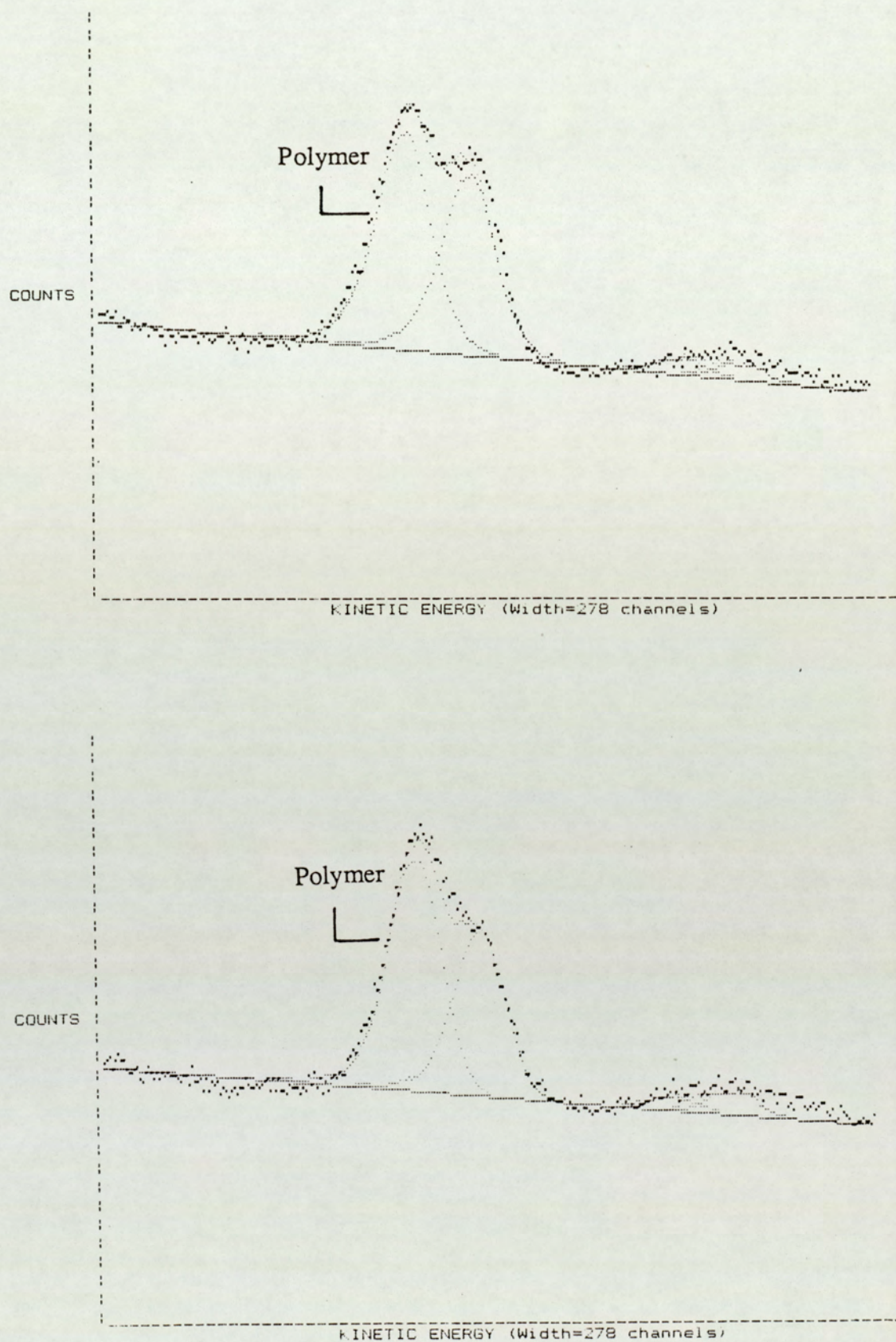


Figure 6.39 XPS Scans for Oxygen on (a) Unused side 0 head (b) Used side 0 head.

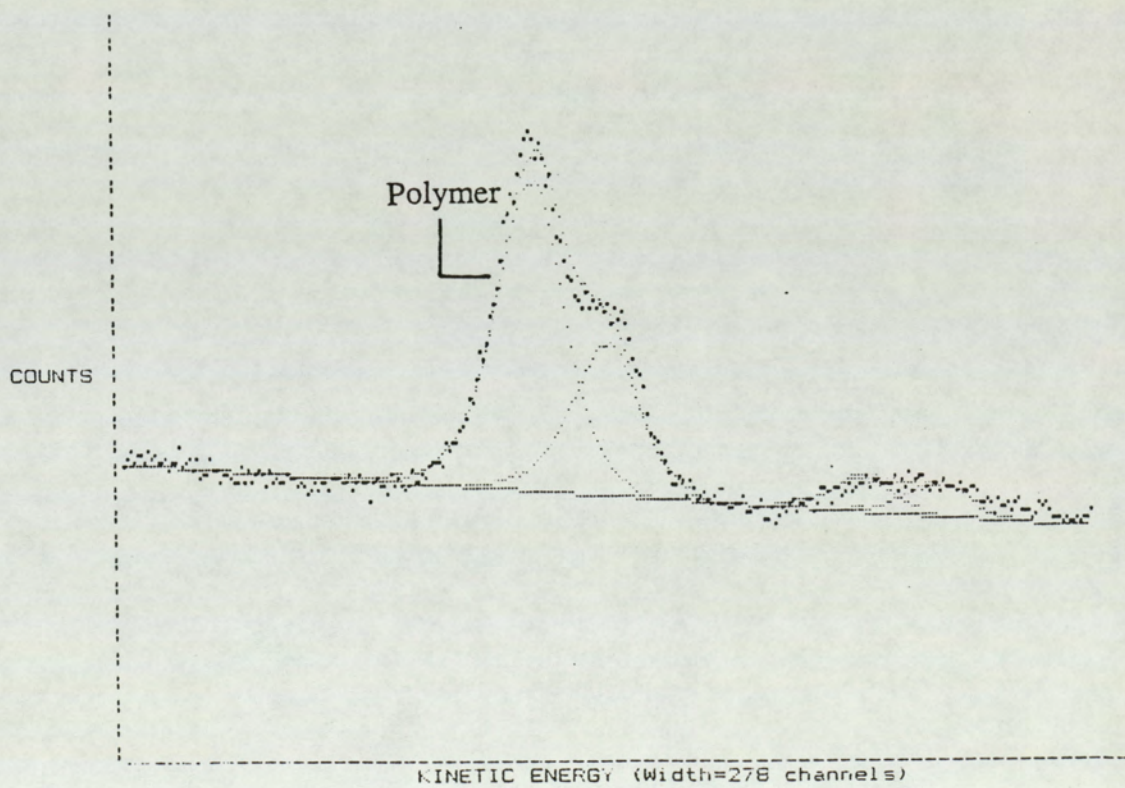
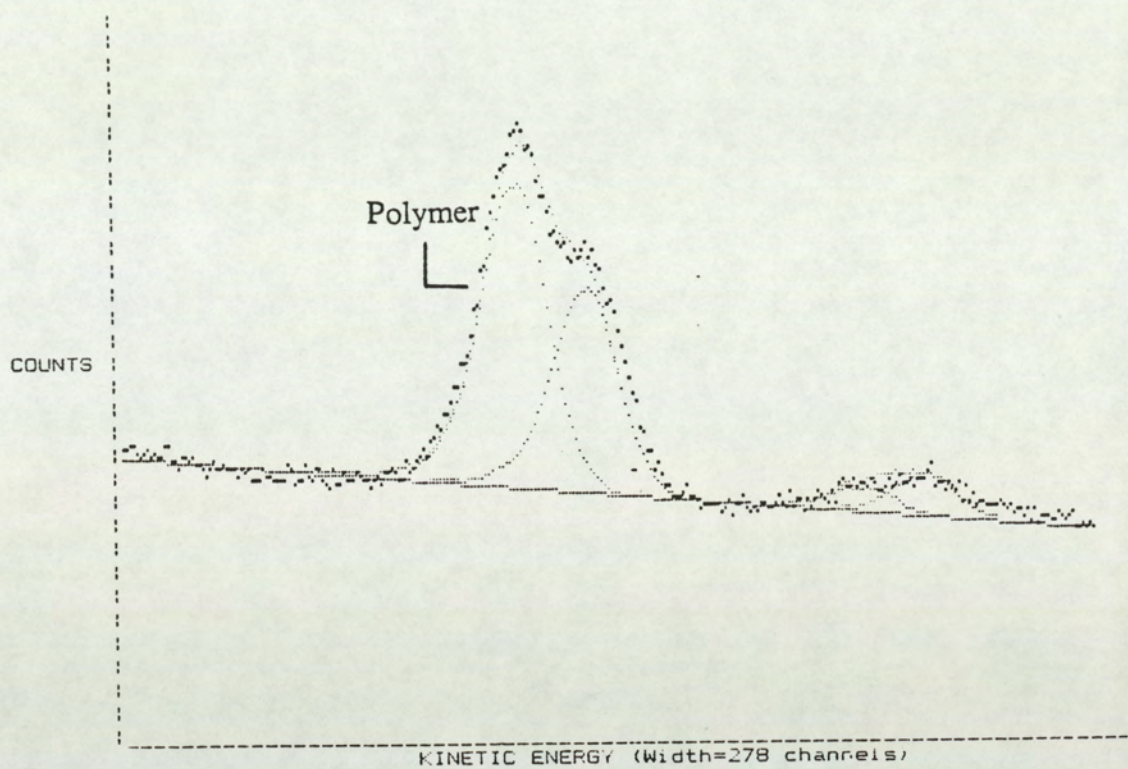


Figure 6.40 XPS Scans for Oxygen on (a) Unused side 1 head (b) Used side 1 head.

boundary lubrication of samples. The removal of these layers by the use of unlubricated media is effected by microscratching of the material by the Alumina particles in the media's magnetic layer which is the head cleaning agent.

Additional confirmation of the existence of these polymeric layers is provided by the XPS scans looking at the Oxygen signal, Figs. 6.39 and 6.40. The unused head has oxygen (apart from the dust and adsorbed layers of gas) primarily in the form of the Titanate ion in the ceramic and the Oxide ion in the form of the ferrite material. The modification of this peak may be caused by larger contributions from the Oxygen in the form found in the organic molecules of the magnetic layer.

In concluding this chapter, it may be said that the "raw" data has been presented with a small amount of explanation of it where this has been found to be necessary. The main part of the discussion, however, has been left to the next chapter but it is worth commenting here, before starting the discussion, that under ideal circumstances it would be possible to examine the samples under test at any time and to inspect the wear scar for true wear. However, for proper inspection, in the real conditions prevailing, the diskette has to be removed and sections cut out from it for analysis by most of the techniques used. Thus if the scar is only due to burnishing effects, as, in fact, it is in the majority of cases, it is not possible to continue the test. This is one of the reasons, that of consistency, that the criterion of visible scar formation has been used, as has been done in the tests carried out by researchers at 3M. Unfortunately this is what can lead to misleading durability data. Recommendations regarding this are offered later.

Chapter 7

Discussion of Results

Chapter 7.

Discussion of Results.

Introduction.

In this chapter the results presented in the preceding chapter have been discussed. The relevance of the information gained to the aims of the project has been considered. In particular, the effects of burnishing and lubrication on the durability of samples has been discussed. Also, the mechanisms of wear applicable to the media have been considered and a theory has been proposed based on the features found on the surface of tested samples. The durability has been discussed individually for each of the rigs used in this investigation and wear mechanisms for each of these rigs have also been considered. These mechanisms have been considered in a single section for all of the rigs as the similarities between these rigs are quite marked.

The final part of the chapter concentrates on the two simulation rigs and discusses their potential for use as accelerated testing devices for this and any future diskette media.

7.1 Durability.

Looking first at the durability aspect, the durability of samples is affected independently by the roughness and lubrication states of the media's magnetic layer. In fact, it is far more important to look at the effects of burnishing time rather than the surface roughness. This is because the process of burnishing does not simply produce a smoother surface. Burnishing also produces fundamental changes in the surface which constitute initiation of the wear

process. Each sample can, therefore, be studied from the point of view of how burnishing affects durability or how the presence or absence of one or both lubricants affects durability. Both of these contributions have been discussed for the different rigs. One important factor in the determination of durability is the criterion used to define sample wear. The details of this have been described earlier and need not be repeated here. However, the possibility of changing these criteria and the implication of doing so are discussed in this section.

7.1.1 Durability: The Effects of Burnishing.

Two effects have been noticed as regards the burnishing of samples and its relationship to their durability. The result is, in fact, dependent on the criterion adopted for monitoring sample wear. If this is set as adopted by 3M and for the present work, *viz.* that the sample is to be discarded if it has visible damage of any sort, then the least burnished, and roughest, samples tend to exhibit very low durability on all of the rigs used in this study. This has been illustrated by the correlation between the interferometric scans shown in Fig. 6.3 and the friction traces of Figs. 6.7 and 6.8, Chapter 6. The burnished media tends to exhibit greater durability as the the shape of the graphs of Figs. 6.5, 6.10 and 6.11 show. As can also be seen from these graphs, there appears to be a point at which further burnishing becomes detrimental to durability; there is an optimum burnish time. This needs to be discussed further before the rigs are considered individually.

The process of burnishing is carried out using abrasives papers which act on the media surface through the hard particles embedded in these papers. These papers appear to act in different ways simultaneously. The nature of the actions has been concluded from a knowledge of the process and observation of the surface as well as a knowledge of the materials used in diskette binders. One

consequence appears to be to make the surface smoother. The results of this can be seen in the interferograms of Fig. 6.3. This smoothing is caused by extensive plastic flow of the surface. This would appear to be the case because the surface is left more reflective than the unburnished surface. The reason for suspecting this plastic flow is that the tests performed for this project have produced shiny scars. These scars have been observed to be caused by plastic flow of materials. Additionally, the SEM micrographs presented in Chapter 6, for example Fig. 6.30, show plastic flow in the region of these scars. The surrounding surface, however, also shows some plastic flow, *albeit* to a lesser degree.

An important effect of burnishing is the physical removal of material from the diskette surface. This contrasts with moving material around on the surface during the asperity plastic flow stage. The removal of material is effected by a micro-abrasive action and thus represents the first stages of wear. Evidence for this is presented in the form of badly produced media. Some examples of this abrasion were found in burnished SR4 samples which were unusable as a result of clear grooving. The fact that this grooving occurred during burnishing, tends to suggest that the removal of material from the surface is a normal action during this process. In addition to this abrasive effect, the burnishing process can also be expected to cause frictional heating. This can cause melting of the polymer in the binder. Subsequent cooling may then produce re-crystallisation in the co-polymer. This is likely to result in a harder surface after initial burnishing. However, further burnishing can be expected to cause damage to this harder surface. This would occur as extensive plastic flow is caused in the subsurface regions. The result of forcing polymeric material to flow around the hard oxide particles could cause sub-surface failure. Also, migration of polymer towards the surface could be effected through a "settling" of the oxide particles. The "settling" of the magnetic particles creates a polymer-rich upper layer and a corresponding relatively particle-rich lower layer. Both of these consequences

imply that too much burnishing would result in a poorer media. This may explain the shape of the durability curves in respect of the burnishing time presented in Chapter 6. The shape of the curve may be understood by considering the head-media contact. This contact causes smoothing of the surface through plastic flow. This apparent "wear" scar (in fact, surface plastic flow) is easily detected on the unburnished samples. Hence the lower durability. Initial burnishing smoothes the surface and increases the durability by making the scar less easily visible as well as affecting the surface crystallinity. It also initiates sub-surface changes. Further burnishing causes substantial sub-surface changes, as described, and leads to poorer media through crack initiation and real wear in the polymer-rich surface created. The mechanics of this real wear are discussed in a later section.

7.1.1.1 Drives.

The drives show similar trends in sample durability to the other rigs, with the unburnished and the most burnished samples exhibiting a greatly reduced durability. The dominating factor here is the criterion used for determining durability. The fact that any visible damage is accepted as "wear" of the media, can produce misleading results. The reason for this is that the unburnished media initially has a matt appearance. As a consequence, any small amount of smoothing of the media surface caused by plastic flow of asperities becomes easily visible in contrast. The plastic flow is most likely to be caused by temperature effects. This would be by local frictional heating and softening of the polymer. The result of this plastic deformation is to produce a smoothed area which is easily visible against the matt normal appearance of the unburnished media surface. This condition does not, however, represent removal of material and hence wear.

In the case of burnished media, the initial appearance is much more

shiny. This means that any smoothing of the media due to head contact is much more difficult to detect as a consequence. Furthermore, it would be expected that melting and re-crystallisation of the polymer during burnishing would leave it more crystalline and harder than the unburnished media surface, as discussed above. The harder surface would be less prone to plastic deformation since the critical pressure required for plastic deformation is directly proportional to the hardness; this has been discussed in Chapter 3. The reformed surface produced by burnishing may be expected to result in changes in the temperature at which the new surface undergoes phase transition. An important transition in this context is the "softening temperature". This is the temperature at which the polymer material suddenly becomes very easy to deform plastically; it flows more readily under lower stresses. With a reduction in proportion of the polymer component at the surface, the consequence of this may be to raise the temperature at which significant softening of the binder occurs towards the melting point of the co-polymer. This may be due to greater heat dissipation via the oxide particles. Plastic flow under normal use therefore may be reduced. This would mean that not only is any plastic flow more difficult to detect against the background, but less of it is likely to occur for initially burnished media. However, beyond a certain burnishing period, the burnishing process would be expected to cause further changes as discussed above. Furthermore, since it uses abrasive materials, burnishing can be expected to cause fundamental damage to the surface through ploughing wear as seen in the faulty media received. Thus burnishing may be seen as starting the wear process. The most burnished media, therefore, shows reduced durability as the wear process resumes during head-media contact. This wear is rapid in its progression, as explained later, and results in rapid deterioration of the media.

Melting of the binder still occurs even in less burnished media due to localised high temperature "hot spots" ("flash" temperatures) caused by local

adhesion. Reasons for believing this are the very smooth regions seen near wear sites and on potential wear particles. An example of this may be seen in Fig. 6.30. These areas are regions where extreme softening or melting appears to have occurred before resetting with the head's very smooth surface planing over during cooling or re-solidification. In fact, this melting would also be expected to occur during burnishing. A more elastic media surface may be beneficial [83], [91].

A more elastic surface should be investigated to determine whether it shows better durability, particularly under the criteria applied here. It would be expected that a sample produced with a binder having a high value of the product (Se) would be beneficial (equation (3.1.1.11) in Chapter 3); S is the ultimate breaking stress and e the elongation, also at fracture. As Fig. 7.1 shows this could result in a material which exhibits substantially only elastic deformation so that the problems associated with increases in the real area of contact could be avoided. The Curve "A" illustrated exemplifies the material with the desired properties. This shows a high elasticity so that a large real area of contact can be avoided. The large value of elongation before fracture would result in fewer wear particles being produced and can be expected to reduced three-body wear as discussed in the wear mechanism section later. Such a material is often termed "hard and tough" [138]. The other curves illustrated show materials with some undesirable properties. Curve "B" shows a material with low elasticity but a moderate elongation at fracture; this is typical of a "soft and tough" material. The material may be expected to exhibit large areas of contact and hence high friction. The "soft and weak" material relating to Curve "C" [138] could be the worst of all showing low elasticity as well as low elongation before fracturing. This would mean large real areas of contact and many wear particles being liberated. Curve "D" shows a material with high elasticity and may be described as being "hard and strong", [138], but it exhibits low elongation and could result in many

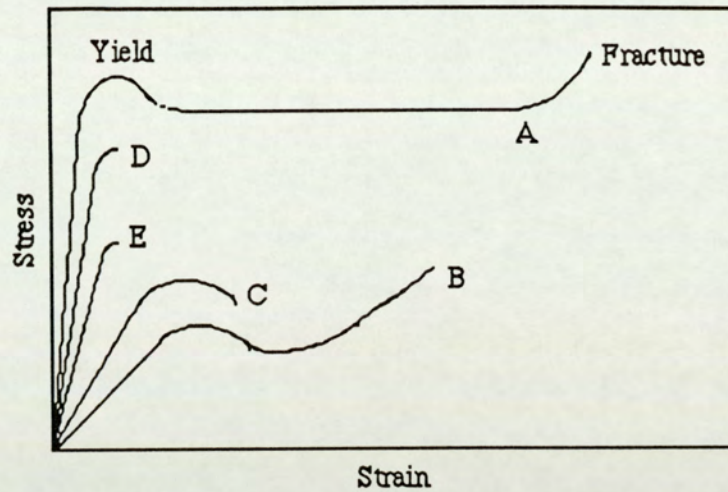


Figure 7.1 The curve "A" shows that the desired material would show elastic deformation even for relatively large stresses as well as having a high elongation strain before it fractures.

wear particles being produced. The Curve "E" exemplifies a "hard and brittle" material [138] which is undesirable because it shows low yield stress and fracture stress.

These general considerations may be applied to all of the rigs but there are some factors which are important in the drives alone.

One important factor to consider in studying durability of media in the drives is the fact that several different drives have been used to study the media. In doing so the drive-to-drive variation must be considered. Probably the most important factor in this drive-to-drive variation is the finite differences in the alignment of the head carriage assemblies. Clearly, in the ideal system, these would all be aligned such that the flat of the side 0 head is horizontal, as illustrated in Fig. 2.9. However, it is likely that these will, in fact, be at some small angle to the horizontal. This tilt can be either in the diskette's radial

direction or perpendicular to this direction. More likely, it is more complex with a contribution in both directions to varying degrees. In order to determine the effect of such tilts, the relatively simple case of a tilt perpendicular to the radial direction can be examined. This is illustrated in Fig. 7.2 where the tilts are shown exaggerated.

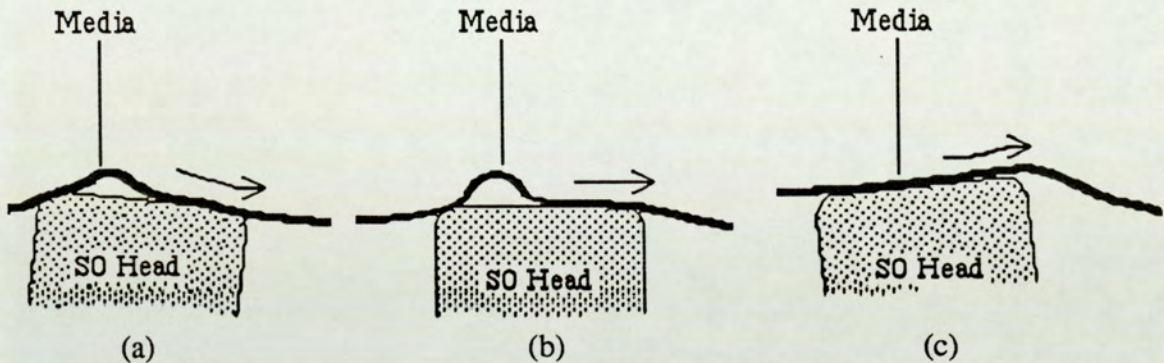


Figure 7.2 The effect of side 0 head tilt (a) negative gradient, (b) ideal orientation and (c) positive gradient.

In the case of the negative tilt of Fig. 7.2 (a), the leading edge of the head is higher than the trailing edge. In this condition the head could cause excessive ploughing wear of the media as its edge cuts into the moving diskette. Wear by the trailing edge could be caused in a similar fashion by a positive tilt but it could also affect the formation of the side 0 bubble resulting in increased wear through an increase in the head-media contact.

7.1.1.2 In-situ Friction Tester.

The friction testing apparatus data shows that friction is fundamentally related to wear in magnetic media. The sudden rise in the friction as a scar is formed shows how friction indicates wear of the media. The durability ranking of media in respect of burnish time is consistent with that found in the drives. What this

implies is that it is immaterial whether real wear, in the material removal sense, or a visible scar is taken as the criterion for terminating tests. The durability ranking produced would be the same. This is because the drives tend to produce wear scars showing mainly surface plastic flow; other rigs, including the friction tester, tend to produce real wear but the durability ranking is still the same. The connection between friction and wear may be more closely examined.

There are believed to be two separate mechanisms responsible for the rise in friction at the onset of wear. One is the increase in the real area of contact caused by plastic flow of the polymer surface. The second is the ploughing mechanism discussed in Chapter 3. The first mechanism results in higher friction because the frictional force is directly proportional to the real area of contact. In the second case, the extra work done in causing plastic flow of the material, either due to ploughing deformation or wear, is done by the force translating the head across the media. This extra resistance to the motion is seen in the form of an increase in the force of friction. The friction is different, however, for the two heads.

It can be seen that the friction force at the side 0 head is consistently higher than that at the side 1 head. This may arise from the media being forced against the trailing edge of the side 0 head by the side 1 head, as seen in Fig. 2.9.

Furthermore, the flexing in the media required to form the side 0 bubble is caused by the side 0 head as it is responsible for deflecting the diskette upwards [60]. The work done in causing this deflection is reflected in the friction force measured at the side 0 head-media interface. Another reason may be the removal of boundary lubricant by scraping at the leading edge of the side 0 head as described by Skelcher [60]; no such effect is considered to occur at the side 1 head.

The friction at both heads seems to show an apparently curious effect. This has been observed on the friction tester apparatus and can be seen from the

friction data graphs of Fig. 6.8. These graphs show a fall in the initial force of friction with increase in burnish time. Durability is not seen to behave in such a linear manner with increases in burnish time, as may be observed from the data in the preceding chapter. This apparently anomalous and contradictory effect is particularly pronounced for the side 0 head-media interface. It would be expected that the smoother, that is more burnished, media should produce higher friction as a result of the increased real area of contact. However, the initial friction measured, in fact, shows a fall. This result may provide circumstantial evidence for the earlier assertion that burnishing of media can provide a relatively hard surface. The consequence of this is less plastic flow of the asperities and the observed resultant trend in the friction. Burnishing is thus beneficial for the less burnished samples as the durability data from the drives and the rigs shows. However, the most burnished samples exhibit a reduced durability because burnishing tends to initiate the process of wear. This happens through the micro-abrasion and possibly also through the creation of a polymer-rich surface region, as discussed above. This process is then continued when these diskettes are tested producing less reliable media. This explains why the initial force of friction is less for the most burnished media; it rises rapidly as the wear processes initiated during burnishing are resumed.

Similar effects occur in the tests performed on the rigs as is discussed now starting with the supported sample simulation rig.

7.1.1.3 Supported sample simulation rig.

The durability ranking with respect to the burnish time is also repeated with this rig. However, the durability of every sample is considerably reduced. One observation to note which may indicate why this is so, is the friction force

measured during the durability tests. The increased friction force is a reflection of higher stresses in the media surface and consequently more rapid wear. The reason for the friction is most likely the larger area of contact between the side 1 head used and the media. This is because the head sits flat on the media when used on this rig. This compares with the very much smaller area of contact found in the drives as illustrated in Fig. 2.9 of Chapter 2. As shown in that figure, the side 1 head inside a drive makes contact at the apex of the side 0 bubble and at the trailing edge of this head. In the case of the present rig, the head sits flat on the media and considerably greater contact results. Moreover, the media cannot flex in any direction, particularly the circumferential direction. This means that the media can be expected to experience much greater stresses as it passes below the head. This increased stressing manifests itself in the form of a rise in frictional force. A similarly higher friction is seen in the data gained from the unsupported sample simulation rig.

7.1.1.4 Unsupported sample simulation rig.

Similar arguments may be used for this rig as have been presented for the supported sample rig above. It shows consistency in durability ranking with the other apparatus. It also shows consistency with the in-situ friction tester in the trends shown for the friction forces measured. Although the two simulation rigs have loosely been compared to the side 0 and side 1 head-media interfaces in the drives, the comparisons are not completely valid. Indeed, this was not the primary purpose of these rigs as explained earlier in Chapter 4. However, the friction trends showing broad consistency with the in-situ friction measurements indicates some similarities between the simulation rigs and the side 0 and side 1 interfaces. Careful inspection of the data, however, does reveal some inconsistencies. It can be seen from this data that the durability of the media

samples is greater on the unsupported sample rig than on the supported sample rig. This is despite the fact that friction is found to be higher for the unsupported sample; the in-situ work shows higher friction on side 0 which also shows surface damage first. The reason for this is that it is very probable that the higher friction is not due to an increased real area of contact (as in the friction tester) on the unsupported sample rig. It is more likely to be a consequence of hysteresis losses due to the sample flexing away from the side 0, head which is used. Energy is expended in the same way as described in an earlier chapter for the in-situ work where the flexing component also exists. This means that the area of contact is relatively small and, with the side 1 head absent on the present rig, the media is not forced onto the trailing edge. This prevents high stresses in the media at the trailing edge thereby leading to increased durability. The increased friction here is due mainly to the work done in flexing of the media.

Clearly, the burnish time experienced by the media is important in the friction and durability of the media. Equally important is the effectiveness of the lubrication which can help to reduce stresses at the head-media interface and thus reduce friction and wear. The details concerning lubrication are discussed in the following sub-section.

7.1.2 Durability: The Effect of Lubrication.

In this sub-section the effect of lubrication on the durability of the media is to be discussed. This is an important aspect as the data shows that the different stock rolls, representing different lubrication conditions, show greatly varying durability. It is important to note that the lubrication conditions have a fundamental effect on the media durability because they can change the nature of the head-media interface. This has been illustrated by the fact that all media samples show a similar dependence on burnish time. The shape of the curves of durability versus burnish time presented in Chapter 6 is such that they indicate an

optimum burnish time. This optimum appears to be independent of the lubrication state of the tested sample. However, although the general shape of the curve is consistently reproduced, the differently lubricated samples show a large difference in the actual durability. This latter difference is due to their different lubrication conditions.

7.1.2.1 Unlubricated Media: SR2 Samples.

All of the data, regardless of the rig used for testing, shows that the unlubricated media exhibits very low durability. This means that the lubricants are essential for the production of reliable floppy diskette media. However, there are two lubricants used, a surface and a bulk lubricant. Of these it is necessary to establish which of these lubricants is the most effective and whether both are necessary. Each of the lubricant samples has been discussed below.

7.1.2.2 Surface Only Lubricated: SR1 Samples.

The SR1 samples are lubricated only with the surface lubricant. This lubricant is a mixture of Oleic acid and Hexadecyl stearate as described in Chapter 6; the molecular structures of these are illustrated in Fig. 6.1. It can be seen from the data presented in that chapter, that these samples consistently show a high durability regardless of the rigs used for testing.

The desired effect of a lubricant is to cause separation of the mating surfaces and thereby reduce friction and wear. The lubrication regime concerning floppy diskette media is considered to be in the boundary and mixed lubrication regimes described by the Stribeck Curve [59] as discussed in Chapter 3 and by Skelcher [60]. Under these regimes the lubricant is likely to produce quite effective separation of the two surfaces. This would be expected to result

in reduced stresses on the media asperities thus leading to a reduction in plastic deformation and in the local heating effects. This reduced plastic deformation can in turn prevent gross increases in the real area of contact, which leads to wear through increased stresses and which is manifested as higher friction. The reduced stressing of the media asperities can be expected to be achieved because the surface lubricant distributes the loading of the head over a larger area. How this occurs is illustrated in Fig. 7.3 below.

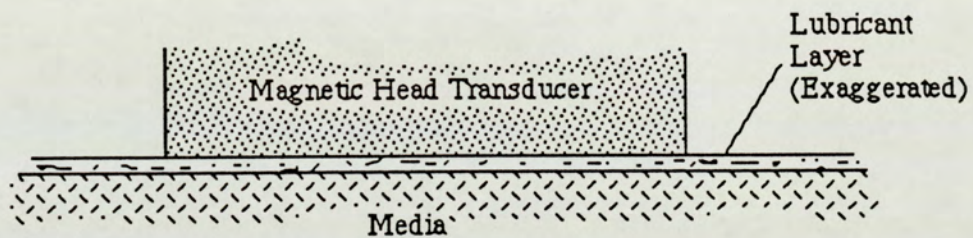


Figure 7.3. The surface lubricant reduces wear by separating the transducer and the media as well as distributing the loading of the head.

Another effect of the surface lubricant is to shear and/or flow itself under the translational stresses imposed by the head. This reduces further the stresses imposed on the media asperities. Load sharing is effected in another way according to Skelcher [139]. He has reported that the surface lubricant can lead to the increased exposure of the Head Cleaning Agent, Al_2O_3 . This then enables the Al_2O_3 particles to be more effective in their second function, that of load bearing. As this reduces the stresses on the relatively soft polymeric binder, the consequence is to improve the durability of the media. Skelcher [139] has not discussed the mechanism by which the effect occurs and no other discussion of the effect has been found in literature. However, his observations do imply that the surface lubricant should be very beneficial, as has been found here.

One other important consequence of the surface lubricant shearing rather than the asperities is that less energy would probably need to be input. This would result from the fluid lubricant shearing more easily than the asperities of the solid, *albeit* soft, binder polymers. The surface asperities receiving less energy is likely to result in reduced flash temperatures and consequently less softening or melting of the polymeric materials of the binder. It must be stated that, qualitatively, evidence of smoothed areas near wear sites is seen on all samples and that they do still occur, even on the surface lubricated media. These sites have been discussed in an earlier section as probably being caused by melting and resetting. This, however, does not reduce the validity of the present argument concerning the lubricant action in reducing flash temperatures. The reason is that the tested media has all shown the same grade of failure and similar surface damage may be expected as a result; the length of time it takes to produce this damage is the crucial factor which indicates the effectiveness of the lubricants. This effectiveness results in the less frequent formation of hot spots and hence increased durability.

The bulk lubricant is expected to behave in a similar fashion to the surface lubricant when at the head-media interface. It is this appearance at the interface which needs to be considered and is done below.

7.1.2.3 Bulk Only Lubricated: SR4 Samples.

These samples contain only Oleic acid as the bulk lubricant. This is absorbed into the body of the magnetic layer. The way in which the bulk lubricant is perceived to act is two-fold:

- (a) The first effect of the bulk lubricant is surmised from Chambers [75] to be to migrate to the surface of the media whenever and wherever the latter is stressed through the head(s) being loaded onto it. This may be likened to the reaction of a sponge full of liquid. The exuded lubricant then acts in the same fashion as the surface lubricant to produce a protective film and thus preventing damage at the head-media interface.
- (b) The second way in which it should act is to be gradually "revealed" as the surface of the media is successively worn away. Some depth profiles of this have been performed on both VHS video tape [140] and on floppy diskette media [75] by Chambers for 3M. The desired effect here is to prevent the starvation of the head-media interface from a lubricating polymer so that wear does not progress suddenly at a catastrophic rate if the lubricating substances at the surface are removed with the erosion of this top surface. The prevention of a lubricant starved interface is clearly important as mentioned above with regard to the unlubricated samples SR2.

The bulk lubricant also has a secondary effect. This effect is due to its behaviour as a plasticiser. This could either be beneficial or destructive depending on the details of the interaction and its effects. Details of this are discussed in the section concerning the mechanisms of wear later, but it can be mentioned here that the two apparently opposite effects may be understood provided the mechanisms of wear are also understood. These mechanisms are discussed in a later section.

Looking now at the data from all of the rigs presented in Chapter 6, it is clear that the SR4 samples, which contain only the bulk lubricant, show only a very marginal improvement in durability compared to the unlubricated samples, SR2. It would appear, then, that either one or both of the above two effects do

not take place at the point where head and media form a contact. In view of Chambers' work [75], it is highly likely that it is the effect described in (a) that is not being seen here. It is quite possible that the rate of migration of the lubricant being used in this case is too low under the head loading stresses commonly used in the drives (0.2 N). Also, the rate of cyclical stressing of the media, which is 5 rev.sec⁻¹, may mean that it is not stressed for long enough at any particular point to allow migration of the lubricant to the surface. This may or may not be cured by the use of some other substance as the bulk lubricant. It is possible that the rate of revolution is too high to permit the use of large molecular chains for the bulk lubricant. This, however, suggests the use of a lighter, and presumably more mobile, molecule but these would be expected to have a higher volatility and consequent loss at the surface. A reduction in volatility may be achieved by adding polar groups to the chain but this would be very likely to defeat the original objective as it would reduce mobility through electrostatic dipole-dipole interactions between the lubricant molecules themselves and the polar groups present in the binder's co-polymer. This co-polymer consists of a polyester-polyurethane structure (see Figs. 2.4 and 2.5 in Chapter 2) and, therefore, contains many such polar groups. In addition to this, it can be expected that migration of fluid lubricant in the fashion of a sponge would be difficult in the matrix of such a highly filled system as a diskette's magnetic layer.

The contribution of the bulk lubricant in the combined effect of the two lubricants does not appear to be very large. The effectiveness of fully lubricating the media is to be discussed next.

7.1.2.4 Fully Lubricated Media: SR3 Samples.

These samples most closely resemble the media produced for commercial use and contain both the bulk and surface lubricants. The durability of these samples is high. The presence of both lubricants does not, however, appear to give these

samples a very much greater durability than the SR1 samples which contain only the surface lubricant. Some extension in the lifetime can be seen with the use of both lubricants compared to the SR1 samples discussed above. This, together with the data from the bulk only lubricated and unlubricated samples, indicates that the bulk lubricant has some effect in increasing the useful commercial life of the media. This synergetic effect appears to be only a small one, however, and most change can be seen in the data taken from the durability tests in the drives. The data from the simulation rigs shows very much less difference between the SR1 and SR3 media. The data from the drives may be complicated by the effects of transferred layers from previous samples as discussed in the preceding chapter. As also discussed there, the effects of these transferred layers are likely to be less on the rigs for reasons concerning the lengths of the tests.

Although in all of these cases the samples with similar burnish times should be compared, the general shape of the durability curve in each case is so similar to the others that a detailed comparison becomes unnecessary. A comparison of the time units used for the co-ordinate axis reveals the difference in durability.

The durability of the media in terms of superficial damage considerations is important from the customer's point of view. It is clear from earlier discussion, however, that the ranking of durability that this criterion produces is consistent with that produced by looking for real wear. Clearly this wear needs to be reduced if better media is to be produced. In this regard, the mechanisms of wear must be considered.

7.2 Mechanisms of Wear.

In order to enable the production of better media, it is important to establish the

means by which the surface appearance of the media becomes altered. This is important because it is the criterion expected to be applied by the consumer. The results of the durability investigation concern this criterion and have been discussed above in this context. In the longer term, however, wear of the media surface is the more important aspect. This is so because it involves the removal of material which carries the magnetic signal. Wear of the media has been discussed in this section and conclusions drawn from the features seen on the surface of worn media samples.

Two types of wear have been considered in literature for floppy diskettes. Green [63] has described these as "tapping" and "abrasive" wear. In the former, the read/write heads are loaded onto and unloaded off the media. The same spot on the media is affected as the media is not rotated while the heads repeatedly make and break contact with its surface. This mode of wear is not important for this study as the drives used do not have the capability of automatically loading and unloading the heads. This is usually done by electro-mechanical means when the drive is accessed in drive units which possess this feature. Even in these drives the loading and unloading occurs at different points in normal use and the test is arguably unrealistic. The process of abrasive wear is much more important as it can occur in any drive unit. Its importance comes more from what leads to it rather than the abrasive wear process itself. Green [63] considers the abrasive wear of media by the heads but this is not considered important until the heads are damaged. When this happens, abrasion by the heads becomes the dominating factor. However, three-body abrasive wear is considered to be of fundamental importance. This mechanism is illustrated in Fig. 7.4.

The key point to note is that the third body is often likely to be a particle which is a result of wear. It is this source of third body particles which is very important as it implies that wear has already taken place at this stage by a different

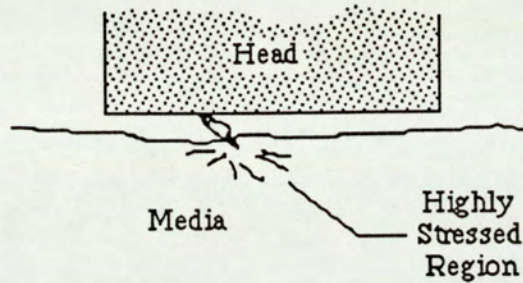


Figure 7.4. The three body interaction which is of primary importance.

mechanism. In order to discover the nature of this mechanism, the surface wear features shown in the micrographs of Chapter 6 need to be studied (Fig. 6.19 to Fig. 6.26). It is clear from these micrographs that where materials have been removed, the edges of the adjacent material are raised. The micrographs of the samples tested on the simulation rigs particularly show these features (Figs. 6.25 and 6.26). Also, the debris described in Chapter 6 has a distinctive shape, it is laminar in nature (Figs. 6.22, 6.23 and 6.27). The first observation indicates that a mechanism involving sub-surface failure leads to the initial production of wear particles. The second, the particle's shape, indicates that delamination is probably the initial cause of wear. The Suh theory of delamination wear has been described, as applied to metallic wear for which it was originally proposed, in the literature survey of Chapter 3. It was also mentioned that some of the conditions described in that theory also exist in magnetic media. One such aspect is the existence of hard objects in the sub-surface region.

Delamination wear in metals may involve these hard phases. These phases often cause the pinning of dislocations at some form of defect in the crystalline lattice. Plastic flow around the hard phases then initiates sub-surface crack formation. These cracks are then caused to grow in the sub-surface region by cyclical stressing. Eventually the cracks are so long that the material in

contact with the bulk can no longer withstand the stresses imposed by the second body. This weakly bonded material then yields to liberate the material above the crack forming a laminar wear particle. In polymers, particularly the present highly filled type, the picture is slightly different.

In these polymeric materials crystallinity in the metallic sense does not exist. In the case of the magnetic media's top, active, layer the place of metallic defects has been taken by the hard particles naturally, and necessarily, included in the binder matrix. Before looking at how delamination may occur in this situation, the included particles may be studied.

There are three suitable candidates. One of these, (b) below, is a weak one. Nevertheless, it deserves to be mentioned because it possibly contributes, *albeit* only to a very small degree compared to (a) and (c) in causing wear:

- (a) The most likely sites for crack nucleation are the most essential part of the magnetic layer, the magnetic particles of $\gamma\text{-Fe}_2\text{O}_3$ themselves. These are quite small (approximately $0.1\ \mu\text{m}$ cross-sectional diameter \times $0.5\ \mu\text{m}$ long) and, probably more significantly, have an acicular shape. This would make them ideal sites for the nucleation of sub-surface micro - cracks as the soft phase of the binder's co-polymer can easily flow around them if forced to do so by the force of the head causing plastic flow of the material on the surface. The crack nucleation is especially likely to occur at the sharp tips of these particles which are readily available in the binder.
- (b) The Head Cleaning Agent's particles (Al_2O_3 particles) provide possible sites where sub-surface cracks may be initiated but these cannot be considered to be the primary source of sites as they have a diameter approximately equal to the thickness of the whole of the magnetic layer and so are probably too large for micro cracks to form around them to any great extent and, as mentioned in the preceding section, their load

bearing action is probably extremely beneficial and far outweighs the damage that they may cause.

- (c) The hard phase of the co-polymer forming the top layer exists within the soft phase. This is the crystalline region intended to give the magnetic layer some rigidity and to prevent the easy plastic flow of this layer which could otherwise occur readily under the stress imposed by the head. These sites are quite possibly one of the regions that lead to the initiation of the sub-surface cracking which eventually results in the delaminative wear of the media.

To look more closely at this delaminative wear process, the sub-surface crack nucleation and propagation needs to be considered.

The basic process starts with plastic flow of the surface asperities. This results in the production of a smoothed surface. This plastic flow is aided by heating of the surface and consequent more rapid flow due to polymer softening and melting. For small area asperity contact, dissipation of heat to the bulk is through this small mutual area. Thus large temperatures can be developed; Bowden and Tabor [141] estimate temperatures of 500°C for non-conducting materials. These localised "hot spot" temperatures are limited by the lowest melting point of the mating non-conducting bodies. In this case that material is the binder of the magnetic layer. As softening and/or melting of the polymer occurs, the greatly increased plastic flow increases the real area of contact causing greater friction and transfer of the polymer towards the surface. This transfer of polymer to the surface leaves the upper layer polymer rich. This polymer rich layer and the relatively particle rich layer below have an effective discontinuity between them. This discontinuity can be compared to that formed in metallic delamination where the same is produced due to dislocation pinning. It is at this discontinuity that crack nucleation can occur due to concentration of the stresses

imposed by the head. The whole process is helped by the presence of the acicular magnetic particles which provide further nucleation sites. The stresses at the tips of the hard $\gamma\text{-Fe}_2\text{O}_3$ particles due to the frictional drag at the surface can be very high. This is a result of their acicular shape and sharp ends. As material is forced against these ends, it can be caused to shear. This is crack nucleation under these conditions. Cyclical stressing then provides for further cracks and growth of existing ones. The way in which this proceeds may be understood if an asperity is considered to move over the media surface from left to right as shown in Fig. 7.5 below.

In the shaded region of Fig. 7.5 (a) compression of the leading edge of

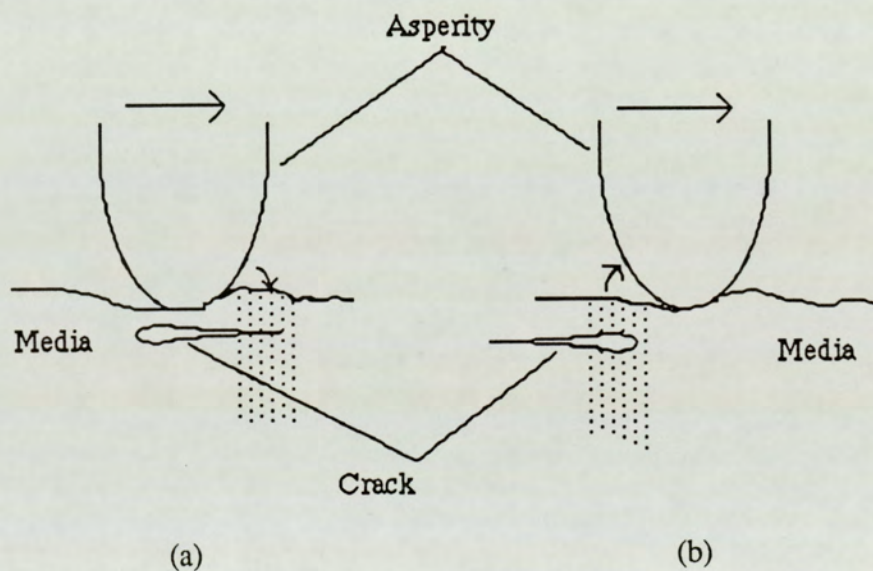


Figure 7.5. Method of sub-surface crack propagation: (a) compression of the leading tip of the crack, and (b) tensioning of the same region.

the crack occurs. This does not produce an extension of the crack. In the same region tension is applied after the deforming asperity has passed over and beyond the crack's leading edge. The stress then experienced by the leading edge of the crack pulls the two surfaces of the crack apart causing it to be elongated. The

greatest stress is experienced at the tip of the crack as determined by the stress field around features such as cracks. This determined is by the commonly recognised "stress intensity factor" which was also mentioned briefly in Chapter 3 where delamination wear of metals was considered. As discussed there, the value of this factor, K , falls as $1/r$ where r is the distance from the tip of the crack.

Considering a crack parallel to the surface under tensile stress perpendicular to that surface, the stress intensity factor is given by

$$K = \sigma \sqrt{(\pi \cdot a)} \quad (7.2.1)$$

Where σ = tensile stress perpendicular to the surface

a = width of crack parallel to the surface but perpendicular to its length (and direction of growth)

The smoothed area formed by plastic flow discussed above results in higher friction due to an increased real area of contact. Clearly, higher friction is likely to imply an increase in the applied tensile stress, σ . This produces an increase in the propagation speeds of nucleated cracks as well as the rate of crack nucleation in the polymer rich layer at the surface.

The cyclical stressing produced by the head eventually leads to the formation of wear particles by delamination. These then become trapped between the head and media and produce three-body abrasive wear as illustrated in Fig. 7.4 by high stress concentration. This abrasive ploughing wear results in the production of further wear particles. The process is thus accelerated and becomes an avalanche with three-body wear dominating and rapid deterioration of the surface occurs.

Another aspect of ploughing wear is through the action of the edges of

the heads. This type of wear has been particularly noticeable in the bit analysis tests. Here it has been found that the data errors only occur after much of the magnetic layer has been removed. In fact, all of the layer is removed at the edges of the wear track by the action of the heads. Obviously this is an important contribution to wear but it is not noticeable until the ploughing wear involving a three-body action has produced catastrophic failure at the other parts of the wear track.

Looking a little more closely at the stresses in the sub-surface region, the stress fields produced may be considered. A qualitative consideration of the stress fields produced in the compressed and tensioned regions illustrated in Fig. 7.5 leads to a conclusion briefly mentioned in Chapter 3. This arises because the combination of the two stresses will determine the depth of the polymer rich layer. It will thus determine the depth at which crack nucleation and propagation rates are maximised. This maximisation occurs because the two stress fields, compressive and tensile, combine to produce a maximum stress somewhere in the sub-surface region. Since the size of both of these fields is dependent on the frictional force, friction is likely to determine the depth at which their combined result is maximum. As the friction rises this depth will increase; conversely if the friction is reduced, then this depth will decrease. It can thus be concluded that the higher friction forces will produce thicker wear particles and consequently mean lower media durability. It is important, therefore, to reduce friction. The reduction of friction is also considered important by other researchers [36],[83].

This fact that frictional forces appear to exert a definite influence in the wear of floppy diskette media is also borne out by the micrographs of the samples which show apparent smoothed areas preceding areas of wear, such as those of Figs. 6.20, 6.21, 6.25 and 6.26 presented in Chapter 6. The smoothed areas are probably produced by local melting and subsequent resetting as the smooth head moves over the media.

The tribological interface of floppy diskettes with the magnetic transducer has not been studied to any great degree in a systematic manner. Of course, in any interacting system such as this the friction and wear are important. It would appear in this case that, unlike the majority of situations encountered in tribology, the two phenomena are closely related in the case of floppy diskettes. In fact, this is probably true for all flexible magnetic media, as has been indicated earlier in Chapter 3. For example, cyclical stressing is often also produced in paused video tape scanned by rotating R/W heads and similar effects may be observed in that case.

The data obtained on the two simulation rigs and the friction tester has shown that the frictional force rises consistently for all samples as the test progresses. This is as is to be expected in light of the way in which the surface of the media is thought to be affected by the head: plastic flow of the surface asperities causes smoothing of this surface creating an interface with increased real area of contact. It may be argued that the classical effects occur here. These are described in texts such as the one by Johnson [107]. The effects to note are, in summarised form, that the rougher surface tends to produce a situation whereby intense stresses are present at the tips of the asperities but these do not penetrate into the bulk of the material. In smoother surface interfaces, the real area of contact causes these stresses to be spread out through out the bulk of the material below this increased area of contact leading to a reduction in the intensity of the surface stresses. Without further consideration this may be expected to imply that the smoother surface interface should produce less wear as less stress would mean a reduction in the rate of sub-surface void formation and the rate of crack propagation. This may be true for these conditions prevailing in metal-metal contacts as are considered by Johnson [107]. However, in the present situation the abrader, in the form of the hard ceramic/ferrite structure of the read/write head, is very much harder than the polymer of the magnetic media. In

this situation, it can be expected that the extremely high stresses experienced by the large asperities causes their plastic deformation through temperature and mechanical effects. This results in the production of a large real area of contact. But, since this larger real area of contact is still between a very hard and a much softer material, even the smaller stress present on the smoother polymer will cause failure to occur in the magnetic media's surface layers. Some evidence of this relationship between the frictional force at the head-media interface and wear has been presented by Cummings [36] for various samples. He has shown that higher friction leads to lower resistance to wear. These observations have been confirmed by the work performed on the supported sample, unsupported sample and in-situ friction testing apparatus.

In conclusion of this sub-section, it may be said that evidence for all stages of the delamination process have been observed. These range from the initial surface smoothing to the lifted lamina and the delaminated particles. These been observed and photographed on the media surface after testing. The holes left after delamination have also been similarly observed and have all been presented in the micrographs of the samples in Chapter 6. The evidence for delaminative wear is, therefore, substantial. It is firmly believed now that this is the initial mechanism involved in the wear of floppy diskette media. The wear particles thus produced subsequently cause three-body abrasive wear through high localised stressing as illustrated earlier in Fig. 7.4. The ploughing out of material by this action causes the media to fail very rapidly from this point. Very rapid catastrophic failure results due to the creation of new wear particles and their own three body action.

In order to reduce both the initial delamination and subsequent ploughing wear, lubrication may be used. The action of lubricants is discussed now in the following sub-section.

7.2.1 Effect of Lubrication on Wear.

It is worth noting again that the surface lubricant has a profoundly beneficial effect on the media whereas the bulk lubricant does not appear to improve it very much. The effect on the media which has been discussed so far has involved consideration of the formation of only superficial scars. However, it could be expected that this may also extend into the domain of wear. The present subsection considers these effects.

7.2.1.1 The Surface Lubricant.

As discussed earlier, the surface lubricant can be expected to act as a load distribution agent. This means that no particular part of the media surface is left very much more stressed than another part. Also, the reduction in friction provided by the lubricant would be expected to reduce the depth at which sub-surface stresses are maximised as described earlier. Temperature effects would be expected to be reduced producing less plastic flow as the lubricant aids in the dissipation of heat. The production of a more elastic surface could be very beneficial here [83], [91] as the stresses applied would cause less plastic deformation (see the suggestions for further work in the next chapter). The real area of contact would be increased more slowly leading to increased durability. Although the more elastic surface may not combat the effects of hot spots, the lubricant applied to the surface could help in dissipating heat [141]. The desired result of lubrication and an elastic surface would be to reduce the sub-surface damage and thus to reduce delamination wear. However, some delamination will still occur. These wear particles can then act as third body abrasive wear agents as shown in Fig. 7.4 earlier. The presence of the surface lubricant, however, can be expected to reduce this type of wear also. This may be achieved by the

distribution of these higher stresses in the same fashion as for the much lower usual stresses. Some evidence of this has been seen in that "micro-scratches" have been seen on the surface of fully lubricated media. An illustration of this is the shown in micrograph of Fig. 7.6 where such a micro-scratch can be seen behind the foreign particle on the surface.

This result is seen because the media sample has most of the stresses imposed via the surface lubricant but a slight increase is seen in the contact region of the third body. This is illustrated in Fig. 7.7 below.

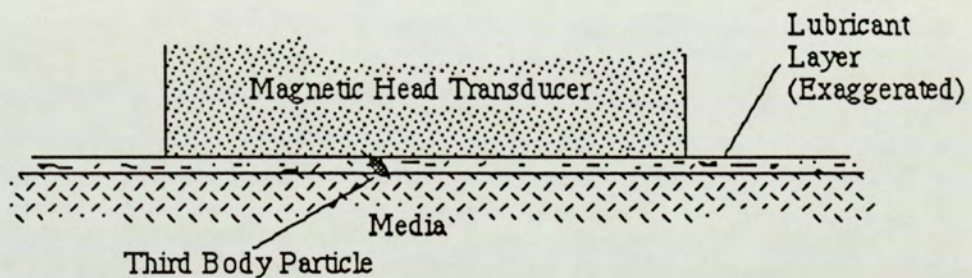
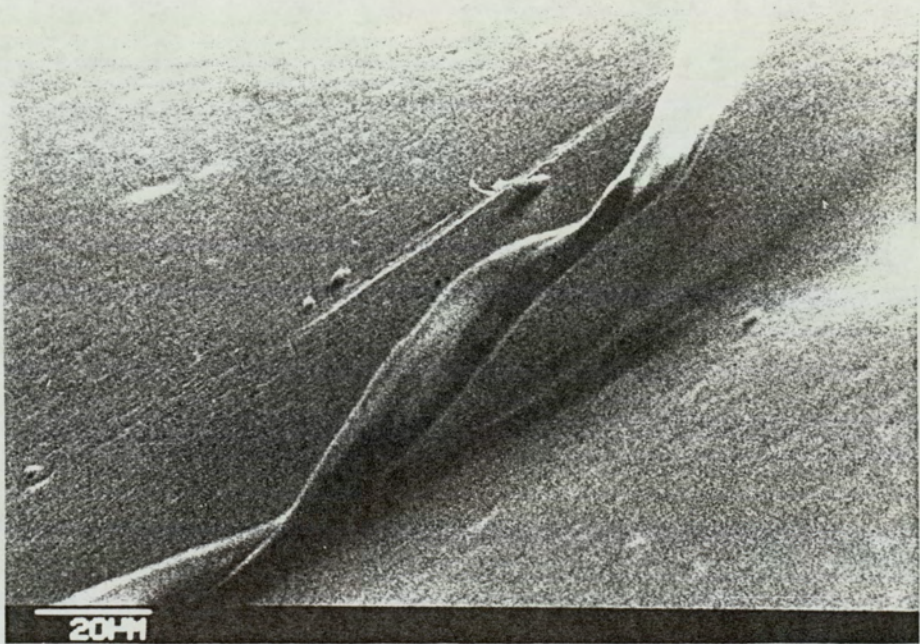


Figure 7.7 The protection afforded by the surface lubricant from a third-body ploughing wear action.

It would be wrong to assume that the surface lubricant is a fluid which is free on the surface as may be implied by the schematic diagram of Fig. 7.7 showing an exaggerated layer. There is a combination of physisorption and chemisorption of the lubricant onto the surface. Some of it undoubtedly migrates into the sub-surface region. However, as long as sufficient is available on the surface it will act. This action is in the reduction of friction by acting as a boundary layer which helps in the reduction of localised surface stressing. It is because of this boundary action that the surface lubricant is considered to be most effective. The bulk lubricant cannot produce this action and thus appears relatively ineffective. By the time that the bulk lubricant has migrated to the surface to produce this action, the damage is expected to have been done. The

Figure 7.6 Micro-scratch caused on the surface of a fully lubricated media probably by a three body action.



bulk lubricant may have other useful features, however, and it is discussed below for this reason.

7.2.1.2 The Bulk Lubricant.

The purpose of the bulk lubricant has been discussed earlier. It is supposed to act in two ways: to migrate to stressed areas of the surface and to prevent lubricant free head-media interfaces as the top layers of the media surface become worn away. Its effect as a plasticiser has also been mentioned and may have one of two opposing effects. The destructive effect could be to make the whole of the magnetic layer prone to much easier plastic flow, under lower stresses, leading to easy destruction of the resulting soft layer. This may occur through larger stresses with high friction and could be caused by larger real areas of contact. The opposite result, that is increased durability, including less wear, may be realised if the plasticising effect was to reduce the number of "hard" sites in the magnetic layer's co-polymer. This would result in fewer sites for wear initiation, in the form of crack nucleation sites, being present. Alternatively, this sub-surface flow could close the nucleated voids. It may, however, be argued that the acicular magnetic particles provide far more such sites in the highly filled polymer than does the hard phase of the co-polymer and so the reduction in the sites is minimal with this plasticising effect.

Another effect of the bulk lubricant could be to migrate within the sub-surface region and to fill any "voids" which form after crack nucleation. It could then act in two ways. The stresses imposed by the head translating over the media could be absorbed by the bulk lubricant or concentrated at the crack tip. In the first case, it would reduce wear and in the latter case it would increase wear. It is interesting to note that this would occur in the compressed part of the media illustrated in Fig. 7.5. However, neither effect appears to be occurring in the

present media. This can be seen by comparing the data for the samples with and those samples without bulk lubrication. No definite effect can be seen as the durabilities for both sets are similar; no effects of this nature have been reported in the literature but may prove to be an interesting investigation.

7.3 Justification of the Simulation Rigs.

One of the aims of this project was to consider whether it was reasonable to use the two simulation rigs as accelerated testing rigs for fast and reliable testing of the media. In order to make a definite decision, there are certain points to consider.

The first of these is whether the methods of wear remain the same under these drastically different circumstances: the removal of certain parameters, the absence of the jacket and hence the liner, the loading of the head onto the media, etc. Quite clearly, if these two methods (rigs and drives) exhibit different mechanisms of wear, then the data from the drives is the more useful since it represents the "real" tribological interface encountered by the media in its normal use. In discussion of this point, it is necessary to recall the original consideration that the side 1 head in a drive causes wear without flexing whereas the side 0 head was thought to cause flexing of the media and thus possibly causing fatigue failure (akin to repeated bending of a wire) through the creation of the side 0 "bubble" illustrated in Fig. 2.9. It has been proposed that the wear on both sides is, in fact, caused by a micro-fatigue process leading to delamination and the flexing of the sample would not contribute in any significant way. This is borne out by the fact that the wear scars are similar no matter where the sample has been tested. This implies that the use of the simulation rigs is quite justified in view of the fact that they produce surface features after testing which are similar to those seen in the drives. Moreover, it is further justified considering the observation

that the rigs tend to produce a worn sample faster than the drives. This is probably due to the increased friction detected on these rigs and reported in Chapter 6. Arguments relating to the increased depths of crack nucleation and thick wear particle production discussed earlier apply here. Thus, genuine accelerated wear is produced by the rigs as is required. This is illustrated by the comparison of the durability data for the two simulation rigs and the in-situ data from the drives as presented in Chapter 6 and discussed there and earlier in this chapter.

7.4 Effect of Head Wear on Media.

The effect of the damage to the heads themselves by, for example, the head cleaning agent in the media binder has been considered to a small extent and it has been found that certain parts of the head tend to wear more than others; some examples can be seen in the Figs. 6.28 to 6.31. This work was prompted by the work done by Blevins et al [33] and Skelcher [139]. Their work appears to show that the side 1 and side 0 heads wear at different relative points. This is, perhaps, to be expected in light of the way in which the head-media interface is different for both heads with the formation of the side 0 bubble.

The work carried out here was of a provisional nature and a fuller investigation has been presented by Blevins et al [33] but further work on this can be strongly recommended. The effects of transferred lubricant layers may also be investigated in this regard. The transfer of "friction polymers" from the binder also need to be considered. A method of detecting the molecular nature of the materials transferred to the head must be developed. Fluorine tagging of molecules may be useful.

The preferential wear of certain parts of the heads due to material discontinuities may be reduced by removing such discontinuities. Green [63]

has suggested the use of Mn-Zn ferrite for the magnetic read/write core and non-magnetic Zn ferrite for the support structure. These materials are similar and may allow better heads to be produced.

In concluding this chapter, it merely needs to be said that the implications of the trends seen in the data presented in Chapter 6 have been considered. This has led to a detailed explanation of the surface wear features and the proposition of a mechanism of wear. The fundamental effect of the lubricants on the durability and wear of the media have also been explained.

Chapter 8
Conclusions
and
Recommendations

Chapter 8.

Conclusions and recommendations.

Introduction.

In this final chapter, the conclusions to be drawn from the above work are presented. Also the relation of these conclusions to the aims set out at the beginning are considered. Some recommendations are offered as a conclusion of these observations. Finally, suggestions for the work that is envisaged as necessary at this stage to further confirm the observations made or which may improve the quality of the data obtained have been made.

8.1 Conclusions.

8.1.1 Media.

The data has been split into two separate categories, burnishing time and lubrication as these clearly have their individual effects. For this reason it is beneficial to consider the two parts separately here.

(a) Lubrication: The surface lubricant, or top coat, appears to be very beneficial in increasing the lifetime of floppy diskette media whether the criterion used is that of wear or that of superficial surface damage. Clearly the surface lubricant must be used in any media for it to be usable.

It would appear from the present work that the bulk lubricant used in diskette media is of only limited use in increasing the durability of the media in terms of the apparent superficial damage. Furthermore, it does not appear to

inhibit real damage. It is possible that different compounds need to be utilised; fatty acid esters may be more effective for reasons of mobility, as discussed earlier. However, it appears from this work that the bulk lubricant alone, at least the oleic acid used here, does not help in any appreciable way to improve the media. Equally, alone it does not appear to have any detrimental effects either. Some improvement is seen in media lubricated with both lubricants compared to surface only lubricated but the effects of transferred layers need to be eliminated by more frequent changing of the heads in order to confirm this.

(b) Burnishing: Clearly the extent of burnishing of the media has an important effect on the durability, particularly when the superficial damage criterion is used. It can be seen that some burnishing of the surface is beneficial but too much tends to cause the media to wear rapidly under test. In fact, it is suspected that the burnishing process, however short the time period, initiates the wear process and leads to the production of defects in the media. From a purely tribological considerations, the media should be produced in rougher form. The reason for this is that this should reduce friction due to a reduced real area of contact. In order to overcome the problem of rapid plastic flow of the large asperities on the rougher surface, a more elastic surface must also be produced [83],[91]. The use of more elastic materials should produce mostly elastic deformation of the asperities and avoid the creation of a smooth scar. The latter requirement can also be expected to effectively reduce the rapid plastic flow of material in the sub-surface region with the effect of reducing void formation and subsequent failure. The main problem, however, with very rough media is magnetic: it tends to produce amplitude modulation of the magnetic signal as the read/write transducer moves towards and away from the surface. This means that some means of smoothing the surface is required. In this case the requirement for a more elastic surface becomes even more critical.

(c) Wear: The observation of features produced on the surface of worn media

show the initial mechanisms of wear to be based on the fatigue processes involved with delamination. All of the evidence appears to show that the surface is damaged consistently in the same fashion and the wear particles are characteristic of this mechanism. This is followed by a three-body action which causes rapid deterioration of the surface.

8.1.2 Rigs.

The first point to note concerning the simulation rigs is that they do provide a genuine method of accelerated media testing. This is possible with some of the parameters removed so the effects of others may be seen more clearly. It is clear from the data that the rigs show durability trends which are similar to those found in the drive. The trends in the friction are also consistent with those produced on the in-situ friction tester. Furthermore, all of these trends are confirmed on the two rigs in a reduced test time. The extra benefit is that these rigs may be used at different rates of rotation to see the effects of relative speed with the confidence that they are producing similar damage to that which may be seen in the drives. There are improvements which may be made, however, and these should be considered before further use.

In particular, both of the simulation rigs would both benefit from the employment of a bearing in which the main shaft could run. The bush used tends to allow runout of the disc used to support the media.

The friction tester needs to be tested for long term tests. In this regard, it would be beneficial to produce a means of easily replacing the heads used which will become worn with long term testing. It would also be useful to produce a rig which could have its heads aligned better than at present, by eye. It is possible that optical methods may be employable. This may also then allow for media to be removed mid-test for examination, if required.

8.2 Recommendations.

The requirement for smooth media for magnetic reasons means that the production of more elastic media is even more necessary. A harder surface would also be beneficial provided it does not prove detrimental to the heads. Probably the best solution is to produce calendered media. This has the effect of creating a smoother surface as required by magnetic considerations but at the same time compresses the media's magnetic layer. This compression tends to pack the magnetic coating and produces a harder surface which can be expected to suffer less plastic flow. Calendering also packs the magnetic particles and produces a better magnetic layer for signal recording and reproduction. Furthermore, calendering can be expected not to cause the initiation of the wear processes in the same way that burnishing does. Excessive lubricant may need to be used as some will be lost in the calendering process. The excess lubricant can be collected and recycled.

The bulk lubrication of media can become important if the top coat should become removed, for example by wear. Different substances should be tried to see if they can be more effective than the oleic acid used for this work. The effects of other materials, with different physical and/or chemical properties should be investigated. In particular fatty acid esters may be effective because of their higher mobility compared to the fatty acids themselves. The mobility arises from the ability to rotate around the ester link.

8.3 Further Work Suggestions.

The effects of surface imperfections should be investigated as it appears that if such an imperfection is present, then the wear will initiate at that point. Also the effects of different surface imperfections need to be investigated to determine which can be ignored without detrimental effects.

A more elastic surface should be investigated to determine whether it shows better durability, particularly under the criteria applied here. It would be expected that a sample produced with a binder having a high value of the product (Se) would be beneficial. This product refers to equation (3.1.1.11) in Chapter 3; S is the ultimate breaking stress and e the elongation, also at fracture. As discussed in Chapter 7, this could result in a material which deforms substantially only elastically so that the problems associated with increases in the real area of contact can be avoided. The large value of e would result in fewer wear particles being produced, thereby reducing the final three-body interaction. Also, an elastic material would be beneficial for reducing the sub-surface plastic flow.

At the same time it would probably be interesting to compare calendered "plastic media" and calendered "elastic media". This could be done for media produced with differing calendering pressures.

The effectiveness of different bulk (and surface) lubricants need to be investigated.

In concluding this chapter, it can be stated that all of the original requirements of the project have been met:

- (a) The effect of different lubrication conditions has been reported;
- (b) The effect of roughness and burnishing has also been considered;
- (c) The mechanisms of wear have been studied and a new theory of wear has been proposed for the media;
- (d) The use of the simulation two rigs for accelerated testing has been investigated and found to be possible.

With regard to roughness and burnishing, it has been found that this process is not merely one which produces a smoother media surface. In fact it is

responsible for the initial micro-abrasion which initiates the processes of wear. These processes resume on media use leading to final failure by the delaminated particles starting an avalanche process with three body abrasive wear.

References

References.

- [1] V Poulsen, United States Patent No. 661619, 13th Nov. 1900.
- [2] V Poulsen, "The Telegraphone", Electrician, 30th Nov. 1900
- [3] R E B Hickman, "Magnetic Recording Handbook", George Newnes Ltd., London, 1956.
- [4] F A Bellis, "A multi-channel digital sound recorder", Proc. of the Conf. on Video and Data Recording, 20 - 22 July 1976, IERE Conf. Proc. No. 30.
- [5] J L E Baldwin, "Digital Television Recording", Proc. of the Conf. on Video and Data Recording, 10 - 12 July 1973, IERE.
- [6] "Super Tape challenges CDs", New Scientist, 12 Sept. 1987.
- [7] "Digital Video breaks standard barriers", New Scientist, 12 Dec. 1987.
- [8] C Corns, Private Communication, 3M (United Kingdom) PLC, Bracknell, England.
- [9] J McRedmund, "How to maintain long life and quality of diskettes", The Office, Nov. 1982.
- [10] B Fox, "Optical memories for home computers", New Scientist, 11th Apr. 1985.
- [11] B Fox, "Technologies compete for optical storage", New Scientist, 25th Feb. 1988.
- [12] B Fox, "Tandy erases its claims to CD first", New Scientist, 12th May 1988.
- [13] "Optical Disc System", Walton Data Systems, Farnborough, Hants., England.
- [14] "Gold discs stop the rot", New Scientist, 9 June 1988
- [15] B Fox, "Tests prove CDs can self-destruct", New Scientist, 7 July 1988.
- [16] J J Burke, "The Optical Data Storage Center", Digest of Papers, IEEE Symposium on Mass Storage Systems (Emerging Solutions for Data

References

- Intensive Applications), Ed.K Friedman, 11 - 14 May 1987, Tucson, Arizona, USA.
- [17] J J Newman, R D Fisher, "Signal-to-noise limitations of particulate disc coatings", IEEE Trans. Magn., Vol. MAG-16, No. 1, Jan. 1980.
- [18] T Osaka, H Matsubara, K Yamanishi, H Mizutami, H Okabe, "Recording Characteristics of Electro-less Plated Perpendicular Media for Floppy Diskettes", IEEE Magn., Vol. Mag-23, No. 3, May 1987.
- [19] E D Daniel, D F Eldridge, "Magnetic recording media", Chapter 3 of "Magnetic recording in Science and Industry", Ed. C B Pear, Jr., Reinhold Publishing Corp., New York, 1967.
- [20] W L Skelcher, "Further durability analysis of Hi-Density diskettes", 3M Internal Report, Mar. 1987.
- [21] "Maxell - A Floppy Diskette Primer", Hitachi - Maxell Ltd., Tokyo, Japan.
- [22] "Technical and market observations on 3M floppy disk media", Special report to 3M DRP by 'Magnetic Media Information Services', (First part), 21st May 1985.
- [23] R L Bradshaw, B Bhushan, "Friction in magnetic tapes III: Role of chemical properties", ASLE Trans., Vol. 27, No. 3, July 1984.
- [24] H J Greenberg, "Flexible disk - read/write head interface", IEEE Trans. Magn., Vol. Mag-14, No. 5, Sept. 1978.
- [25] G G Adams, "Procedures for the study of flexible-disk to head interface", IBM J. of Res. and Dev., Vol. 24, No. 4, July 1980.
- [26] R R Stromsta, D Egbert, "Head media flying characteristics on double sided 5 in. and 8 in. flexible disk drives", 1981 IEEE Workshop on Applied Magnetic Recording, 16-17 June 1981, San Francisco.
- [27] P M Dickens, "The sliding wear of polymers under various fluids", Ph.D. Thesis, University of Aston in Birmingham, England, 1984.
- [28] W L Skelcher, Private communication, (Binder coatings information),

References

- 1985.
- [29] B Bhushan, B S Sharma, R L Bradshaw, "Friction in magnetic tapes I: Assessment of relevant theory", ASLE Trans., Vol. 27, No. 1, Jan. 1984.
- [30] F E Talke, J L Su, "The mechanism of wear in magnetic recording disk files", Tribology International, Feb. 1975.
- [31] F E Talke, R C Tseng, "An investigation of the wear and material transfer in magnetic recording disk files", Wear, Vol. 28, 1974.
- [32] R D Weiss, "Abrasion wear in magnetic disk files", J. App. Phys., Vol. 50, No. 3, March 1979.
- [33] I R Blevins, P J Moran, W L Skelcher, "Preliminary measurements on the abrasivity of 5.25 in. flexible diskette media", 3M Internal report, Sept 1983.
- [34] P U Bagatta, "Fluorocarbon lubricants for surface lubrication", MMIS conference, Hawaii, May 1983.
- [35] "Technical and market observations on 3M floppy disk media", Special report to 3M DRP by 'Magnetic Media Information Services', (Second part), 21st May 1985.
- [36] D K Cummings, "Friction testing of diskettes", 3M Internal report, May 1985.
- [37] D E Speliotis, "Barium Ferrite Magnetic Recording Media", IEEE Trans. Magn., Vol. Mag-23, No. 1, Jan 1987.
- [38] T Fujiwara, "Magnetic properties and recording characteristics of Barium Ferrite Media", IEEE Trans. Magn., Vol. Mag-23, No. 1, Jan 1987.
- [39] D E Speliotis, "Destructive characteristics of Barium Ferrite Media", IEEE Trans. Magn., Vol. Mag-23, No. 1, Jan 1987.
- [40] C B Pear, Jr., (Ed.), "Magnetic Recording in Science and Industry", Reinhold Publishing Corp., New York, 1967.
- [41] S J Begun, "Magnetic Recording", Murray-Hill Books, England, 1949.

References

- [42] W E Stewart, "Magnetic Recording Techniques", McGraw-Hill, New York, 1958.
- [43] A S Hoagland, "Digital Magnetic Recording", Wiley, New York, 1963.
- [44] V N Hudson, "A digital magnetic recording system for high density applications", M.Phil. Thesis, Manchester Polytechnic, Manchester, England, 1985.
- [45] "OEM Operating and Service Manual TM100-1, TM100-2 drives 48 Tracks per Inch", Tandon Corporation, California, USA.
- [46] N J Suwarnasarn, "White light interferometry for VHS Head - media spacing", 3M Internal Report, Jan - May, 1984.
- [47] F P Bowden, D Tabor, "The friction and lubrication of solids: Part 1", Oxford, 1953.
- [48] F P Bowden, D Tabor, "The friction and lubrication of solids: Part II", Oxford, 1964.
- [49] S S Athwal, "Wear of low alloy steels at elevated temperatures", Ph.D. Thesis, University of Aston, Birmingham, England, 1983.
- [50] W L Skelcher, "The wear of polymers during sliding under fluid-contaminated conditions", Ph.D. Thesis, University of Aston, Birmingham, England, 1982.
- [51] B Briscoe, "Fundamental aspects of the sliding wear of polymers", Selection and performance of dry bearings, National Centre of Tribology, Risley, 25th May 1983.
- [52] J S Halliday, "Surface examination of reflection electron microscopy", Proc. Inst. of Mech. Eng., No. 169, 1955.
- [53] J A Greenwood, J P B Williamson, "Contact of normally flat surfaces", Proc. Roy. Soc. London, Ser. A295, 1966.
- [54] E Rabinowicz, "Friction and wear of materials", Wiley, New York, 1965.
- [55] S B Ratner, I I Farberova, O V Radyukevich, E G Lur'e, "Connection between wear - resistance of plastics and other mechanical properties", from

References

- 'Abrasion of rubber', D I James Ed., McLaren and Sons, 1967.
- [56] J Lancaster, "Practical aspects of polymer wear", Selection and performance of dry bearings, National Centre of Tribology, Risley, 25th May 1983.
- [57] S Bush, "Polymer types and their general properties", Selection and performance of dry bearings, National Centre of Tribology, Risley, 25th May 1983.
- [58] J C Anderson, "A review of NCT work on commercially available dry materials", Selection and performance of dry bearings, National Centre of Tribology, Risley, 25th May 1983.
- [59] R Stribeck, "Die Wesentlichen Eigenschaften der Gleit - und Rollenlager", Zeitschrift des Vereines Deutscher Ingenieure, Vol. 46, No. 36, 6th Sept. 1902 (in German).
- [60] W L Skelcher, "Diskette friction measurements", 3M Internal Report, May 1986.
- [61] N Hall, "Erasable Compact Disc takes on Digital Audio Tape", New Scientist 10th Sept. 1987.
- [62] "Tandon TM100-1, TM100-2 Flexible Disk Drives Product Specification and User's Manual", Tandon Corporation, California, USA.
- [63] B Green, "Reducing wear when using double sided diskettes", New Electronics, 4 May 1982.
- [64] R A von Behren, "Diskette accelerated wear test", 3M Internal correspondence to R F Dubbe, 31 August 1984.
- [65] A E T Chiou, "The effect of spring pad loading and head penetration on flight of flexible diskette over a spherical head", IEEE Trans. Magn., Vol. Mag-21, No. 1, Jan 1985.
- [66] C F Lin, R F Sullivan, "An application of white light interferometry in thin film measurements", IBM J. Res. and Dev., May 1972.
- [67] R A Bengal, K A Boyles, "Drag and normal transducer for head to disk

References

- interface", IBM Tech. Discl. Bull., Vol. 22, No. 3, Aug. 1979.
- [68] L C Anderson, E T Yen, "Detection of damages and defects in particulate disk media", IBM Tech. Discl. Bull., Vol. 25, No. 5, Oct. 1982.
- [69] R E Linder, P B Mee, "ESCA determination of Fluorocarbon lubricant film thickness on magnetic disk media", IEEE Trans. Magn., Vol. Mag-18, No. 6, Jan 1982.
- [70] L J Hedlund, "Infra-red lubricant quantitation and dispersion tester for magnetic disks" IBM Tech. Discl. Bull., Vol. 25, No. 11A, Apr. 1983.
- [71] J L Crowley, L P Dawson, W I Maino, L Nebenzahl, B Smith, A Wu, "Non-destructive in-situ analytical for magnetic disk lubricant and magnetic film thickness measurement", IBM Tech. Discl. Bull., Vol. 26, No. 7B, Dec. 1983.
- [72] V Au-Yeung, "FTIR determination of fluorocarbon lubricant film thickness in magnetic disk media", IEEE Trans. Magn., Vol. Mag-19, No. 5, Sept. 1983.
- [73] F T Walder, D W Vidrine, G C Hansen, "The analysis of lubricants on magnetic disks by Fourier Transform Infra-red Spectroscopy", Appl. Spectroscopy, Vol. 38, No. 6, 1984.
- [74] H Hinkel, U Kuenzel, M Schrader, W Steiner, H Weiss, "Method of detecting the lubricant distribution on magnetic recording media", IBM Tech. Discl. Bull., Vol. 26, No. 9, Feb. 1984.
- [75] S A Chambers, "Surface characterisation of 3M Floppy Diskettes in various stages of development - X-ray Photoemission and Scanning Auger Microprobe", 3M report to G M Robinson, DRP, 3M, 2 Nov. 1982.
- [76] H Hinkel, J Kempf, U Kuenzel, E Prinz, "Reducing the viscous force (stiction) of magnetic head sliders on magnetic disks", IBM Tech. Discl. Bull., Vol. 25, No. 9, Feb. 1983.
- [77] V Heinrich, J Kofler, H G Nauth, H Stricker, H Tandjung, "Magnetic head

- stiction detector", IBM Tech. Discl. Bull., Vol. 26, No. 9, Feb. 1984.
- [78] V DePalma, D Nepala, "Selection of load bearing materials for compatibility with commonly used magnetic material lubricants", IBM Tech. Discl. Bull., Vol. 25, No. 9, Feb. 1983.
- [79] M R Lorentz, R D Miller, E T Yen, "Controlled pore formation in magnetic disk coatings to optimise lubricant retention", IBM Tech. Discl. Bull., Vol. 26, No. 9, Feb. 1984.
- [80] G Kraus, U Kuenzel, M Schrader, "Method of lubricating the surface of organic magnetic storage media", IBM Tech. Discl. Bull., Vol. 27, No. 4A, Sept. 1984.
- [81] M Hamada, S Fukushima, T Suenaga, K Itoh, S Ogawa, "A new lubrication for high density magnetic coated disks", J. Appl. Phys., Vol. 55, No. 6, 15 Mar. 1984.
- [82] W L Skelcher, J L Sullivan, J F Dirks, "Durability analysis of various control numbers of high density diskettes", 3M Internal Report, Apr. 1986.
- [83] B Bhushan, "Analysis of the real area of contact between a polymeric magnetic medium and a rigid surface", Trans of the ASME, Vol. 106, Jan. 1984.
- [84] H Hiratsuka, H Hanafusa, K Nakamura, S Hosakawa, "Durability of magnetic recording tape for Mass Memory Systems", Review of the Electrical Communications Labs., Vol. 28, No. 5-6, May - Jun. 1980.
- [85] "Method cuts out drop-outs on flexible media", Computer Design, Dec. 1983.
- [86] B Bhushan, R L Bradshaw, B S Sharma, "Friction in magnetic tapes II: Role of physical properties", ASLE Trans., Vol. 27, No. 2, Apr. 1984.
- [87] H Hiratsuka, H Hanafusa, K Nakamura, S Hosakawa, "Material requirements for highly durable magnetic recording tape", Electronics and Communications in Japan, Vol 63-C, No. 6, 1983.

References

- [88] H Hanabusa, H Hiratsuka, K Nakamura, "Study of wear resistance of magnetic tape from the point of view of raw materials", *Denshi Tsushin Gakkai Ronbunshi*, C82/5 Vol. J65-C, No. 5.
- [89] J Kelly, "Tape and head wear", Chapter 2 of 'Magnetic media for the eighties', NASA Publication 1075, F Khalil Ed., Apr. 1982.
- [90] B Bhushan, "Influence of test parameters on the measurement of the coefficients of friction in magnetic tapes", *Wear*, Vol. 93, 1984.
- [91] K Miyoshi, D H Buckley, B Bhushan, "Friction and morphology of magnetic tapes in sliding contact with Ni-Zn Ferrite", NASA Technical Paper 2267, Jan. 1984.
- [92] I E Jurek, D J Keller, "Electron beam curable polyurethane blends as magnetic media binders", *J. of Radiation Curing*, Vol. 12, No. 1, Jan. 1985.
- [93] M M Reznikovskii, G I Brodskii, "Features of the abrasion of highly elastic materials", from 'Abrasion of rubber', D I James Ed., McLaren and Sons, 1967.
- [94] S B Ratner, "Comparison of the abrasion of rubbers and plastics", from 'Abrasion of rubber', D I James Ed., McLaren and Sons, 1967.
- [95] N P Suh, "The Delamination Theory of Wear", *Wear*, Vol. 25, 1973.
- [96] J F Archard, "Contact and rubbing of flat surfaces", *J. of Appl. Phys.*, Vol. 24, No. 8, Aug. 1953.
- [97] D Hull, D J Bacon, "Introduction to dislocations", 3rd Edition, Pages 88-90, Pergamon Press, 1984.
- [98] A H Cottrell, "Dislocations and plastic flow in crystals", Pages 54-57 and 103-104, Oxford, 1953.
- [99] D Hull, D J Bacon, "Introduction to dislocations", 3rd Edition, Pages 49-51 and 215-224, Pergamon Press, 1984.
- [100] A H Cottrell, "Dislocations and plastic flow in crystals", Pages 58-62, Oxford, 1953.

- [101] P Feltham, "Deformation and strength of materials", Butterworth, 1966.
- [102] N P Suh, S Jahanmir, E P Abrahamson III, A P L Turner, "Further investigations of the delamination theory of wear", J. of Lubrication Technology of the ASME, Vol. 96, Oct. 1974.
- [103] N P Suh, "An overview of the delamination theory of wear", Wear, Vol. 44, 1977.
- [104] S Jahanmir, N P Suh, "Mechanics of sub-surface void nucleation in delamination wear", Wear, Vol. 44, 1977.
- [105] J R Fleming, N P Suh, "Mechanics of crack propagation in delamination wear", Wear, Vol 44, 1977.
- [106] J R Fleming, N P Suh, "The relationship between crack propagation rates and wear rates", Wear, Vol 44, 1977.
- [107] K L Johnson, "Contact Mechanics", Cambridge, 1985.
- [108] N P Suh, H-C Sin, "On prediction of wear coefficients in sliding wear", ASLE Trans., Vol. 26, No. 3, Jul. 1983.
- [109] "PAT-2+TM Performance and alignment tester - owner's manual", Dysan Corporation, Sunnyvale, California, USA.
- [110] W L Skelcher, "Diskette friction measurements", 3M Internal Report, May 1986.
- [111] D B Pendergrass, Private communications, 3M Center, St. Paul, Minnesota, USA.
- [112] M Andrews, "Apple Roots: Assembly Language Programming for the Apple //e and //c", McGraw-Hill, California, 1986.
- [113] J Crossley, "Applesoft internal entry points points", The Apple Orchard, March/April 1980.
- [114] J Uhley, "Use of the Disk II Interface Card through your own software", The Apple Orchard, April 1983.
- [115] C Bongers, "In the heart of Applesoft", MICRO - the 6502 Journal, No.

- 33, Feb. 1981.
- [116] "Applesoft II BASIC Programming Programming Reference manual", Apple Computers Inc. Product #A2L0006 (030-0013-E), 1981.
- [117] "Apple // DOS User's Manual for II, II+, IIe" Apple Computers Inc. Product #A2L2002, 1983.
- [1118] L Poole, M McNiff, S Cook, "Apple II User's Guide", McGraw-Hill, California, 1981.
- [119] "Apple II real-time clock construction", Everyday Electronics, May 1983.
- [120] "Dysan 224/2A Analog Alignment Diskette - Alignment instructions", Dysan Corporation, Sunnyvale, California, 1984.
- [121] D Lichtman, "A comparison of the methods of surface analysis and their application", from 'Methods of surface analysis', A W Czanderna Ed., Elsevier, 1975.
- [122] W M Riggs, M J Parker, "Surface analysis by X-ray Photoelectron Spectroscopy", from 'Methods of surface analysis', A W Czanderna Ed., Elsevier, 1975.
- [123] A Joshi, L E Davis, P W Palmberg, "Auger Electron Spectroscopy", from 'Methods of surface analysis', A W Czanderna Ed., Elsevier, 1975.
- [124] C D Wagner, "Sensitivity of detection of elements by photoelectron Spectroscopy", Analytical Chemistry, Vol. 44, No. 6, May 1972.
- [125] D Briggs, "Application of XPS in polymer technology", from 'Practical Surface Analysis', D Briggs, M P Seah Ed., Wiley, 1983.
- [126] D W Dwight, W M Riggs, "Fluoropolymer surface studies", J. of Colloid and Interface Science, Vol. 47, No. 3, Jun. 1974.
- [127] D Briggs, J C Riviere, "Spectral interpretation", from 'Practical Surface Analysis', D Briggs, M P Seah Ed., Wiley, 1983.
- [128] C D Wagner, "Auger lines in X-ray photoelectron spectroscopy", Analytical Chemistry, Vol. 44, No. 6, May 1972.

References

- [129] J L Sullivan, "Surface analysis techniques", Final Year Undergraduate Lecture Course University of Aston, Birmingham, England, 1985-6.
- [130] C E Hall, "Introduction to Electron Microscopy", McGraw-Hill (London), 1953.
- [131] R D Heidenreich, "Fundamentals of Transmission Electron Microscopy", Interscience Monographs and Texts in Physics and Astronomy: Vol. XIII, Interscience Publications, (Wiley), 1966.
- [132] "Mirau interference equipment operating instructions", Zeiss, W. Germany.
- [133] G M Robinson, T J Szezech, C D Englund, R D Cambronne, "Relationship of roughness of video tape to its magnetic performance", IEEE Trans. Magn., Vol. Mag-21, Sept. 1985.
- [134] D M Perry, G M Robinson, R W Peterson, "Measurement of surface topography of magnetic recording materials through computer analyzed microscopic interferometry", IEEE Trans. Magn., Vol. Mag-19, No. 5, Sept. 1983.
- [135] R W Peterson, G W Robinson, R A Carlsen, C D Englund, P J Moran, W M Wirth, "Interferometric measurements of the surface profile of moving samples", Applied Optics, Vol. 23, No. 10, 15th May 1984.
- [136] G W Robinson, P J Moran, R W Peterson, C D Englund, "Applications of interferometric measurements of surface topography of moving magnetic recording materials", IEEE Trans. Magn., Vol. Mag-20, No. 5, Sept. 1984.
- [137] W L Skelcher, Private Communications.
- [138] L E Nielsen, "Mechanical Properties of polymers", Reinhold Publishing, New York, 1962.
- [139] W L Skelcher, "The abrasivity of 5.25-inch diskettes", 3M Internal Report, August 1986.
- [140] S A Chambers, "Surface characterisation of 3M VHS video tape via - X-ray

References

- Photoemission and Scanning Auger Microscopy", 3M report to G M Robinson, DRP, 3M, 12 Mar. 1984.
- [141]F P Bowden, D Tabor, "Friction and Lubrication", Methuen, London, 1956, (Chapter V).

Appendix A.

Calibrations.

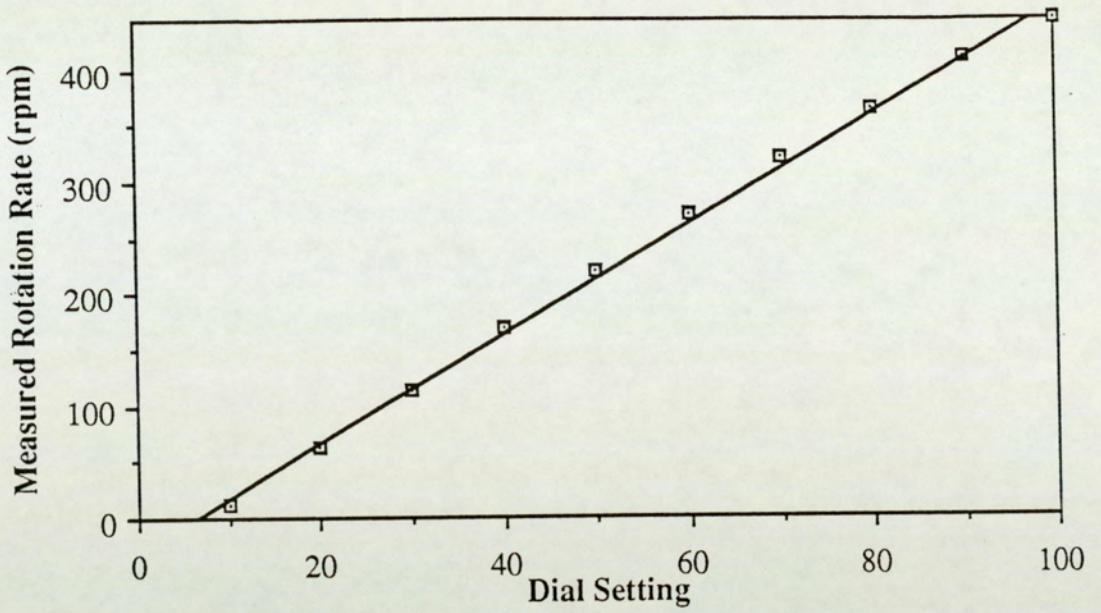


Figure A.1 Operating calibration for the supported sample rig.

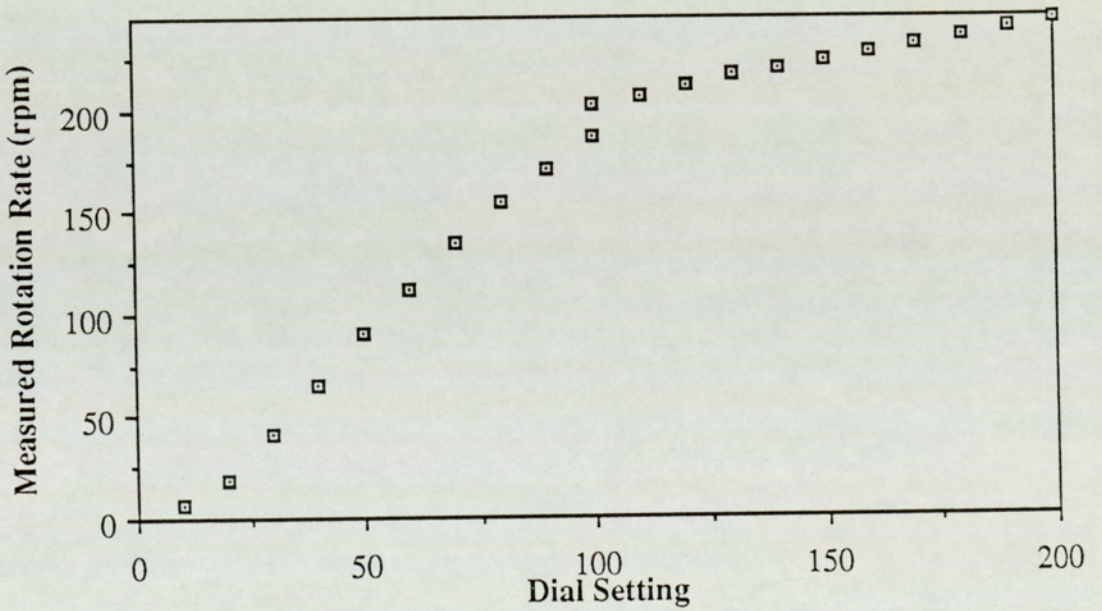


Figure A.2 Operating calibration for the unsupported sample rig. The discontinuity at the dial setting of 100 is due to switching from one range to another on the control face.

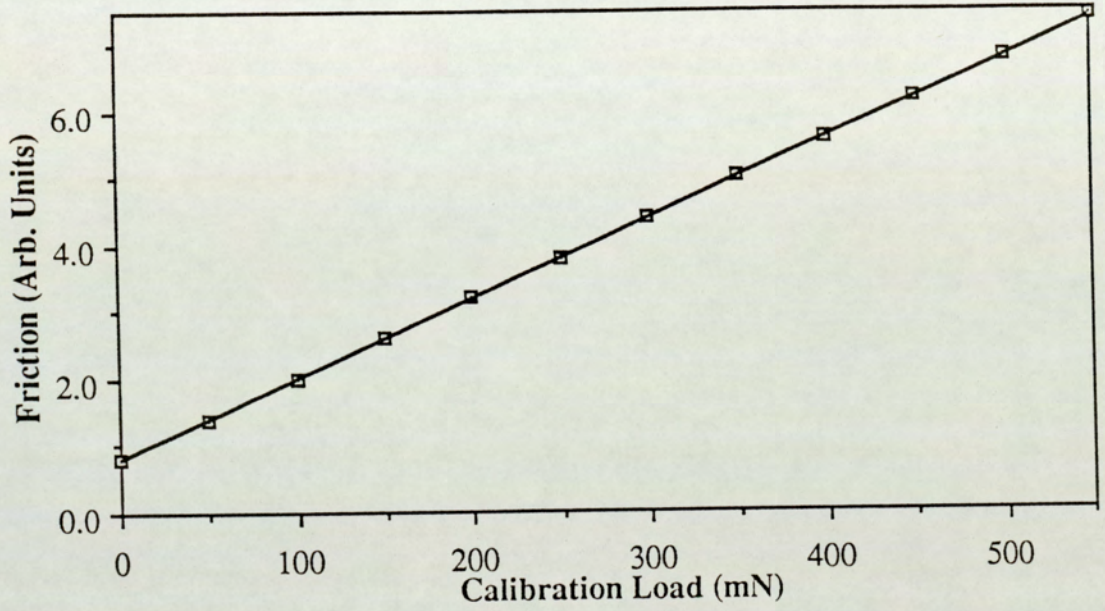


Figure A.3 Calibration for the friction measuring transducer used on the supported sample and unsupported sample simulation rigs

Appendix B.

Computer Programs Employed in
Bit Analysis of the Media.

Appendix B

The program listed below is the master control program used in reading the test drives and for recording the data to files on data diskettes on the Apple //e micro computer. It was used in conjunction with the machine code routines listed second and the data file reader listed last.

```

10 gosub 20 : goto 60
20 text : home : print "*** Digital Write Read Tester ***" : Vtab 7 : return
30 rem
40 rem find drives and tracks to test, signal reduction factor
50 rem
60 dim ds(8) : dim tr(8) : sl(8) : dim dr(8) : dim hd(8) : dim fl$(8) : dim sm$(8) :
  dim ct(8) : dim sec(8) : dim tk(8) : dim bt(8) : dim fa(8)
70 for i=1 to 8 : ds(i)=0 : tr(i)=40 : sl(i)=7 : dr(i)=3 : hd(i) = 3 : fl$(i)="" :
  sm$(i)=""
80 if (i=3 or i=4) then 230 : rem omit slot 3
90 gosub 20 : print "Use drive number "i"? (y/n): "; : get a$ : print a$ : if a$
  <>"y" and a$ <>"n" then print chr$(7) : goto 90
100 if a$="n" then vtab 17 : print "Not using drive "i". ok? (y/n): "; : get a$ : print
  a$ : if a$="y" then 230
110 rem
120 rem calculate slot and drive for sequential drive number=i
130 rem
140 ds(i)=1:sl(i)=int((i+1)/2 + 1) : dr(i)=(i=2*int(i/2))
150 rem
160 rem get track to test, head to use and file to store data under
170 rem
180 vtab 9 : input "Track to test (0 to 39): ";tr$ : tr(i)=val(tr$) : if tr(i)<0 or
  tr(i)>39 or (tr(i)=0 and tr4<>"0") or (len(tr$)>2) then 180
190 vtab 11 : print "Head to use for test (0/1): "; : get hd$ : print hd$ :
  hd(i)=val(hd$) : if hd(i)<0 or hd(i)>1 or (hd(i)=0 and hd$<>"0") or (hd(i)=1
  and hd$<>"1") then 190
200 vtab 13 : print "Set up drive "i" on track "tr(I)" using head "hd(i).": vtab 15
  : print "Is this data ok? (y/n): "; : get a$ : print a$ : if a$<>"y" and a$<>"n"
  then print chr$(7) : goto 200
210 if a$<>"y" then ds(i)=0 : goto 90
220 vtab 17 : print "Output file for drive "i; : input " data: ";fl$(i) : vtab 19 : input
  "Enter sample name: "; sm$(i) : print chr$(4) "open "fl$(i)",s6,d2" : print
  chr$(4) "close "fl$(i)
230 next
235 gosub 20 : input "Signal reduction factor? ";rd$
240 rem
250 rem set up clock read routine
260 rem
270 dim d$(7) : dim m$(12)
280 for i=1 to 7 : read d$(i): next
290 for i=1 to 12 : read m$(i) : next
300 data "Sunday", "Monday", "Tuesday", "Wednesday", "Thursday",
  "Friday", "Saturday"
310 data "January", "February", "March", "April", "May", "June", "July",
  "August", "September", "October", "November", "December"
320 rem
330 rem next line is the same as 10 to 100 of initialising routine
340 rem
350 poke - 16207,56 : poke - 16208,15 : poke 16207,60 : poke - 16205,56 :

```

Appendix B

```

poke - 16206,15 : poke - 16205,60 : poke - 16208,0 : poke - 16206,0 : poke
- 16205,52 : poke - 16205,60
360 poke - 16205,56 : rem access ddrb
370 poke - 16206, 0 : rem port B as inputs
380 poke - 16205,60 : access port B
390 rem
400 rem machine code routine to read clock registers. Call 768 reads registers
and stores them in locations 801 to 812 (801=reg1)
410 rem
420 rem load necessary machine code
430 rem
440 print chr$(4) "bload clkread.obj,s6,d1"
450 rem
460 rem gosub clock read routine for start time of test = ts$
470 rem
475 gosub 1200 : ts$ = t$
480 rem
490 gosub 1500 : rem display testing message
500 rem
510 rem set up drive and write $FF to test track - use BETL
520 rem
530 for i = 1 to 8
540 rem
550 rem check if drive selected; if not, skip
560 rem
570 if ds(i) = 0 then call 2087(s,sl(i),dr(i),hd(i),0,1,0,0) : ds(i) = 0 : goto 720 :
rem ensure select LED is off
580 rem
590 rem else place head on track tr(i)
600 rem
610 call 2087(s,sl(i),dr(i),hd(i),1,1,1,40) : call2087(s,sl(i),dr(i),hd(i),1,1,0,tr(i))
620 rem
630 rem write $FF strings to test track
640 rem
650 call 2087(wi,sl(i),dr(i),hd(i),er)
660 if er = 0 then 720
670 if er = 128 then gosub 20 : print chr$(7)"No index found on drive "i"."
680 if er = 255 then gosub 20 : print chr$(7)"Diskette in drive "i" is write-
protected"
690 print "Do you wish to continue test or restart? (c/r): ";get a$ : if a$ <> "c"
and a$<>"r" then 690
700 if a$ = "r" then print chr$ (7) : run 10
710 if a$ = "c" then gosub 20 : print "Okay. Trying again ..." : goto 610
720 next
725 gosub 1500
730 rem
740 rem do read tests on each drive - read > full track = 4 kByte
750 rem
760 for i = 1 to 8 : if ds(i) = 0 then 1070
770 call 2087(ri,sl(i),dr(i),hd(i),0,er)
780 rem
790 rem error code = 128 => no index on diskette.
800 rem error code = 255 => disk read failed : location $08 = sector
810 rem $07 = byte# and $09 = bad byte value
820 rem
830 if er = 0 then 1070
840 if er = 128 then gosub 20 : print chr$ (7)"No index found on drive "i"." :

```

Appendix B

```

    print "Continue on next drive or re-read? (c/r): "; :get a$ : print a$ : if a$
    <>"r" and a$ <>"c" then 840
850 if (er = 128 and a$ = "r") then gosub 1500 : goto 770
860 if (er = 128 and a$ = "c") then gosub 1500 : goto 1070
870 if er = 255 then fa(i) = fa(i) + 1 : rem another soft error
880 rem
890 rem got end of test time and stored it in te$
900 rem now check data consistency
910 rem
920 rem get binary byte value of bad byte
930 rem
940 gosub 1300
950 if ((peek(8) = sec(i)) and (peek(7) = bt(i)) and (bi$ = bb$(i))) then ct(i) = ct(i)
    + 1 : goto 970
953 rem
955 rem if new error location, record and reset ct(i) = 1
957 rem
960 if ((peek(8) <> sec(i)) or peek (7) <> bt(i)) or (bi$ <> bb$(i))) then ct(i) = 1 :
    sec(i) = peek (8) : bt(i) = peek (7) : bb$(i) = bi$
970 if ct(i) < 3 then 1070
975 gosub 1200 : te$ = t$
980 print chr$(4)"append "fl$(i)",s6,d2"
990 print chr$(4)"write "fl$(i)
1000 print "Sample used = "sm$(i)", , : print "Drive = "i",    Track = "tr(i)",
    Head = "hd(i) : print "Test started at = "ts$ : print "Test ended at = "te$ :
    print "Bad byte at "peek(8)"the sector, "peek(7)"th byte, bad byte = "bi$
1005 print "Total soft read errors = "(fa(i) - 2) : print "Signal reduced to "rd$" *
    head read signal>"
1010 print chr$(4)"close "fl$(i)
1020 print chr$(4)"pr#1" : print chr$(9)"80n" : print "Sample used = "sm$(i)",
    , : print "Drive = "i",    Track = "tr(i)",    Head = "hd(i) : print "Test started
    at = "ts$ : print "Test ended at = "te$ : print "Bad byte at "peek(8)"th sector,
    "peek(7)"th byte, bad byte = "bi$
1025 print "Total soft read errors = " (fa(i) - 2) : print print "Signal reduced to "
    rd$" * head read signal" : print "Data file = "fl$(i) : print : print : print
    chr$(4)"pr#0"
1030 rem
1040 rem turn motor off for this drive and deselect it
1050 rem
1060 gosub 1500 : call (s,sl(i),dr(i),hd(i),0,1,0,0) : ds(i) = 0
1070 next
1080 rem
1090 rem check all drives stopped else return to read tests.
1100 rem
1110 for j = 1 to 8
1120 if ds(j) then j = 9 : got 760
1130 next
1140 rem
1150 rem all drives stopped now
1160 rem exit program after message.
1170 rem
1180 gosub 20 : vtab 15 : print htab (5); te$ : print : print "chr$(7)"*** All tests
    complete ***"
1190 end

1200 rem

```

References

Appendix B

The listing below presents the entire set of machine code utility programs which were employed in the bit analysis work in conjunction with the master control program listed above.

```

1  *BETL 00.01.02 5/14/86 10:42AM - AMENDED - PJS
2  *****
3  *
4  * BIT ERROR TEST LANGUAGE (BETL)*
5  * WEAR TEST PROGRAMS 1/86
6  *
7  *****
8          ORG $0800
0800:00   9          HEX 00          ;zero byte required by
                                basic
0801:15 08   10         DA LINK          basic link field
                                11         HEX 0A00          basic line number (10)
0805:8C 32 30
0808:37 31 3A 12         HEX 8C323037313A ;call 2071:
080B:B9 31 30
080E:34 2C 31
0811:31 3A   13         HEX B93130342C31313A ;poke 104,11:
0813:AC 00   14         HEX AC00          run token & eol mark
0815:00 00   15 LINK    HEX 0000          ;temp end of basic prog
16 *-----*
17 * THE SHORT BASIC PROGRAM
18 * ABOVE CALLS THE INITIALISATION
19 * ROUTINE BELOW & CHANGES THE
20 * POINTER TO THE BEGINNING OF
21 * BASIC SO THAT LIST AND LOAD
22 * WILL WORK FROM $0B00. THIS
23 * ALLOWS THE MACHINE LANGUAGE
24 * ROUTINE TO BE SAVED WITH THE
25 * APPLESOFT PROGRAM IN ONE FILE
26 * 1) BLOAD THIS PROGRAM
27 * 2) TYPE POKE 104,11 <CR>
28 * 3)LOAD THE APPLESOFT PROGRAM
29 * 4)TYPE POKE 104,8 <CR>
30 * 5)SAVE THE COMBINED PROGRAM
31 * UNDER A NEW NAME
32 * I SUGGEST THAT YOU INCLUDE
33 * POKE 104,8 AS THE LAST LINE
34 * OR STATEMENT EXEC'D TO AVOID
35 * ACCIDENTAL LOSS OF THE M'CHINE
36 * LANGUAGE PORTION OF THE
37 * PROGRAM - ESPECIALLY AFTER THE
38 * EARLY DEBUGGING IS FINISHED
39 *-----*
0817:A9 00   40         LDA #$00          zero byte required by
0819:8D 00 0B 41         STA $0B00         new applesoft program
42 *-----*
43 *SET ALL DAC REF VOLTAGES = 0 V
44 *-----*
081C:A2 10   45         LDX #$10
081E:A9 80   46         LDA #$80          $80 = 0 VOLTS

```

Appendix B

```

0820:9D EF C0 47 NZERO STA DACADC+3,X ;start at $C0FF (slot 7)
0823:CA 48 DEX
0824:D0 FA 49 BNE NZERO stop after $C0F0 (slot 7)
0826:60 50 RTS ;return for 'run'
51 *-----*
52 *START PROGRAM CODE *
53 *-----*
54 COUNT1 EQU $06
55 COUNT2 EQU $08
56 IFLG EQU $1B =I or comma
57 SL2 EQU $8A slot# * 2
58 SL16 EQU $8B slot# * 16
59 DRNUM EQU $8C drive #
60 REVCNT EQU $8D bytes per rev
61 INTVAL EQU $A0 integer value from intget
62 BYTE EQU $A1 1 byte from getbyt
63 CHRGET EQU $B1 next Asoft chr -> A-reg
64 BUF EQU $2000 buffer for disk track read
65 P0L EQU $C080 phase 0 LO
66 P0H EQU $C081 phase 0 HI
67 P1L EQU $C082 phase 1 LO
68 P1H EQU $C083 phase 1 HI
69 P2L EQU $C084 phase 2 LO
70 P2H EQU $C085 phase 2 HI
71 P3L EQU $C086 phase 3 LO
72 P3H EQU $C087 phase 3 HI
73 DOFF EQU $C088 drive motor off (unused)
74 DON EQU $C089 drive motor on (R/W)
75 D0SEL EQU $C08A select drive 0
76 D1SEL EQU $C08B select drive 1
77 Q6L EQU $C08C set Q6 LO
78 Q6H EQU $C08D set Q6 HI
79 Q7L EQU $C08E set Q7 LO
80 Q7H EQU $C08F set Q7 HI
81 *
82 * Q6 Q7 use of Q6 and Q7 lines
83 -----
84 LO LO read (disk -> shift register)
85 LO HI write
86 HI LO sense write protect
87 HI HI data bus -> shift register
88 *
89 DACADC EQU $C0EC base add adc/dac s7
90 HDLOAD EQU $C0F4 base add hdload s7
91 *
92 DATA EQU $D995 move txtptr to eol or ;
93 CHKCLS EQU $DED8 ) ?
94 CHKOPN EQU $DEBB ( ?
95 CHKCOMEQU $DEBE , ?
96 SYNERR EQU $DEC9 generate a syntax err
97 PTRGET EQU $DFE3 var stor (lo=$83hi=$84)
98 INTGET EQU $E105 eval expr -> intval
99 ILLQUAN EQU $E199 illegal quantity message
100 GIVAYF EQU $E2F2 AH,YL -> FAC
101 GETBYT EQU $E6F8 eval exp @ txtptr -> byte
102 MOVMF EQU $EB2B stores fac-> mem (yl,xh)
103 *

```

Appendix B

```

104 WAIT      EQU $FCA8      monitor WAIT routine
105 *
106 *-----*
107 * GENERAL NOTES: CALL THESE *
108 * ROUTINES AT THE LABEL 'ENTER' *
109 * WITH AN ARGUMENT LIST IN *
110 * PARENTHESES AS INDICATED AT *
111 * EACH FUNCTION. THE FIRST *
112 * ARGUMENT WILL BE A ONE OR TWO*
113 * LETTER OP-CODE (NOT A STRING *
114 * VARIABLE) FOLLOWED BY A COMMA*
115 * AND THEN THE NUMERICAL VALUES*
116 * OR APPLESOFT VARIABLES AS *
117 * REQUIRED BY THE FUNCTION - *
118 * REMEMBER THAT ARGUMENTS THAT*
119 * RECEIVE RETURN VALUES MUST BE *
120 * NAMED APPLESOFT VARIABLES! *
121 * E.G. ER IN READ/WRITE AND *
122 * THE LAST ARGUMENT OF *
123 * THE FIND COMMAND *
124 *-----*
0827:20 BB DE 125 ENTER JSR CHKOPN start of arguments?
082A:C9 57 126 CMP #'W'
082C:F0 1F 127 BEQ WRITE
082E:C9 52 128 CMP #'R'
0830:F0 0F 129 BEQ TOREAD
0832:C9 53 130 CMP #'S'
0834:F0 11 131 BEQ TOSEEK
0836:C9 46 132 CMP #'F'
0838:F0 0A 133 BEQ TOFIND
083A:C9 54 134 CMP #'T'
083C:F0 0C 135 BEQ TOTIME
083E:4C C9 DE 136 JMP SYNERR
0841:4C DC 08 137 TOREAD JMP READ jump table
0844:4C 3C 09 138 TOFIND JMP FIND
0847:4C 75 09 139 TOSEEK JMP SKSET
084A:4C BA 0A 140 TOTIME JMP TIMER for command parser
141 *-----*
142 * WRITE 2F TO DISK FOR >1 REV. *
143 * CALL2087(W,SL,DR,HD,ER) *
144 * CALL2087(WI,SL,DR,HD,ER) *
145 * VARIABLE SL=SLOT NUMBER 2 -> 5 *
146 * VARIABLE DR=DRIVE # 0 / 1 *
147 * VARIABLE HD=HEAD # 0 / 1 *
148 * ER=ERROR CODE RETURNED: *
149 * 0 = OK *
150 * 128 = NO INDEX FOUND *
151 * 255 = WRITE PROTECTED *
152 *-----*
084D:20 B1 00 153 WRITE JSR CHRGET expect I or comma
0850:85 1B 154 STA IFLG save indexed flag
0852:C9 49 155 CMP #'I' is it indexed?
0854:D0 0C 156 BNE GOWRITE
0856:20 B1 00 157 JSR CHRGET eat the I
0859:20 3A 0A 158 JSR PARMS slot, head, drive
085C:50 65 0A 159 JSR FNDINDX is index present?

```

Appendix B

085F:4C	65 08	160		JMP	WPROT	
0862:20	3A 0A	161	GOWRITEJSR	PARMS		set slot, drive, head
		162	*-----*			
		163	* CHECK WRITE PROTECT STATUS *			
		164	*-----*			
0865:A6	8B	165	WROT	LDX	SL16	
0867:BD	8D C0	166		LDA	Q6H,X	Q6 HI, Q7 LO
086A:BD	8E C0	167		LDA	Q7L,X	to read write prot status
086D:10	0A	168		BPL	NPROT	write protected?
086F:20	BE DE	169		JSR	CHKCOM	eat a comma
0872:A0	FF	170		LDY	#\$FF	write prot'd
0874:A9	00	171		LDA	#\$00	error flag HI byte
0876:4C	AC 0A	172		JMP	STUFFIT	set flag var. rtn to basic
0879:A5	1B	173	NPROT	LDA	IFLG	is it indexed?
087B:C9	B9	174		CMP	#'I'	indexed?
087D:D0	10	175		BNE	NORM	
		176	*-----*			
		177	* FIND THE PLACE TO START *			
		178	* * *			
		179	* ...NNNNNN NNNNNNNN... *			
		180	* IIIII *			
		181	* * *			
		182	* ...-----WWWWWW... *			
		183	* * *			
		184	* NOTE THAT WRITE SHOULD GO *			
		185	* PAST INDEX SO THAT THE WRITE *			
		186	* SPLICE WILL BE FOUND SOON *			
		187	* AFTER AN INDEXED READ STARTS *			
		188	*-----*			
087F:A6	8A	189		LDX	SL2	DACADC offset
0881:BD	EC C0	190	IND1	LDA	DACADC,X	
0884:C9	D0	191		CMP	#\$D0	index?
0886:90	F9	192		BCC	IND1	yes, wait
0888:BD	EC C0	193	IND2	LDA	DACADC,X	
088B:C9	D0	194		CMP	#\$D0	index?
088D:B0	F9	195		BCS	IND2	no. wait
088F:A9	00	196	NORM	LDA	#\$00	count for
0891:85	8D	197		STA	REVCNT	non indexed
0893:A9	20	198		LDA	#\$20	write (\$2000 bytes?)
0895:85	8E	199		STA	REVCNT+1	
0897:A9	FF	200		LDA	#\$FF	write all 1's pattern
0899::A6	8B	201		LDX	SL16	
089B:A4	8D	202		LDY	REVCNT	init counter (LO byte)
		203	*-----*			
		204	* CODE FROM HERE TO STALL MUST *			
		205	* BE ON ONE MEMORY PAGE FOR *			
		206	* CORRECT TIME COUNTS *			
		207	*-----*			
089D:9D	8F C0	208		STA	Q7H,X	Q6H,Q7H (A) to sh reg
08A0:1D	8C C0	209		ORA	Q6L,X	Q6L,Q7H write on disk
08A3:EA		210		NOP		
08A4:E4	1B	211		CPX	IFLG	(stall 3 cycles)
08A6:EA		212	MORE	NOP		
08A7:20	DB 08	213		JSR	STALL	wait 12 cycles
08AA:EA		214	WRITE1	NOP		
08AB:EA		215		NOP		
08AC:9D	8D C0	216		STA	Q6H,X	

Appendix B

08AF:1D	8C C0	217		ORA Q6L,X	write on disk
08B2:88		218		DEY	
08B3:D0	F1	219	BNE	MORE	256 bytes
08B5:48		220		PHA	
08B6:68		221		PLA	
08B7:C6	8E	222		DEC REVCNT+1	
08B9:D0	EF	223		BNE WRITE1	not revcnt bytes yet
08BB:A9	FF	224		LDA #\$FF	not create 1 or 2 errors
08BD:E4	1B	225		CPX IFLG	per track to stop reads
08BF:9D	8D C0	226		STA Q6H,X	
08C2:1D	8C C0	227		ORA Q6L,X	write on disk
08C5:20	DB 08	228		JSR STALL	give it time to finish
08C8:EA		229		NOP	
08C9:EA		230		NOP	
08CA:48		231		PHA	
08CB:68		232		PLA	
08CC:BD	8E C0	233	ALLOC	LDA Q7L,X	Q7 LO, Q6 LO
08CF:BD	8C C0	234		LDA Q6L,X	set read mode
08D2:20	BE DE	235		JSR CHKCOM	eat a comma
08D5:A9	00	236		LDA #\$00	flag=0 for normal return
08D7:A8		237		TAY	;HI byte of flag
08D8:4C	AC 0A	238		JMP STUFFIT	return error code
08DB:60		239	STALL	RTS	
		240		*-----*	*
		241		* READ THE DISK TO A BUFFER	*
		242		* CALL2087(R,SL,DR,HD,V,ER)	*
		243		* CALL2087(RI,SL,DR,HD,V,ER)	*
		244		* VARIABLE SL=SLOT NUMBER 2 -> 5	*
		245		* VARIABLE DR=DRIVE # 0 / 1	*
		246		* VARIABLE HD=HEAD # 0 / 1	*
		247		* VARIABLE V=VOLTAGE 0 TO 128	*
		248		* ER=ERROR CODE RETURNED:	*
		249		* 0 = OK	*
		250		* 128 = NO INDEX FOUND	*
		251		*-----*	*
08DC:20	B1 00	252	READ	JSR CHRGET	expect I or comma
08DF:85	1B	253		STA IFLG	save indexed flag
08E1:C9	49	254		CMP #'I'	is it indexed?
08E3:D0	ID	255		BNE GOREAD	
08E5:20	B1 00	256		JSR CHRGET	eat the I
08E8:20	3A 0A	257		JSR PARMS	slot,head,drive
08EB:20	4B 0A	258		JSR SETDAC	set ref voltage
08EE:20	65 0A	259		JSR FNDINDX	is index present?
08F1:BD	EC C0	260	RIND1	LDA DACADC,X	X=offset sl2+dr#
08F4:C9	D0	261		CMP #\$D0	index?
08F6:90	F9	262		BCC RIND1	yes, wait
08F8:BD	EC C0	263	RIND2	LDA DACADC,X	
08FB:C9	D0	264		CMP #\$D0	index?
08FD:B0	F9	265		BCS RIND2	no, wait
08FF:4C	08 09	266		JMP RDNOW	time to start reading
0902:20	3A 0A	267	GOREAD	JSR PARMS	set slot, drive, head
0905:20	4B 0A	268		JSR SEDAC	set ref voltages
0908:A9	00	269		LDA #\$00	save counters for
090A:85	07	270		STA \$07	no. of bytes read
090C:85	08	271		STA \$08	and no. of sectors read
090E:A6	8B	272		LDX SL16	set slot to read

Appendix B

0910:A0	00	273		LDY #\$00	read next sector
0912:BD	8E C0	274		LDA Q7L,X	clear readswitch I/O
0915:BD	8C C0	275	READBYT	LDA Q6L,X	ensure read mode
0918:10	FB	276		BPL READBYT	is data read?
091A:DD	8C C0	277		CMP Q6L,X	sure?
091D:D0	F6	278		BNE READBYT	
091F:C9	FF	279		CMP #\$FF	test data read
0921:D0	0D	280		BNE DUMP	if non-\$ff, break
0923:C8		281		NIY POSITION	for next byte
0924:D0	EF	282		BNE READBYT	no? back for next byte
0926:E6	08	283		INC \$08	set at next sector
0928:A5	08	284		LDA \$08	check to see if
092A:C9	10	285		CMP #\$10	last sector done
092C:DO	E7	286		BNE READBYT	no? retn for next sector
092E:4C	CC 08	287		JMP ALLOK	return error code = 0
0931:84	07	288	DUMP	STY \$07	store addr of bad byte
0933:85	09	289		STA \$09	save bad byte value
0935:20	BE DE	290		JSR CHKCOM	
0938:4C	72 08	291		JMP \$0872	set er = 255
093B:60		292		RTS	
		293		*-----*	
		294		* BUFFER IS NOW FULL	*
		295		*-----*	*
		296		*	
		297		*-----*	*
		298		* SEARCH BUFFER FOR NON-\$FF	*
		299		* CALL2087(F,START,FOUND)	*
		300		* START=ADDRESS TO SEARCH FROM*	*
		301		* 8192 <= START < 24576	*
		302		* \$2000 \$6000	*
		303		* FOUND=ADDRESS OF NON-\$FF	*
		304		*-----*	*
093C:20	B1 00	305	FIND	JSR CHRGET	eat the F
093F:20	BE DE	306		JSR CHKCOM	eat the comma
0942:20	05 E1	307		JSR INTGET	expr -> intval H,L bytes
0945:A5	A0	308		LDA INTVAL	get HI byte
0947:C9	20	309		CMP #\$20	starting address
0949:90	04	310		BCC F1	too low
094B:C9	60	311		CMP #\$60	end of buffer
094D:90	03	312		BCC F2	range ok
094F:20	99 E1	313	F1	JSR ILLQUAN	issue ill quan msg
0952:20	BE DE	314	F2	JSR CHKCOM	eat a comma
0955:A5	A0	315		LDA INTVAL	count HI byte
0957:A4	A1	316		LDY BYTE	Y=LO of ptr
0959:85	A1	317		STA BYTE	swap to create
095B:A9	00	318		LDA #\$00	base address
095D:85	A0	319		STA INTVAL	pointer
095F:B1	A0	320	F3	LDA (INTVAL),Y	get next data byte
0961:C9	FF	321		CMP #\$FF	is byte ok?
0963:D0	0B	322		BNE F4	no? go back to program
0965:C8		323		INY	;increment counter
0966:D0	F7	324		BNE F3	keep going
0968:E6	A1	325		INC BYTE	HI byte of counter
096A:A5	A1	326		LDA BYTE	set cntr HI byte for cmpr
096C:C9	60	327		CMP #\$60	done?
096E:D0	EF	328		BNE F3	no? keep going
0970:A5	A1	329	F4	LDA BYTE	get count ready (Y=LO)

Appendix B

```

0972:4C AC 0A 330          JMP STUFFIT      COUNT HI=A,LO=Y
331 *
332 * CALL287(S,SL,DR,HD,ON=1/OFF=0,LD=1/UP=0,
          U=0/D=1,TRK CNT)
333 * SELECT SLOT,HEAD,DRIVE - SL16 & SL2
334 * MOTO ON OR OFF, LIFT/LOAD HEAD
335 * SET DIRECTION TO MOVE HEAD AND
336 * MOVE HEAD TO DESIRED RELATIVE TRACK
337 *
338 * PHASE 2      PHASE 3      USAGE OF PHASE 2,3
339 * -----
340 *      LO      LO      SELECT HEAD 0
341 *      HI      HI      SELECT HEAD 1
342 *      LO      HI      TURN MOTOR ON
342 *      HI      LO      TURN MOTOR OFF
344 *
345 * NOTE: BE CAREFUL NOT TO TURN THE MOTOR
346 * ON OR OFF BY ACCIDENT WHILE CHANGING
347 * HEADS! GO THROUGH P2L,P3L FIRST
0975:20 B1 00 348 SKSET   JSR  CHRGET   remove the command S
0978:20 E6 09 349         JSR  SETUP    set up slot, drive, head
097B:20 BE DE 350         JSR  CHKCOM   eat a comma
097E:20 F8 E6 351         JSR  GETBYT   motor on=1/off=0
0981:8A          352         TXA
0982:A6 8B      353         LDX  SL16    load slot o/set for hd sel
0984:29 01      354         AND  #1      leave a 0 or a 1
0986:DO 09      355         BNE  B1
0988:BD 85 C0 356         LDA  P2H,X    MOTOR
098B:BD 86 C0 357         LDA  P3L,X    OFF
098E:4C 97 09 358         JMP  B2
0991:BD 84 C0 359 B1     LDA  P2L,X    MOTOR
0994:BD 87 C0 360         LDA  PH3,X    ON
0997:20 DB 09 361 B2     JSR  TIME     enable and wait
099A:20 BE DE 362         JSR  CHKCOM   eat a comma
099D:20 F8 E6 363         JSR  GETBYT   head load=1,lift=0
09A0:8A          364         TXA
09A1:A6 8A      365         LDX  SL2     get offset=slot*2+dr#
09A3:29 01      366         AND  #$1     leave a 0 or 1
09A5:F0 04      367         BEQ  LIFT
09A7:A9 FF      368         LDA  #$FF    +5 V
09A9:D0 02      369         BNE  DOIT    (always)
09AB:A9 80      370 LIFT     LDA  #$80    0 V
09AD:9D F4 C0 371 DOIT    STA  HDLOAD,X send voltage to sl#7 line
09B0:20 BE DE 372         JSR  CHKCOM   eat a comma
09B3:20 F8 E6 373         JSR  GETBYT   direction up=0,down=1
09B6:8A          374         TXA
09B7:29 01      375         AND  #1     leave a 0 or 1
09B9:18          376         CLC
09BA:65 8B      377         ADC  SL16
09BC:AA          378         TAX
09BD:BD 82 C0 379         LDA  P1L,X    set direction
09C0:20 BE DE 380         JSR  CHKCOM   eat a comma
09C3:20 F8 E6 381         JSR  GETBYT   get track step count
09C6:20 B8 DE 382         JSR  CHKCLS  end of argument list?
09C9:8A          383         TXA
09CA:A6 8B      384         LDX  SL16

```

Appendix B

09CC:A8		385	TAY MOVE	counter
09CD:F0	16	386	BEQ FINI	do not move
09CF:BD	81 C0	387 PULSE	LDA P0H,X	pulse inverted by board
09D2:BD	80 C0	388	LDA P0L,X	drive expects ----_----
09D5:20	E0 09	389	JSR TIME2	time delay
09D8:88		390	DEY	
09D9:D0	F4	391	BNE PULSE	more steps?
09DB:A6	8B	392 TIME	LDX SL16	get slot*16
09DD:BD	89 C0	393	LDA DON,X	turn on motr to fool card
09E0:A9	70	394 TIME2	LDA #\$70	time delay
09E2:20	AB FC	395	JSR WAIT	~ 0.01 Sec
09E5:60		396 FINI	RTS	fall to here from skset
		397	*-----*	
		398	*READ PARAMETERS FROM CALL LIST *	
		399	*... SLOT, DRIVE, HEAD ...	*
		400	* LEAVES SLOT*16 IN SL16	*
		401	* SLOT*2+HEAD IN SL2	*
		402	* SELECTS HEAD AND DRIVE	*
		403	*-----*	
09E6:D8		404 SETUP	CLD	
09E7:20	BE DE	405	JSR CHKCOM	eat a comma
09EA:20	F8 E6	406	JSR GETBYT	slot#?
09ED:8A		407	TXA	
09EE:C9	02	408	CMP#\$2	check range of slot
09F0:90	04	409	BCC BADSLOT	(< 2)
09F2:C9	06	410	CMP #\$6	
09F4:90	03	411	BCC SLOK	(<5)
09F6:4C	99 E1	412 BADSLOTJMP	ILLQUAN	out of range 2-5
09F9:0A		413 SLOK	ASL	*2
09FA:85	8A	414	STA SL2	
09FC:0A		415	ASL	*4
09FD:0A		416	ASL	*8
09FE:0A		417	ASL	*16
09FF:85	8B	418	STA SL16	
0A01:20	DB 09	419	JSR TIME	ensure card is turned on
		420	*-----*	
		421	* PICK THE DRIVE	*
		422	*-----*	
0A04:20	BE DE	423	JSR CHKCOM	eat a comma
0A07:20	F8 E6	424	JSR GETBYT	drive#?
0A0A:8A		425	TXA	
0A0B:29	01	426	AND #1	leave 1 or 0
0A0D:85	8C	427	STA DRNUM	
0A0F:18		428	CLC	
0A10:65	8B	429	ADC SL16	
0A12:AA		430	TAX	
0A13:BD	8A C0	431	LDA D0SEL,X	select drive
0A16:A6	8B	432	LDX SL16	slot*16=offset
0A18:BD	84 C0	433	LDA P2L,X	force head select to
0A1B:BD	86 C0	434	LDA P3L,X	head 0 - leave mtr on/off
		435	*-----*	
		436	* PICK HEAD TO USE	*
		437	*-----*	
0A1E:20	BE DE	438	JSR CHKCOM	eat a comma
0A21:20	F8 E6	439	JSR GETBYT	drive#?
0A24:8A		440	TXA	
0A25:29	01	441	AND #1	leave 1 or 0

Appendix B

```

0A27:18      442      CLC
0A28:65 8B   443      ADC SL16      add slot offset
0A2A:AA      444      TAX
0A2B:BD 84 C0 445      LDA P2L,X    select
0A2E:BD 86 C0 446      LDA P3L,X    head

447 *-----*
448 *CALCULATE DACADC OFFSET AND *
449 *LEAVE IT IN SL2 AND THE X-REG *
450 *-----*
0A31:A5 8A   451      LDA SL2      slot*2
0A33:18      452      CLC          prep for add
0A34:65 8C   453      ADC DRNUM    dr#=1/0
0A36:85 8A   454      STA SL2      $4-B for S2,d0 to S5,d1
0A38:AA      455      TAX          leave it for later
0A39:60      456      RTS

457 *-----*
458 *GET SLOT & DRIVE, TURN MOTOR ON*
459 *LEAVE X=DACADC OFFSET *
460 *-----*
0A3A:20 E6 09 461 PARS   JSR SETUP    read parameter list
0A3D:A6 8B   462      LDX SL16    slot offset
0A3F:BD 84 C0 463      LDA P2L,X    motor
0A42:BD 87 C0 464      LDA P3H,X    ON
0A45:20 DB 09 465      JSR TIME     do it and wait
0A48:A6 8A   466      LDX SL2      get dacadc offset
0A4A:60      467      RTS

468 *-----*
469 *READ VARIABLE FOR VOLTAGE *
470 *(SHOULD BE 0 -> 127) AND *
471 *CONVERT IT TO $80 -> $00 THEN *
472 *SET DAC TO THE VOLTAGE *
473 *-----*
0A4B:20 BE DE 474 SETDAC JSR CHKCOM eat a comma
0A4E:20 F8 E6 475      JSR GETBYT  eval variable
0A51:A5 A1   476      LDA BYTE    should be $0 -> $80
0A53:C9 81   477      CMP #$81    is it less than $81?
0A55:90 03   478      BCC SETDAC1 OK
0A57:4C 99 E1 479      JMP ILLQUAN issue ill quant message
0A5A:A9 80   480 SETDAC1 LDA #$80
0A5C:38      481      SEC
0A5D:E5 A1   482      SBC BYTE    now $80 -> $0
0A5F:A6 8A   483      LDX SL2     dac offset
0A61:9D EC C0 484      STA DACADC,X set voltage
0A64:60      485      RTS

486 *-----*
487 *CONFIRM THAT INDEX IS PRESENT *
488 *OR RETURN ERROR CODE 128 *
489 *AFTER CMP #$D0 CARRY CLEAR *
490 *IMPLIES INDEX IS PRESENT *
491 *-----*
0A65:A9 20   492 FNDINDX LDA #$20    load
0A67:85 07   493      STA COUNT1+1 counter
0A69:A9 00   494      LDA #$00    to see if
0A6B:85 06   495      STA COUNT1  index changes
0A6D:A6 8A   496      LDX SL2     get o/set to 2*slot+drive

```

Appendix B

```

497 *-----*
498 *FIND STARTING PLACE - COUNT *
499 *CYCLES WITH INDEX NOT PRESENT *
500 *-----*
0A6F:EA 501 C0      NOP
0A70:C6 06 502      DEC COUNT1    count 32 cycles
0A72:D0 07 503      BNE C1         loops while
0A74:C6 07 504      DEC COUNT1+1   looking for index
0A76:D0 05 505      BNE C2
0A78:4C A3 0A 506     JMP NOIND      no index found
0A7B:48 507 C1     PHA          waste time
0A7C:68 508     PLA
0A7D:EA 509     NOP
0A7E:EA 510     NOP
0A7F:EA 511     NOP
0A80:BD EC C0 512     LDA DACADC,X  read adc
0A83:C9 D0 513     CMP #$D0      is it index?
0A85:B0 E8 514     BCS C0       no, go back and wait
0A87:4C 8B 0A 515     JMP C4       kill time cont. count
516 *-----*
517 *COUNT INDEX BY 32 CYCLE LOOPS *
518 *-----*
0A8A:EA 519 C3     NOP
0A8B:C6 06 520 C4     DEC COUNT1    continue counting
0A8D:DO 07 521     BNE C5
0A8F:C6 07 522     DEC COUNT1+1
0A91:D0 05 523     BNE C6
0A93:4C A3 0A 524     JMP NOIND      no index found
0A96:48 525 C5     PHA          waste time
0A97:68 526     PLA
0A98:EA 527 C6     NOP
0A99:EA 528     NOP
0A9A:EA 529     NOP
0A9B:BD EC C0 530     LDA DACADC,X  read adc
0A9E:C9 D0 531     CMP #$D0      is it index?
0AA0:90 E8 532     BCC C3       yes, keep counting
0AA2:60 533     RTS
534 *-----*
535 *NO INDEX FOUND: SET ERR FLAG *
536 *-----*
0AA3:20 BE DE 537 NOIND JSR  CHKCOM   eat a comma
0AA6:68 538     PLA         remove return address
0AA7:68 539     PLA         so prog goes to basic
0AA8:A9 00 540     LDA #$00    high byte for error
0AAA:A0 80 541     LDY #$80    decimal 128 bad ind flag
0AAC:20 F2 E2 542 STUFFIT JSR  GIVAYF   float AH,YL into FAC
0AAF:20 E3 DF 543     JSR PTRGET   find where it goes
0AB2:AA 544     TAX         prep for store in variable
0AB3:20 2B EB 545     JSR MOVMF    store it
0AB6:20 95 D9 546     JSR DATA    eat rest of statement
0AB9:60 547     RTS
548 *-----*
549 * READ THE DISK IMMEDIATELY *
550 *WITHOUT WAITING FOR DISK TO *
551 *COME TO SPEED, LOOK FOR *
552 *$FF'S AND COUNT TIME UNTIL *
553 *ONE APPEARS. *

```

Appendix B

```

554 *CALL2087(T,SL,DR,HD,V,CT) *
555 *VARIABLE SL=SLOT NUMBER 2 -> 5 *
556 *VARIABLE DR=DRIVE NUMBER 0/1 *
557 *VARIABLE HD=HEAD NUMBER 0/1 *
558 *VARIABLE V=VOLTAGE 0 ->128 *
559 *CT=COUNT RETURNED *
560 *EACH COUNT=19.437 MICROSEC. *
561 *-----*
0ABA:20 B1 00 562 TIMER JSR CHRGET eat the T
0ABD:20 E6 09 563 JSR SETUP slot,head,drive
0AC0:20 4B 0A 564 JSR SETDAC set ref voltage
0AC3:20 BE DE 565 JSR CHKCOM eat a comma
0AC6:A6 8B 566 LDX SL16 get slot offset
0AC8:BD 89 C0 567 LDA DON,X turn on card
0ACB:A9 00 568 LDA #$00
0ACD:85 06 569 STA COUNT1 counter low byte
0ACF:A8 570 TAY counter high byte
0AD0:BD 84 C0 571 LDA P2L,X turn on the motor
0AD3:BD 87 C0 572 LDA P3H,X and start looking for data
0AD6:BD 8E C0 573 LDA Q7L,X ensure read mode
0AD9:BD 8C C0 574 LDA Q6L,X start looking
0ADC:E6 06 575 TLOOP INC COUNT1
0ADE:D0 07 576 BNE T1
0AE0:C8 577 INY
0AE1:C0 80 578 CPY #$80 counter full?
0AE3:F0 0B 579 BEQ CNTFULL
0AE5:D0 02 580 BNE T2 ALWAYS
0AE7:48 581 T1 PHA waste time
0AE8:68 582 PLA waste more
0AE9:BD 8C C0 583 T2 LDA Q6L,X look at data
0AEC:C9 FF 584 CMP #$FF is it good?
0AEE:D0 EC 585 BNE TLOOP keep counting
0AF0:98 586 CNTFULL TYA arrange count
0AF1:A4 06 587 LDY COUNT1
0AF3:4C AC 0A 588 JMP STUFFIT count high=a, low=y
589 *-----*
590 *END OF PROGRAM CODE *
591 *PROGRAM MUST END BY $0AFF OR *
592 *CHANGES MUST BE MADE IN THE *
593 *'POKE 104,XX' STATEMENTS AT *
594 *THE BEGINNING OF THE PROGRAM *
595 *-----*
0AF6:00 01 02 596 HEX 000102 Version 0.1.2
0AF9:44 42 50 597 ASC 'DBP'

```

End of assembly

764 bytes

Errors: 0

Appendix B

The program listed below enables reading back of the data stored on disk in relation to the bit analysis carried out by the above software. The above master control program does provide a "hard copy" with a printer always on-line. However, it is useful to produce copies of the data later. The following program is intended to fulfill this function.

```
10 print chr$(4) "mon i" : goto 60
20 text : home : print " *** prog to read text files ***"
30 print " *** created by the program ***"
40 print " *** digiwear using the BETL ****"
50 print " *** utility (#0.1.2.m) ****" : vtab 11 : return
60 gosub 20 : onerr goto 210
70 print "Enter number of files to analyse" : input "or print out: ";n$ : n = val (n$)
  : in n = 0 and n$ <> "0" then chr$(7) : goto 70
80 dim fl$(30) : dim p$(30) : rem file, printed?
90 for i = 1 to n
100 gosub 20 : print "Enter filename of file #";i : input": ";fl$(i) : p$(i) = ""
110 next
120 rem
130 rem now read files
140 rem
150 i = 1
160 gosub 20 : print "List "fl$(i)" directly to printer? (y/n): "; : get a$ : print a$ : if
  a$ <> "y" and a$ <> "n" then print chr$(7) : goto 160
170 p$ = a$ : if a$ = "y" then print chr$(4)"pr#1" : print
180 print chr$(4)"open "fl$(i)",s6,d2"
190 print chr$(4)"read "fl$(i)
200 get b$ : print b$ : goto 200
210 if a$ = "y" then print chr$(4)"pr#0" : goto 250
220 print : print "Any key to continue ... "; : get a$
230 gosub 20 : print "Hard copy now? (y/n): "; : get a$ : print a$ : if a$ <> "y"
  and a$ <> "n" then print chr$(7) : goto 230
240 if a$ = "y" then print chr$(4)"close" : goto 170
250 print chr$(4)"close"
260 if i < n then i = i + 1 : goto 160
270 for i = 1 to n
280 if p$(i) = "n" then 300 : rem check all files printed
290 next : goto 320
300 gosub 20 : print "Print all or some of " : print "the remaining files? (y/n): "; :
  get a$ : print a$
310 if a$ = "y" then 160
320 print chr$(4)"nomon i" : stop
330 end
```